FRI-UW-8413
December 1984

FISHERIES RESEARCH INSTITUTE
School of Fisheries
University of Washington
Seattle, Washington

RENTON SEWAGE TREATMENT PLANT PROJECT:

SEAHURST BASELINE STUDY

K. K. Chew and Q. J. Stober, Principal Investigators

VOLUME III

Section 4

Water Column Ecology

by

J. Anderson, A. Copping, T. Jagielo, J. Postel,
W. Peterson, B. Dumbald, G. Heron, R. Hood, M. Strom

Draft Final Report
for the period
1 April 1982 to 31 December 1984
for
The Municipality of Metropolitan Seattle
Seattle, Washington

Approved:

Submitted:_____

_____
Director

RENTON SEWAGE TREATMENT PLANT PROJECT:
Seahurst Baseline Study
K. K. Chew and Q. J. Stober, Principal Investigators

VOLUME SUBTITLES

Volume	Section	Title
I	1	Executive Summary
II	2	Puget Sound: A Fjord System Homogenized with Water Recycled over Sills by Tidal Mixing.
	3	Circulation in South Central Puget Sound Basin and Seahurst Bay.
III	4	Water Column Ecology
IV	5	Intertidal and Shallow Subtidal Benthic Ecology
V	6	Subtidal Benthic Ecology
VI	7	Fish Ecology
VII	8	Fish Health
VIII	9	Microbiology
	10	Virology
IX	11	Marine Chemistry
X	12	Marine Toxicology
XI	13	Vertical Transport of Freon Extractable and Non-extractable Material and Bacteria (fecal coliform and enterococci) to the Surface of Marine Waters: Some Experimental Results Using Secondary Sewage Effluent.
	14	The Influence of Floatable Materials From Treated Sewage Effluents on Shorelines

TABLE OF CONTENTS

LIST OF FIGURES

Number Page

LIST OF TABLES

LIST OF APPENDIX FIGURES

LIST OF APPENDIX TABLES

PREFACE

Expansion of the Renton Sewage Treatment Plant to meet the needs of a growing population in the Seattle metropolitan area was begun in 1982. The secondary effluent from this plant has been discharged into the Duwamish River near Tukwila, Washington since its construction in the mid-1960's. The increased capacity of this plant from 36 million gallons per day to 72 mgd would not allow continued compliance with established water quality standards in the Duwamish River and a plan to construct a pipeline, tunnel and marine outfall system to divert effluent directly to Puget Sound was adopted. A site due west of the plant in the south central Puget Sound basin at Seahurst was selected as the marine receiving water.

The Seahurst Baseline Study as a part of the expansion plan was designed to obtain pre-discharge ecological data in the marine environment in the East and Colvos Passage areas of south central Puget Sound (Figure 1.1). Although facility planning by METRO and an environmental impact statement by the U.S. Environmental Protection Agency predicted no water quality problems were likely to occur as a result of the proposed discharge, the Seahurst Baseline Study was initiated to carefully document a comprehensive and integrated understanding of the marine ecological conditions in the receiving waters. These data were utilized to minimize potential impacts of the design, to aid in ongoing planning efforts, to evaluate several outfall alignments in Seahurst Bay and to assess changes which could occur once effluent was discharged at the site. The principal purpose for this effort was to establish environmental conditions, organism assemblages and predictive water quality information prior to a planned event using appropriate scientific procedures which could be repeated during later monitoring efforts. The

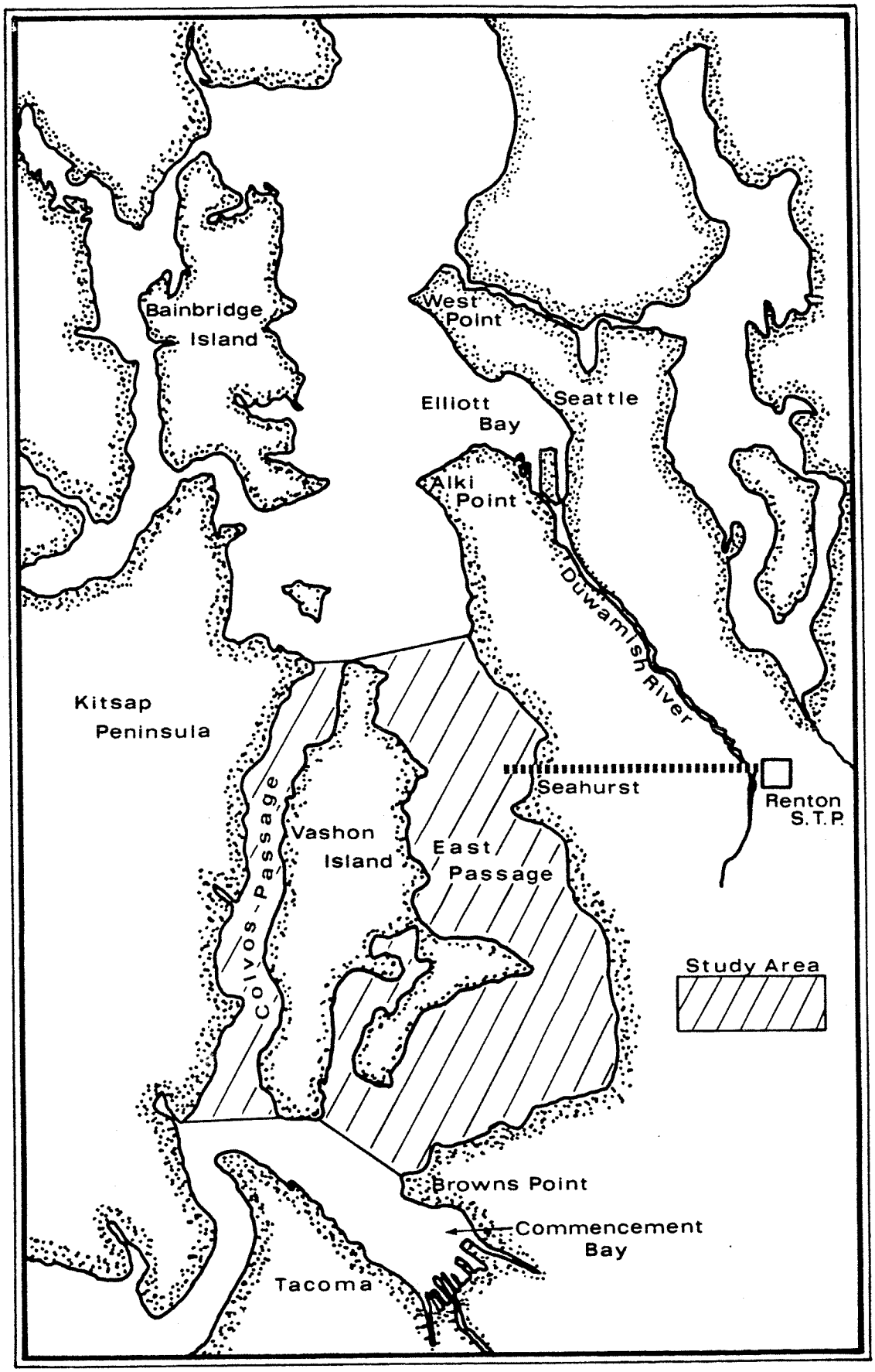

Figure 1.1. The Central Puget Sound basin showing the location of the Renton Sewage Treatment Plant and the study area in the south central basin

Seahurst Baseline Study was initiated in April 1982. It was to extend for a three year period with field sampling designed to terminate in March 1984 followed by analysis of the data, a final report and a post-effluent discharge monitoring plan in March 1985. In April 1984 the METRO Council decided to move the Renton Treatment Plant outfall site to Duwamish Head in Elliott Bay as the culmination of ongoing planning and design efforts. As a result of that decision a final report was authorized on a shortened time schedule to prevent the loss of ecological data obtain for Seahurst Bay and the East Passage of Puget Sound.

The Seahurst Baseline Study was originally designed with three broad objectives: (1) to collect, analyze and interpret the significance of physical, chemical and biological data around the proposed sewage treatment plant outfall at Seahurst to determine the properties and characteristics of the receiving environment; (2) to utilize the information obtained to aid in the siting and design of the outfall pipe and diffuser; and (3) to recommend a post-effluent discharge monitoring plan that will effectively and efficiently determine if the presence of the new outfall significantly changes the receiving water environment described in the first objective. The latter objective was not fulfilled after the Seahurst site was dismissed from further outfall siting consideration.

The technical organization of this study is illustrated in Figure 1.2. The major tasks identified which consistently interacted were grouped together under water column, environmental health, sediment investigations and chemistry. The studies of the water column included monitoring of the physical/chemical characteristics of the water and the indigenous pelagic biota. Sediment investigations included the ecological studies of the intertidal and subtidal benthos and fishes. Environmental health included the

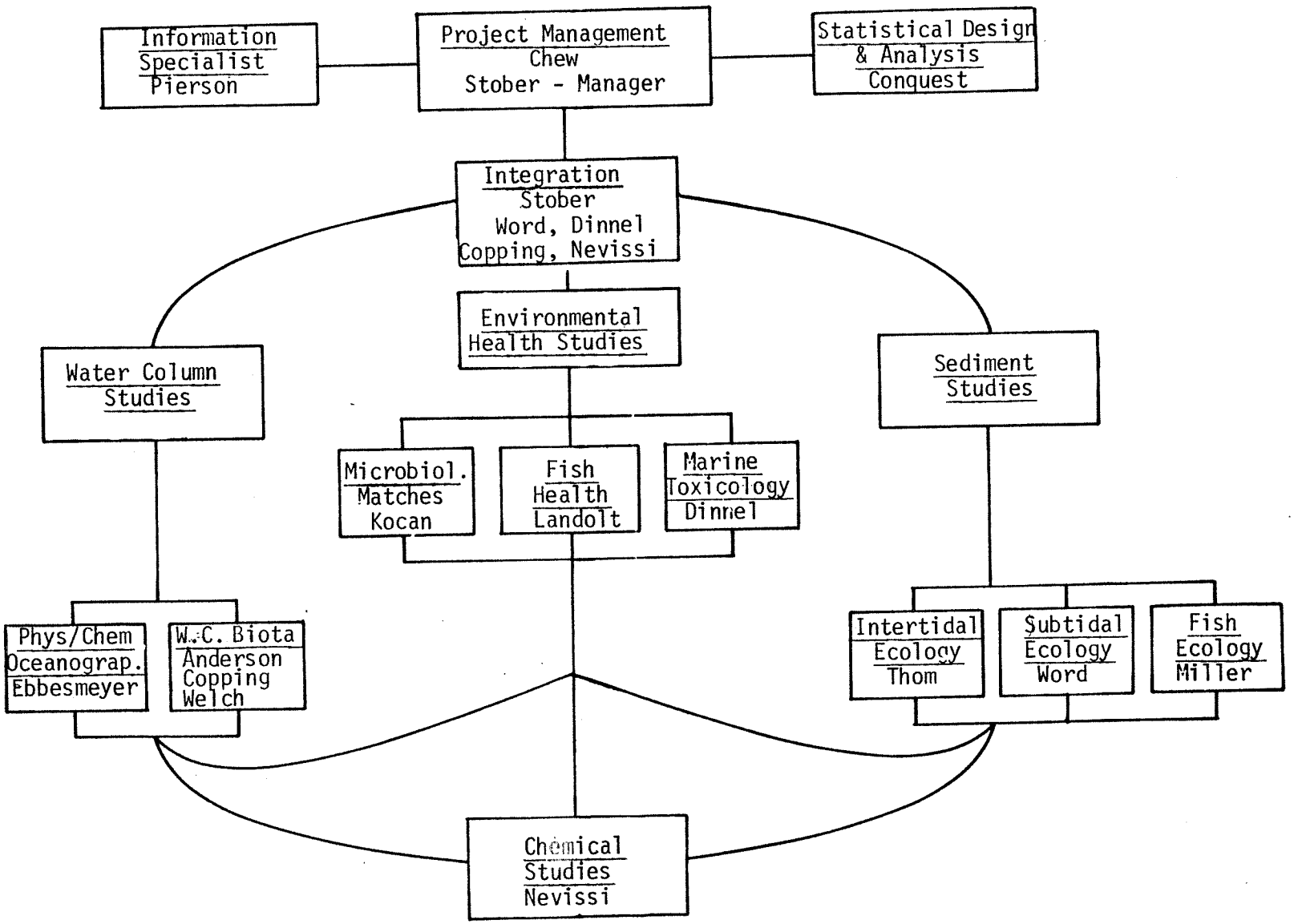

Figure 1.2. Organization of the Renton Sewage Treatment Plant Project, Seahurst baseline study indicating major project divisions, specific tasks, and responsibilities of selected personnel.

monitoring and isolation of human pathogens (bacteria and viruses), fish pathology (fish health) and marine toxicology (water column, sediments and effluent). The chemical analyses were focused on the presence of trace metals in water, biota and sediment, in addition to a variety of support services to the entire project. The organizational structure of this study facilitated efficiency, fiscal control, interdisciplinary integration within and between tasks and ensured that the study scope and schedules were met in a timely manner. This report is similarly organized by task.

Statistical expertise was provided on a regular basis to faculty, staff and students associated with the project by Dr. Loveday Conquest in the Center for Quantitative Sciences in Forestry, Fisheries and Wildlife. Areas of investigation included computation of required sample sizes in various experimental designs, appropriate transformations of data, use of parametric and nonparametric tests, and general statistical approaches to data analysis.

Organizational and coordination meetings were held routinely throughout the study period within and between task groups to plan sampling and analytical activities and to discuss developing interpretations of the data. The Project Manager and Project Leaders were in daily contact with METRO staff throughout the study in an effort to find solutions to problems and to ensure the maximum performance of all investigators during this study.

ACKNOWLEDGMENTS

The Seahurst Baseline Study is sponsored by the Municipality of Metropolitan Seattle (METRO) through a research services contract with the University of Washington College of Ocean and Fishery Sciences. This study is a part of the Renton Sewage Treatment Plant Project. The Study Coordinator for METRO is Mr. Robert I. Matsuda.

We would like to thank Messers. Rick Adler, Cory Miller and Jeff Brown for their help in collecting samples, and Mr. Lauren Rice for this help at the Occupational Skills Center, Highline Public Schools, Marine Laboratory at Seahurst Park.

Our thanks also to Dr. Bruce Miller for lending his induction salinometer, and to Dr. Carl Lorenzen, U.W. School of Oceanography for his continuing loan of equipment and for his advice.

ABSTRACT

Studies of the water column ecology were designed to focus on a resolution of the seasonal patterns. Phytoplankton (chlorophyll) and nutrient levels in the photic zone were related to the seasonal light cycle with the zooplankton cycle following chlorophyll. The cycles were coupled in terms of the rates of change of the properties. The phytoplankton rate of change was positive in the spring and negative in the autumn with respective minimum and maximum levels near the winter and summer solstice, respectively. A larger positive rate of change in zooplankton in the spring followed chlorophyll with a negative rate of change in autumn. Maximum zooplankton abundance was observed about the summer solstice and minimum abundance about the winter solstice. The rates of change of nutrients were inverse to the chlorophyll resulting in maximum and minimum concentrations about the winter and summer solstices, respectively.

Plankton and nutrient levels exhibited a large variability about the seasonal pattern. The spatial variation between stations on a given day was about 15% for nutrients, 30% for plankton biomass, and 40% for plankton species abundance. The temporal variation was about 2 to 3 times larger. Thus, the total variability about the seasonal smoothed averages was about 15 to 30% for nutrients, 100% for plankton biomass, and 150 to 200% for plankton species.

The chance of observing a high level of chlorophyll in the photic zone ($\geq$10 mg Chl/m^3) was larger in the summer of 1983 (15%) than in the summer of 1982 (7%). During the summer of 1983 chlorophyll levels were about twice that observed in 1982 or any year observed over the last decade. A major El Nino affected the waters of the Northeast Pacific Ocean in 1983 and resulted in an

average water column temperature increase of about 1°C in Puget Sound. It is possible that this had a positive effect on phytoplankton growth in Puget Sound, however, the cause of the doubling in chlorophyll from 1982 to 1983 is not fully understood.

The dominant phytoplankton species in Puget Sound were diatoms, which had maximum rates of growth in the spring. Dinoflagellates were second with maximum numbers in midsummer. Microflagellates were the third most abundant group with maximum numbers in midsummer. Toxic dinoflagellates were infrequently observed in small numbers. The dominant zooplankton observed in the main basin and Seahurst Bay were Paracalanus sp. and Corycaeus angilicus. Calanus pacificus was not numerically abundant but because of its size contributed a large biomass.

4.0 WATER COLUMN

J. Anderson, A. Copping, T. Jagielo, J. Postel, W. Peterson,

B. Dumbauld, G. Heron, R. Hood, M. Strom

4.1 Introduction

Natural daily and seasonal fluctuations in the Puget Sound marine environment can produce extremely high and low levels of chemical and biological properties in the water column and the nearshore environment. Presently, the evidence indicates that the discharge of treated effluent at depth will have a small impact on the average levels and frequency of extreme fluctuations in the water properties. Without prior documentation, natural daily and seasonal fluctuations might easily be misinterpreted as the result of effluent discharge. Conversely, long term changes to the environment by continuous discharge of effluent into Puget Sound might go unnoticed. The purpose of the water column study was to provide a baseline of the physical, chemical and biological properties which can be used for post-effluent discharge monitoring, and to contribute a statistically meaningful data set from which long-term changes in the Puget Sound environment can be assessed.

The water column study focused on the biological and chemical properties that are likely to be directly affected by effluent. These properties include dissolved nutrients, phytoplankton, zooplankton and particulate material. All observations were collected in statistically significant quantities so that the probability of observing differing levels of the properties can be determined. In addition, the sampling plan was designed to identify specific possible impacts and to assess their significance. The study focused on the following goals:

1. To determine the probability and cause of high and low plankton and nutrient levels in the Seahurst Bight.
2. To define the ecological differences between East Passage, Dalco Passage off Brown's Point, Colvos Passage and the main basin off West Point.
3. To document the seasonal changes in plankton biomass and nutrient concentrations in the intertidal region of Seahurst Park.
4. To describe freshwater sources in East Passage.
5. To determine the quantity and quality of sediment flux in the Seahurst/East Passage area.

4.2 Description of Study Area

The main basin of Puget Sound lies between a 44 m deep landward sill at Tacoma Narrows and a 66 m deep seaward sill at Admiralty Inlet (Figure 4.1). Tidal action causes upwelling at the landward sill and downwelling at the seaward sill. This drives an active two-layer circulation with net seaward flow above sill depth and landward flow below sill depth. The short residence time of water in the lower layer (about 3 weeks) causes this layer to closely follow the seasonal cycles in the upper layer. The upper layer circulates clockwise around Vashon Island and results in a net southwards flow through East Passage and a northward flow through Colvos Passage.

Seahurst Bight (Figure 4.1) is an open embayment on East Passage. Brace Point demarks its northern end and Three Tree Point its southern end. The bottom rapidly deepens into East Passage allowing free exchange of water between East Passage and Seahurst Bight. The circulation is reduced in the Bight and an anticyclonic eddy induces a nearshore northward drift while the main flow in the passage is southward. The intertidal zone of Seahurst Park

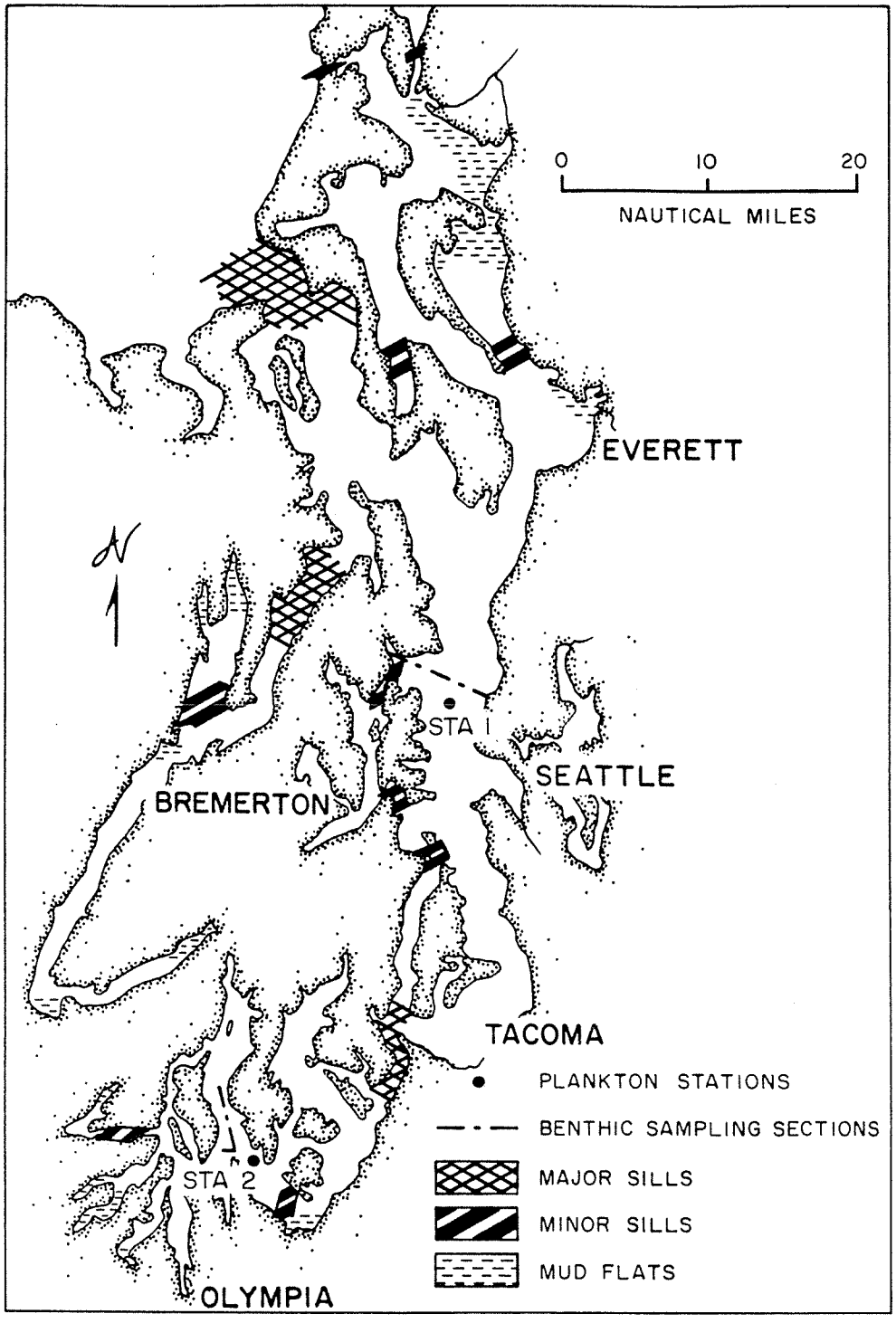

Figure 4.1. Puget Sound and sills.

beach is large; between 50 and 100 m of tide flat is exposed during low tides.

The basic interactions of plankton, nutrients, sunlight and mixing are illustrated in Figure 4.2. Phytoplankton growth is controlled by the amount of light that a cell receives (Flux 1, Figure 4.2) which varies with season, the depth to which the cells are mixed, and the clarity of water which is a function of the shading from phytoplankton and silt in the water. Phytoplankton are lost from the surface layer by zooplankton consumption (Flux 2) and the sinking of cells into the deep layer (Flux 3). Phytoplankton require nutrients for growth (Flux 4) but unless the nutrient concentration in the photic zone is near zero, nutrients do not limit growth.

Phytoplankton uptake (Flux 4) is the major nutrient removal mechanism in the surface layer. The major replacement mechanism is mixing from the nutrient rich deep layer by upwelling (Flux 5). A secondary replacement occurs from zooplankton leakage, sloppy feeding and excretion of digested phytoplankton (Flux 6). Other sources of nutrients to the surface layer include river runoff, land drainage and sewage outfalls (Flux 7). Deep layer nutrient inputs include zooplankton excretion (Flux 8) and the inflow of oceanic water across the seaward sill (Flux 9). Nutrients leave the deep layer by upwelling (Flux 5).

In general, the rates of cycling of organic carbon and nitrogen through the water column food chain are controlled by the amount of sunlight energy available for growth. Thus the rates and concentrations of properties have dominant seasonal cycles that follow the seasonal cycle of day length and sunlight intensity. Phytoplankton, with doubling times of a few days, respond quickly to changes in sunlight and thus a phytoplankton bloom occurs near the vernal equinox when the daily increase in day length is most rapid. Zooplankton egg production generally increases when the phytoplankton food

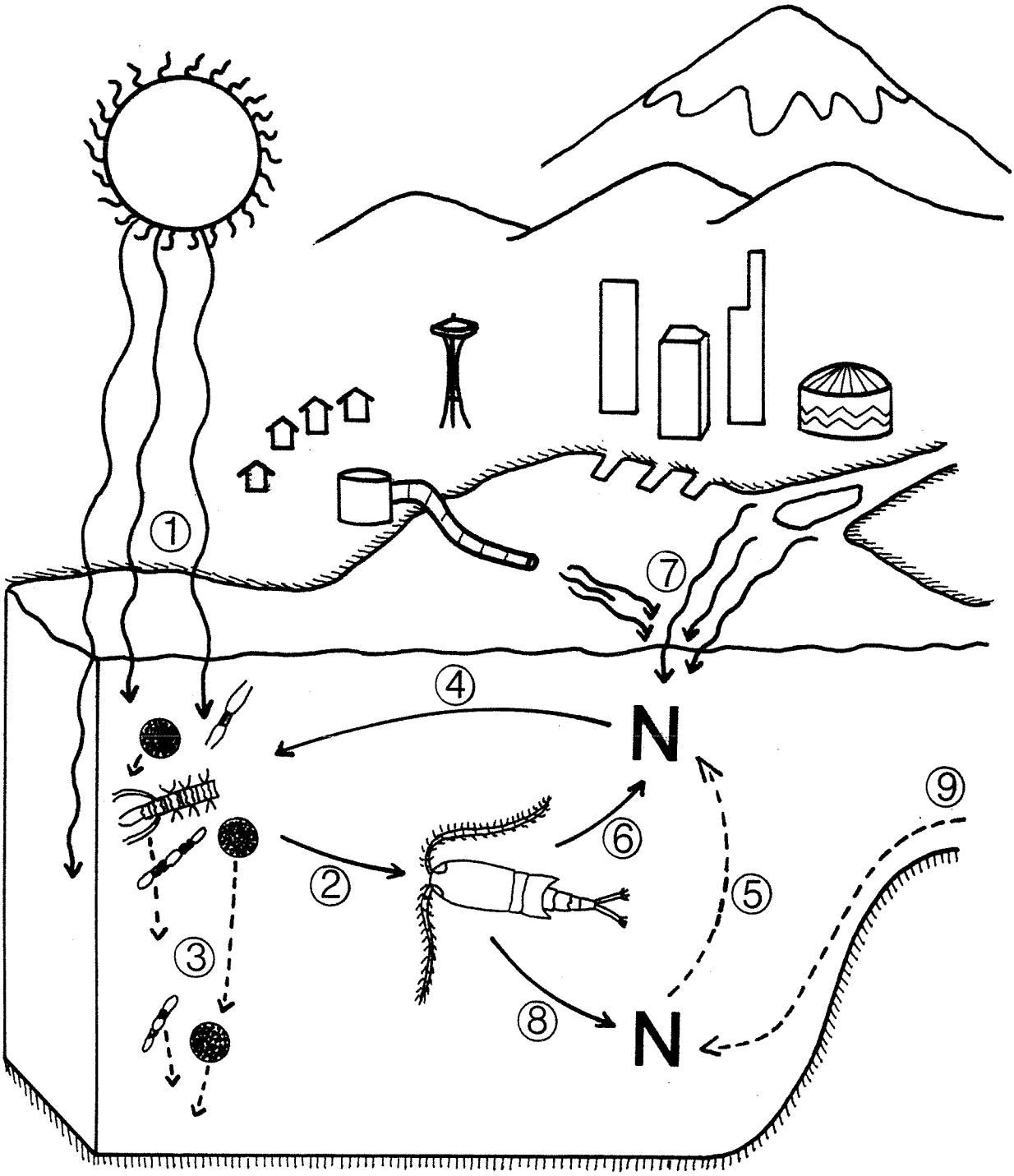

Figure 4.2. Diagram illustrating flux of material and energy through the water column. See text for description.

source becomes abundant. Zooplankton development takes several weeks so that zooplankton population increase lags the spring phytoplankton bloom by that amount of time. Replenishment of surface layer nutrients is constant over the year so changes in concentration follow changes in the uptake rate of nutrients by phytoplankton.

The minimum and maximum levels of water column properties correspond with seasonal transitions. Minimum phytoplankton and zooplankton levels occur near the winter solstice when light intensity and day length are at a minimum. Maximum plankton levels occur near the summer solstice when the light intensity and day length are at a maximum. Rapid increases in the plankton levels occur near the vernal equinox when the day length increases most rapidly and maximum loss occurs near the autumnal equinox when day length decreases most rapidly. The nutrients reach maximum values near the winter soltice when phytoplankton growth is minimum, and minimum levels near the summer solstice when phytoplankton growth is near maximum.

4.3 Materials and Methods

4.3.1 Field Program

To accomplish the study goals a sampling program including intertidal, nearshore, and wide area stations was conducted.

Six water column stations, numbered five through ten (Table 4.1), were sampled in the nearshore region of Seahurst Park in order to determine levels of physical and chemical parameters and their spatial variability in the area. Levels of phytoplankton and zooplankton biomass were measured and probability distributions of their abundance constructed for post-discharge comparison. Station 4, in the center of East Passage, was sampled with the nearshore stations as a link to the environment of the open Sound. In response to

Table 4.1. Location of discrete sampling stations and bottom depths (see also Figure 4.1).

Station No.	Latitude	Longitude	Bottom depth (m)	Location
1	47°39.6'N	122°28.8'W	220	West Point
2	47°29.9'N	122°29.5'W	100	Colvos Passage
3	47°19.1'N	122°28.3'W	170	Commencement Bay
4	47°28.8'N	122°24.7'W	180	East Passage
5	47°28.3'N	122°22.7'W	110	Seahurst
6	47°29.3'N	122°22.3'W	110	Seahurst
7	47°28.8'N	122°22.3'W	100	Seahurst
8	47°28.8'N	122°22.2'W	60	Seahurst
9	47°28.8'N	122°22.0'W	30	Seahurst
10	47°28.7'N	122°21.9'W	10	Seahurst

METRO's request, sampling at stations 5, 8 and 9 was discontinued after July of 1983, and two new stations (12 and 13) were introduced. Stations 12 and 13 were close to the proposed location of the pipeline southern alignment. Figure 4.3 shows their location in the Seahurst/East Passage area.

Discrete sampling stations were chosen in the south central basin of Puget Sound to provide information about wide area differences. They are located at: West Point (station 1), chosen as an historical station occupied in previous METRO studies (Campbell et al., 1977); Dalco Passage near Brown's Point (station 3), chosen to represent the environment of Commencement Bay; Colvos Passage (station 2), chosen as an unimpacted control station and East Passage (station 4), chosen to represent the study area (Figure 4.4).

Cruise tracks for underway mapping were chosen as midchannel representations of the areas linking the wide area stations: from West Point heading south, around Vashon Island and north to West Point (Figure 4.4). A new cruise track for the inshore transect at Seahurst Park was established in January of 1983 to better determine the onshore and offshore differences in surface water properties in the area from Point Pully to Brace Point and from Seahurst Park to midchannel (Figure 4.3).

The Seahurst inshore studies have their basis in a sampling station of opportunity. Students at the Occupational Skills Centre marine facility, Highline School District, collected water samples for chlorophyll and nutrient analysis from the beach in front of the laboratory. Incident radiation data was collected with a pyroheliometer mounted on the roof of the lab, and zooplankton hauls were taken at a fixed point about 500 meters offshore.

Sediment traps were deployed at 47^{o} 27.9'N and 122^{o} 22.9'W, approximately half a mile from shore, south of Seahurst Park. The bathymetry of the Seahurst bight is so steep that this location presented the only flat spot

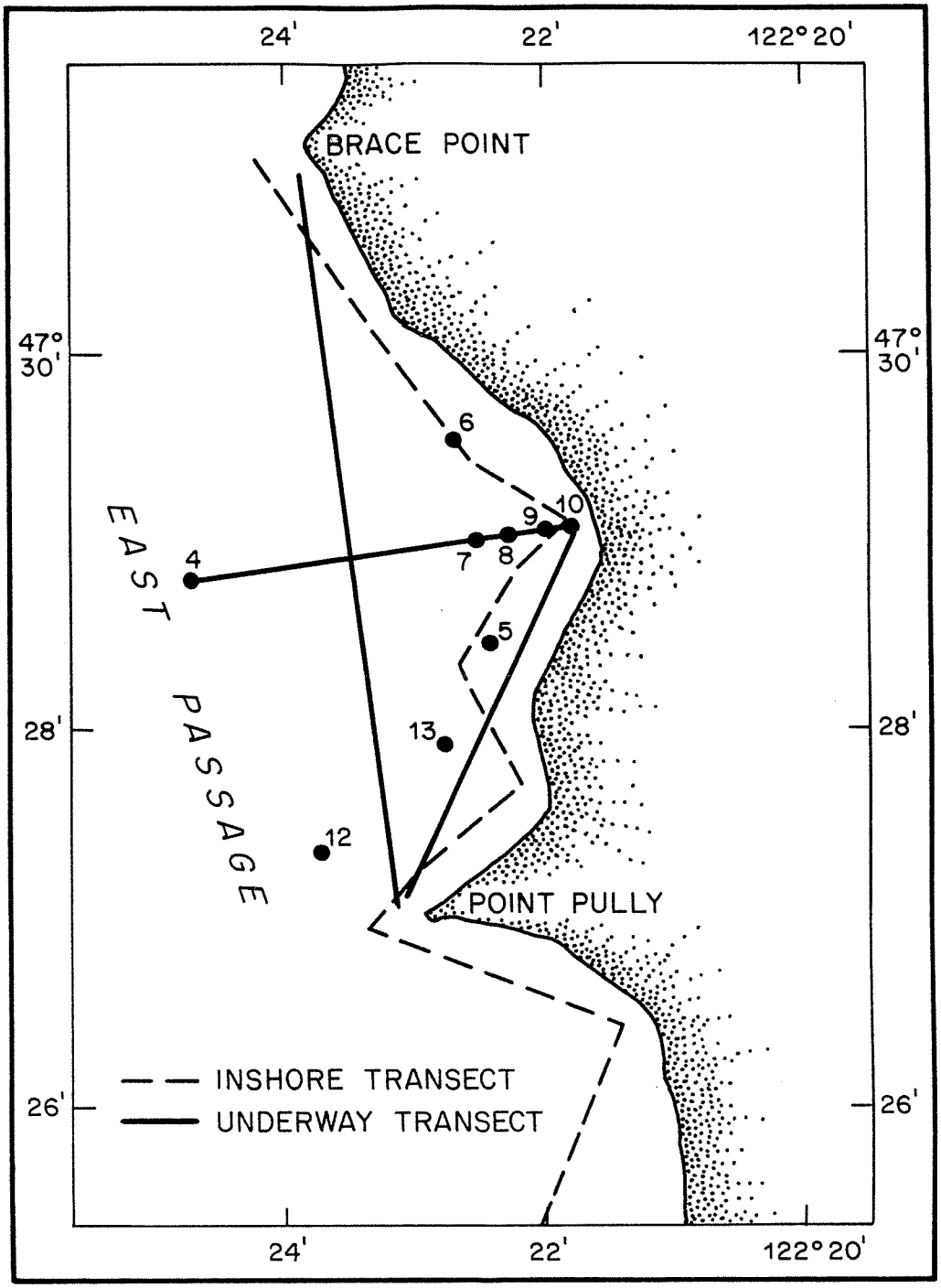

Figure 4.3. Location of stations in Seahurst Bight and positions of inshore and underway transects.

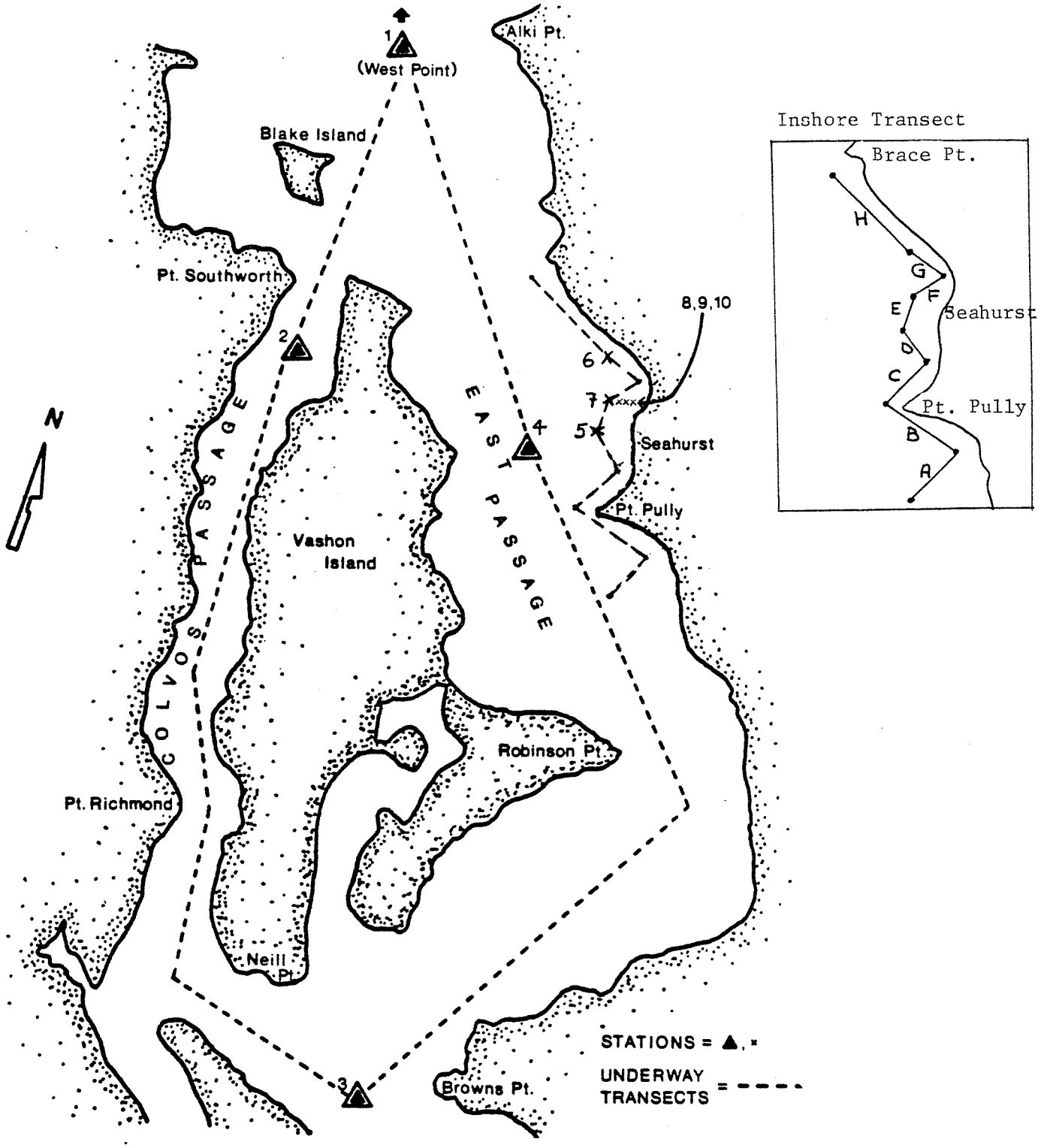

Figure 4.4. Main basin station locations and position of main basin underway cruise transect.

where it was possible to deploy a mooring close to shore in water approximately 65 meters deep.

4.3.2 Laboratory Program

4.3.2.1 Discrete Water Samples and CTD Calibration

Water samples were collected with a General Oceanics Rosette containing eleven 5-liter bottles. The Interocean CTD and rosette were mounted together in a frame containing a Martek transmissometer and a Licor quantum meter. One bottle was equipped with reversing thermometer racks. The depths sampled at each station are summarized in Table 4.2A. Temperature, conductivity, dissolved oxygen, light transmittance, irradiance and depth were measured on each cast. Calibration samples for temperature, salinity and dissolved oxygen were taken at intermediate and/or bottom sampling depths.

4.3.2.2 Temperature

Temperature was determined using duplicate reversing thermometers, provided with the rosette. The thermometers were read onboard, and the values adjusted by computer, based on periodic calibration checks for each thermometer performed at the School of Oceanography, Univ. Washington.

4.3.2.3 Salinity

Salinity samples were collected in standard salinity bottles and were analyzed on the University of Washington conductance salinometer. Each batch run was standardized using Copenhagen standard seawater.

Table 4.3 summarizes the type of samples which were analyzed from the sediment traps. Chlorophyll, phaeopigment, dry weight and CHN sampling was carried out as indicated for wide area discrete samples. Lead-210 samples were placed in pre-washed 2 liter jugs and returned to the University for analysis in order to calibrate the rate of sedimentation in the sediment traps versus that occurring on the sea floor. Samples for microscopic analysis were

Table 4.2A. Water bottle sampling depths for Phase II.
n = nutrient and chlorophyll analysis
P = phytoplankton species samples
c = carbon-14 uptake experiments
0 = oxygen and salinity calibration samples

z (m) \ St. no.	Wide Area			Discrete nearshore							Sample Totals
	1	2	3	4	5	6	7	8	9	10	
0	nP	n	n	nPc	n	n	nPc	n	n	nPc	
3	nP	n	n	nPc	n	n	nPc			nPc	
5	nP	n	n	nPc	n	n	nPc				
10	nP	n	n	nPc	n	n	nPc			nPo	
20	nPo	no	no	nPco	no	no	nPco		no		
50	n	n	n	n	n	n	n	no			
75	n	n	n	n	n	n	no				
100	n	no	n	n	no	no					
150	n		no	no							
200	no										
	10n 5p 2o	8n 2o	9n 2o	9n 5P 5c 2o	8n 2o	8n 2o	7n 5P 5c 2o	2n 1o	2n 1o	3n 3P 2c 1o	2076n 604P 550o 456c

preserved as phytoplankton species.

4.3.2.4 Dissolved Oxygen

Water was collected in Carpenter oxygen bottles, treated according to Carpenter (1964) and the samples kept cool and dark until analyzed by the School of Fisheries Water Quality Laboratory and by the Water Column group using the method of Carpenter (1964).

4.3.2.5 Nutrients

Nutrient samples were collected in acid-washed 250 ml plastic bottles and frozen immediately on board.

The nutrients nitrate, nitrite, ammonia, phosphate and silicate were analyzed as soon as possible after each cruise, and not later than one month. Analysis was performed by the routine chemistry laboratory of the School of Oceanography using the methods of Strickland and Parsons (1972). The instrument was standardized every 4 hours with standards made with low nutrient North Pacific seawater. Unknown standards were included with the analyses to maintain additional checks on the data quality.

4.3.2.6 Chlorophyll

Chlorophyll samples were collected at each depth. Up to 280 ml were filtered over glass fiber filters and analyzed by the fluorometric method of Strickland and Parsons (1972).

4.3.2.7 Zooplankton

Vertical net hauls were made according to the schedule shown in Table 4.2B. A 1/2 m 209 um Puget Sound closing net was used. Hauls were split with a Folsom splitter. One half was filtered for dry weight analysis and the other preserved with formalin for species analysis.

Zooplankton biomass estimates were obtained by dry weight analysis. One quarter to one half split from each zooplankton haul was filtered over a pre-

Table 4.2B. Schedule for zooplankton net hauls. Wide area stations (1-3) were sampled 27 times per year and near field stations (4-10) 38 times per year.

	Station No.								
	1	2	3	4	5	6	7	10	Total
No. of hauls	1	1	1	1	1	1	1	1	274
Volume analysis	1	1	1	1	1	1	1	1	274
Species identification	1	0	1	0	0	0	1	1	108
Archived	1	0	1	0	0	0	1	1	108

Table 4.3. Analysis of sediment trap samples.

Type	Reason	Analysis By
Chlorophyll and Phaeopigments	organic matter fallout and passage through zooplankton trophic level	Water Column Group
CHN	total organics	Water Column Group
Dry Weight	sedimentation rate of inorganic portion	Water Column Group
Microscopic Analysis	characterization of living/dead material	Water Column Group and/or Sediment Fingerprint Group
Lead-210	sedimentation rate	Chemistry Group

weighed glass-fiber filter. The filters were oven-dried on board and weighed again when completely dry to obtain a dry weight estimate (Lovegrove 1966).

Zooplankton species were identified and the dominant species counted. Dominant copepod species were further divided into life-stages. Quarterly, replicates were counted to determine error limits of the counting. Gayle Heron of the School of Oceanography carried out the analysis.

4.3.2.8 Phytoplankton

Phytoplankton species and cell volumes were determined with an inverted microscope using the methods of Lund et al. (1958) and Strathman (1967). Major species were identified and quarterly replicate samples were counted to determine error limits of counting. James Postel of the School of Oceanography carried out this analysis.

4.3.2.9 Primary Production

Primary productivity was determined by the C-14 uptake method as outlined in Strickland and Parsons (1972). Samples were taken from up to five light depths as determined by quantum meter traces, or secchi disc casts. The samples were incubated on deck using neutral density light filters, from local apparent non until sunset. Carbon-14 activity was measured using a Packard Tricarb Liquid Scintillation Spectrometer Model 3310. The data analysis was carried out by Willis Peterson of the School of Oceanography. Surface incident radiation was measured using a Licor quantum meter and integrator, throughout each incubation day.

4.3.2.10 Underway Sampling

The underway sampling system measured surface water properties using the sea water system onboard the R/V Liberty. Continuous measurement of ammonia and *in vivo* fluorescence followed that of Strickland and Parsons (1972). Temperature and salinity was measured using an Ocean Data Equipment

instrument. Chlorophyll was measured on a Sequoia-Turner Model 111 or 112 fluorometer with a flow-through sampling cell. Particle scattering was measured using a Monitek Model 31 continuous-flow nephelometer. All sensors are computer compatible and were monitored with an HP-41CV programmable calculator and interface loop, controlling a data acquisition system.

4.3.2.11 Seahurst

Chlorophyll and nutrient samples were collected daily beginning in June 1982, from the beach area off the marine laboratories at Seahurst Park. A clean bucket was used to take the sample and approximately 300 ml of water was filtered for chlorophyll analysis. Additional unfiltered water was frozen for nutrient analysis. All analyses was carried out at the University.

Vertical net hauls for zooplankton were taken several times a week beginning in October of 1982 at a fixed station off Seahurst Park. A 1/4 um mesh zooplankton net was towed from the bottom (approximately 11 meters) to the surface, and the samples preserved with formalin. Samples were analyzed for species identification, and distributional trends at weekly and seasonal intervals.

Physical oceanographic data was collected along four transects in the Seahurst Park area in order to investigate the existence of an onshore movement of bottom water, from October 1982 until January 1983. Sampling occurred at one week to one month intervals. The transects were perpendicular to the shoreline and consisted of four stations each, with bottom depths of approximately 3, 5, 7 and 10 meters, respectively (Figure 4.5). Conductivity, temperature and salinity were measured at one meter intervals from the bottom, using a Beckman RS5-3 Induction Salinometer.

4.3.2.12 Sediment Trap Studies

In November of 1982 and in March 1983, sediment trap arrays was deployed

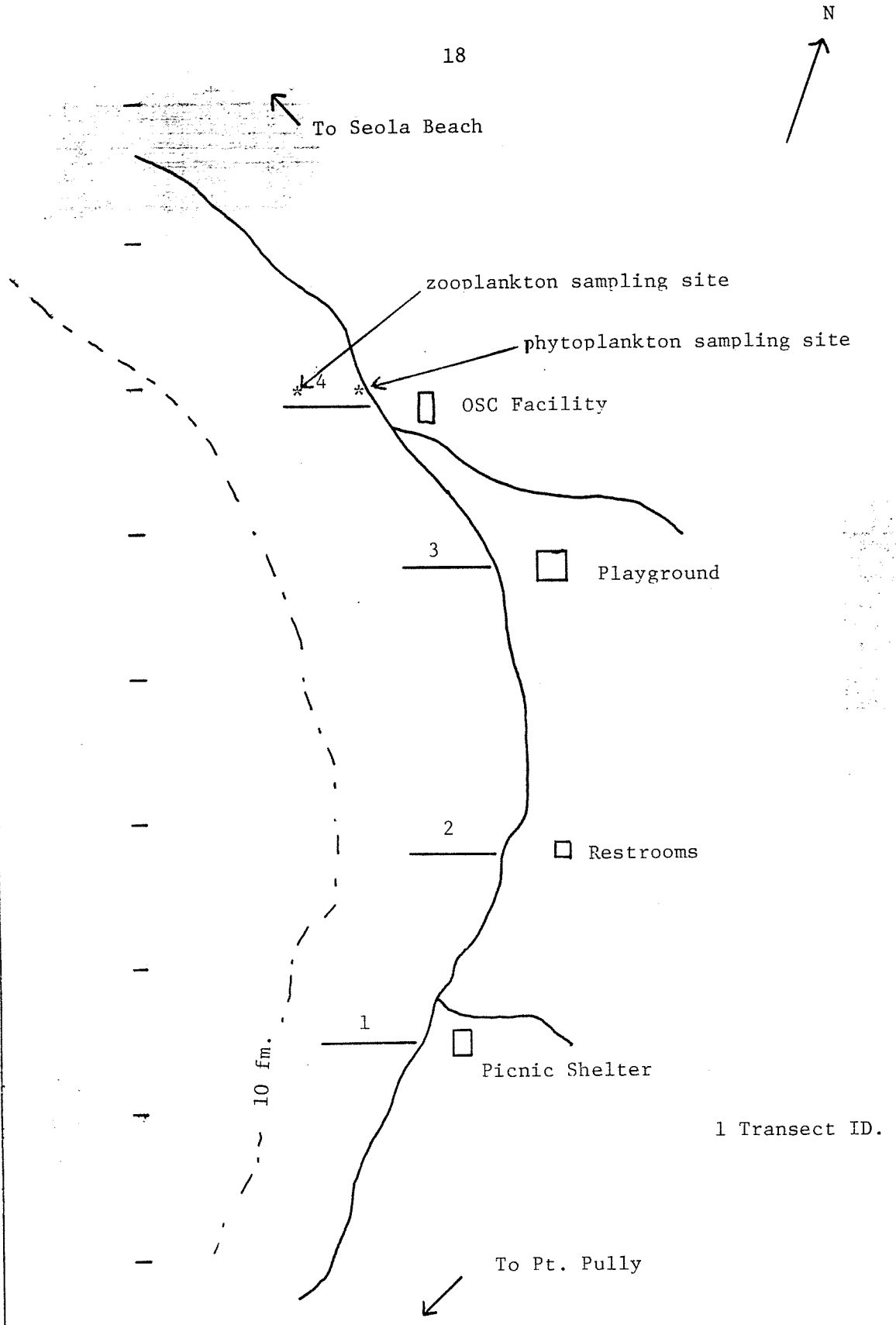

Figure 4.5. Positions of transects for study of onshore flow of bottom water in Seahurst Bight, including intertidal sampling site.

in the Seahurst area in order to examine sediment loading in the area and was to quantify the following:

1. Organic fallout from the water column.
2. Sedimentation of terrigenous material, and
3. Rate of incorporation of organic material into the sediments.

The array was deployed in approximately 65 m of water south of Seahurst Park. The array consisted of a pair of sediment traps placed below the photic zone which were closed electronically, after the design of Lorenzen et al. (1981). The mooring had subsurface flotation and was released by electronically-triggered explosive devices. Ground lines improved the chances of recovery. The University of Washington research vessel ONAR was used to deploy and recover the sediment trap arrays. The deployment site for the array was 47°17.9'N 122°22.9'W with the flotation at 10 m depth.

4.3.2.13 Quality Control

Quality control of data analysis was performed in five steps:

1. On-board cross-checks of sample numbers.

Each discrete sample taken on-board ship and from Seahurst and Indianola beaches was recorded on two separate log forms, to allow cross-checks for accuracy of sample identification. Underway transect data was checked by frequent time and location notations independent of the computerized system.

2. Duplicate sample analysis.

Duplicate oxygen, salinity, nutrient and chlorophyll samples were taken regularly and analyzed "blind" in order to check the precision of analyses. C-14 experimental results and temperature determinations were the result of two measurements at each depth. Results of duplicate oxygen analysis are seen in Table 4.4. Rejection levels for difference

Table 4.4. Duplicate Analysis of Dissolved Oxygen.

Sample No.	Date	Duplicate A (run by Water Column personnel) D.O. (ml/l)	Duplicate B (run by School of Oceanography lab.) D.O. (ml/l)	% Diff.
1	4/12/83	6.11	6.17	1.0
2	4/12/83	6.00	6.04	0.6
3	4/12/83	6.24	6.28	0.7
4	4/12/83	5.73	5.87	2.3
5	4/12/83	7.80	7.86	0.7
6	4/12/83	5.79	5.82	1.0
7	4/12/83	5.88	5.91	0.4
8	4/12/83	6.11	6.15	0.6
9	4/12/83	8.81	8.83	0.2
10	4/12/83	6.74	6.73	0.1
11	4/12/83	5.75	5.79	0.7
12	4/22/83	6.49	6.50	0.3
13	4/22/83	6.10	6.17	1.1
14	4/22/83	5.91	5.84	0.7
15	4/22/83	6.68	6.74	0.8
16	4/22/83	6.65	6.56	1.0
17	4/22/83	6.26	6.30	0.7

between duplicate samples differs with the type of sample, and is summarized in Table 4.5. Rejection levels have been calculated based on confidence limits of sampling and analysis procedures (Strickland and Parsons 1972).

3. Removal of outliers from the data set.

After analysis, data were reviewed and questionable values rechecked for sample identification accuracy. Unacceptable values were removed from the data set before going onto keypunch forms.

4. Computer entry of data.

Keypunching of data was carried out by experienced personnel of the water column group. Hardcopies of all data files were made after entry and all numbers were checked for accuracy.

5. Graphical check of the data.

Data files were plotted by computer and the results reviewed by trained personnel in order to establish trends in the data and to act as an additional screening process for outliers and unlikely trends. Cross-checks to original data forms resulted from errors spotted at this stage. This step provided an important check on the underway data points which were handled by computer up to this point.

4.3.3 Underway Data Analysis

Data acquisition of (all) underway instruments was controlled by a Hewlett-Packard system and monitors each channel every 13 seconds which recorded the data on a mini data cassette. The data was transferred to a Hewlett-Packard model 87 microcomputer and stored on 5-1/4" disc.

Chlorophyll a and ammonia channels were calibrated on each cruise. Turbidity calibrations were performed periodically in the laboratory and temperature and salinity calibrations were checked against field samples. All

Table 4.5. Rejection levels for differences between duplicates.

Sample type	Rejection level (% difference)	Means of correction
Oxygen	1.5	Eliminate from data set check for systematic error
Salinity	2.0	Eliminate from data set
Temperature	0.5	Eliminate from data set change thermometers
Chlorophyll	7.0	Use more reasonable value (trend analysis) if one exists
Nutrient	5.0	Use more reasonable value
C-14	7.0	Use more reasonable value

All calibrations were applied to raw data on the microcomputer. Plots of concentration versus distance were constructed to check for instrument error. The information was stored on flexible disc, resulting in one calibrated and one uncalibrated copy of the data.

To determine the effect of Commencement Bay water in East Passage, underway surface mapping was carried out from Shilshole Bay, south through East Passage, and around Vashon Island (Figure 4.4) from July 1982 to March 1984. Cruises occurred once every two weeks during the growing seasons of 1982 and 1983, and once every three weeks during the winters of 1982-1983 and 1983-1984.

Data collected between Point Pully and station 3 in East Passage was examined in detail to:

1. characterize Commencement Bay water in terms of temperature, salinity, turbidity, chlorophyll and ammonia.
2. examine the relative importance of the forces which determine the amount of Commencement Bay water in East Passage.

4.3.4 Statistical Methods and Models

4.3.4.1 Probability Distributions

The probability models decribe the chance of observing specified levels of nutrients and plankton on a seasonal basis. The parameters of the models are related to ecological variables.

In a specified interval of time the probability of property y having a value greater than y_0 and less than y_1 is expressed:

$$P(y_0 < y < y_1) = \int_{y_2}^{y_1} p(x)dx \qquad (1)$$

where p(x) is the probability density function (pdf) that models the dynamics controlling the distribution of y over time. The meaning of eq(1) is graphically represented in Figure 4.6 depicting the pdf as a function of y. The total area under the pdf is equal to 1 and the area of the shaded area is equal to the probability that y will fall within the range y_0 and y_1. With y_1 equal to infinity the area represents the probability that y will be greater than y_0.

Probability density functions are developed using stochastic calculus. First, the rate of change of a property x in a fluctuating system is modeled with a stochastic differential equation (SDE)

$$dx/dt = h(x) + f\ e(x)\ i(t) \qquad (2)$$

where i(t) is a stochastic or random input to the process, e(x) describes the effect of x on the input, f is the intensity of the input, and h(x) describes the rate of change of x in the absence of the stochastic input. Using Ito calculus, (Nisbet and Gurney 1982) the mean rate and variance in the change of the probability of the population are defined

$$m(x) = h(x)$$

$$v(x) = [fe(x)]^2 \qquad (3)$$

Where m(x) is the mean rate of change of the probability of the population and v(x) is the variance in the change of the probability of the population.

Using a Fokker-Planck equation, the rate of change in the pdf over time and x is described by the equation

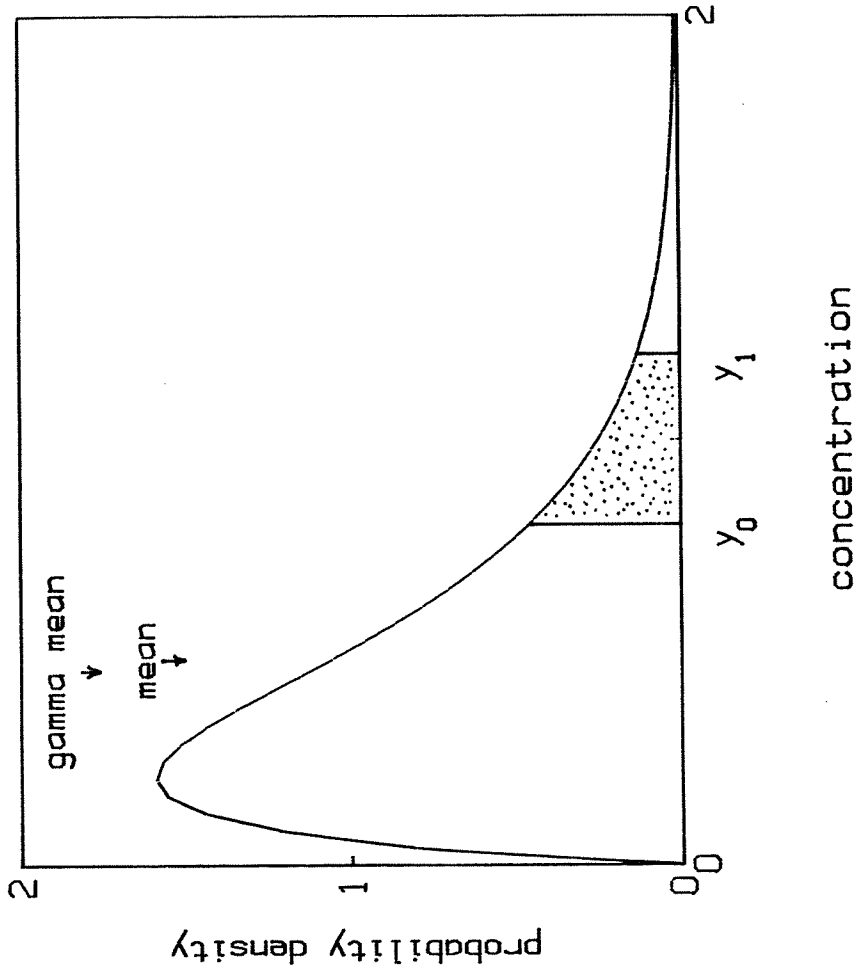

Figure 4.6. Illustration of gamma probability density function with location of gamma mean and arithmatic mean. Ratio of the shaded area to the total area under the curve gives the probability of a observing a concentration between yo and yl.

$$\partial p(x)/\partial t = - \partial[m(x)p(x)]/\partial x + (1/2)\partial^2 [v(x)p(x)]/\partial x^2 \qquad (4)$$

These equations are useful in making primitive statistical models of biological systems. The deterministic behavior can be represented by the dynamic equation dx/dt = h(x) and the remaining unknown fluctuations can be approximated by f e(x) i(t) where i(t) is a white noise function. The process converts the deterministic dynamic equation, which describes x as a function of time, to a stochastic dynamic equation, which describes the probability of x as a function of time and the level of x.

The time resolution of probability distributions are often mathematically complex but over intermediate time intervals (long compared to the scale of the random processes but short compared to seasonal variations), the pdf can be assumed to be at equilibrium. In this intermediate scale the process approaches stochastic equilibrium where x changes with time but the pdf is constant. The pdf at stochastic equilibrium is simply defined

$$P(x) = \frac{C}{v(x)} \int \exp[2 \quad m(x)/v(x)\ dx] \qquad (5)$$

where C is a constant of integration that scales the pdf to a unit area.

4.3.4.2 Phytoplankton Model

The pdf for phytoplankton is based on a model in which growth is limited by light through self-shading over the water column and loss is controlled by a combination of grazing and sinking of cells (Ebbesmeyer, Okubo, Anderson, and Conquest, in preparation). The model yields a SDE based on the logistic growth equation

$$dx/dt = rx(1-x/K) + f \times i(t) \qquad (6)$$

where x is the phytoplankton concentration integrated over the photic zone, r is the net growth rate, K is the carrying capacity of the deterministic process, i(t) is the white noise representation of the random process and f is the intensity of the random processes.

The net growth rate is defined as $r = gI - l$ where g is a growth rate coefficient per unit light intensity, I is the average light intensity over the photic zone in the absence of chlorphyll, and l is the average loss rate of phytoplankton over the photic zone from sinking and zooplankton grazing. Light intensity is defined as $I = I_0 e^{-kz}$ where k is the extinction coefficient of water, I_0 is the incident surface radiation, and x* is an integration depth.

The carrying capacity is $K = (l - 1/gI)/m$ where m is the extinction coefficient for the absorption of light per unit chlorophyll. This phytoplankton carrying capacity is defined in terms of a balance between a grazing rate and growth rate proportional to the average light intensity in the water column. K will increase with surface light intensity and the growth coefficient, and will decrease with zooplankton abundance and the loading of river borne silt in the water column.

Equation (6) is a specific form of eq(2), so the rate of change of the mean and variance can be written according to eq(3). To solve for the steady state pdf eq(4) is set equal to zero. The boundary conditions are such that no probability flows from the interval $0 < x < \infty$ and the resulting solution of eq(4) is the gamma probability density function which has the form

$$P(x) = \frac{(x/a)^{b-1}}{a\,\Gamma(b)} \exp(-x/a) \qquad (7)$$

where $\Gamma(b)$ is the gamma function, and a and b are the scale and shape parameters of the gamma pdf. They are related to the logistic SDE by

$$a = K\ R$$
$$b = 2/R \qquad (8)$$

where $R = (f\hat{}2)/r$ is a randomness coefficient, or rate variability coefficient, that describes the intensity of the random process to the deterministic process.

The gamma pdf is positively skewed with the modal value below the carrying capacity and mean value (Figure 4.6). The relationship between these equations is given by the following equations (Goel and Richter-Dyn 1974, p. 131-143):

$$\text{mean} = M = K$$
$$\text{variance} = V = R\ K\ /2 \qquad (9)$$
$$\text{mode} = Xm = K(1 - R)$$

4.3.4.3 Zooplankton Model

Histograms of zooplankton net catch exhibit skewed distributions that are characteristic of population data as described in Anderson (Appendix 4.A). On theoretical grounds Anderson and Okubo (1984, Appendix 4.B) demonstrated that net catch is expected to have a gamma type distribution and an underlying dynamic equation that takes the form of a stochastic logistic equation. The equation can be expressed

$$dx/dt = ax - mx^2 + f \times i(t) \qquad (10)$$

where x is the rate of change of catch in a net, (a) describes the rate at which aggregations of zooplankton break up and (m) is an aggregation term that is a function of zooplankton total population and the dynamics by which zooplankton aggregations form. The term f x i(t) is the stochastic rate process and is formulated as in the phytoplankton equation. A draft of this work is given in Appendix 4.A. Several forms of m are possible. In the most reasonable form the mean value and variance of the catch are defined in term of the zooplankton dynamics by the relations

$$\text{mean} = M = Z\ V\ a'/(b'\ A1)$$
$$\text{variance} = V = M^2\ \ f^2/2a' \qquad (11)$$

where Z is the zooplankton abundance per unit volume of habitat, a' is the swarm split rate, b' is the swarm merge rate, A1 is the cross-sectional area of swarms encountered by the net, and f is the intensity of the random processes from swarming and variations in the zooplankton growth dynamics.

To estimate the mean zooplankton abundance per unit volume of habitat the swarm factors a', b', and A1 are required. These parameters are simply not known, so all estimates of zooplankton abundance are relative. The situation is even more tenuous since the swarm factors may change from season to season, and year to year. In virtually every zooplankton study using net data to estimate the abundances over the seasons it is assumed the swarm factors are invariant and that the major change in seasonal data is from changes in population Z. On intuitive grounds Z should be the major factor that alters catch but the changes in the nature of swarming from season to season and year to year may also be of importance.

4.3.4.4 Nutrient Model

For nutrients in stochastic equilibrium the input of the nutrient into a layer is balanced by loss due to diffusion and uptake. A stochastic dynamic equation with these features can be expressed

$$dx/dt = u - vx + f\ i(t) \qquad (12)$$

The deterministic input rate is $u = wx_o - rB$, where x_0 is the concentration of the input, w is the rate coefficient of the physical input of x, and r is the concentration independent biological uptake of x and B is the plankton biomass. The term v is the deterministic loss rate $v = w - q$, where q is the concentration dependent uptake rate. The term f scales the intensity of the fluctuating rate and is assumed to be independent of concentration.

Equation (12) has the form of eq(2) so the rate of change of the mean and variance from eq(3) are $m(x) = u - vx$ and $v(x) = f^2$. Solving eq(5) with the boundary conditions that no probability flows from the interval $0 < x < oo$. The steady state pdf for eq(12) is a gaussign pdf where

$$P(x) = C_1 \exp[-\frac{v}{f^2}(x-\frac{u}{v})^2] \qquad (13)$$

where C_1 is a constant making the integrated probability equal to one. The mean, variance and mode are

mean $M = u/v$

variance $V = 2 f^2/v$ (14)

mode $Xm = M$

See Appendix 4.C for a complete development of the nutrient model.

4.3.4.5 Model Parameters

The scale and shape parameters of the gamma distribution, a and b are required to estimate statistical properties of the models. The parameters can be estimated by the method of matching moments and by an optimal unbiased inference procedure. In the method of matching moments the parameters are estimated from the arithmetic mean M and the variance V by the equations

scale parameter $a = V/M$

(15)

shape parameter $b = (M\hat{}2)/V$

This method is sensitive to extreme values in the data set and does not provide reliable estimates of the parameters.

A more powerful estimator that centers about the mode of the distribution and also provides two-sided confidence intervals for the parameters is based on an optimal unbiased inference procedure by Engelhardt and Bain (1978). This method is used in this report to estimate the parameters and the 90% two-sided confidence intervals about the best estimates.

The carrying capacity and randomness coefficient for integrated phytoplankton observations are obtained from the scale and shape parameters by the following equations

$K = ab$

$$R = 2/b \tag{16}$$

The zooplankton population estimate and variance of eq(11) are

$$M = ab$$
$$V = a\ 2\hat{}b \tag{17}$$

The mean M and variance of nutrient distributions (see eq(14)) are estimated normal statistics.

A third method to estimate model statistics is through log transformation (Anderson in review Appendix 4.A). For the phytoplankton model the carrying capacity and randomness coefficient can be defined

$$K = \exp\ (E[\ell n(x)]) \tag{18}$$
$$R = 2\ Var[\ell n(x)]$$

The mean and variance of the zooplankton and zooplankton observations can be estimated from the log transformations by the equations

$$M = \exp\ (E[\ell n(x)]) \tag{19}$$
$$V = M\ Var[\ell n(x)]$$

The estimations of the mean and variance by eq(17) and eq(19) differ from the

arithmatic mean and variance in that the estimates are not as sensitive to extreme values in the data. In the analysis of the water column data statistical parameters are obtained from the gamma statistics where the shape and scale parameters are estimated by the optimal unbiased inference procedures.

Two sided 90% confidence intervals on the scale and shape parameters, a and b, are determined by optimal unbiased inference procedures of Englhardt and Bain (1978). The two sided 90% confidence intervals about the mean values and K are determined by the approximation method of Grice and Bain (1980).

The upper and lower 90% confidence limits of R are determined from the upper and lower estimates of the shape parameter according to

$$Ru = 2/bl \qquad (20a)$$

$$Rl = 2/bu \qquad (20b)$$

4.3.4.6 Data Grouping

To estimate the gamma parameters for the data sets over intervals of time and space requires that the data is in stochastic equilibrium over the interval. Specifically this requires that the carrying capacity K, intrinsic growth rate r, the input rate u, the loss rate v, and the randomness scaling factors f are constant over the interval. Then the variability of a property is assumed to be caused by random processes and the property is in stochastic equilibrium. Data groups with station number, data and number of points are given in Table 4.6.

The assumption that a property is in stochastic equilibrium can be assessed by the rate of change of the deterministic rate term over the interval. If the deterministic rate term is near zero over an interval, then

the assumption of a stochastic equilibrium is supported. The rates of change of properties over intervals are determined by smoothing algorithms (section 4.3.4.8 and 4.3.4.9). The data from the Seahurst Intertidal, which is the largest data set, has been used to support the choice of the data temporal groupings in the Seahurst Bight and the main basin data sets. Gradients of chlorophyll and nitrate over time are shown in Figures 4.7.3.1 and 4.7.3.2. The average gradients of chlorophyll and nitrate for each interval are given in Table 4.6. Assumptions of stochastic equilibrium are best for winter and summer periods.

The criterion for spatial uniformity in the data groupings is the absence of high or low trends over time for any station in the group. To test for this criterion a Kruskal-Wallis analysis of variance by ranks was performed (Zar 1974). On the basis of this test, stations 4, 5, 6, 7, 12, and 13 were grouped as Seahurst Bight stations and stations 1, 2, 3, and 4 were grouped as Puget Sound stations.

4.3.4.7 Smoothing Algorithms

Observations of nutrients and plankton collected over time exhibit a combination of random and deterministic (non-random) patterns. The most predominant pattern is the seasonal cycle associated with the winter to summer cycle of changing day length and light intensity. The second dominant light pattern is the 24 hour diel cycle. The nutrients and plankton are affected by currents on a 12 hour interval due to the tidal cycle and on a 28 day interval of spring and neap tides that determine the maximum and minimum daily tidal heights. Superimposed on these regular cycles are a number of patterns that approximate cycles but are largely random. The most dominant of these random patterns is the variation of light intensity associated with the passage of weather fronts through the Puget Sound area. The mode of the time interval

Table 4.6. Data groupings. Pigment and nutrients = Chl, phytoplankton species = Ps, zooplankton species = Zs, primary productivity = PP, chlorophyll rate (mg/m^3/d) = Chl', nitrate rate (mg-at/m^3/day) = NO3', Seahurst intertidal group = It. Stations 4, 5, 6, 7, 12, and 13 grouped as Seahurst Bight stations. Main basin stations 1, 2, 3 and 4 grouped separately.

Seahurst Bight Stations			Data points						Average rate	
Interval	Dates	Days	Chl	Ps	Zs	Zw	PP	It	Chl'	NO3'
Summer solstice 1982	6/2/82 7/15/82	43	15		9			15		0.15
Autumnal equinox 1982	8/30/82 10/11/82	42	48	19	24	21	12	30	-0.05	0.1
Winter solstice 1983	12/06/82 1/17/83	42	21	9	12	19		31	0.0	0.04
Vernal equinox 1983	2/28/83 4/11/83	42	42	19	24	32	12	31	0.6	-0.22
Summer solstice 1983	6/2/83 7/11/83	39	49	14	23	22	14	19	-.03	0.07
Autumnal equinox 1983	8/31/83 10/11/83	41	42	7	15	30	14	31	-0.06	0.1
Winter solstice 1984	11/22/83 1/3/84	42	18		6	15	6	11	0.02	0.08

Seahurst Bight Probability Dist.			Data points			NO3 data		
Interval	Dates	Days	Chl	PP	NH3	Dates	Days	Points
Summer season 1982	6/21/82 9/21/82	92	43	22	38	6/1/82 6/7/82	5	6
Winter season 1983	12/06/82 2/28/83	84	19	6	18	1/18/83 2/28/83	22	11
Summer season 1983	6/21/83 9/21/83	92	57	26	57	6/02/83 6/21/83	18	16
Winter season 1984	12/21/83 3/11/84	80	15	6	15	1/3/84 2/14/84	42	10

Table 4.6 (continued).

Main Basin Stations			Data points		
Interval	Dates	Days	Chl	Zs	Zw
Summer season 1982	6/15/82 9/22/82	69	6	6	6
Winter season 1983	11/15/82 3/1/83	106	6	6	6
Summer season 1983	6/21/83 9/7/83	72	6	6	6
Winter season 1984	12/6/83 1/21/84	105	5	6	6

between the passage of these weather fronts is about 10 days. The ecosystem itself may randomly oscillate with frequencies determined by the turnover time and development time of the major components. Significant frequencies are determined by the phytoplankton doubling time, which is on the order of days, and the zooplankton development time, which is on the order of a week to a month. The spatial pattern of nutrients and plankton also contributes to the variability of properties as measured over time at fixed stations. The spatial patterns of nutrients, phytoplankton and zooplankton are different with zooplankton exhibiting the smallest scales, due to swarming aggregation, and nutrients the largest scales.

The interactions of these meteorological, tidal, ecosystem and spatial processes with different spatial and temporal scales produce differring temporal patterns for nutrients, phytoplankton and zooplankton. In general the seasonal cycle has a well defined effect on nutrients and plankton but the combination of regular and random processes with intervals of days to weeks produce complex and essentially random variations of the properties on time scales less than the seasonal scale. The purpose of the smoothing algorithms is to separate the regular seasonal patterns of the properties from the essentially random patterns with periods of days to weeks. Smoothing algorithms provide estimates of the property values and the rate of change of the properties as a function of time. Different algorithms are required for nutrients and plankton.

4.3.4.8 Nutrient Smoothing

For nutrients and other properties where the rate of change is independent of its concentration, smoothing is based on the Weiner process model where the rate of change of property x with time t can be written

$$dx/dt = r + f\ i(t) \qquad (21)$$

where r is the deterministic rate of change of x, and f i(t) models the random rate of change of x. This random, or stochastic term, is a crude approximation of the random and quasi-random meteorological, ecosystem and spatial processes. The term i(t) is a white noise function that rapidly fluctuates about a zero mean value and has a variance of one. The intensity of the fluctuations are scaled by f.

Equation (21) is an approximation to the more realistic rate equation defined by eq(12) section 4.3.4.4. The assumption of a constant rate r in eq(21) is justified on the grounds that the smoothing algorithm is applied over small intervals of time so that, over an interval, the changes in the deterministic rate are small.

The probability of observing x at a time t given the value of x_0 at time t = 0, with x unrestricted over the range $-\infty < x < \infty$, the pdf is given by (Goel and Richter-Dyn 1974)

$$P(x:x_0,t) = (1/\sqrt{2\pi v(t)})\ \exp[-(x-x_0 - rt)^2 / 2v(t)] \qquad (22a)$$

where the variance is

$$v(t) = f^2\ t \qquad (22b)$$

To smooth a time series one must assume that, over the time interval T, the rate r is constant and x changes according to eq(21). The parameters x_0 and r can be estimated over the interval T using a least squares regression of x vs. t defined by the equation

$$x = a_0 - a_1 t' \qquad (23)$$

where t' is the relative time coordinate defined $t' = t - t_0$, t_0 is the center point of the interval and a_0 is the x value at $t' = 0$ and a_1 is the slope r at $t' = 0$. The least squares regression is carried out by the method of maximum likelihood where the probability distribution of x about the actual distribution is defined by eq(22) with the relative time coordinate t'. The regression is made over the relative coordinate system interval $-T/2 < t' < T/2$.

The variance of the regression is defined by the equation

$$V(t) = vx + f\ 2\ |t'| \qquad (24)$$

where vx is the variance that is constant over time and f 2 t' is the weighted variance associated with the time dependent Weiner process according to eq(22b). The time independent variance is principally the result of the advection of spatial patterns past the sampling location. In effect, with time dependent and time independent components of the variance, the smoothing is weighted by a single parameter T_e, which is the time required for the time independent variance to equal the time dependent variance. This parameter is designated the eigen time and is defined

$$T_e = vx/f\hat{}2 \qquad (25)$$

and the normalized variance becomes

$$V_i = T_e + t' \qquad (26)$$

The regression coefficients a_0 and a_1 are obtained by the equations

$$a_0 = (1/D)(\Sigma^2 t_i /V_i \quad \Sigma xi/V_i \; - \; \Sigma t/V_i \quad \Sigma t_i \; xi/V_i)$$

$$a_1 = (1/D)(\Sigma 1/V_i \quad \Sigma t_i \; xi/V_i \; - \; \Sigma t_i/V_i \quad \Sigma xi/V_i) \qquad (27)$$

$$D = \quad 1/V_i \quad \Sigma t_i{}^2 /V_i - (\Sigma \; t_i{}^2 /V_i)^2$$

where x_i is the x value relative time t_i, and V_i is the normalized variance according to eq(26).

4.3.4.9 Plankton Smoothing

For phytoplankton, zooplankton and other properties where the rate of change over time is dependent on the value of the property, the smoothing algorithm is based on the Ornstein-Uhlenbeck process where the rate of change of the property x over time t is

$$dx/dt \; = \; rxG(x/K) \; + \; fx \; i(t) \qquad (28)$$

The deterministic rate is modeled by an intrinsic growth rate r and a saturation term G(x/K) that describes how the rate approaches zero about population equilibrium value or carrying capacity K. The random processes are modeled by the second term that includes the white noise term i(t) with intensity f. About the carrying capacity the saturation term can be approximated by a log function (Anderson in review, Appendix 4.A). Since $(1/x)(dx/dt) = d\ell n(x)/dt$ the dynamic equation describing the process can be written

$$dy/dt = - ry + f \; i(t) \qquad (29)$$

where

$$y = \ln(x/K) = - G(x/K) \tag{30}$$

The pdf of y can be determined from a Fokker-Planck eq(4). For the boundary conditions -oo < y < oo the probability of the process having the value y at time t when its value was y_0 at t = 0 is

$$P(y:y_0,t) = \frac{\exp[-(y - m(t))^2 / 2v(t)]}{\sqrt{2 \pi v(t)}} \tag{31a}$$

where the growth of the mean value over time is

$$m(t) = y_0 \exp(-rt) \tag{31b}$$

and the growth of the variance is

$$v(t) = (f^2 /2r) (1 - \exp(-2rt)) \tag{31c}$$

To develop a maximum likelihood regression according to the probability distribution of eq(31) note yo = $\ln(x_0/K)$ and with eq(30) and (31b) the regression equation is

$$\ln(x) = \ln(K) - \ln(x/K) \exp(-rt) \tag{32}$$

The exponent term must be expressed as a series using

$$\exp(z) = 1 + z + z^2/2! + z^3/3!.... \tag{33}$$

and the regression equation becomes

$$\ln(x) = \ln(x_0) - \ln(x_0/K)\, rt + \ln(x_0/K)(rt)^2/2! + \ldots \quad (34)$$

The series is truncated at the first power giving

$$\ln(x) = \ln(x_0) - \ln(x_0/K)\, rt \quad (35)$$

This amounts to a linear regression of the form

$$x' = a_0 + a_1 t' \quad (36)$$

where t' is the relative time coordinate $t' = t - t_0$, $x' = \ln(x)$, the intercept at $t' = 0$ is $a_0 = \ln(x_0)$ and $a_1 = r \ln(x_0/K)$ is the slope. The smoothing algorithm again is defined over the moving interval T where

$$-T/2 + t_0 < t < t_0 + T/2 \quad (37)$$

The variance of the regression is divided into time independent and time dependent parts as

$$V(t) = vx + (f^2/2r)(1 - \exp(-2r\, t)) \quad (38)$$

where vx is a measure of the time independent variance and the time dependent variance is defined by the Ornstein-Uhlenbeck process by eq(31c). Equation (38) weights the smoothing algorithm. When the sampling interval is greater

than 1/r the weighting is dependent on a single parameter: the ratio of the time independent and time dependent variances as

$$W = vx/(r/f^2) \tag{39}$$

and the normalized variance is

$$V_i = W + (1 - \exp(-2rt))/2 \tag{40}$$

When $W >> 1$, the algorithm fits a smooth line through a series of data. When $W < 1$, the algorithm gives more weight to points near the relative center point ($t' = 0$) and the algorithm tends to run closer to the data points and the resulting fit is less smooth.

The regression coefficients a_0 and a_1 are given by eq(27) where $x_i = \ln(x)$, V_i is given by eq(4) and t_i is the relative time t.

The smooth value and the smooth temporal gradient for the plankton algorithm are

$$x_0 = \exp(a_0)$$
$$dx/dt = a_1 \exp(a_0) \tag{41}$$

4.3.4.10 Variability

The variability of the observations can be divided into four parts: yearly, seasonal, spatial and temporal. The yearly variability consists of the changes in the seasonal cycles from year to year which are quantified through comparisons of gamma statistics at the equinoxes and solstices of the

years. The seasonal variability consists of the cyclic pattern of changes in the properties with season and is determined with the smoothing algorithm described in sections 4.3.4.7 to 4.3.4.9. The spatial variation consists of variation between stations collected over a short interval of time (1 day). The temporal variation is defined in terms of the difference between observations and the seasonal pattern obtained from the smoothing algorithms.

The spatial variability is a combination of temporal variability on scales smaller than the time required to sample all stations plus random and structured spatial patterns. The temporal variability includes the spatial variability and temporal variations with periods that are small compared to the 75 day interval of the smoothing algorithm. Thus the temporal variability includes variations that have random or regular cycles of a month or less.

The spatial and temporal variability of a property can be characterized over all seasons in terms of relative deviations from a point estimator. The relative spatial variability of an observation is defined.

$$Vs = (x - E[x])/E[x] \tag{42}$$

where the point estimator E[x] is the arithmetic mean value of property x at a group of stations collected on the same day. The relative temporal variability of an observation is defined

$$Vt = (x-X)/X \tag{43}$$

where the point estimator X is the seasonally smoothed value obtained by the smoothing algorithm.

The measures Vs and Vt are random variables with weak seasonal

correlations. Histograms of Vs and Vt over a year are essentially normally distributed with zero mean values. The mean of Vs is identically zero because the daily mean of the relative measures is identically zero. For plankton, the mean value of Vt is slightly positive since the regression of data points is performed on a log transform of the data. For nutrients, where X is obtained from a normal smoothing algorithm, the mean is near zero. Plankton variations tend to be proportional to the mean value, so the relative variations, normalized by the point estimators, are weakly correlated with season.

4.4 Results

The results are presented in six sections covering the Seahurst Bight, the main basin, the Seahurst intertidal zone, freshwater sources, sediment trap studies, and onshore flow of bottom water. Temporal patterns are illustrated in plots of properties vs. Julian days referenced to January 1, 1982. Properties are presented in three ways: discrete depth values, depth integrated values and depth integrated average values. For zooplankton the depth integrated values are the total abundance obtained from a bottom to surface net haul and the integrated average is the integrated abundance divided by the volume of water filtered. For phytoplankton primary productivity, chlorophyll and phaeopigment, integrated values represent the water column from the surface to the 1% light depth and the integrated average is the integrated value divided by the 1% light depth times a unit area. Phytoplankton species counts were from water samples collected at the 50% light depth. Unless otherwise noted, nutrients are represented as integrated average values using the same procedure that was to obtain the phytoplankton integrated averages. When noted, nutrient values from specific depth layers

are presented.

The seasonal trends of the data sets are shown as smooth lines through the temporal plots. These lines are calculated according to the smoothing algorithms described in Sections 4.3.4.7 to 4.3.4.9. A smoothing time interval of 75 days is used for all seasonal distributions unless otherwise noted and the eigen time Te = 15 days. The doubling time for phytoplankton is Td = 3 days and Td = 10 days for zooplankton. The smooth lines are insensitive to the choice of Te and Td with the 75 day smoothing interval.

The similarity of a property from station to station was quantified using the Kruskal-Wallis nonparametric test. The differences and similarities between stations are qualitatively illustrated with trumpet diagrams.

The differences between seasons are illustrated by grouping stations within 6 week periods about the solstice and equinox dates. These intervals were selected to represent times when properties were near steady state. The statistics of the 6 week groups are presented in terms of gamma mean values. The interval dates and number of data points for each property are given in Table 4.6. The models on which the gamma statistics are based are developed in Sections 4.3.4.2 to 4.3.4.5.

The variability of properties about spatial averages and seasonal trends are presented in tables of relative spatial and temporal variability. The theory of these measures is developed in Section 4.3.4.10.

The probability distributions of selected properties are presented as histograms with the gamma probability distributions fit as described in section 4.3.4.1.

4.4.1 Seahurst Bight

4.4.1.1 Physical and Meteorological

Daily sunlight intensities, measured in einsteins/m^2/day, varied over the

year by a factor of 30 with minimum values near 1 and maximum values near 35. The passage of weather fronts caused daily sunlight intensity to change by up to 15 einsteins/m^2/day (Figure 4.7). Weather fronts in 1982 and 1983 occurred at approximately two week intervals and lasted for several days.

The upper layer stratification, as measured by the density difference between the surface and 25 m, followed the seasonal pattern of light (Figure 4.8).

The temperature in the surface water varied between 14.5°C in the summer and 8°C in the winter. The deep water temperature varied with a seasonal cycle between 8 and 12°C (Figure 4.9). In 1983 the water column temperatures on a given day were 1°C higher than in 1982. This warming is attributed to the El Nino, the global weather anomaly in 1983.

The depth of the photic zone (Figure 4.10) is defined by the 1% light depth. The photic zone minimum occurred near the summer solstice in 1982 and 1983 and the maximum depth occurred near the autunmal equinox.

The turbidity data is a measure of the amount of silt in the water column. Surface values of turbidity had a seasonal distribution (Figure 4.11).

4.4.1.2 Phytoplankton

The growth of phytoplankton in Puget Sound is principally controlled by the in situ light intensity available to cells for photosynthesis. The level of surface solar radiation is the principal factor determining the in situ level of sunlight. Of secondary importance is the depth to which cells are mixed, and the particulate content of the water. Nutrients, which are required for growth, are generally present in high concentrations in the water column and do not limit cell growth in Puget Sound.

The rate of primary productivity measured as carbon uptake per 1/2 day

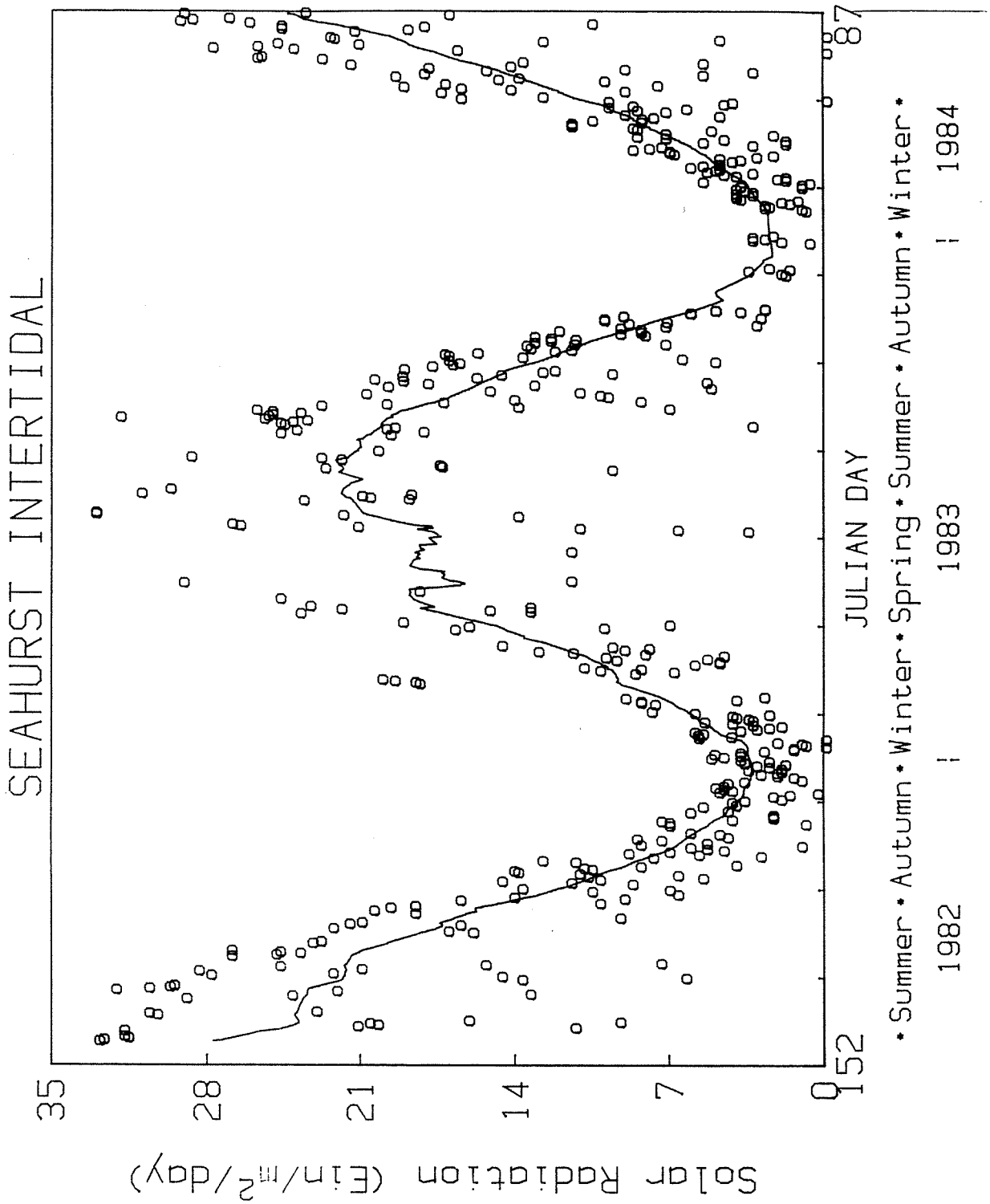

Figure 4.7. Solar radiation at Seahurst. Time axis in consecutive Julian days since Jan. 1 1982. Solstice and equinox points demarked by stars on the time axis. Tick marks every 60 days. Line through data fit with smoothing algorithm. See text for details.

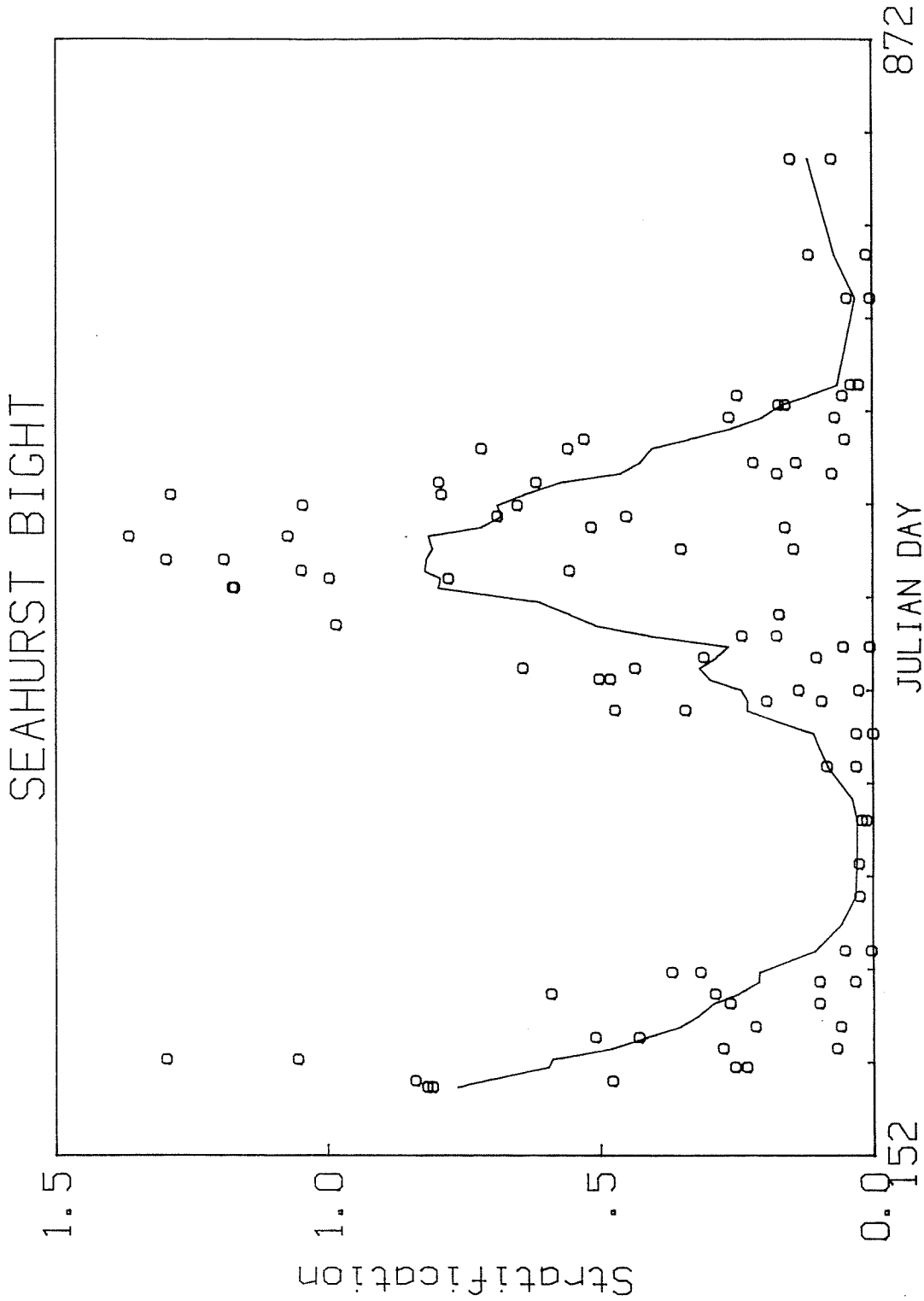

Figure 4.8. Stratification for Seahurst Bight stations with smoothed distribution. Stratification defined as the difference in density between 25 m and the surface.

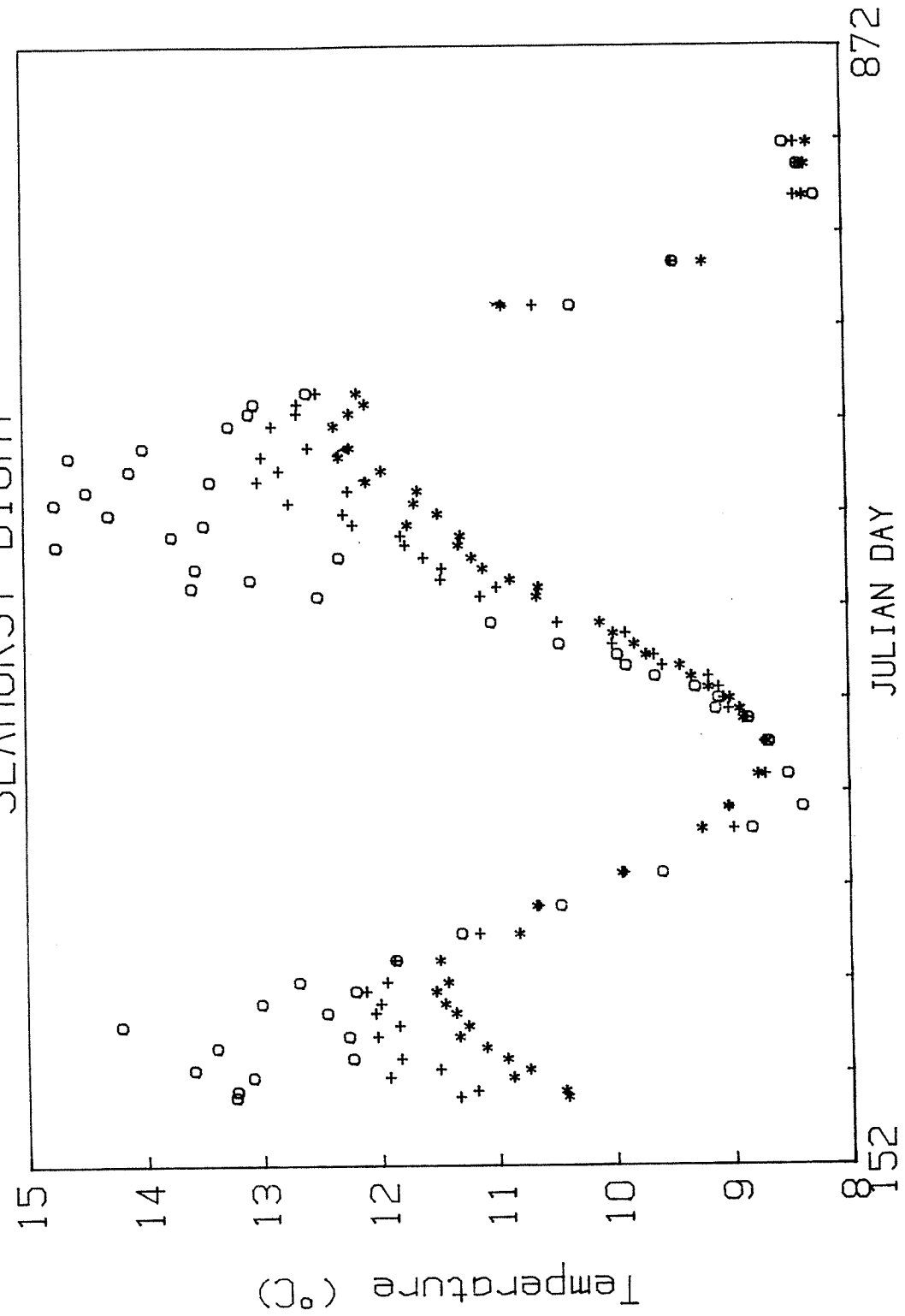

Figure 4.9. Seasonal temperature distribution at surface (o), 50 m (+) and 100 m (*) depths in Seahurst Bight.

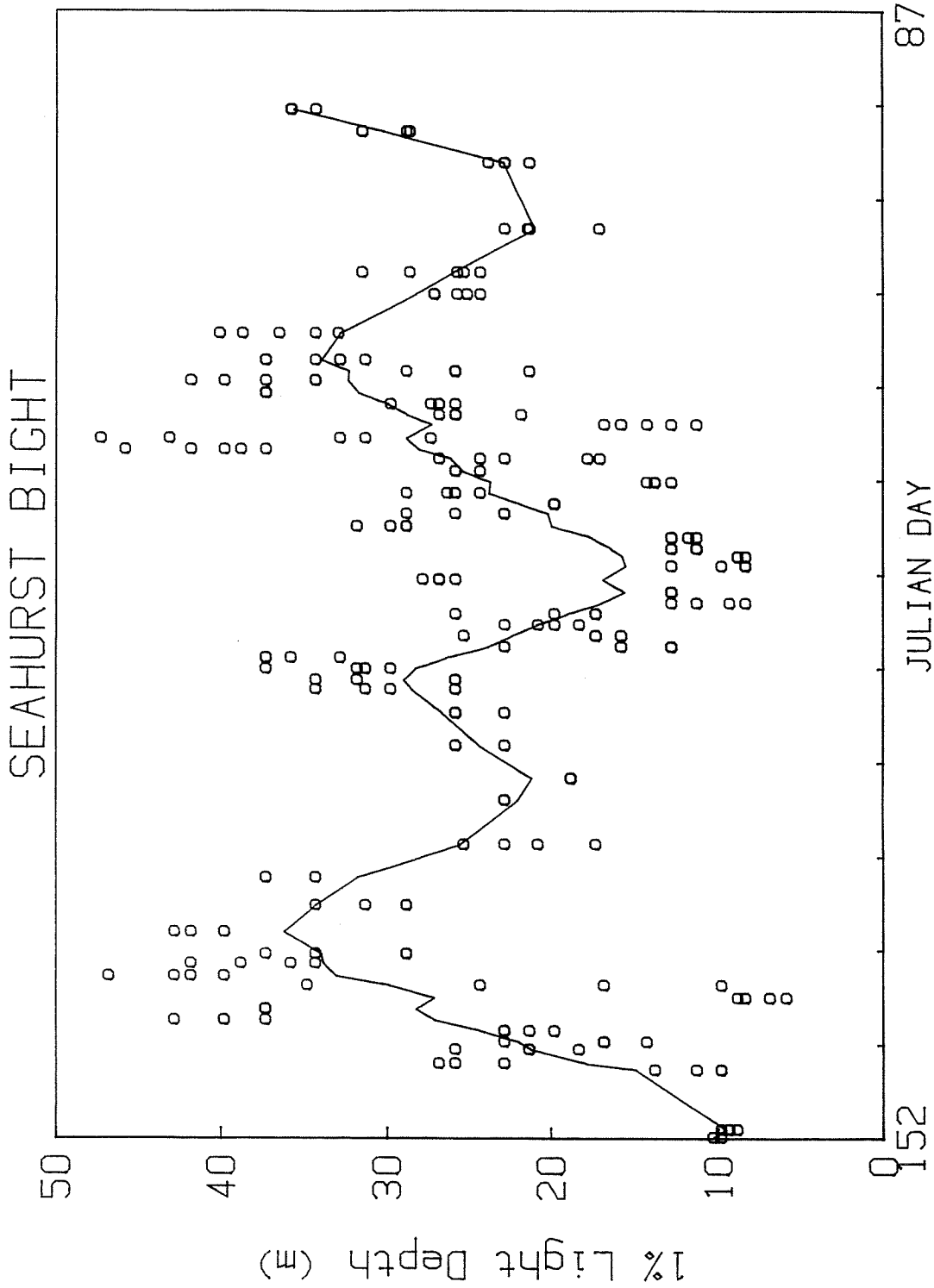

Figure 4.10. Depth of the 1% light level in Seahurst Bight.

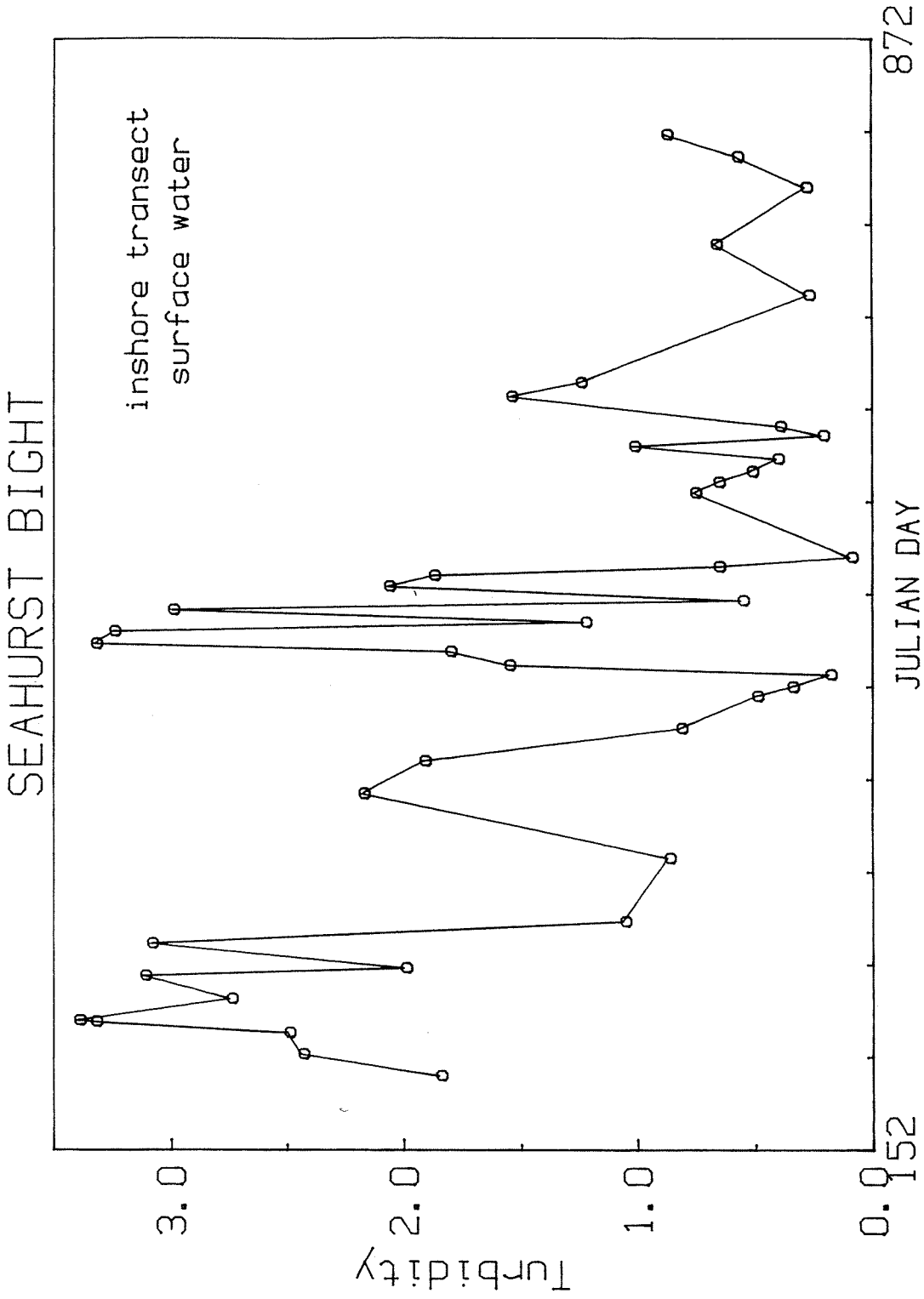

Figure 4.11. Surface water turbidity, in NTU units, from underway cruises in Seahurst Bight. Data are connected without smoothing.

period at stations 4 and 7 is illustrated in Figure 4.12a. The smoothed line obtained with the lognormal smoothing algorithm shows the seasonal pattern with maximum rates in the spring and a steady decline to the autumn and winter minimum. The greatest increase of primary productivity over time (Figure 4.12b) occurred at the vernal equinox and marked the beginning of the spring phytoplankton bloom. The rapid decrease in the growth rate about the summer solstice coincided with changes in other water column properties. The gamma mean primary productivity values were significantly different between seasons but the year to year difference cannot be distinguished at the 90% gamma confidence limits (Table 4.7). The probability distributions of productivity taken over the summer and winter seasons illustrate differences between the two years (Figure 4.13) (see Appendix 4.D).

On a chlorophyll specific basis, productivity (Figure 4.14) in the spring of 1983 reached the maximum specific rate of the major phytoplankton species found in the spring, Chaetoceras sp. (Nakanishi and Monji 1965). The specific rate in the summer of 1982 was greater in the summer of 1983 and the difference is significant at the 90% gamma confidence level (Table 4.7).

The phytoplankton biomass is controlled by the time integration of the growth and loss processes. The growth rate is the most important factor and so phytoplankton biomass follows light via the growth rate. Biomass, as measured by chlorophyll integrated over the photic zone, exhibited a great deal of variability about the seasonal distribution (Figure 4.15a). This pattern is typical of all phytoplankton properties. The seasonal pattern of the net growth rate of chlorophyll is illustrated by the time variation of the slope of the smoothed distribution (Figure 4.15b). The maximum positive net growth rate, which was the spring bloom, was observed near the vernal equinox, and a second maximum was observed in mid summer. About the summer solstice,

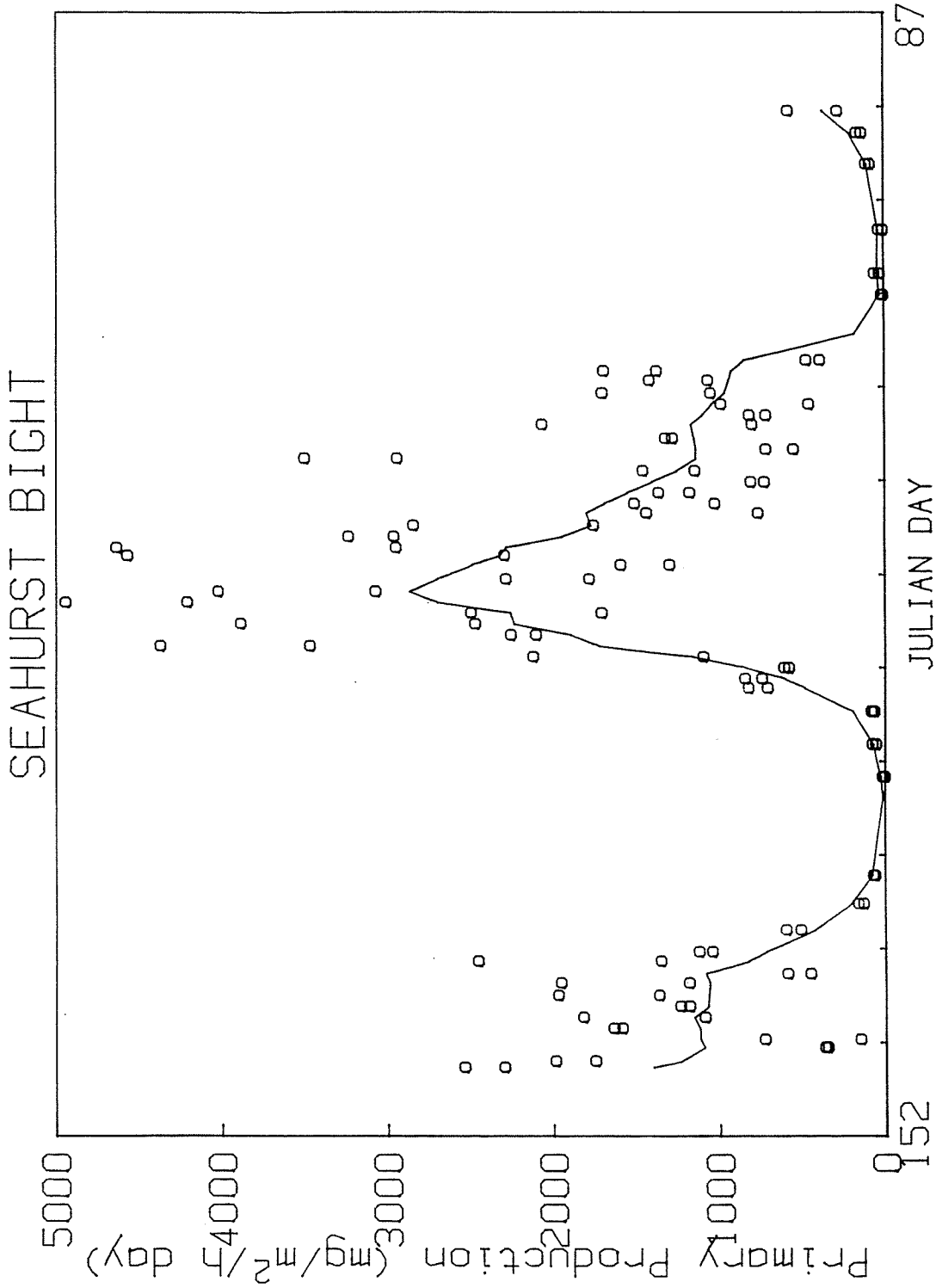

Figure 4.12a. Primary productivity (mg/m^2/half day) for Seahurst Bight with smoothed distribution.

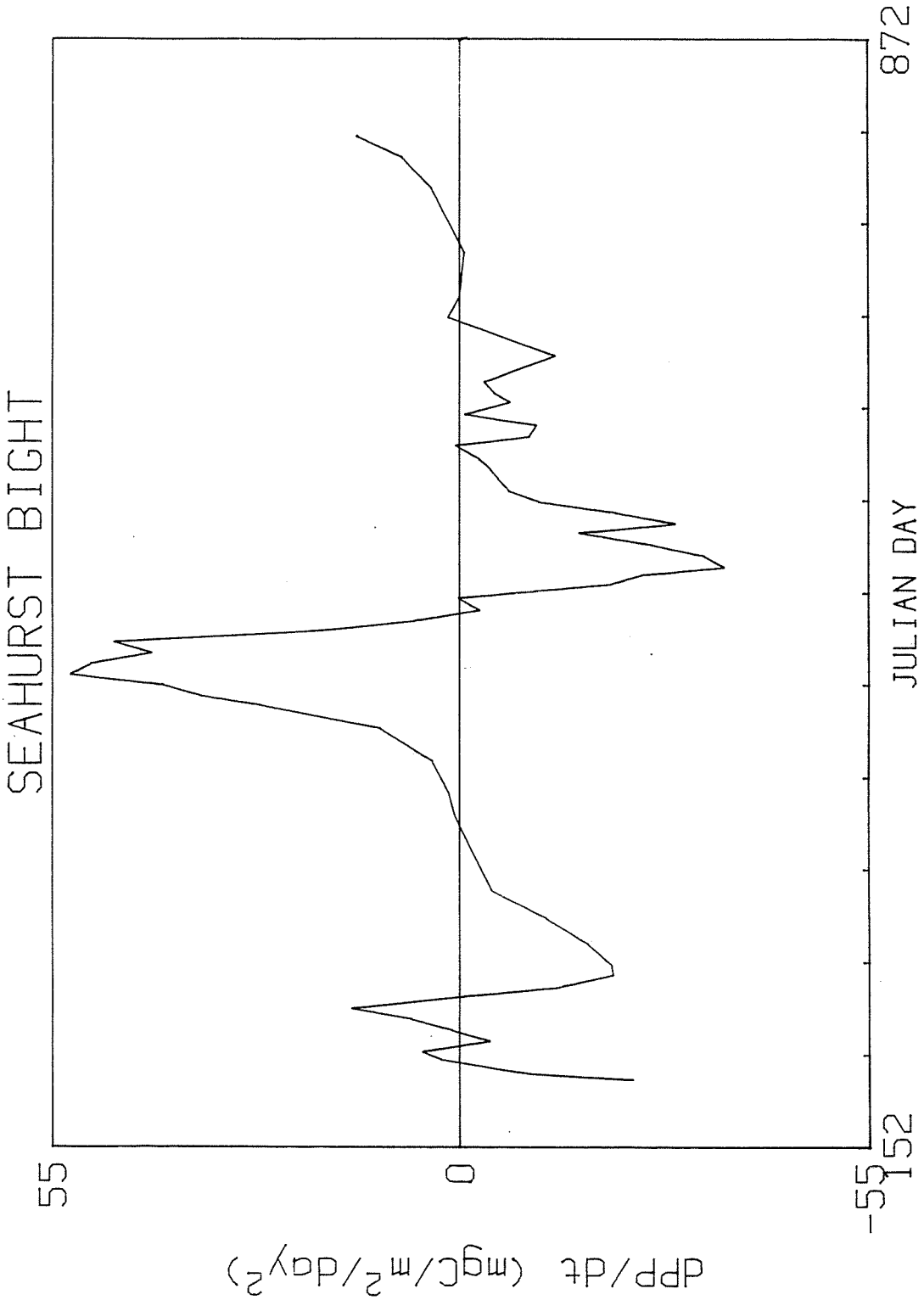

Figure 4.12b. Slope of smoothed distribution from Fig.4.12a depicting the rate of change of primary productivity.

Table 4.7. Carrying capacity and 90% gamma confidence interval for primary productivity (mg C/m^2/.5 day) and chlorophyll specific primary productivity (mg C/mg Chl/.5 day). Data was grouped from 6 week periods about the equinox and solstice dates for 1982 and 1983. Significantly higher levels marked by * Insufficient data to carry out the analysis was collected near the summer solstice and the winter solstices, 1982.

Period	Primary prod. integrated	Chl specific primary prod.
Summer solstice 1982	-	-
Summer solstice 1983	175 (129-287)	28.0 (21.7-39.7)
Autumnal equinox 1982	64 (43-139)	19.9* (16.0-25.8)
Autumnal equinox 1983	43 (32-67)	5.5 (4.9-6.3)
Winter solstice 1982	-	-
Winter solstice 1983	2 (1-2.5)	4.3 (3.0-8.1)
Vernal equinox 1982	53 (35-137)	18.4 (14.4-25.4)

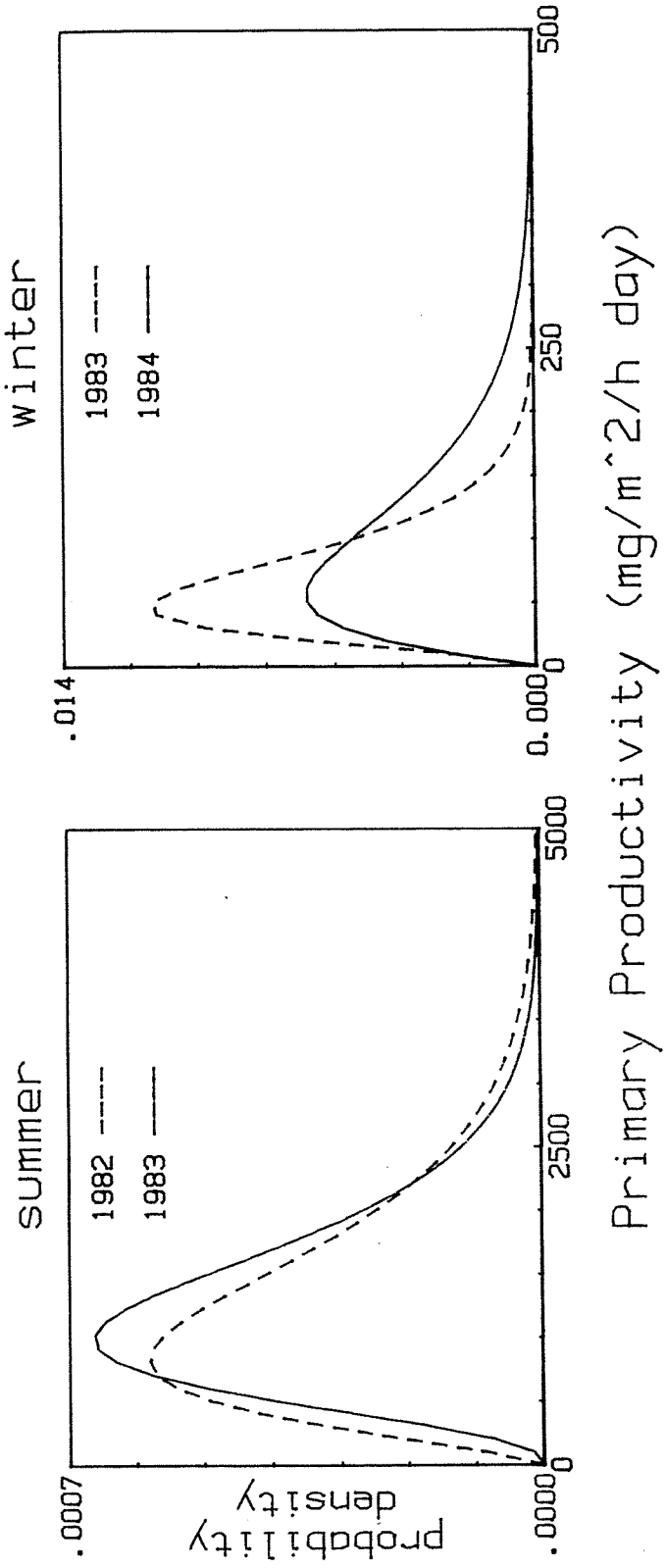

Figure 4.13. Gamma probability distributions for Seahurst Bight primary productivity (mg C/m^2/half day) for summer 1982 and 1983, and winter 1983 and 1984.

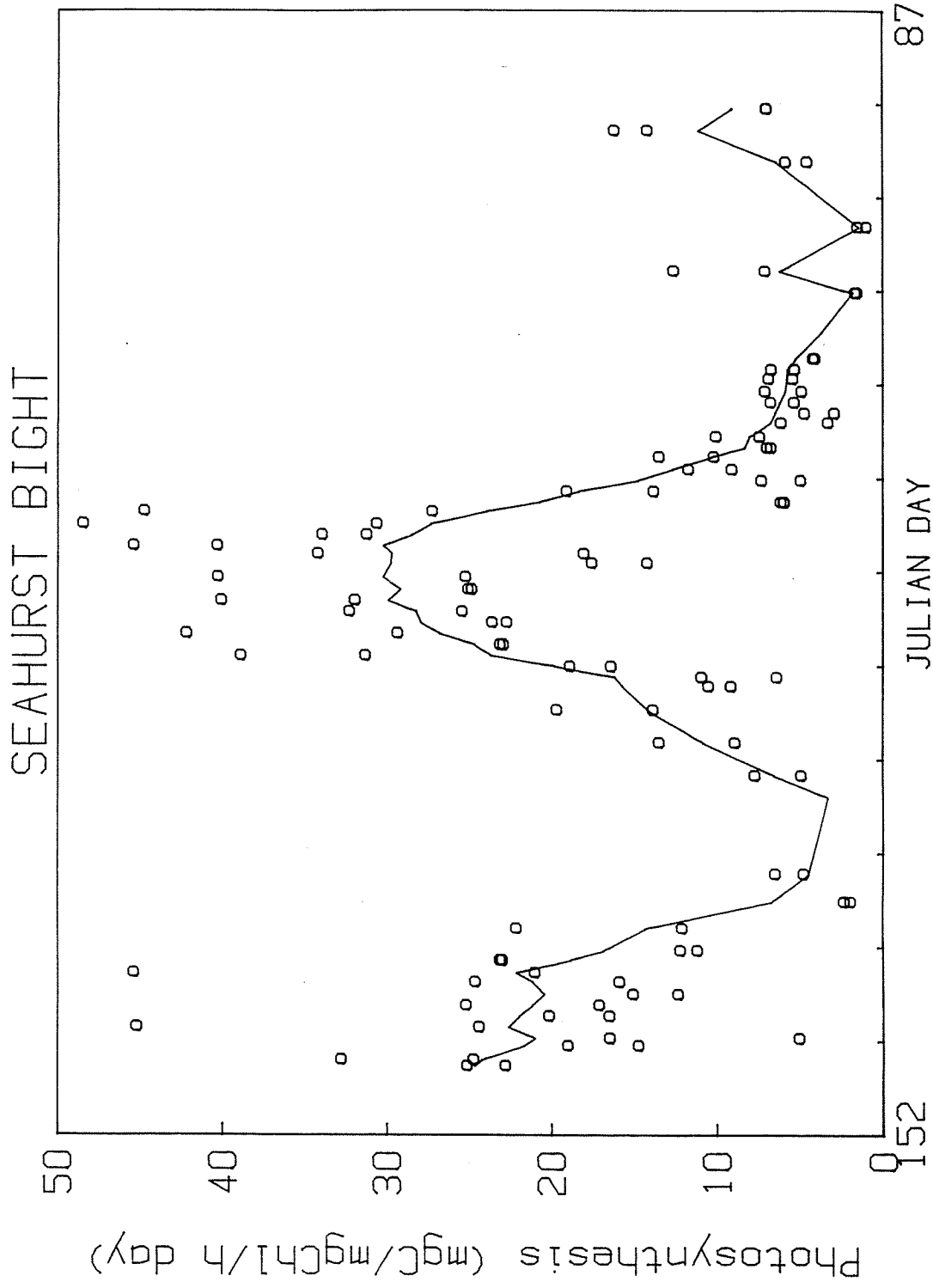

Figure 4.14. Chlorophyll specific photosynthesis for Seahurst Bight with smoothed distribution.

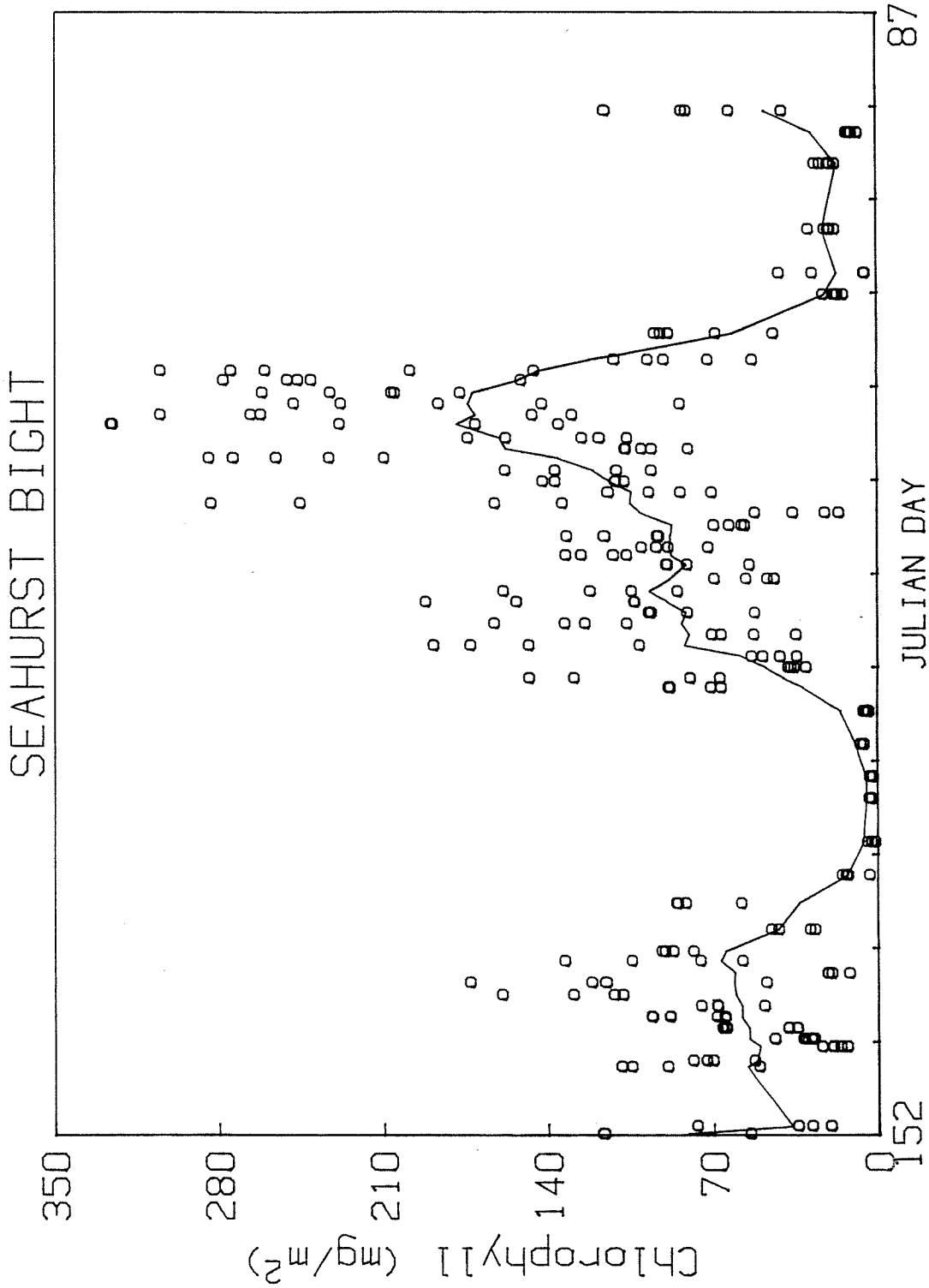

Figure 4.15a. Chlorophyll integrated over to the 1% light depth in Seahurst Bight with smoothed distribution.

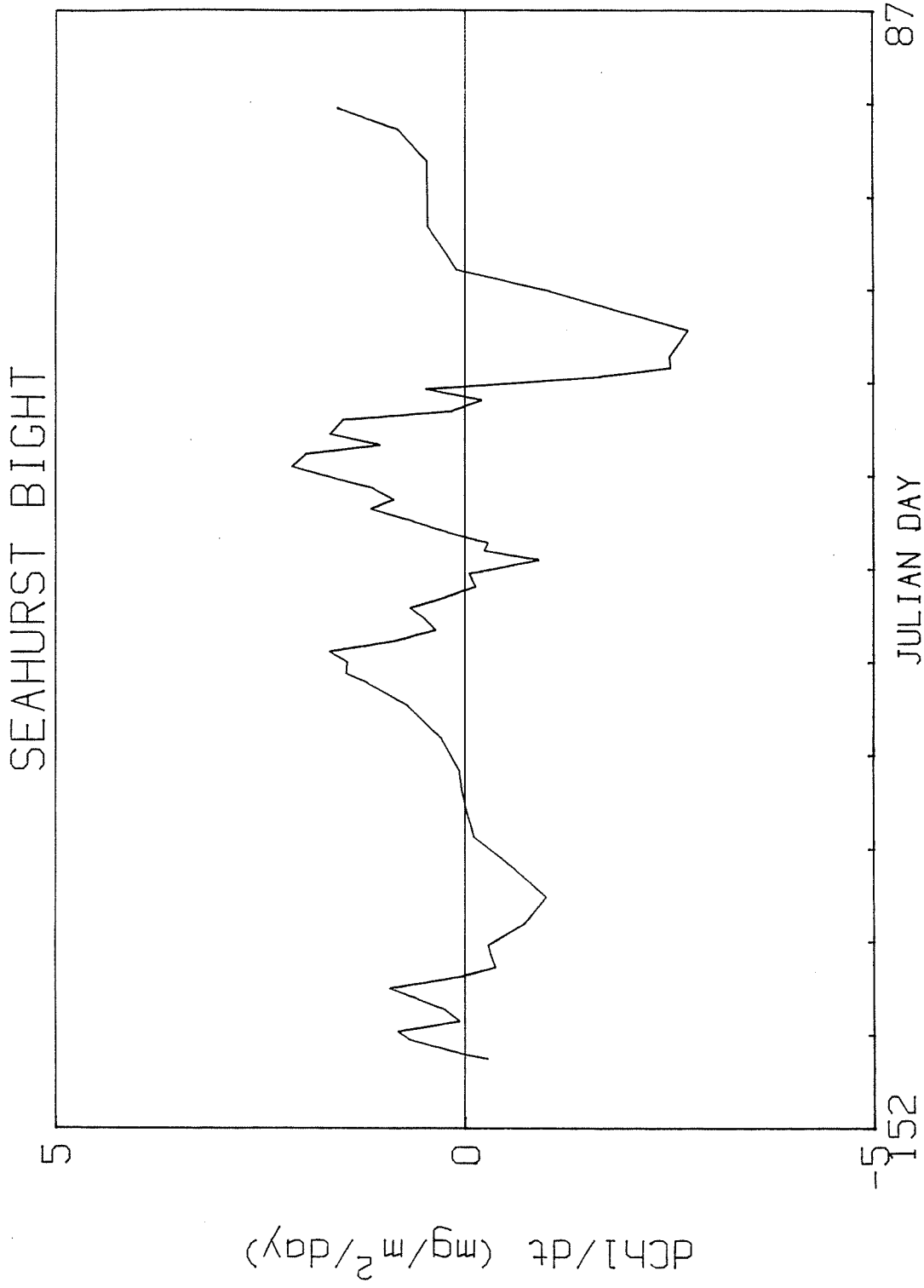

Figure 4.15b. Slope of smoothed distribution depicting rate of change of integrated chlorophyll.

which falls between the two maxima, the chlorophyll net rate was negative. The major loss of chlorophyll occurred in the autumn, and levels were near zero in the winter.

Chlorophyll levels in 1983 were significantly above normal when compared to 1982 and historical levels. At the autumnal equinox in 1983 the integrated chlorophyll was about 3 times higher than in 1982. Winter 1983-84 levels were about 5 times higher than those of 1982-83 (Table 4.8). Probability distributions of chlorophyll for summer and winter seasons are depicted in Figure 4.16. During the summer of 1982 the chance of chlorophyll going above 100 mg Chl/m 2 was 19 out of 100 while during the summer of 1983 the change was 70 out of 100 (see Appendix 4.D).

Chlorophyll concentrations, obtained by dividing the integrated levels by the depth of the photic zone, show a seasonal pattern but the high concentrations about the 1983 autumnal equinox are not as pronounced (Figure 4.17a) due to the autumnal deepening of the photic zone. The spring and summer net increase, the summer equinox loss, and the net decrease in the autumn are evident in terms of concentration (Figure 4.17b). The smooth curves show differences in concentration between 1982 and 1983. Summer solstice concentrations, calculated by gamma statistics, were essentially equal for 1982 and 1983 while the autumnal equinox levels in 1982 were about 40% lower than those in 1983. Within the 90% gamma confidence limits these levels can not be identified as different (Table 4.8).

The differences in chlorophyll concentration in the two summers can be quantified by probability distributions constructed from observations collected during the summer seasons (between the summer solstice and autumnal equinox). The chance of observing a depth integrated average photic zone chlorophyll concentration of greater than 5 mg Chl/m^3 was 23 out of 100 in

Table 4.8. Carrying capacity and 90% gamma confidence interval for phytoplankton chlorophyll and phaeopigments. Chlorophyll integrated over photic zone expressed as (mg/m^2). Chlorophyll and phaeopigment concentrations expresses as average integrated concentrations (mg/m^3). Date was grouped from 6 week periods about the equinox and solstice dates for 1982 and 1983. Significantly higher levels marked by *

Period	Chlorophyll (mg/m^2)	Chlorophyll (mg^m^3)	Phaeopigment (mg^m^3)
Summer solstice 1982	69 (64-79)	6.5 (6.0-7.3)	2.3 (2.1-2.7)
Summer solstice 1983	98 (84-123)	7.0 (5.9-9.6)	2.3 (1.9-3.3)
Autumnal equinox 1982	78 (64-104)	4.4 (3.6-8.4)	0.3 (0.2-0.5)
Autumnal equinox 1983	200 (180-230)	7.8 (6.8-9.7)	0.8* (0.7-1.1)
Winter solstice 1982	4 (4-5)	0.2 (0.1-0.2)	0.1 (0.1-0.1)
Winter solstice 1983	20 (16-26)	0.8* (0.6-1.1)	0.3* (0.2-0.4)
Vernal equinox 1982	66 (53-102)	2.8 (2.3-4.9)	1.2 (0.9-2.0)

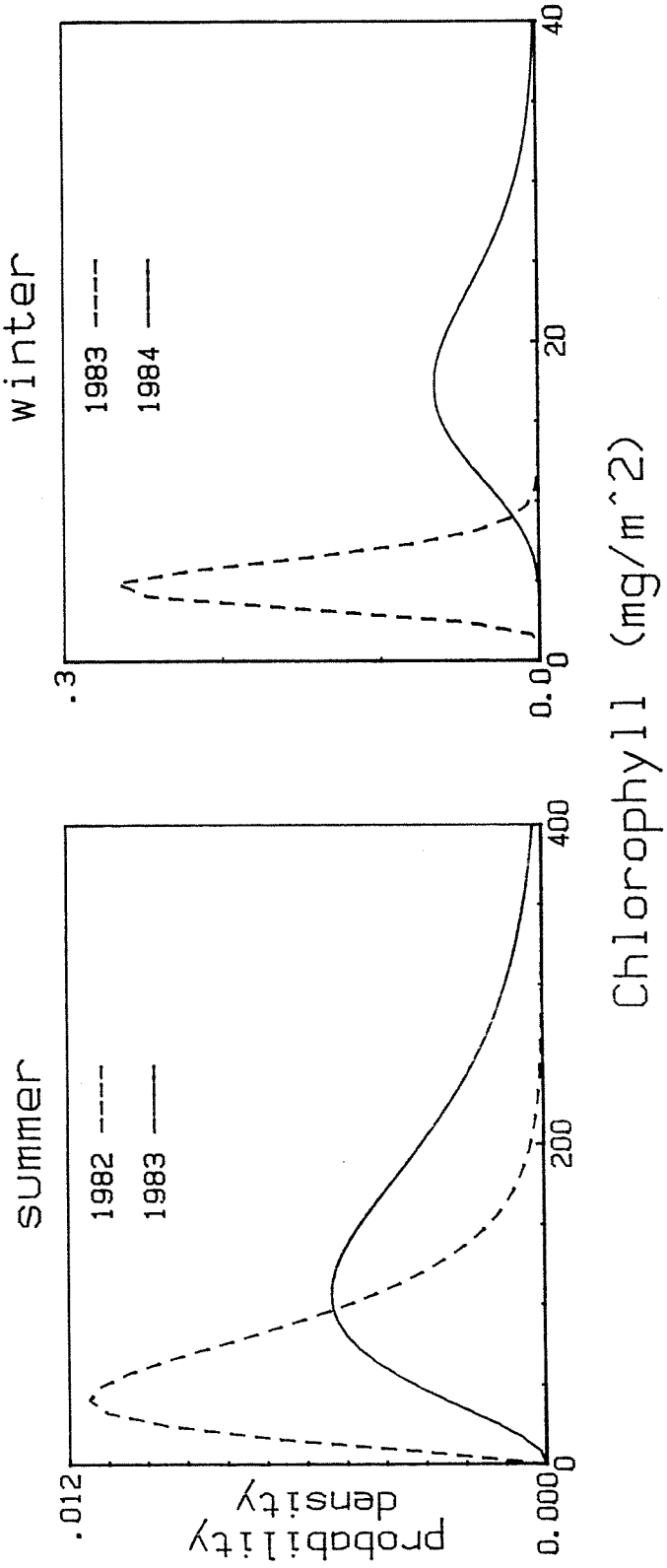

Figure 4.16. Gamma probability distributions for Seahurst Bight integrated chlorophyll (mg Chl/m^2) for summer 1982 and 1983, and winter 1983 and 1984.

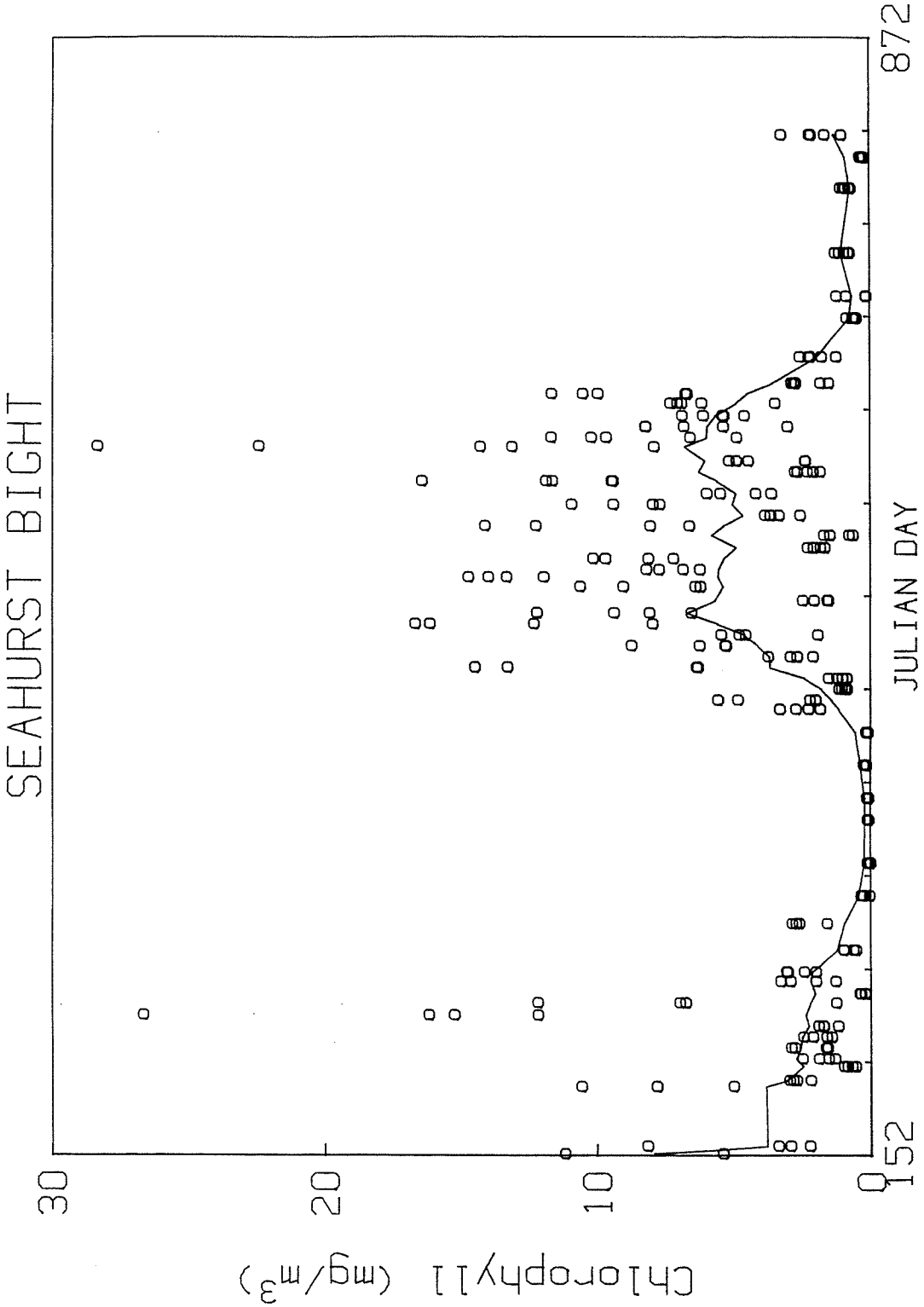

Figure 4.17a. Chlorophyll concentration in Seahurst bight photic zone with smoothed distribution.

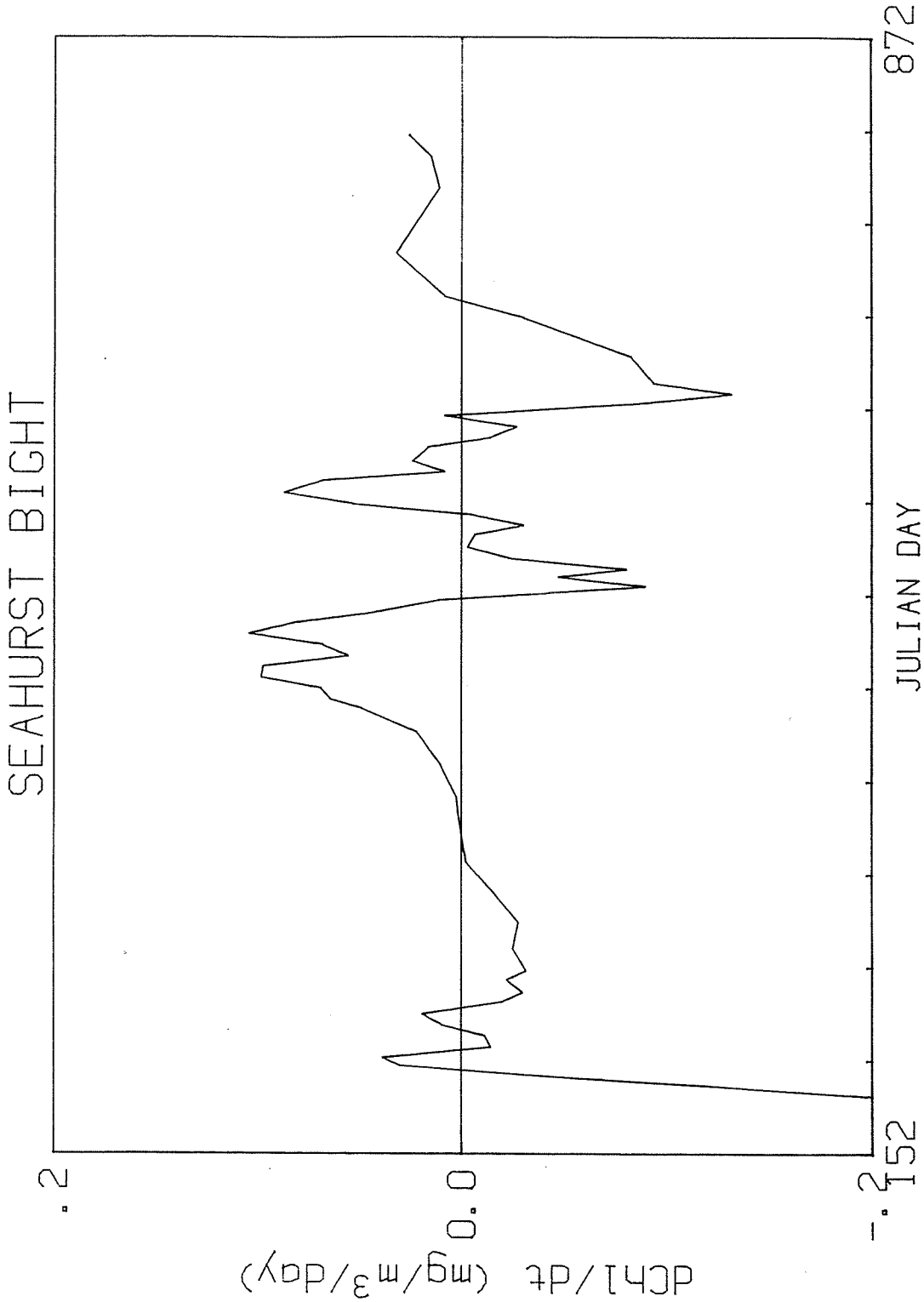

Figure 4.17b. Slope of smoothed distribution depicting rate of change of chlorophyll concentration.

1982 and 52 out of 100 in 1983. The chance of observing higher winter values in 1984 was greater than in 1983 (Figure 4.18) (see Appendix 4.D).

Phaeopigments are produced by the degradation of chlorophyll in the gut of zooplankton. They are excreted into the water and lost by photoxidation and sinking. The peak concentrations occurred in the mid-spring of 1983 (Figure 4.19a). The maximum net rate of production occurred near the vernal equinox and the maximum rate of loss near the summer solstice (Figure 4.19b). Phaeopigment concentration steadily decreased from the spring, in contrast to chlorophyll, which had spring and summer maxima. Summer solstice concentrations of phaeopigments were equal in 1982 and 1983 while autumnal equinox concentrations in 1983 were significantly larger than in 1982. Winter solstice concentrations were significantly larger in 1983 than in 1982 (Table 4.8). Probability distributions of phaeopigments for summer 1982 and 1983 and for winter 1982-83 and 1983-84 are given in Figure 4.20.

The relative variability of chlorophyll and phaeopigment concentrations and integrated primary productivity are about 1.0 for the temporal variability and 0.25 for the relative spatial variability, indicating that from cruise to cruise these parameters varied by on the order of 100% of the seasonally smoothed value while from station to station on a given sampling day the variation was on the order of 25%. For chlorophyll specific productivity and integrated chlorophyll, the relative temporal variability was between 0.5 and 0.6, indicating less variation in the seasonal distribution (Table 4.9).

The seasonal pattern of phytoplankton identified by species followed the seasonal pattern of phytoplankton biomass measured as chlorophyll. An exact comparison of the two measures can not be made since the species data were collected at the 50% light depth only while the chlorophyll concentrations are depth integrated averages. Three major phytoplankton species were abundant in

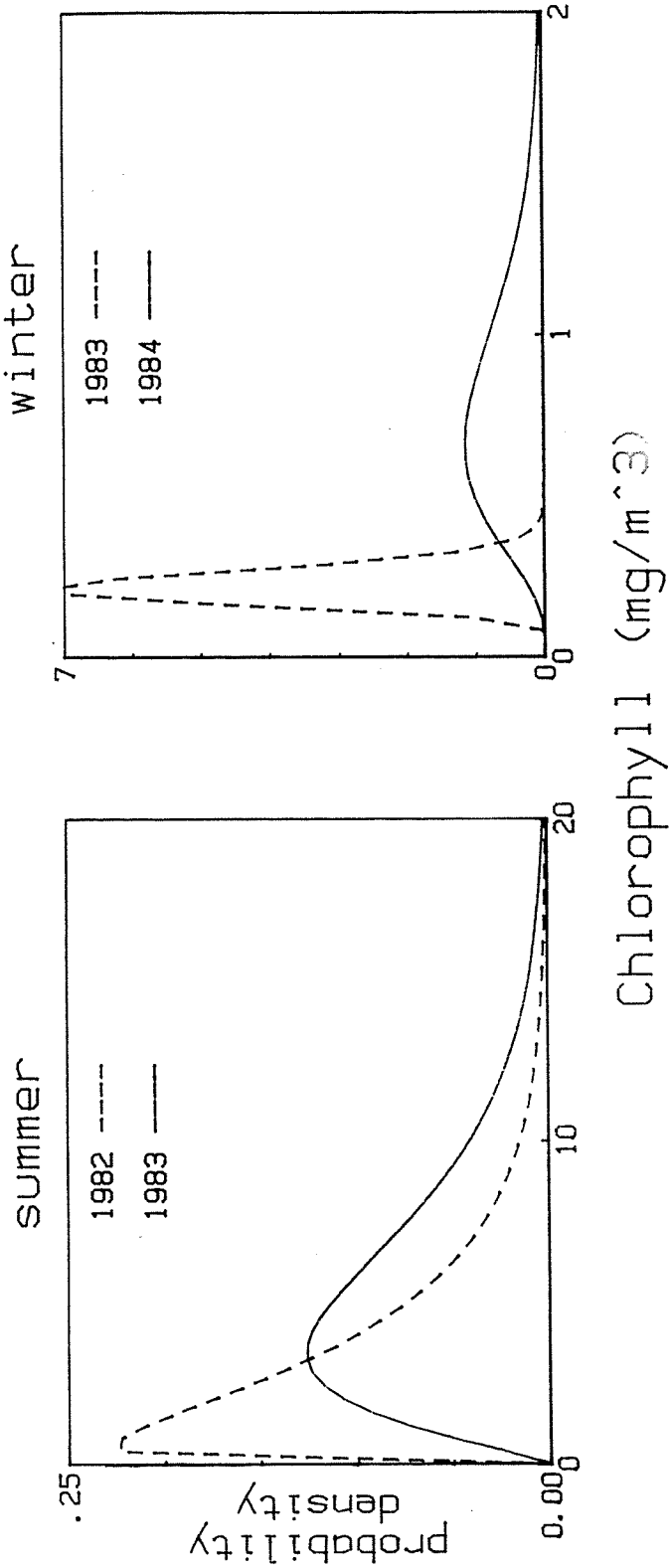

Figure 4.18. Gamma probability distributions for Seahurst Bight chlorophyll concentration for summer 1982 and 1983, and winter 1983 and 1984.

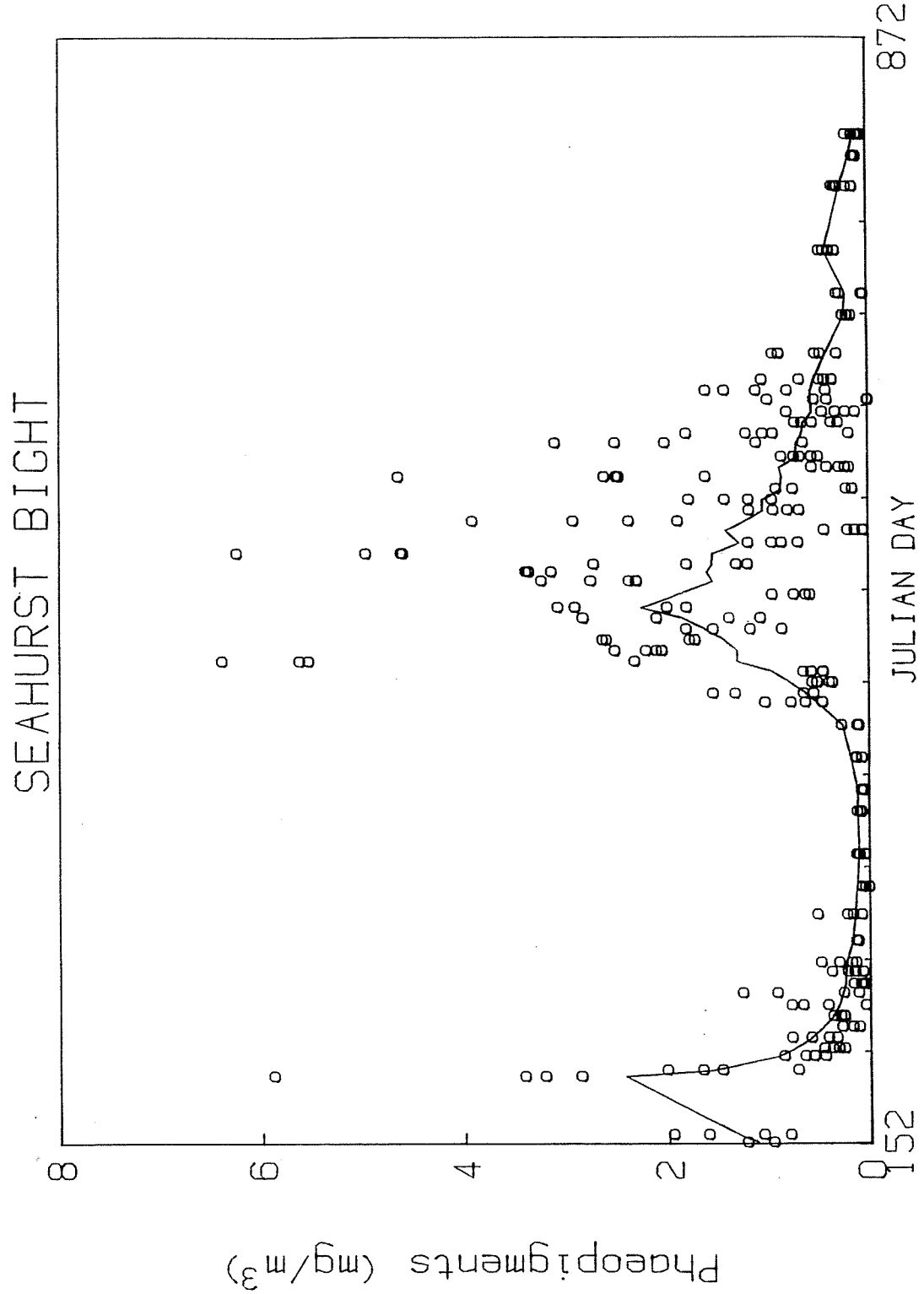

Figure 4.19a. Phaeopigment concentration in Seahurst Bight photic zone with smoothed distribution.

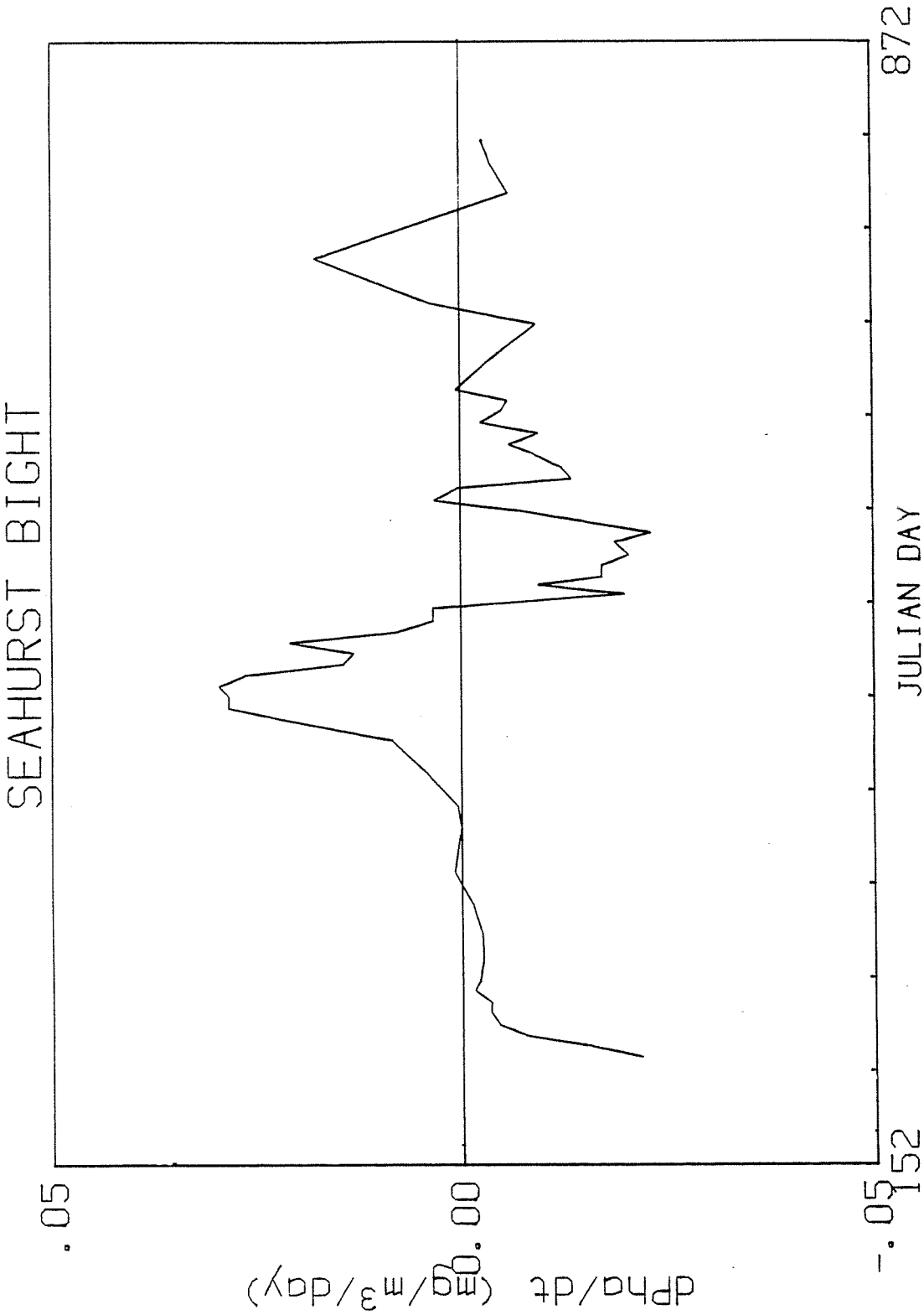

Figure 4.19b. Slope of smoothed distribution depicting rate of change of phaeopigment concentration.

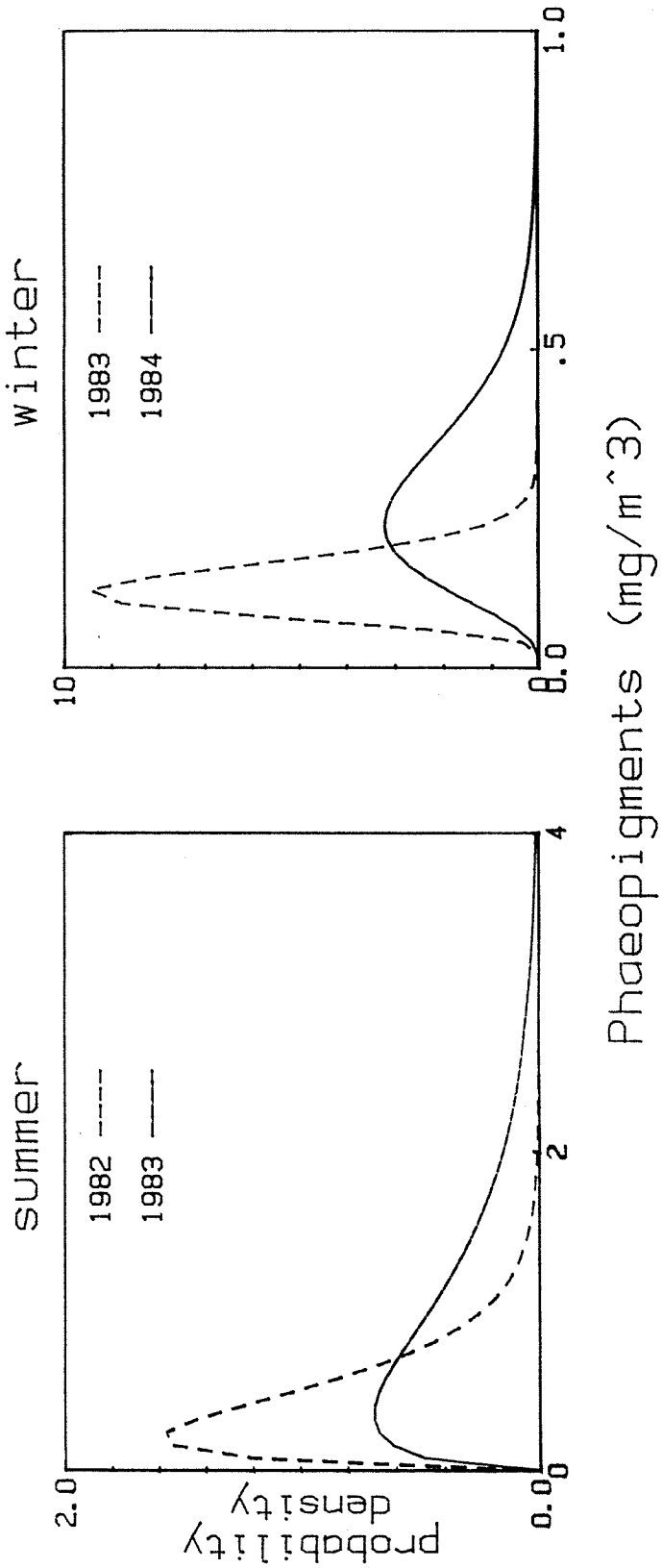

Figure 4.20. Gamma probability distributions for Seahurst Bight phaeopigment concentration for summer 1982 and 1983, and winter 1983 and 1984.

Table 4.9. Relative variability of phytoplankton properties in the Seahurst Bight as computed according to Section 4.6.3.10.

Property	Units	Temporal variability	Spatial variability
Primary Productivity	mg C / m^3 .5 day	0.98	0.25
Specific Primary Prod.	mg C / mg Chl .5 day	0.52	0.18
Chlorophyll	mg Chl/m^2	0.61	0.25
Chlorophyll	mg Chl/m^3	1.16	0.27
Phaeopigment	mg Pha/m^3	0.90	0.27

the Seahurst Bight; diatoms, dinoflagellates, and microflagellates. Diatoms are the largest in size, followed by dinoflagellates and microflagtellates. On a volume basis, the relative sizes are 100:10:1 (Figure 4.21).

A Kruskal-Wallis test was performed on the species data over the standard 6 week time intervals centered about the equinox and solstice periods for stations 4, 7 and 10 (Table 4.10). No systematic difference was found between stations. The smooth seasonal distributions of cell numbers were determined with the lognormal smoothing algorithm using data from stations 4, 7 and 10. Cell volume was determined on a seasonal basis (Table 4.11) using a carbon to volume relationship for diatoms where $\log_{10}$ (Carbon)=0.788 $\log_{10}$ (Volume) - 0.464, and for other phytoplankton where $\log_{10}$ (Carbon=0.792 $\log_{10}$ (Volume) - 0.333, the carbon content of the species was determined.

The phytoplankton blooms in the spring and summer, and the dominance of diatoms over dinoflagellates and microflagellates on a carbon basis is illustrated in the diagram of smoothed data in Figure 4.22. Diatoms had a primary bloom in the spring and a secondary bloom in the summer. Dinoflagellates reached their maximum levels during the summer solstice when diatoms declined. Microflagellates gradually increased through the spring and into the mid-summer and gradually decreased from mid-summer.

The dominant genera of diatoms; Skeletonema costatum, Chaetoceros debilis, other Chaetoceros species, and Thalassiosira species exhibited similar seasonal patterns (Figure 4.23). Diatoms, which were present but never dominant included: Nitzschia spp., Biddulphia longicruris, Coscinodiscus spp., Thalassionema sp., and Melosira spp. Diatom numbers in 1983 increased in the spring and dropped significantly in the summer (Figure 4.24a). The maximum average number (907 cell/ml) was observed near the summer equinox in 1983. The minimum average (3/ml) occurred near the winter solstice of 1982-83. At the autumnal equinox numbers were higher in 1983 than in 1982 (125 vs. 57 cells/ml) but the 90% confidence estimates on the means overlapped

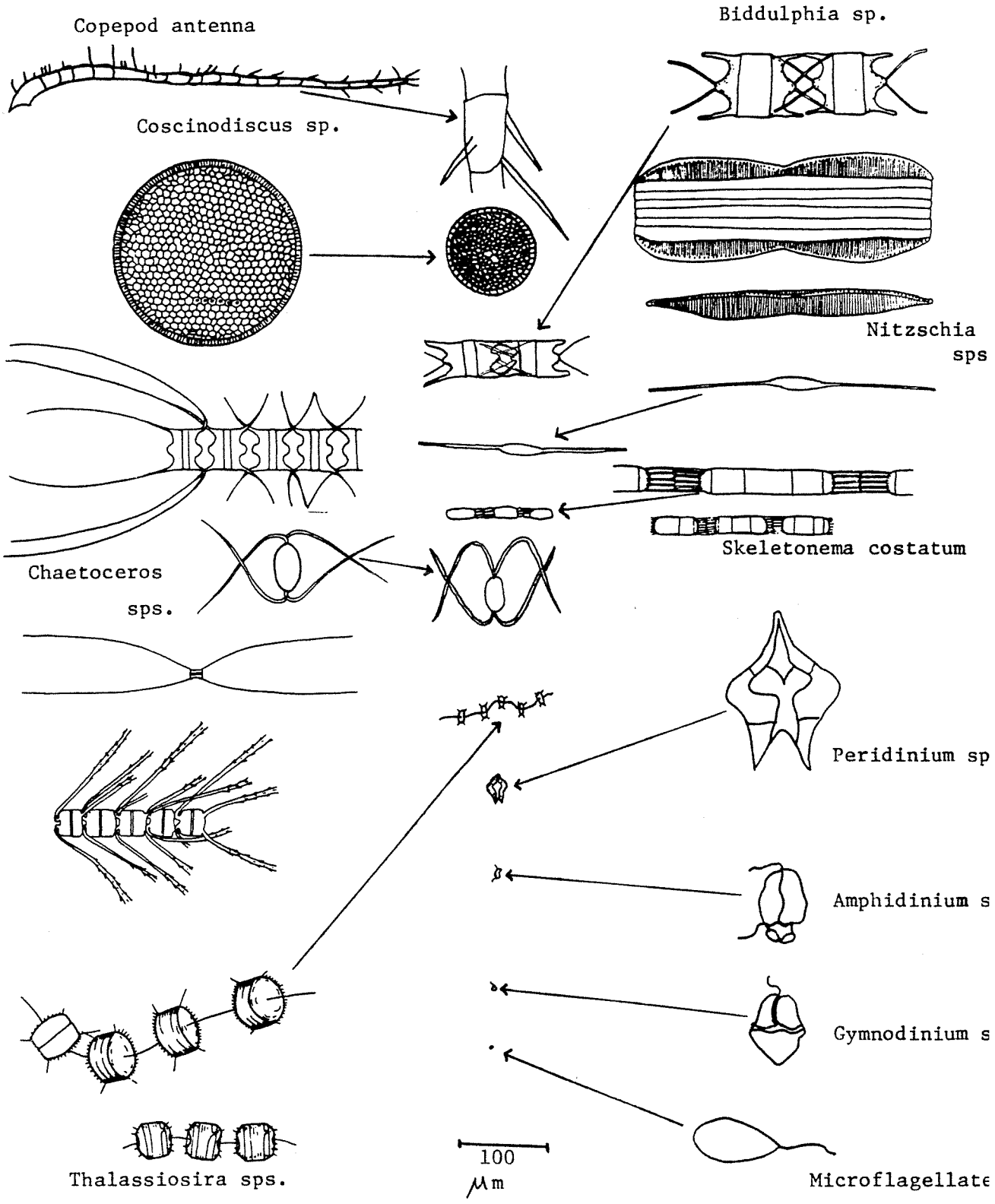

Figure 4.21. Dominant Species of phytoplankton in Puget Sound. Relative cell sizes with 100 um scale are also illustrated.

Table 4.10. Kruskal-Wallis test for differences among phytoplankton species at stations 4, 7 and 10 in Seahurst Bight. Hypothesis; species are not different between stations, is accepted if chi-square > H. Test are significant at the 95% confidence level. H is Kruskal-Wallis statistic.

Season	Degrees freedom	H	chi^2 (0.05, df)	Difference between stations
DIATOMS				
Summer 1982	2	0.05	6	No difference
Winter 1982-83	2	0.06	6	No difference
Summer 1983	2	5.97	6	No difference
DINOFLAGELLATES				
Summer 1982	2	0.81	6	No difference
Winter 1982-83	2	0.39	6	No difference
Summer 1983	2	3.43	6	No difference
MICROFLAGELLATES				
Summer 1982	2	0.36	6	No difference
Winter 1982-83	2	1.59	6	No difference
Summer 1983	2	0.51	6	No difference

Table 4.11. Conversion to cell carbon from cell numbers for total diatoms, dinoflagellates and microflagellates. Cell carbon is in picograms.

Season	Total Diatoms	Total Dinoflagellates	Total Microflagellates
Winter (J Days 300-452 666-809)	301.0	667.6	21.8
Spring/Fall (J Days 196-200 279-284, 459-564, 636-649)	238.0	814.0	31.5
Summer (J Days 207-270, 571-628)	2,829.7	2,308.1	185.2

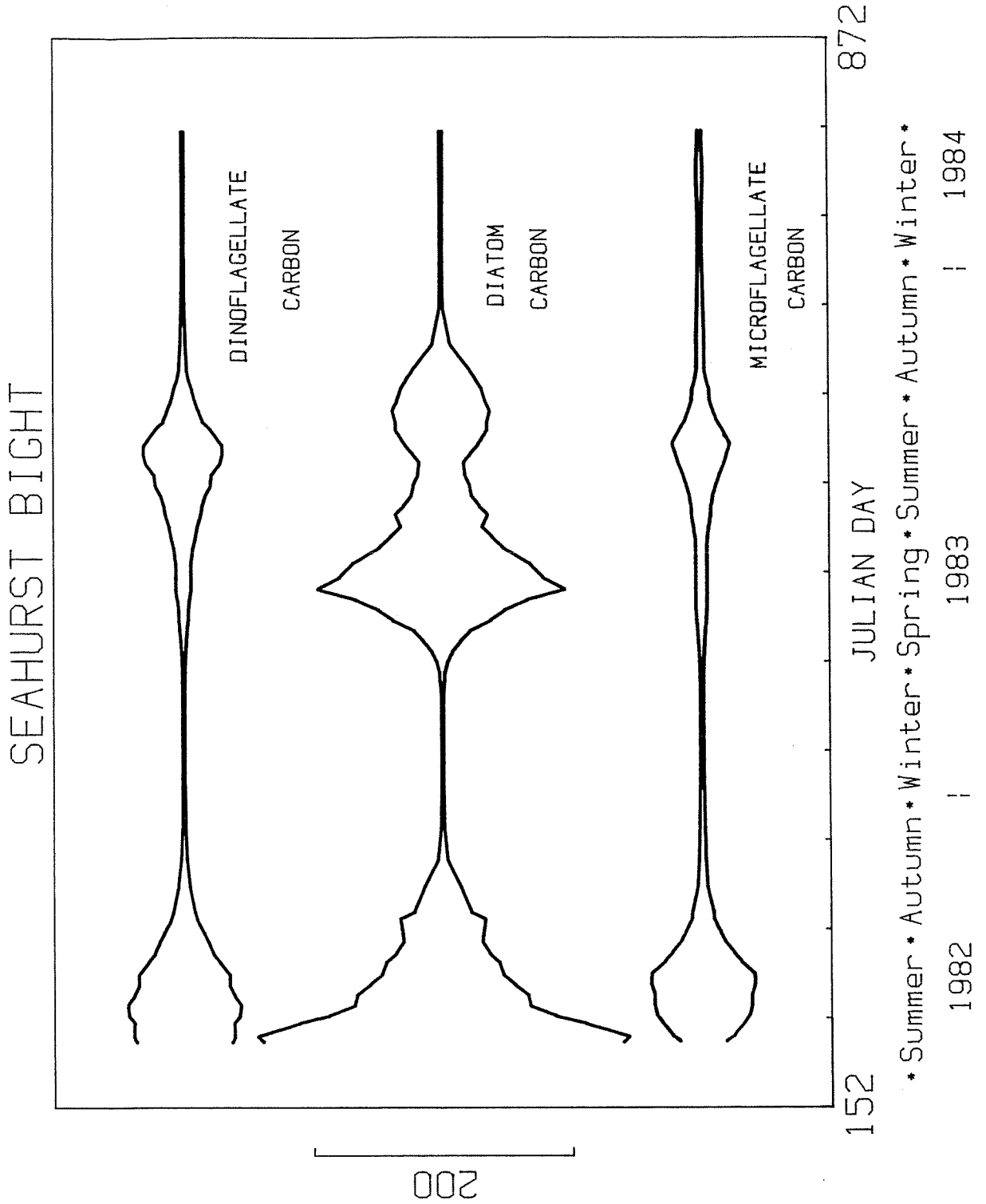

Figure 4.22. Carbon biomass of major phytoplankton groups over time in Seahurst Bight. Scale on left depicts 200 mg/m^3 of cell carbon. All phytoplankton species samples were collected from the 50% light depth at stations 4, 7 and 10.

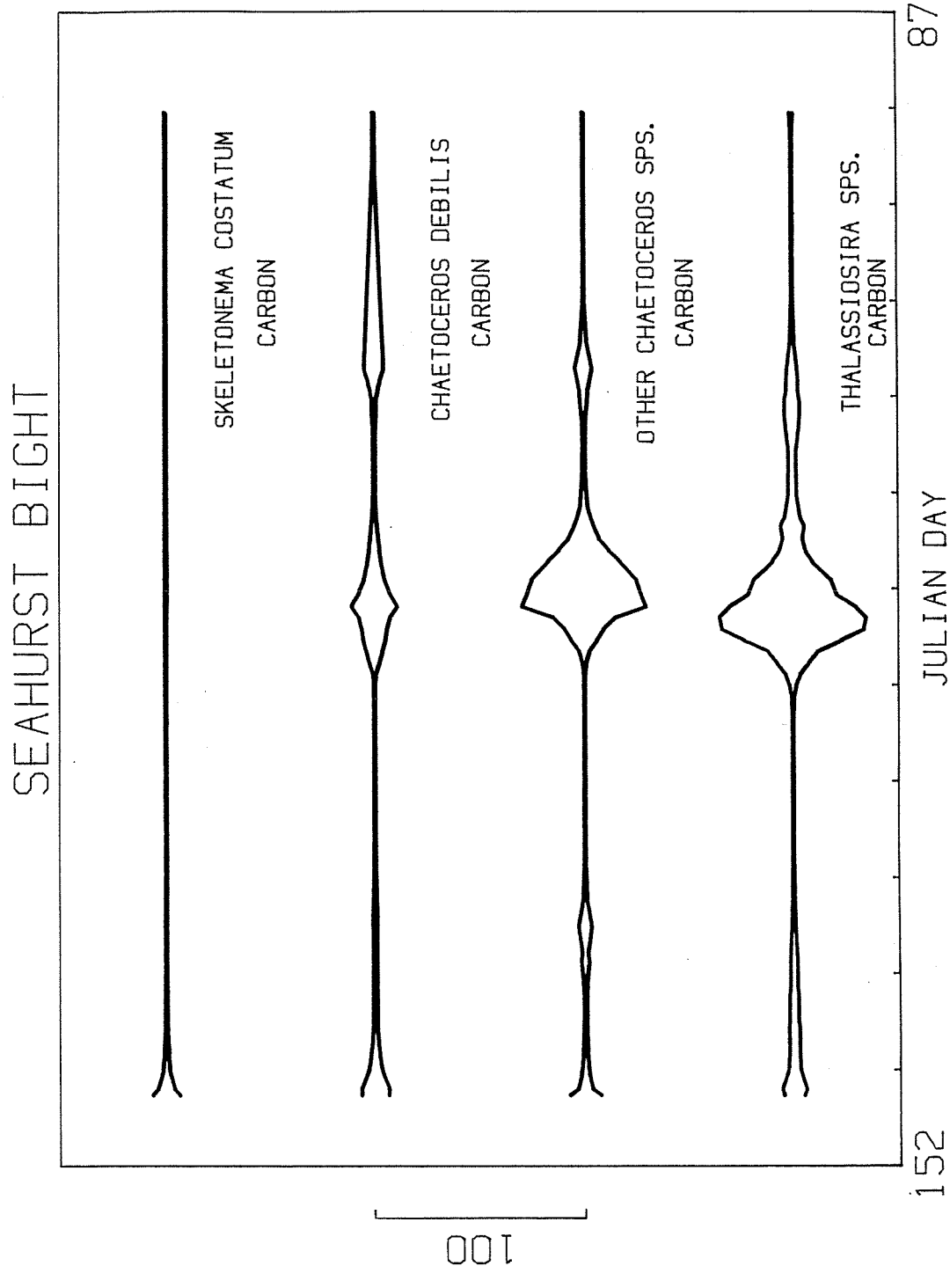

Figure 4.23. Carbon biomass of major diatom species over time in Seahurst Bight. Scale on left depicts 200 mg/m^3 of cell carbon.

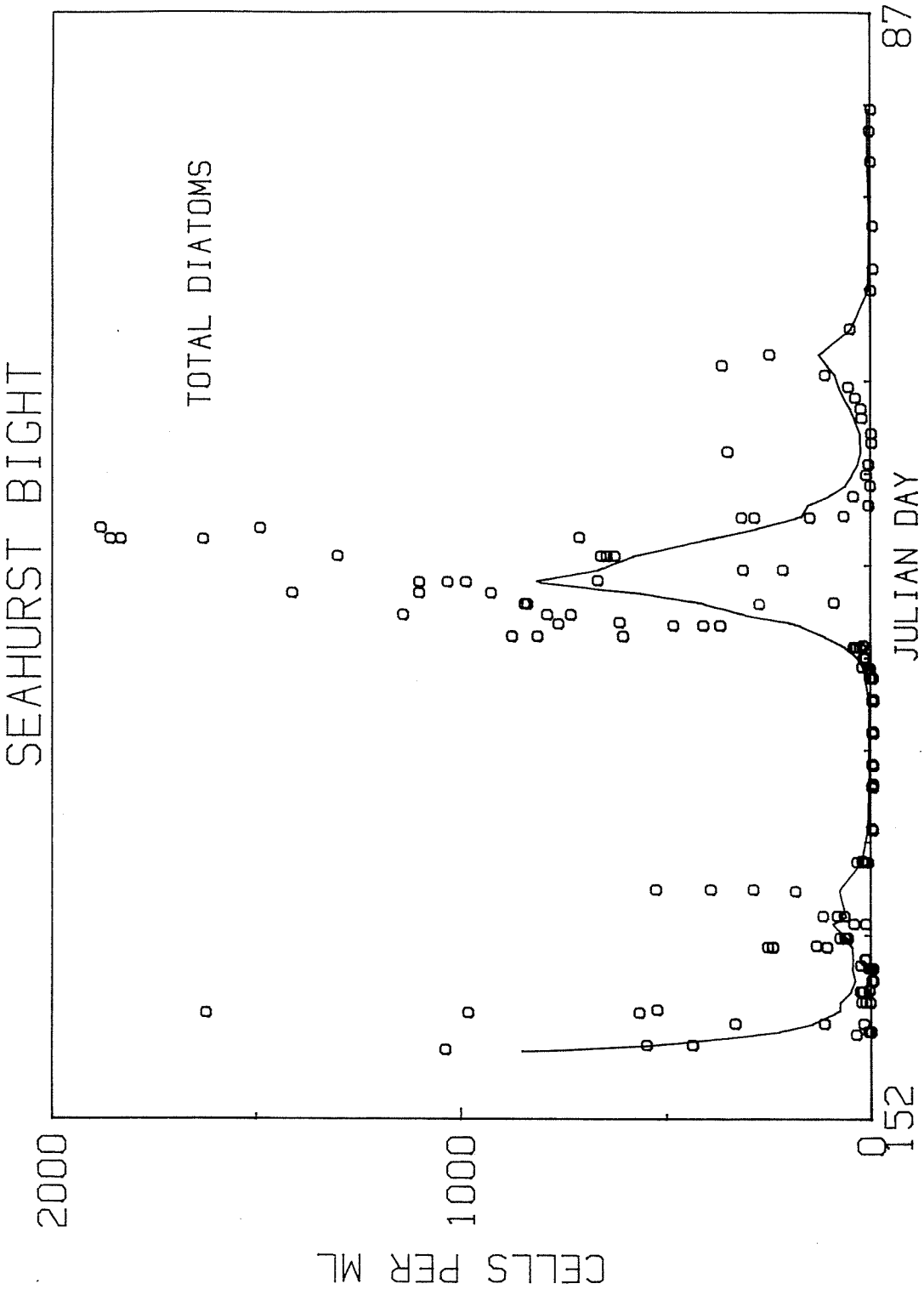

Figure 4.24a. Total diatom numbers from 50% light depth in Seahurst Bight with smooth distribution.

(Table 4.12). The net growth and loss rates of diatom numbers occurred principally in the spring with values of about 20 cells/ml/day (Figure 4.24b).

Dinoflagellates exhibited smooth seasonal changes in cell numbers (Figure 4.25a) with growth rates from spring through mid-summer and losses from mid-summer through autumn (Figure 4.25b). Dinoflagellates at the autumnal equinox in 1982 were 3 times higher than at the autumnal equinox in 1983 (64 vs. 22 cells/ml). The difference is significant at the 90% gamma confidence level (Table 4.12). the most common dinoflagellates observed were: Peridinium spp., Amphidinium spp., Dinophysis acuminata, and Gymndonium splendens. The toxin-producing Gonyaulax catenella was sometimes observed and only in very low numbers.

Microflagellates exhibited smooth seasonal changes in cell numbers similar to the pattern observed in dinoflagellates (Figure 4.26a). The growth rate was maximum in the spring and generally declined from mid-summer through the autumn (Figure 4.26b). The autumnal equinox levels in 1982 were greater than in 1983 (387 vs. 276 cells/ml). The difference was significant at the 90% gamma confidence level (Table 4.12).

The relative spatial and temporal variance of the phytoplankton species is similar to that of chlorophyll with spatial variability on the order of 100% and spatial variability on the order of 25% (Table 4.13).

4.4.1.3 Zooplankton

In the Seahurst Bight trends in the abundance of zooplankton follow those of phytoplankton, as phytoplankton are a principal food for the zooplankton. Zooplankton population changes lag the phytoplankton population changes because the zooplankton development time is on the order of a few weeks while the doubling time of phytoplankton is on an order of a day. In this section the spatial and temporal zooplankton trends in Seahurst Bight are presented in

Table 4.12. Carrying capacity and 90% gamma confidence interval for phytoplankton species (numbers/ml) for diatoms, dinoflagellates and microflagellates from stations 4, 7 and 10 in Seahurst Bight. Data is collected from 6 week periods about the equinox and solstice dates for 1982 and 1983.

Period	Diatoms	Dinoflagellates	Microflagellates
Summer solstice 1982			
Summer solstice 1983	907 (636-1960)	27 (20-44)	276 (226-353)
Autumnal equinox 1982	57 (43-120)	64 (50-153)	387 (329-475)
Autumnal equinox 1983	124 (94-213)	22 (17-40)	229 (180-328)
Winter solstice 1982	3 (2-3)	2 (1-2)	127 (115-145)
Winter solstice 1983			
Vernal equinox 1982	84 (74-331)	6 (4-10)	158 (126-223)

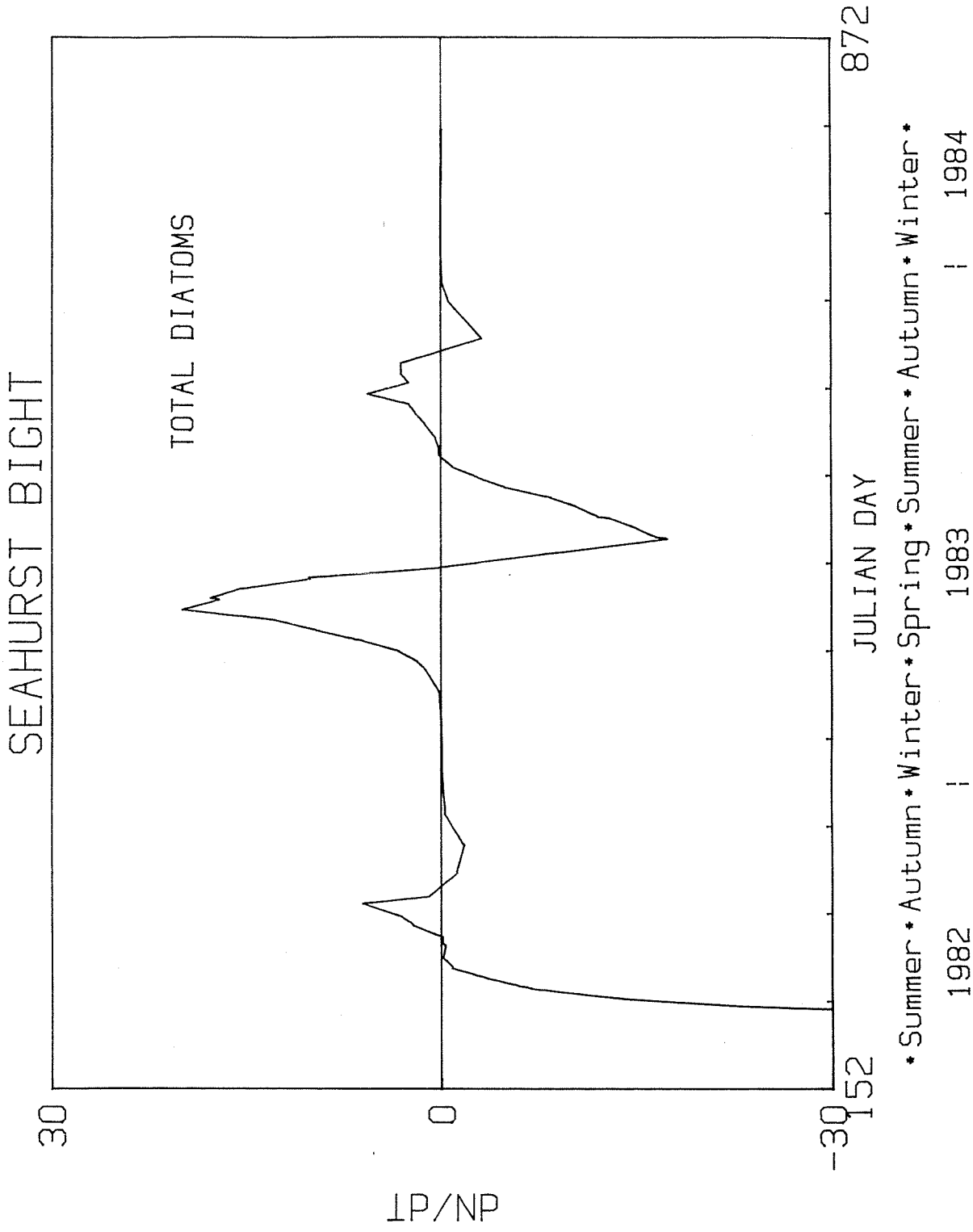

Figure 4.24b. Slope of smoothed distribution depicting rate of change of diatom numbers.

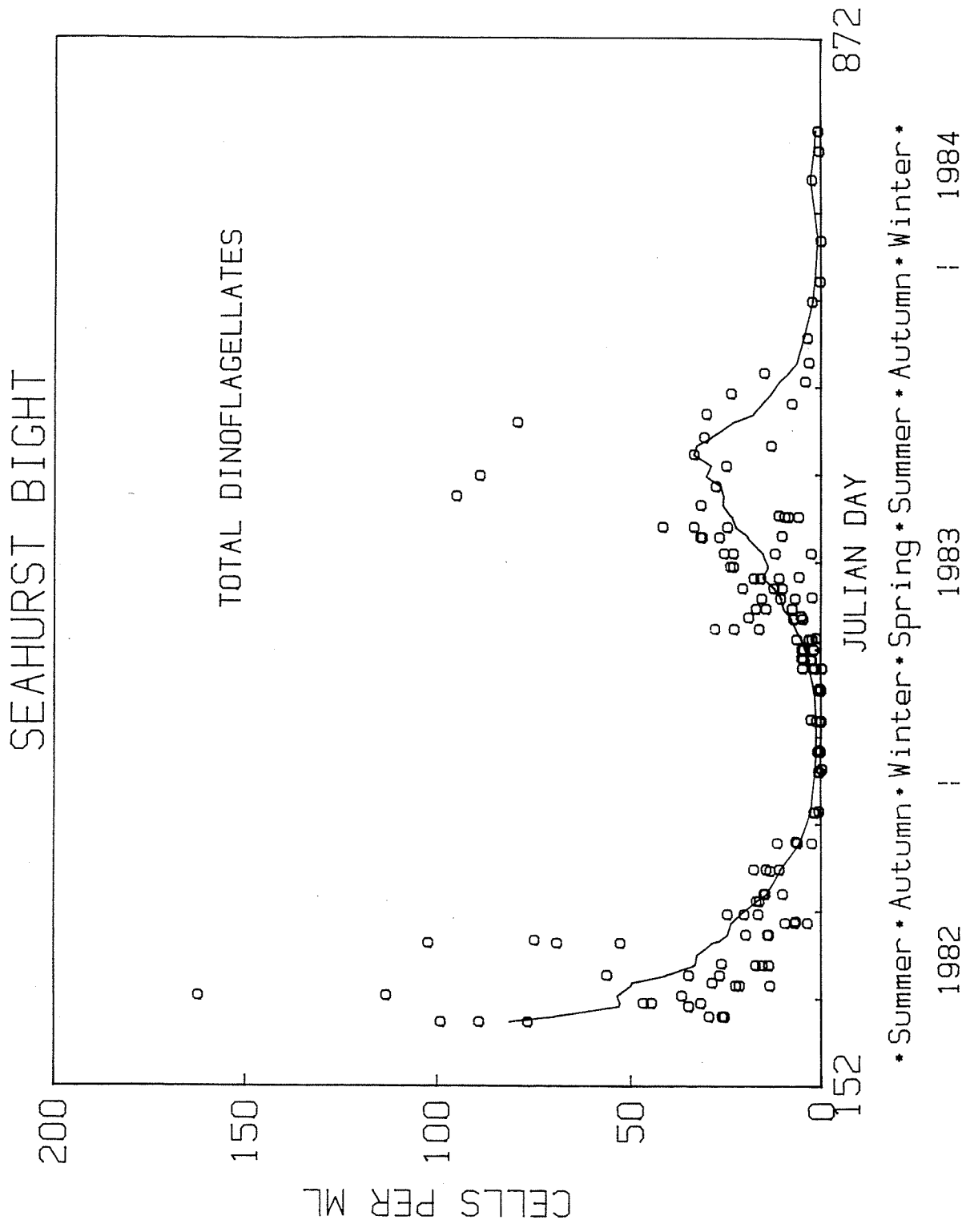

Figure 4.25a. Total dinoflagellate numbers from 50% light depth in Seahurst Bight with smooth distribution.

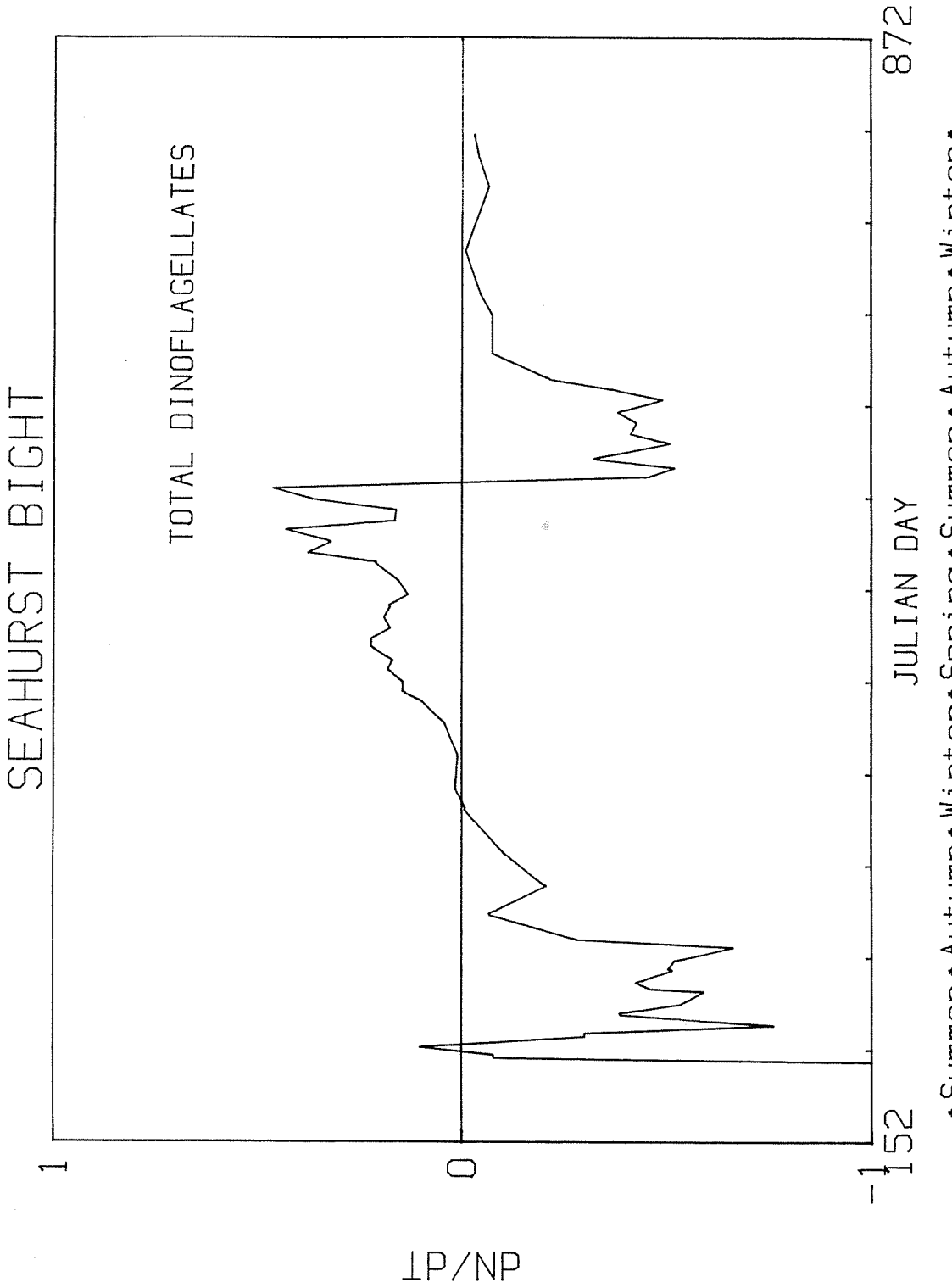

Figure 4.25b. Slope of smoothed distribution depicting rate of change of dinoflagellate numbers.

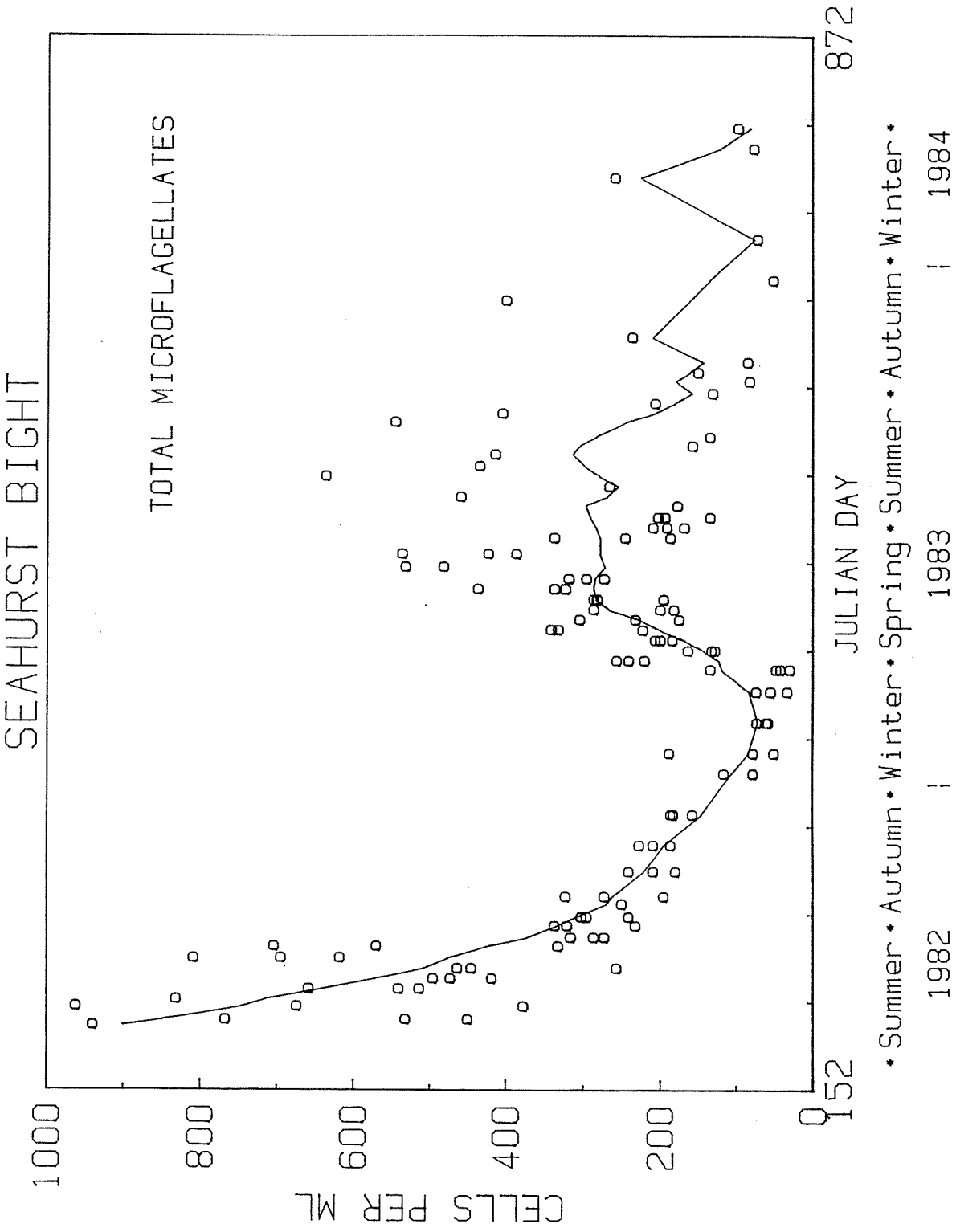

Figure 4.26a. Total microflagellates numbers from 50% light depth in Seahurst Bight with smooth distribution.

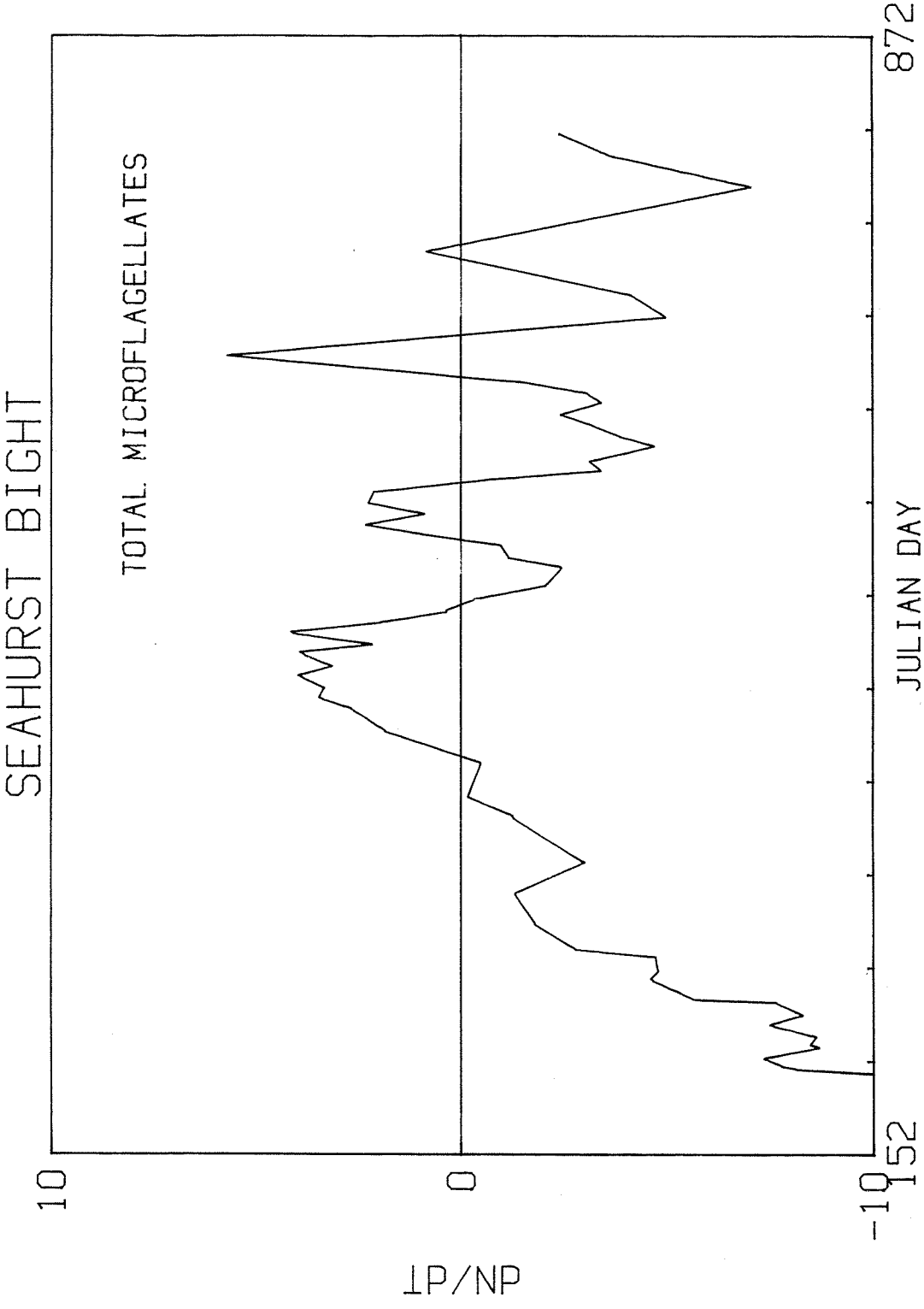

Figure 4.26b. Slope of smoothed distribution depicting rate of change of dinoflagellate numbers.

Table 4.13. Variability of phytoplankton species at stations 4, 7 and 10 in the Seahurst Bight using method of Section 4.3.4.10.

Property	Relative temporal variability	Relative spatial variability
Chlorophyll mg/m^3	1.16	0.27
Diatoms	2.68	0.29
Dinoflagellates	1.70	0.29
Microflagellates	0.45	0.22

terms of dry weight biomass and species numbers. The data includes net hauls from stations 4, 5, 6, 7, 12, and 13.

Only relative zooplankton abundance is obtained by the dry weight of material caught in the 209 um mesh net because the effect of zooplankton swarming and net avoidance on net catch are not understood. In addition the net retains a fraction of the phytoplankton and detritus which biases the zooplankton estimation. Given these problems, the zooplankton data are useful as a relative measure of abundance. The count data provides a better estimate of biomass by species and does not contain the phytoplankton and detritus bias of the dry weight data. An absolute correlation between animal counts and water column abundances can not be obtained because of unknown swarming and net avoidance behavior of the zooplankton.

The seasonal pattern of zooplankton dry weight is shown in Figure 4.27a. Spring and summer levels were significantly higher at the 90% confidence level than autumn and winter levels. In general, on a season by season basis the 1983 levels were greater than 1982 levels but the differences were not significant at the 90% confidence level (Table 4.14). A smoothed maximum dry weight net growth of 1.1 mg/m^3/d, occurred in mid-spring in 1983. The maximum net loss rate, 1.0 mg/m^3/d, occurred after the summer solstice (Figure 4.27b). Dry weight was also calculated from species counts using the conversion factors of Table 4.15. The species dry weights are a factor of 3 to 8 lower than the net dry weights (Table 4.14). The species dry weight only includes only the major zooplankton and excludes fragile forms and detritus that are included in the net haul dry weight.

Eight zooplankton species dominated the Seahurst Bight water column: four calanoids - Calanus pacificus, Pseudocalanus spp., Paracalanus sp., Microcalanus sp.; two cyclopiods - Corycaeus angilicus and Oithona similis;

Table 4.14. Carrying capacity and 90% gamma confidence interval for zooplankton net haul dry weight and species dry weight (mg/m^3). Species dry weight from total zooplankton counts coverted to dry weight according to Table 4.15. Data is collected from 6 week periods about the equinox and solstice dates for 1982 and 1983. Significantly higher levels in a period marked by *.

Period	Net Haul dry weight	Species dry weight
Summer solstice 1982	98.0 (82.3-98.5)	12.7 (11.1-16.0)
Summer solstice 1983	107.8 (95.1-125.8)	22.7 (19.2-28.8)
Autumnal equinox 1982	75.2 (65.3-75.2)	9.3 (8.2-11.0)
Autumnal equinox 1983	71.9 (62.5-88.2)	14.7 (11.3-21.2)
Winter solstice 1983	22.2 (20.1-24.9)	6.1 (4.4-9.8)
Winter solstice 1983	18.3 (14.7-24.4)	5.1 (4.2-6.4)
Vernal equinox 1982	31.7 (27.6-38.8)	4.9 (4.1-6.3)

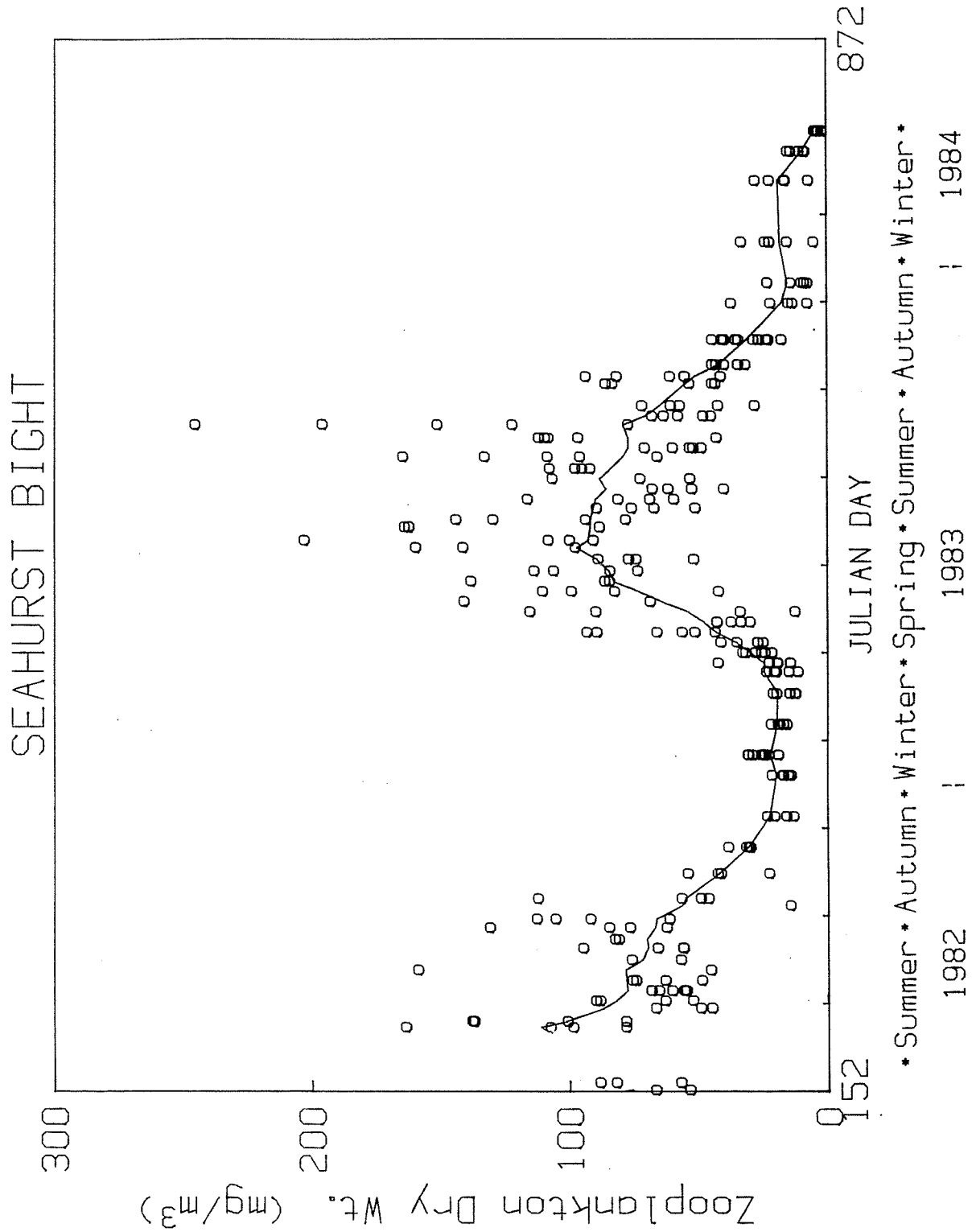

Figure 4.27a. Zooplankton dry weight from Seahurst Bight with smoothed distribution.

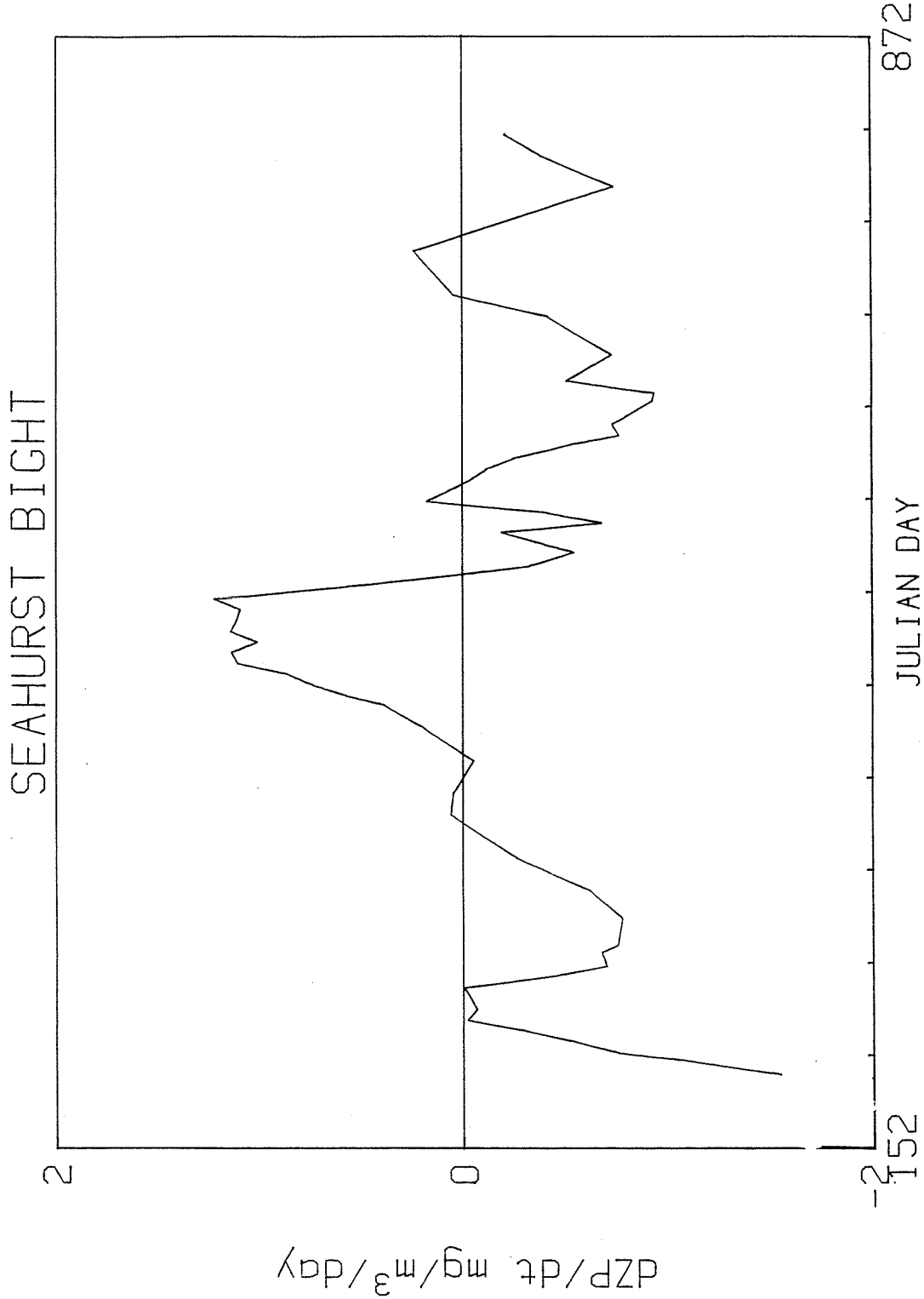

Figure 4.27b. Slope of smoothed distribution depicting rate of change of zooplankton dry weight.

Table 4.15.

DRY WEIGHT CONVERSION FACTORS

Species	Adults	Dry Weight (µg) Copepodid Stages						Average all stages	References
		5	4	3	2	1	ave.		
Calanus pacificus	170	127	55	23	9.3	4.3	44	65	Vidal, 1978, 1980
Pseudocalanus spp.	15	8.6	4.2	2.4	2.0	1.0	3.6	5.5	Vidal, 1978, 1980
Paracalanus sp.	5.9	3.8	2.1	1.3	.5	.2	1.6	2.3	*1
Corycaeus anglicus	4	2.2	1.6	1.0	.7	.2	1.1	1.6	*2
Microcalanus sp.	3.8	-	-	-	-	-	1.1	1.6	*1
Oithona similis	2.0	-	-	-	-	-	.6	.8	Uye, 1982
Oikopleura dioica	3	-	-	-	-	-	-	-	Uye, 1982

*1 Derived from length-weight relationship using Vidals' (1978) data for Pseudocalanus and Calanus and some mean lengths from this study.

*2 Derived from length-weight relationship for Oithona (Uye 1978) and lengths reported for Corycaeus (Gibson & Grice 1978).

and two larvaceans - Oikopleura dioica and Fritillaria borealis (Figure 4.28). These species are primarily herbivores, with the exception of Corycaeus angilicus, which is a raptorial carnivore in the adult stage and Oithona similis, which is an omnivore (Wickstead 1962; Marshall 1973). A full list of species found in Seahurst Bight is given in Appendix 4.E. Zooplankton count data from the stations were grouped by seasons and species. A Kruskal-Wallis test was applied to determine if any station had consistently higher or lower values on a species by species, and season by season basis. With two exceptions the stations could be considered similar and the data grouped (Table 4.16).

The smoothed seasonal distributions of the 8 dominant species are illustrated in terms of numbers (Figure 4.29a) and dry weight (Figure 4.29b). The dry weight was estimated using Table 4.15. Paracalanus sp. and Corycaeus anglicus dominated in number of animals but Calanus pacificus dominated in terms of biomass due to its large size. In general, the seasonal distributions fall into three patterns: Calanus and Pseudocalanus had little seasonality and high variability; Paracalanus, Microcalanus, Corycaeus and Oithona had clear seasonal patterns with relatively low levels of variability; and Oikopleura and Fritillaria had a clear seasonal cycle with a high degree of variability.

Calanus pacificus appeared to have both winter and summer peak abundances (Figure 4.30a) corresponding with peaks in the net growth rate near the winter and summer solstices (Figure 4.30b). Population declines were apparent at the vernal and autumnal equinoxes. The winter peak was presumably due to an overwintering population of late copepodid stages. The summer peak was associated with young copepodid stages. Summer solstice 1982 abundance was three times the 1983 abundance. For other seasons the differences between

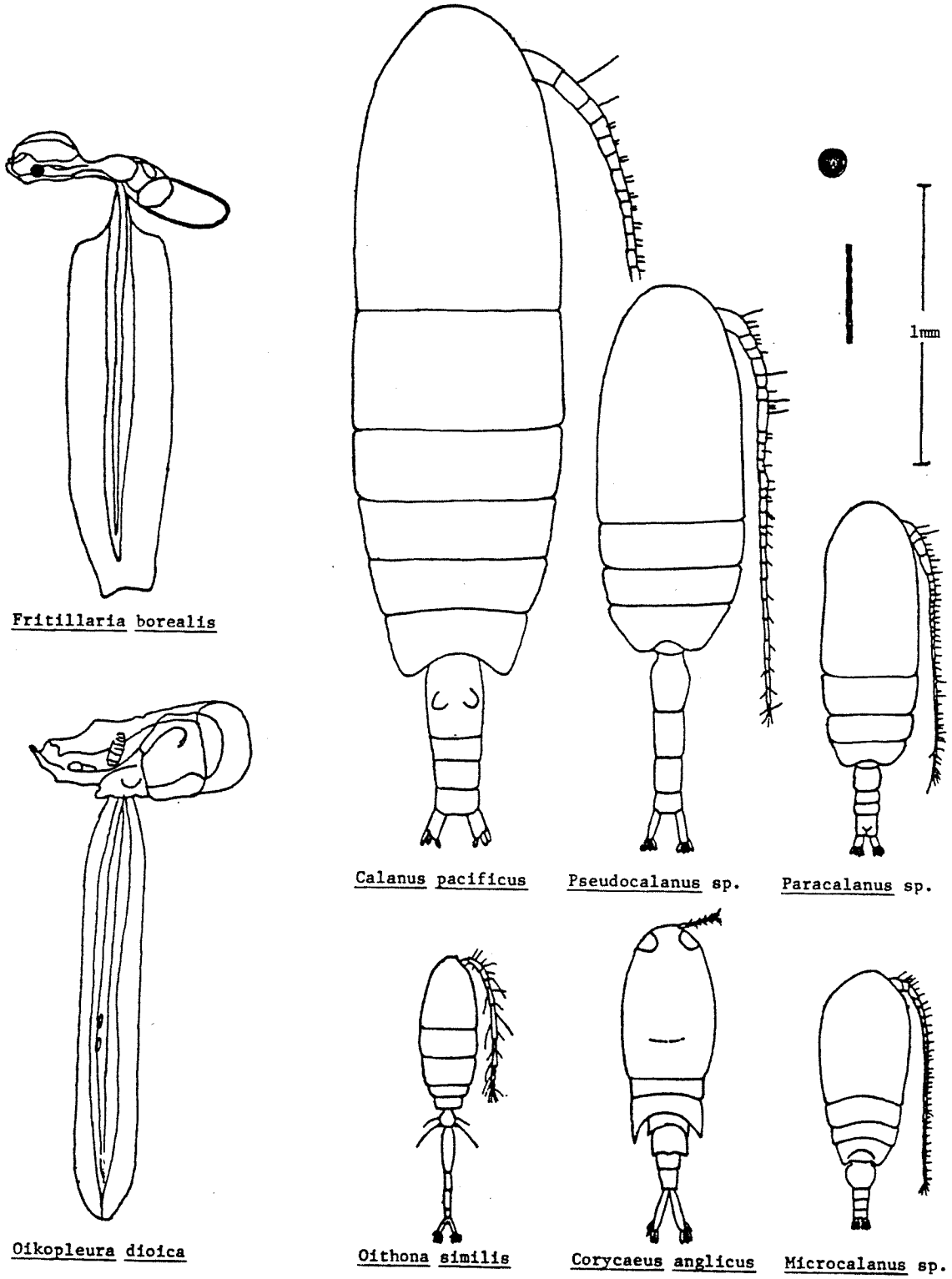

Figure 4.28. Illustrations of major zooplankton species found in Puget Sound. Drawn to a 1mm scale including typical phytoplankton cells.

Table 4.16. Kruskal-Wallis and Mann-Whitney test results for zooplankton species. The null hypothesis tested is H_0: the mean number of animals/m^3 of the given species is the same at the given stations for the given season. Corrections were made for tied ranks in both tests. (CR = cannot reject H_0, R = reject H_0.)

Variable	Season*	Stations	# of Observations	Degrees of freedom	Test statistic	Table value**	Result
Calanus pacificus	Sum 1982	4,5,6,7	43	3	4.07	6.25	CR
	Win 1982-83	4,5,6,7	30	3	.86	6.25	CR
	Sum 1983	4,5,6,7,12,13	62	5	7.24	9.24	CR
	Win 1983-84	4,7	14	-	27	38	CR
Paracalanus sp.	Sum 1982	4,5,6,7	48	3	.71	6.25	CR
	Win 1982-83	4,5,6,7	40	3	.01	6.25	CR
	Sum 1983	4,5,6,7,12,13	100	5	6.93	9.24	CR
	Win 1983-84	4,7	14	-	25	38	CR
Pseudocalanus spp.	Sum 1982	4,5,6,7	23	3	.67	6.25	CR
	Win 1982-83	4,5,6,7	32	3	3.16	6.25	CR
	Sum 1983	4,5,6,7,12,13	80	5	6.93	9.24	CR
	Win 1983-84	4,7	14	-	33	38	CR
Microcalanus spp.	Sum 1982	4,5,6,7	42	3	3.44	6.25	CR
	Win 1982-83	4,5,6,7	27	3	2.25	6.25	CR
	Sum 1983	4,5,6,7,12,13	96	5	14.74	9.24	R
	Win 1983-84	4,7	14	-	27	38	CR
Corycaeus anglicus	Sum 1982	4,5,67	58	3	6.64	6.25	R
	Win 1982-83	4,5,67	40	3	1.36	6.25	CR
	Sum 1983	4,5,6,712,13	100	5	6.54	9.24	CR
	Win 1983-84	4,7	14	-	26	38	CR
Oithona similis	Sum 1982	4,5,6,7	54	3	1.35	6.25	CR
	Win 1982-83	4,5,6,7	40	3	.98	6.25	CR
	Sum 1983	4,5,6,7,12,13	97	5	4.49	9.24	CR
	Win 1983-84	4,7	14	-	31	38	CR

Table 4.16 (continued).

Variable	Season*	Stations	# of Observations	Degrees of freedom	Test statistic	Table value**	Result
Oikopleura dioica	Sum 1982	4,5,6,7	50	3	3.08	6.25	CR
	Win 1982-83	4,5,6,7	16	3	.58	6.25	CR
	Sum 1983	4,5,6,7,12,13	65	5	3.65	9.24	CR
	Win 1983-84	4,7	6	-	5.5	9	CR
Fritillaria borealis	Sum 1982	4,5,6,7	28	3	4.14	6.25	CR
	Win 1982-83	4,5,6,7	3	3	-	-	-
	Sum 1983	4,5,6,7,12,13	37	5	4.09	9.24	CR
	Win 1983-84	4,7	0	-	-	-	-

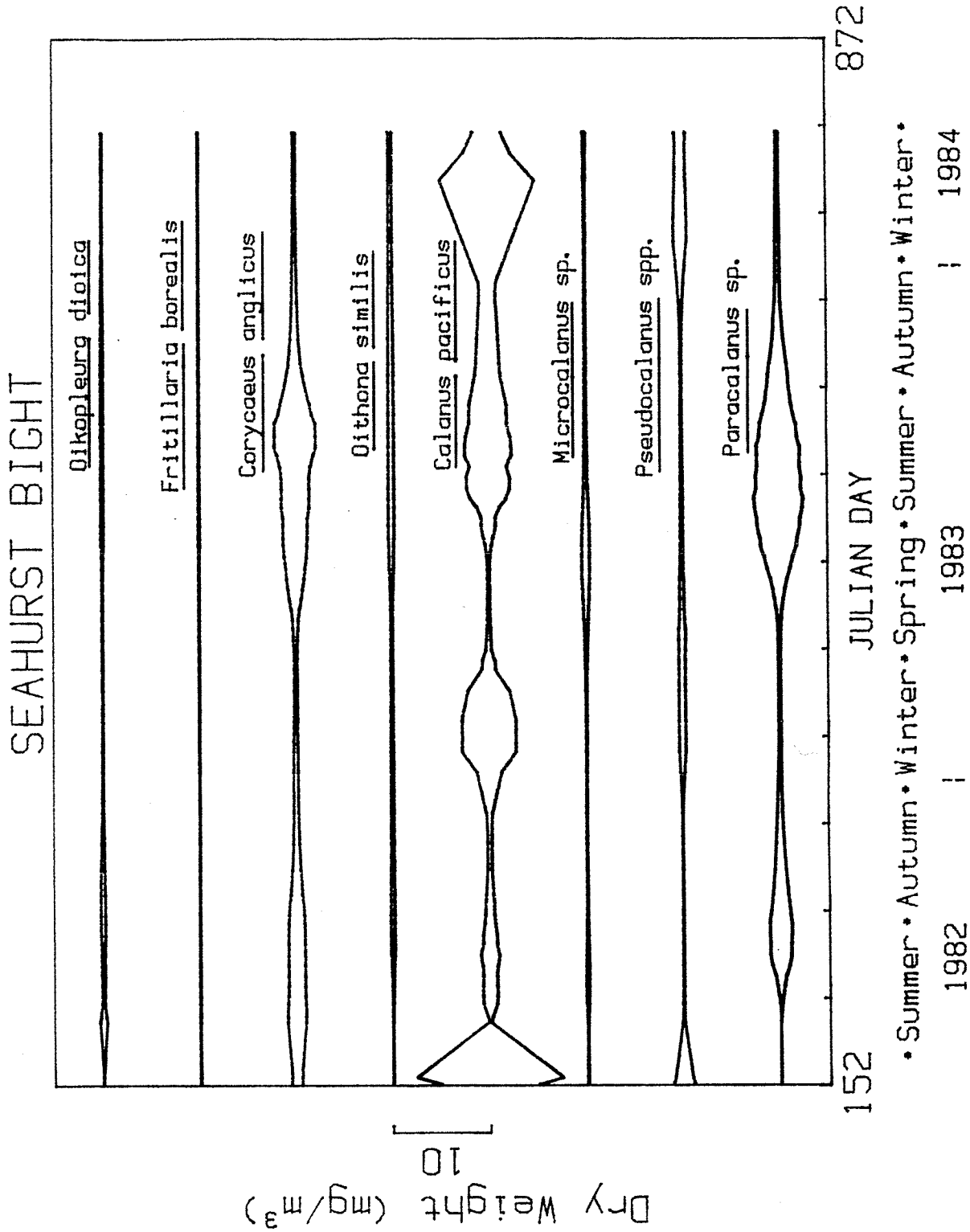

Figure 4.29a. Dry weight biomass of major zooplankton species over time in Seahurst Bight. Scale depicts 10 mg/m^3 of animal dry weight.

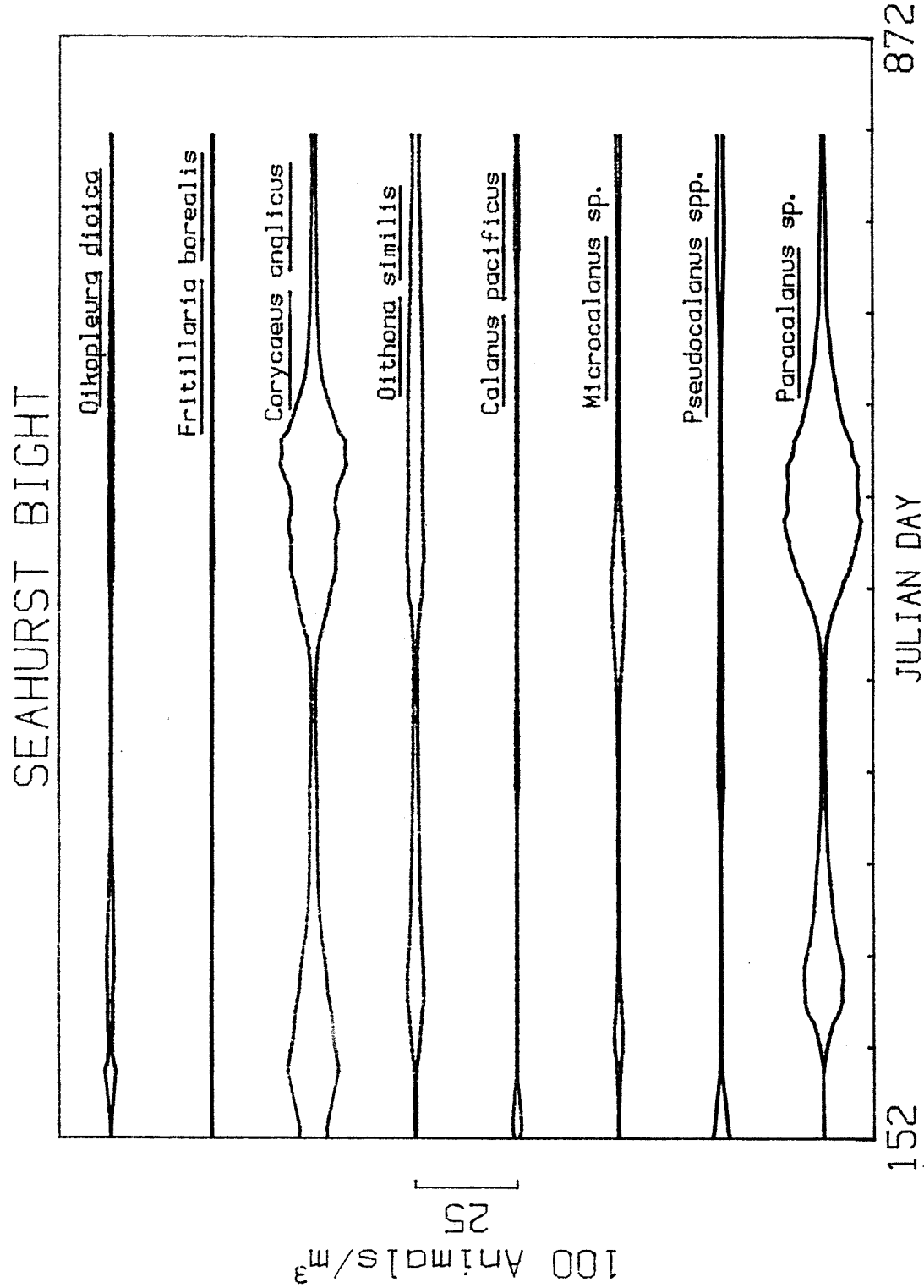

Figure 4.29b. Numbers of major zooplankton species over time in Seahurst Bight. Scale on left depicts 100 animals/m^3.

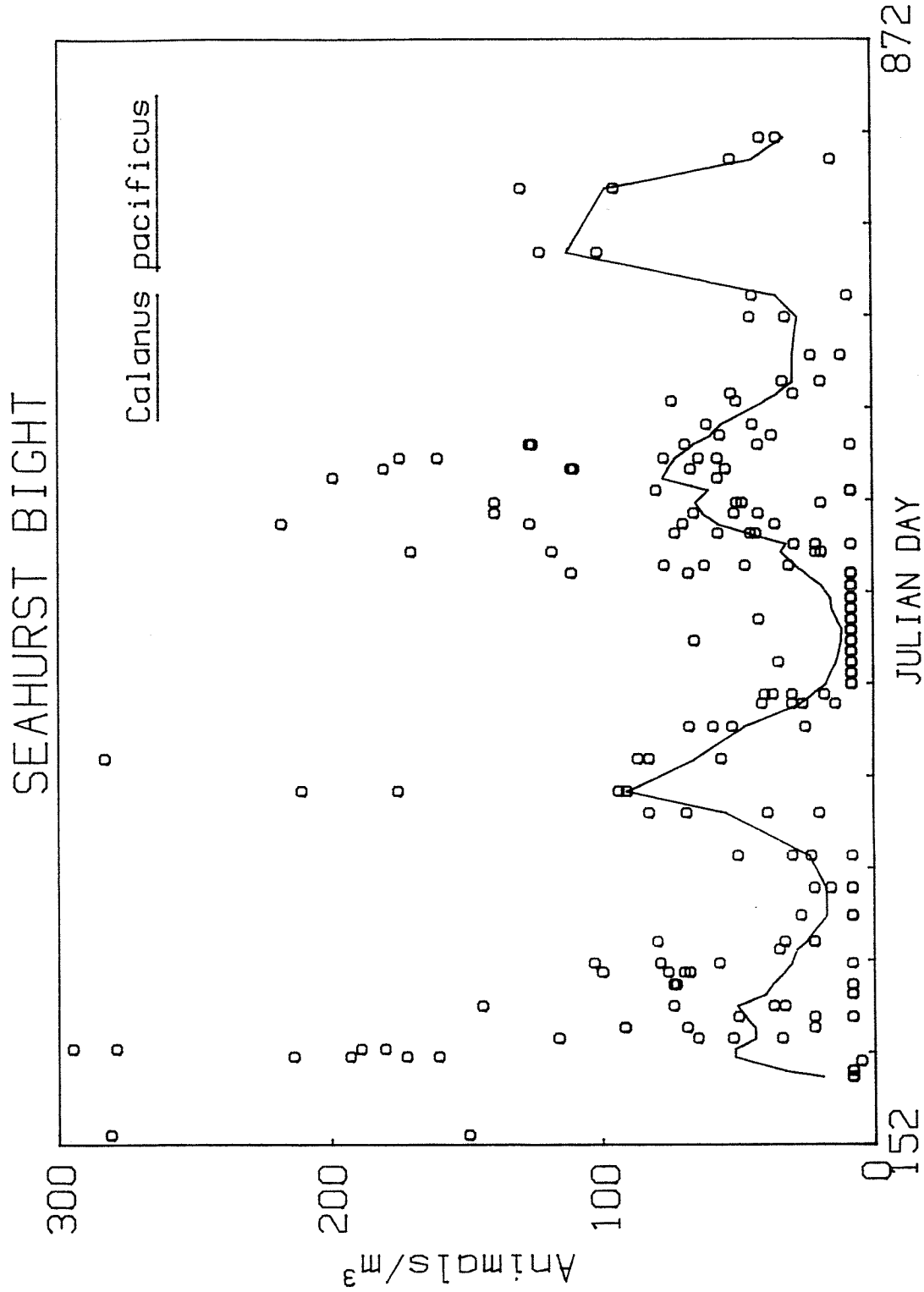

Figure 4.30a. Total numbers of Calanus pacificus in Seahurst Bight with smooth distribution.

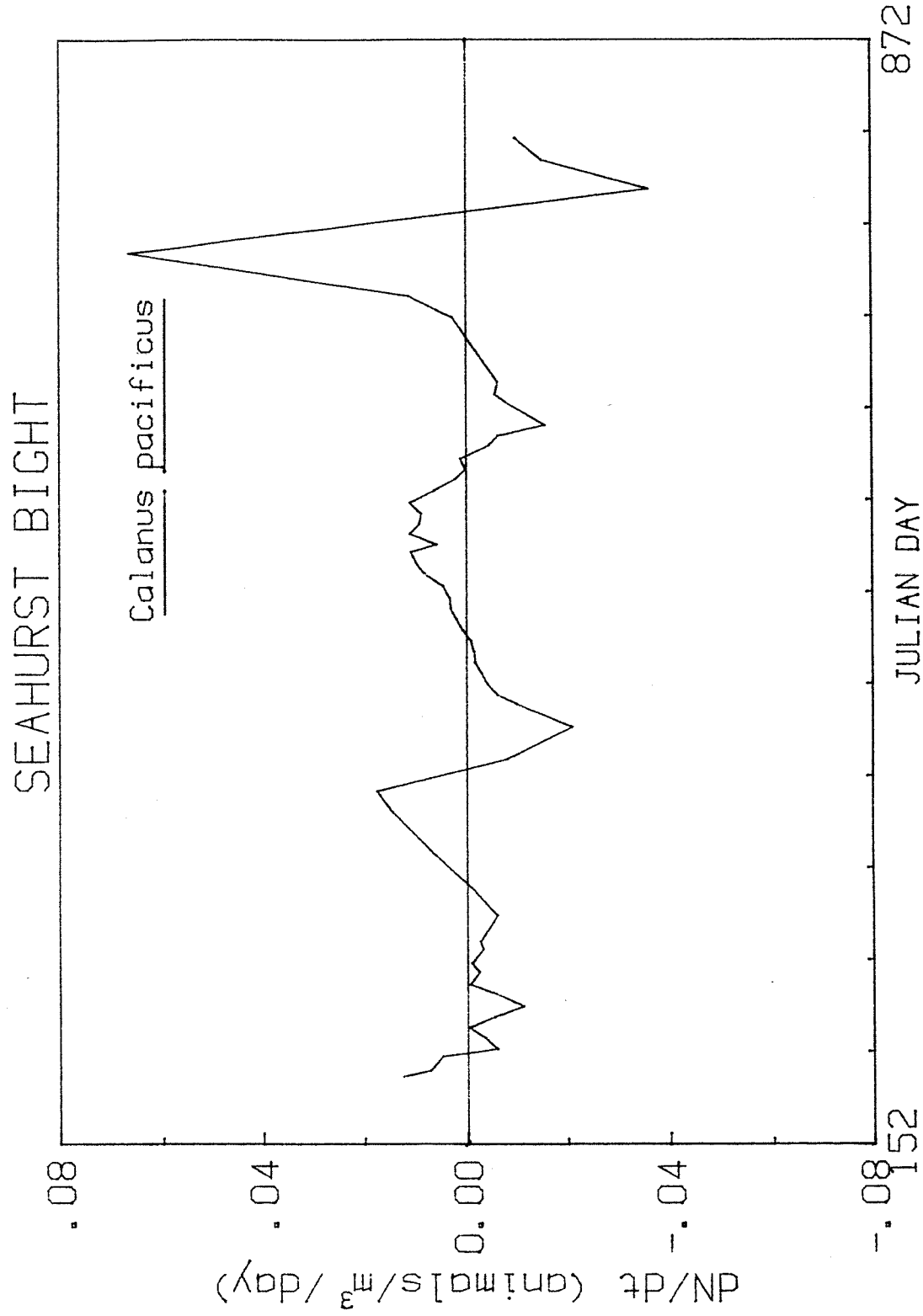

Figure 4.30b. Slope of smoothed distribution depicting rate of change of Calanus pacificus numbers.

years were not significant (Table 4.17). On a biomass basis the seasonal distributions of Calanus pacificus were not significantly different between summer and winter solstices but Calanus pacificus was dominant over other species (Table 4.18).

Pseudocalanus had a weak seasonal cycle and numbers similar to that of the much larger Calanus (Figure 4.31a and 4.31b and Table 4.17). The net growth rate was maximum in the winter. This may reflect the presence of an overwintering late state that became susceptable to capture in the net during the winter season. Pseudocalanus biomass was never significant over the year.

Paracalanus, dominant in terms of numbers and biomass, had a smooth seasonal pattern with maximum numbers (Figure 4.32a) and maximum net growth rates (Figure 4.32b) near the summer solstice. The largest decline in the population occurred after the autumnal equinox. Winter solstice abundance and biomass for 1982 and 1983 are similar within the 90% gamma limits but near the summer solstice of 1982 Paracalanus levels were low while in 1983 they dominated the zooplankton community (Tables 4.17 and 4.18).

Microcalanus had a clear seasonal cycle similar to Paracalanus but was not dominant in either numbers or biomass (Figure 4.33a). The maximum growth rate occurred shortly after the spring equinox and the maximum loss occurred near the summer solstice (Figure 4.33b). Microcalanus populations were low at the summer equinox in 1982 (Table 4.17).

The cyclopoid copepod, Corycaeus anglicus, has a smooth seasonal cycle similar to that of Paracalanus. The population maximum was in the summer of 1983 (Figure 4.34a) and the maximum net growth rate, in the spring, was of the same order and coincident with the Paracalanus maximum rate. The maximum loss occurred about the autumnal equinox (Figure 4.34b). Corycaeus seasonal abundances in 1983 were about twice the 1982 levels. The differences were

Table 4.17. Gamma mean values and 90% confidence interval for the numbers (animals/m^3) of the 8 dominant zooplankton species. Data grouped in 6 week periods about the equinox and solstice periods in 1982 and 1983. Groups contain 5 to 24 data points. Significantly higher levels for a season marked with *.

Species	Summer Solstice 1982	Summer Solstice 1983	Winter Solstice 1982	Winter Solstice 1983
Calanus pacificus	221* (145 - 402)	67 (53 - 78)	79 (55 - 132)	59 (42 - 97)
Paracalanus sp.		1918* (1660 - 2300)	150 (113 - 220)	153 (133 - 177)
Pseudocalanus spp.	250* (221 - 305)	78 (59 - 148)	114 (81 - 187)	154 (134 - 179)
Microcalanus sp.		272 (227 - 352)	40 (32 - 52)	39 (26 - 88)
Corycaeus angilicus	893 (824 - 990)	1356* (1102 - 1915)	199 (170 - 238)	145 (125 - 170)
Oithona similis	175 (151 - 207)	424* (354 - 550)	171 (137 - 223)	252 (213 - 304)
Oikopleura dioica	594 (455 - 1390)	1189 (923 - 1920)	50 (39 - 71)	
Fritillaria borelis		1072 (820 - 1809)		

Species	Vernal Equinox 1982	Vernal Equinox 1983	Autumnal Equinox 1982	Autumnal Equinox 1983
Calanus pacificus	37 (30 - 48)		65 (54 - 84)	58 (46 - 78)
Paracalanus sp.	69 (60 - 85)		1001 (878 - 1180)	1334 (1010 - 2050)
Pseudocalanus spp.	93 (78 - 119)		42* (34 - 55)	10 (7 - 14)

Table 4.17 (continued).

Species	Vernal Equinox 1982	Vernal Equinox 1983	Autumnal Equinox 1982	Autumnal Equinox 1983
Microcalanus sp.	136 (117 - 166)		132* (98 - 225)	47 (33 - 86)
Corycaeus angilicus	144 (119 - 190)		666 (578 - 798)	1895* (1369 - 3474)
Oithona similis	101 (88 - 120)		393 (338 - 480)	428 (354 - 544)
Oikopleura dioica	131 (85 - 249)		310 (250 - 581)	551 (376 - 1418)
Fritillaria borelis			151 (110 - 267)	186 (110 - 529)

Table 4.18. Gamma mean values and 90% confidence interval for biomass (mg/m^3) of the 5 most dominant zooplankton species, total species biomass and zooplankton dry weight from net hauls. Data grouped in 6 week periods about the summer and winter solstice in 1982 and 1983. Groups contain 6 to 24 data points. Significantly higher levels for a season marked with *.

Species	Summer Solstice 1982	Summer Solstice 1983	Winter Solstice 1982	Winter Solstice 1983
Species dry weight	12.7 (11.1-16.0)	22.7* (19.2-28.8)	6.1 (4.4-9.8)	5.1 (4.2-6.4)
Calanus pacificus	5.0 (5.9-15.4)	5.3 (4.2-9.4)	4.0 (2.7-9.2)	2.9 (2.1-4.5)
Paracalanus sp.	0.06 (0.04-0.21)	5.41* (4.64-6.62)	0.23 (0.22-0.47)	0.32 (0.32-0.41)
Corycaeus anglicus	1.43 (1.32-1.58)	3.18* (2.62-4.28)	0.46 (0.39-0.55)	0.37 (0.31-0.46)
Oikopleura dioica	1.03 (1.18-3.05)	2.54 (2.12-6.15)	0.06 (0.04-0.23)	0.06 (0.04-0.5)

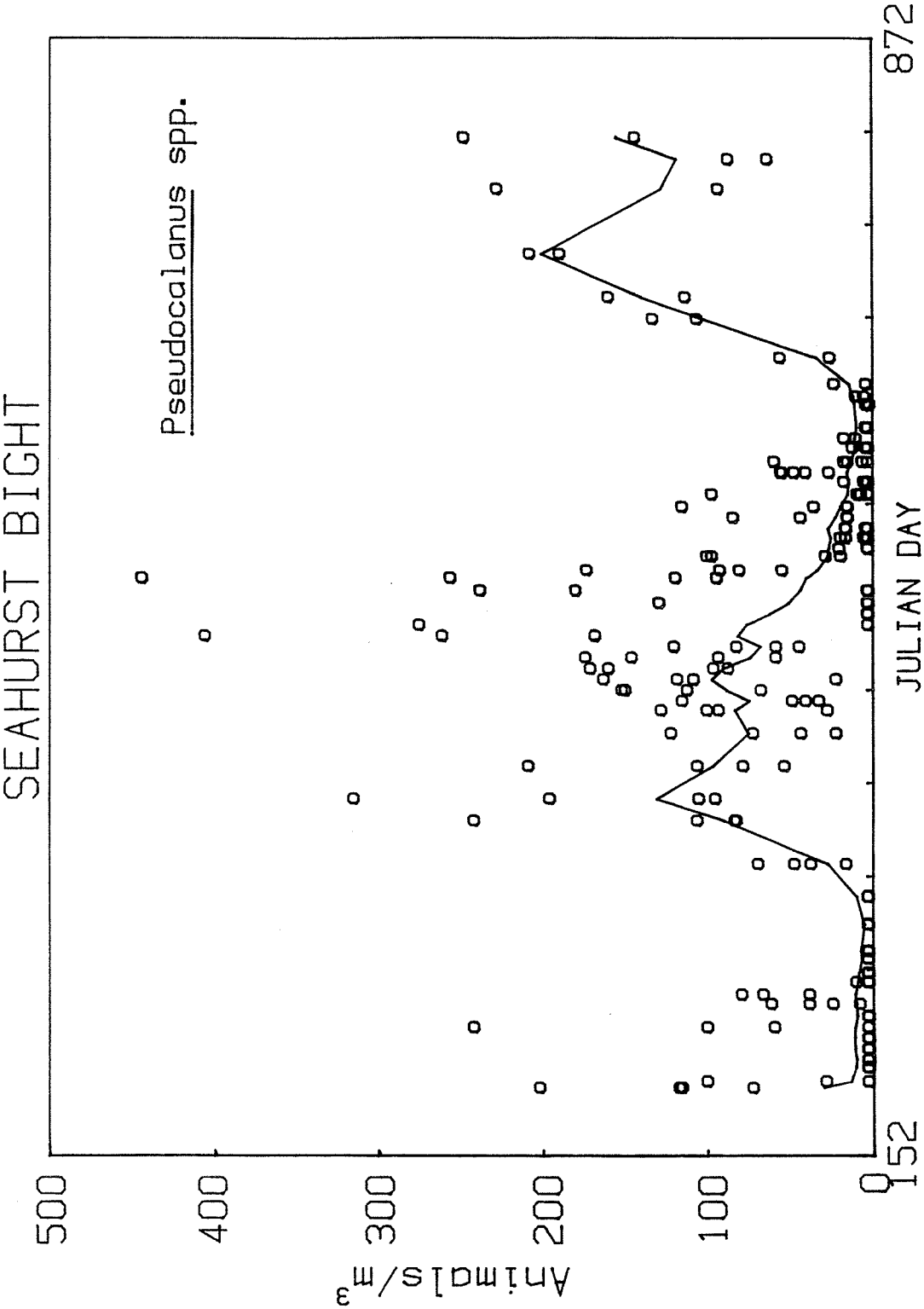

Figure 4.31a. Total numbers of Pseudocalanus spp. in Seahurst Bight with smooth distribution.

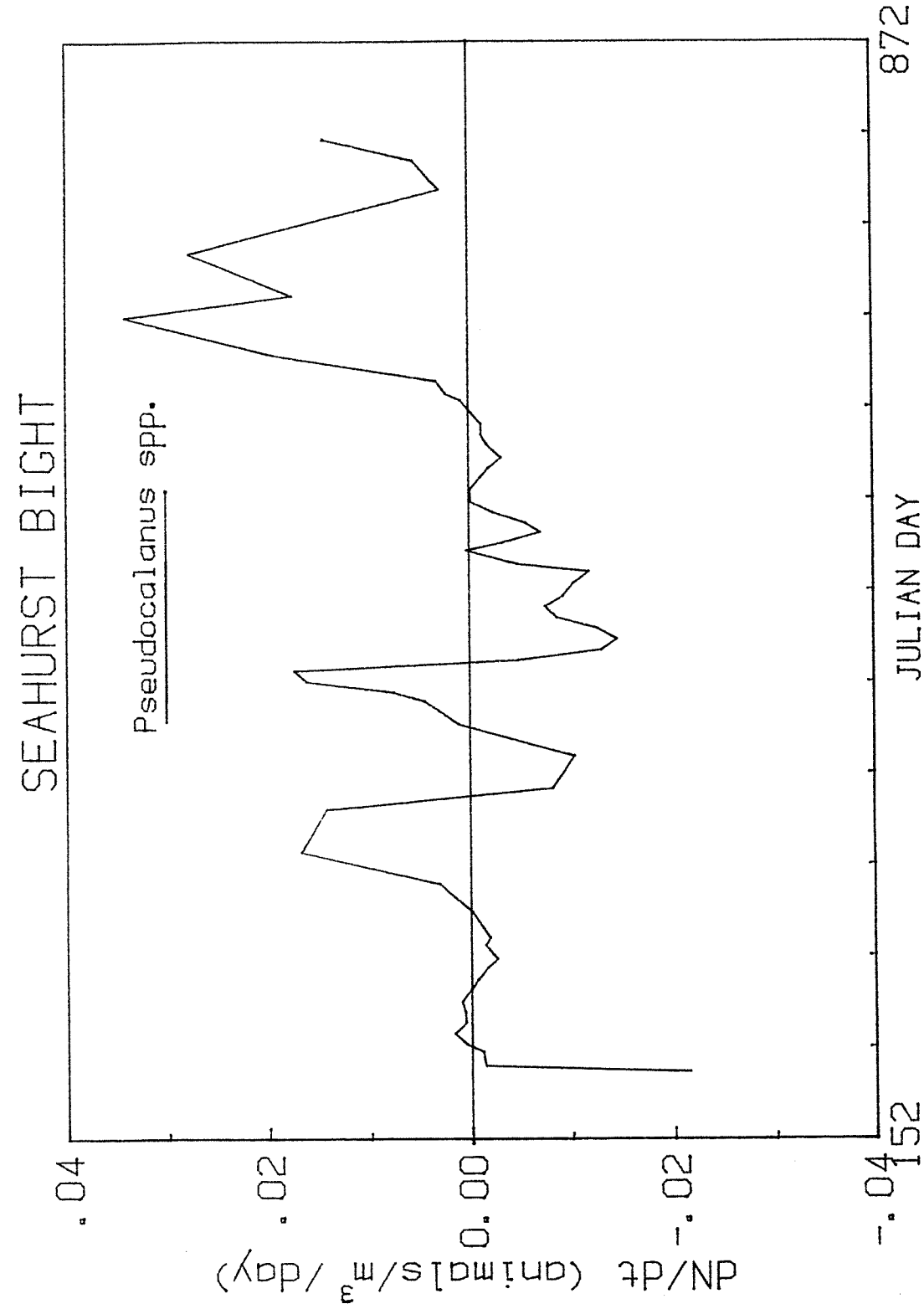

Figure 4.31b. Slope of smoothed distribution depicting rate of change of Pseudocalanus spp. numbers.

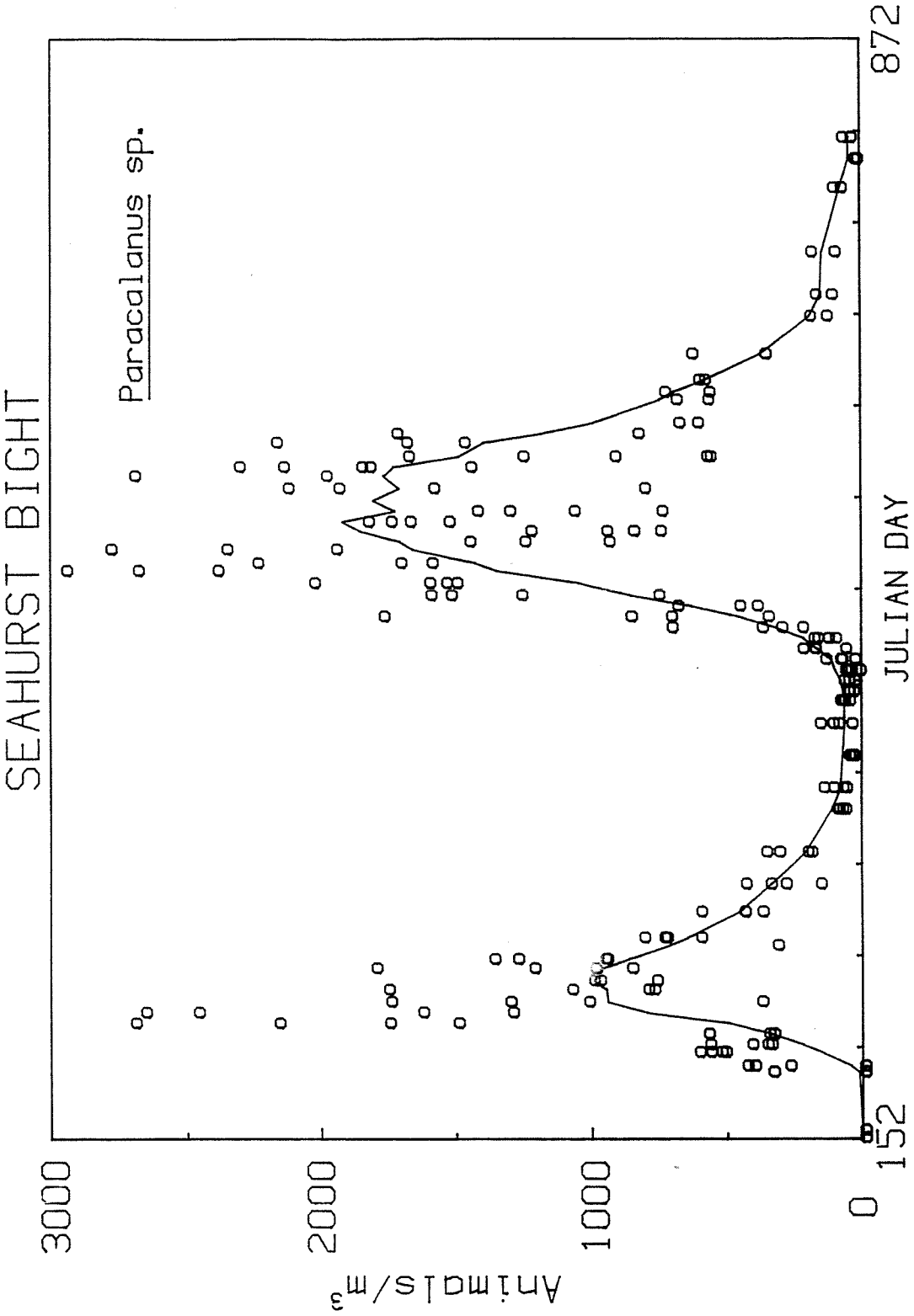

Figure 4.32a. Total numbers of Paracalanus sp. in Seahurst Bight with smooth distribution.

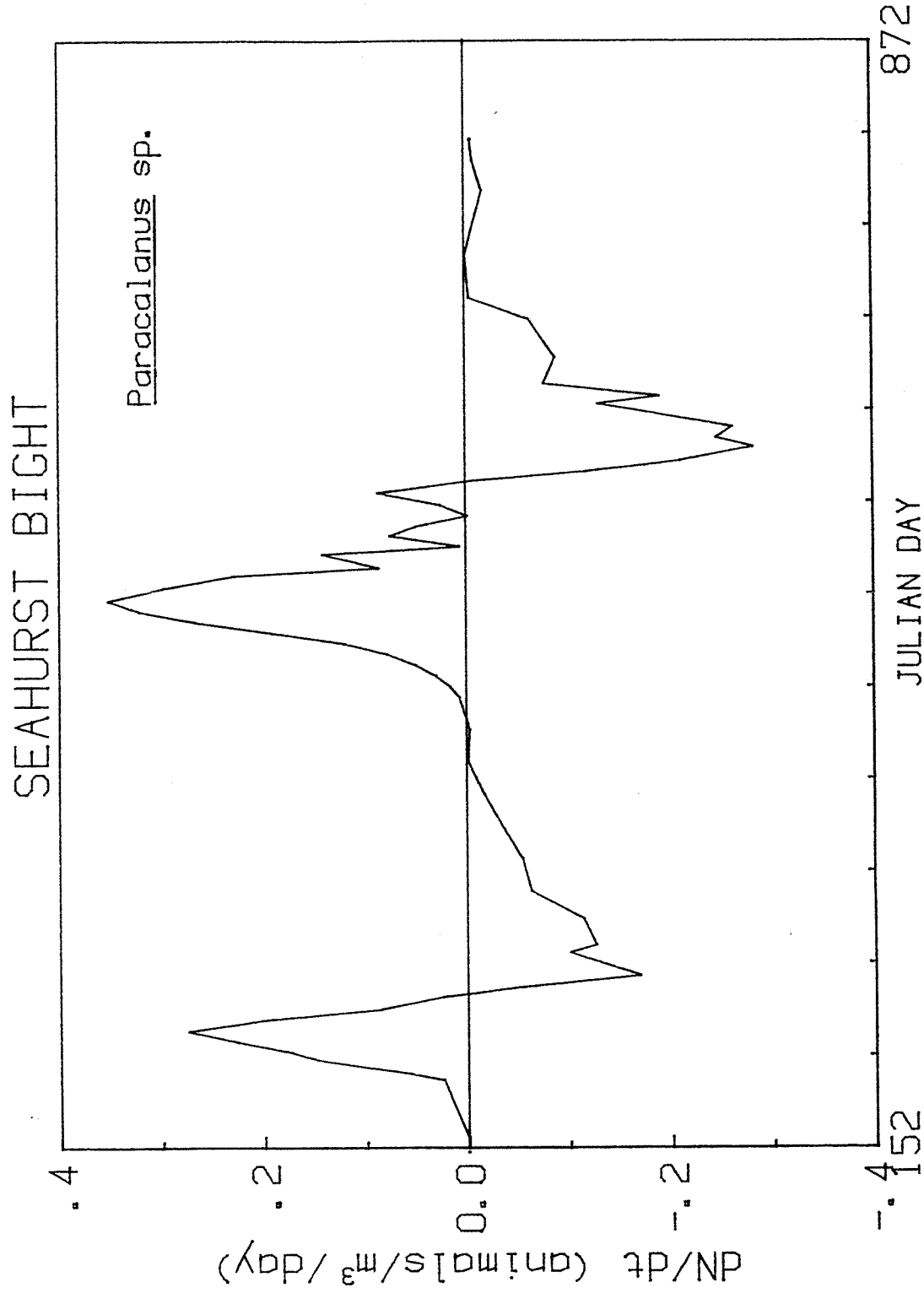

Figure 4.32b. Slope of smoothed distribution depicting rate of change of Paracalanus sp. numbers.

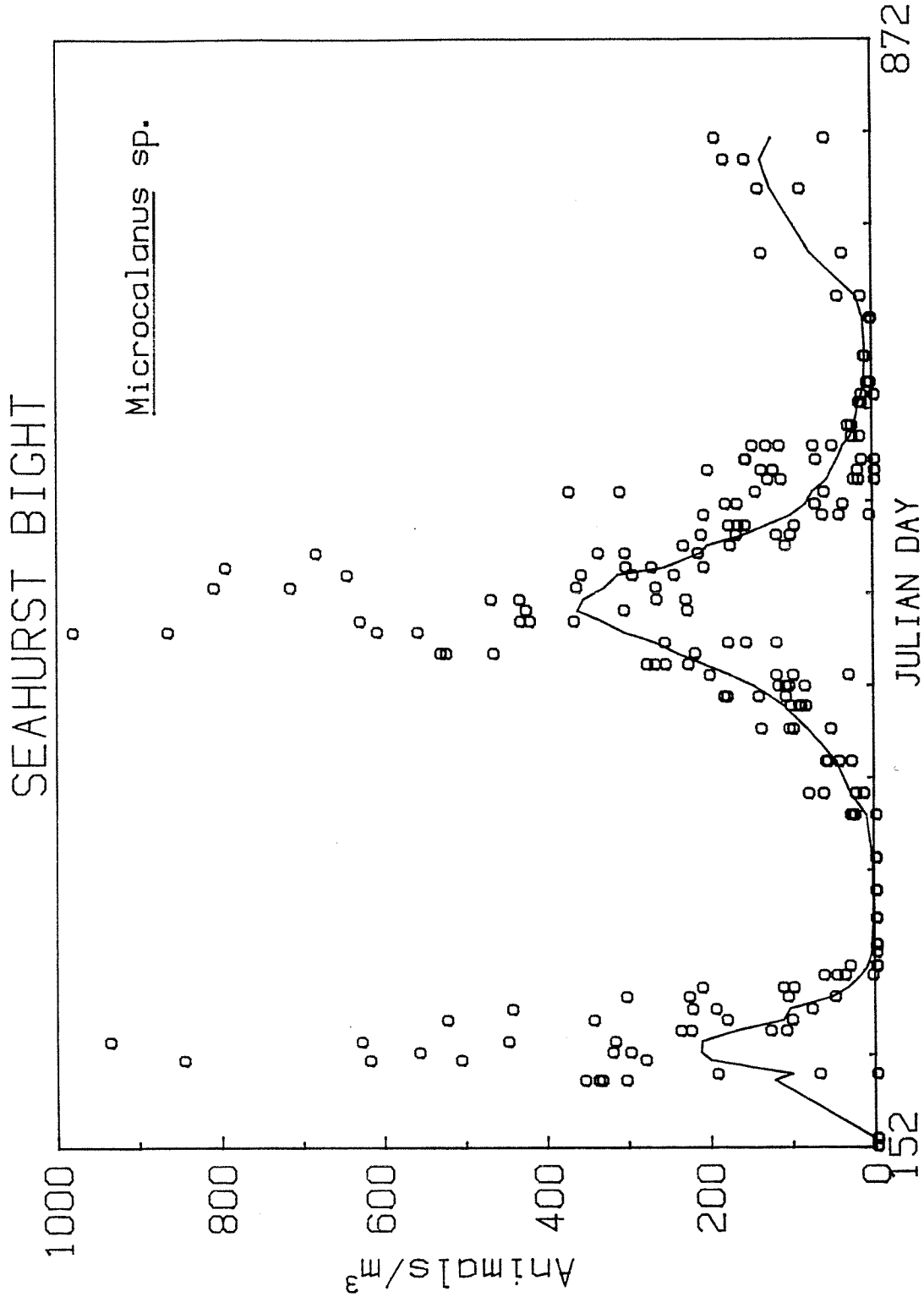

Figure 4.33a. Total numbers of Microcalanus sp. in Seahurst Bight with smooth distribution.

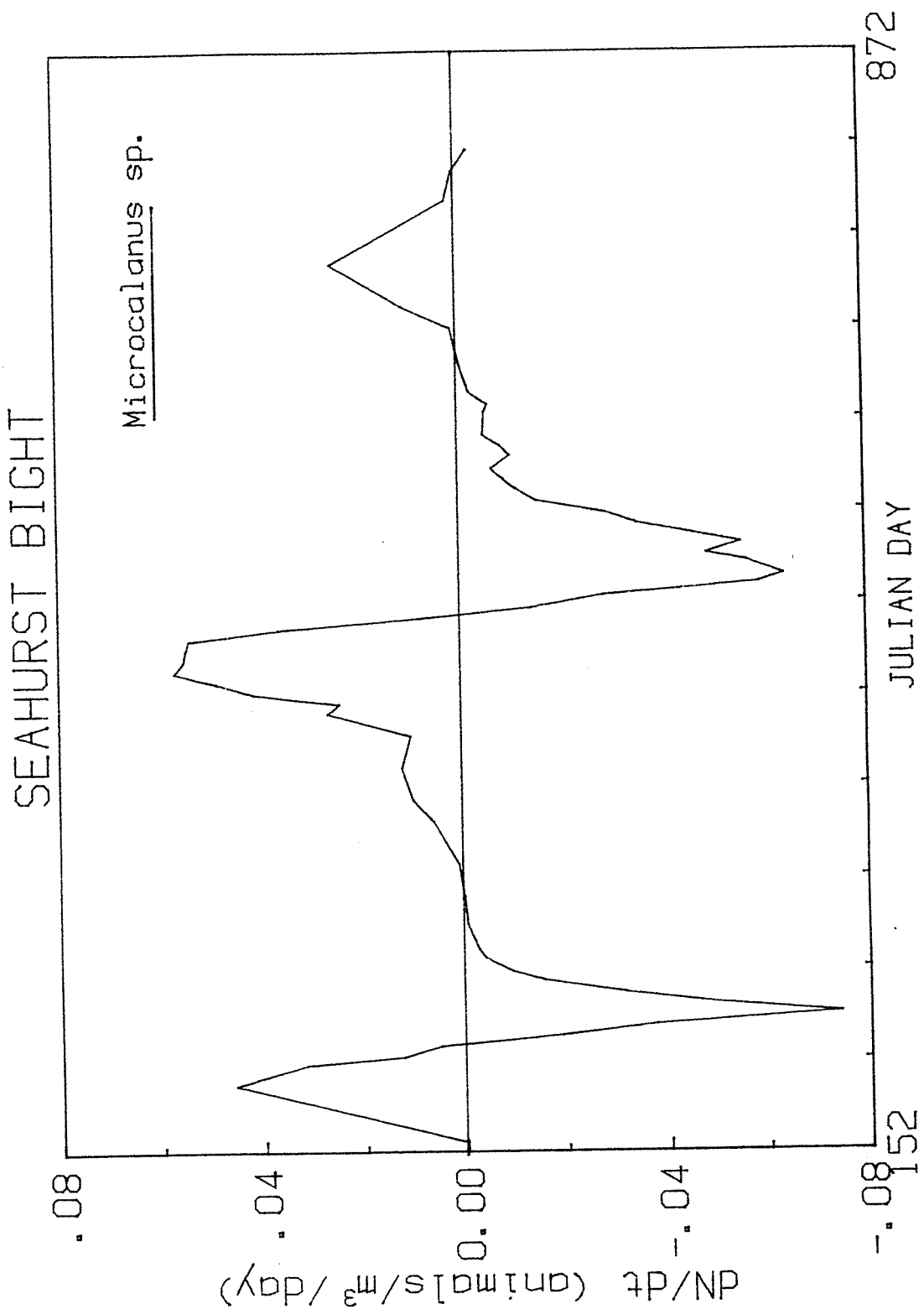

Figure 4.33b. Slope of smoothed distribution depicting rate of change of Microcalanus sp. numbers.

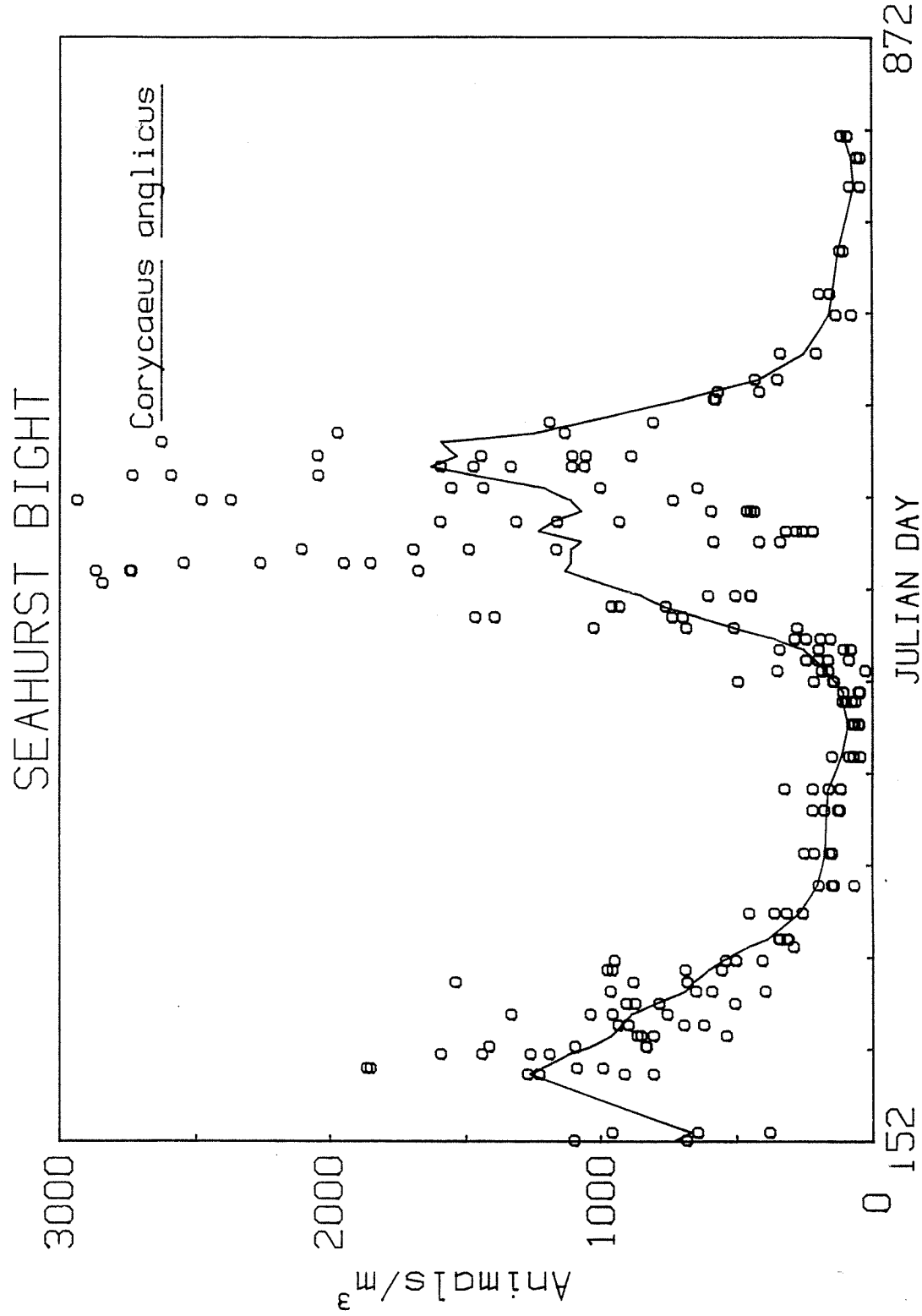

Figure 4.34a. Total numbers of Corycaeus anglicus in Seahurst Bight with smooth distribution.

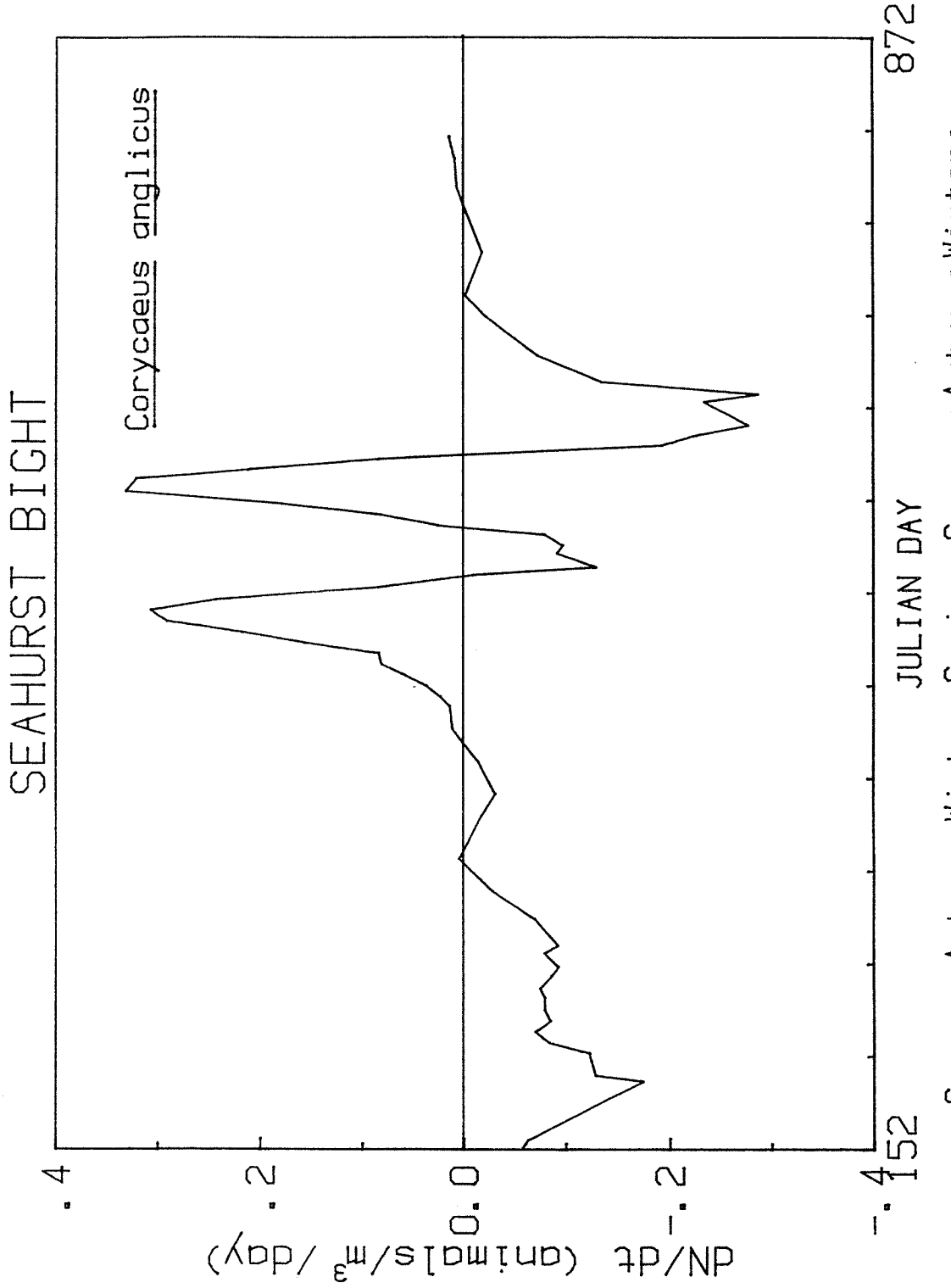

Figure 4.34b. Slope of smoothed distribution depicting rate of change of Corycaeus anglicus numbers.

significant at the 90% gamma limit (Table 4.17).

The cyclopoid copepod, Oithona similis, had a smooth seasonal cycle similar to Corycaeus with the maximum biomass occurring in the summer (Figure 4.35a) and maximum net growth rates in the spring and summer (Figure 4.35b). Oithona contributed little to the total biomass because of its small size (Figure 4.27). Abundances were slightly larger in 1983 than in 1982 (Table 4.17).

The larvaceans showed clear seasonal cycles with high summer and low winter populations. Winter levels were often to low to be counted along with the major species. In these cases the abundances were reported with zero values. For Oikpleura (Figure 4.36a) high summer levels were evident for 1983 but differences between the autumnal equinox in 1982 and 1983 were not significant at the 90% gamma confidence level (Table 4.17). Net growth rate peaks occurred in mid-spring and mid-summer and between these times the rates decreased. In the autumn populations decreased (Figure 4.36b). Fritillaria had spring and summer high values and winter lows (Figure 4.37a). Growth was positive in the spring and negative in the summer with autumn and winter values being near zero (Figure 4.37b).

In all species temporal variability exceeded spatial variability by a factor of 2 to 3. In terms of spatial variability two groups were evident. Low spatial variability species (25 to 30%) included Paracalanus, Corycaeus and Oithona. High spatial variability species (40 to 50%) included Calanus, Pseudocalanus, Microcalaus, Oikopleura and Fritillaria. In terms of temporal variability three groups were evident. Oithona had the lowest temporal variability (47%). An intermediate group (63 to 76%) included Paracalanus, Microcalanus and Coryaeus. The high variability group (90 to 172%) included Calanus, Pseudocalanus, Fritillaria and Oikpleura. The net dry weight

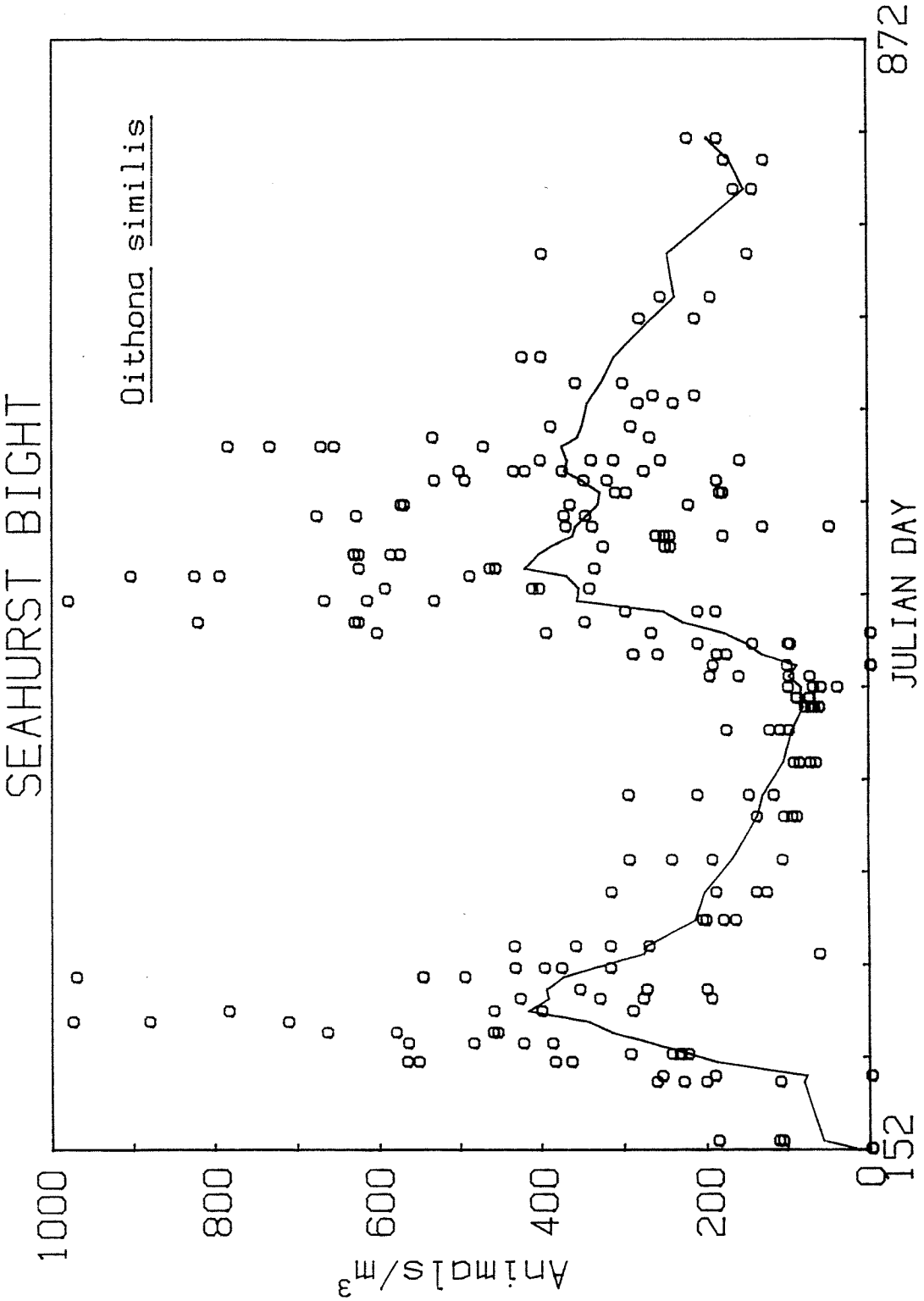

Figure 4.35a. Total numbers of Oithona similis in Seahurst Bight with smooth distribution.

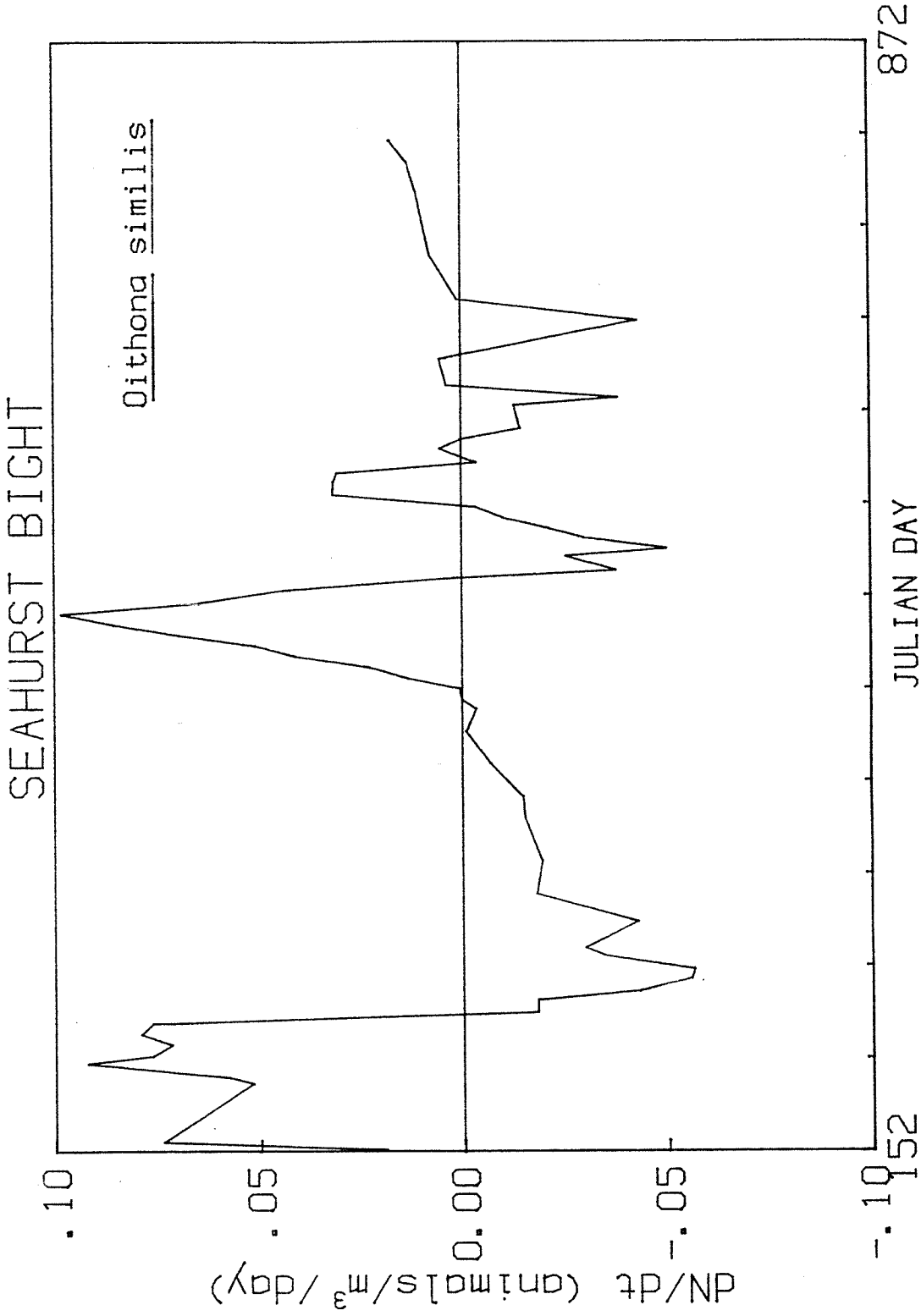

Figure 4.35b. Slope of smoothed distribution depicting rate of change of Oithona similis numbers.

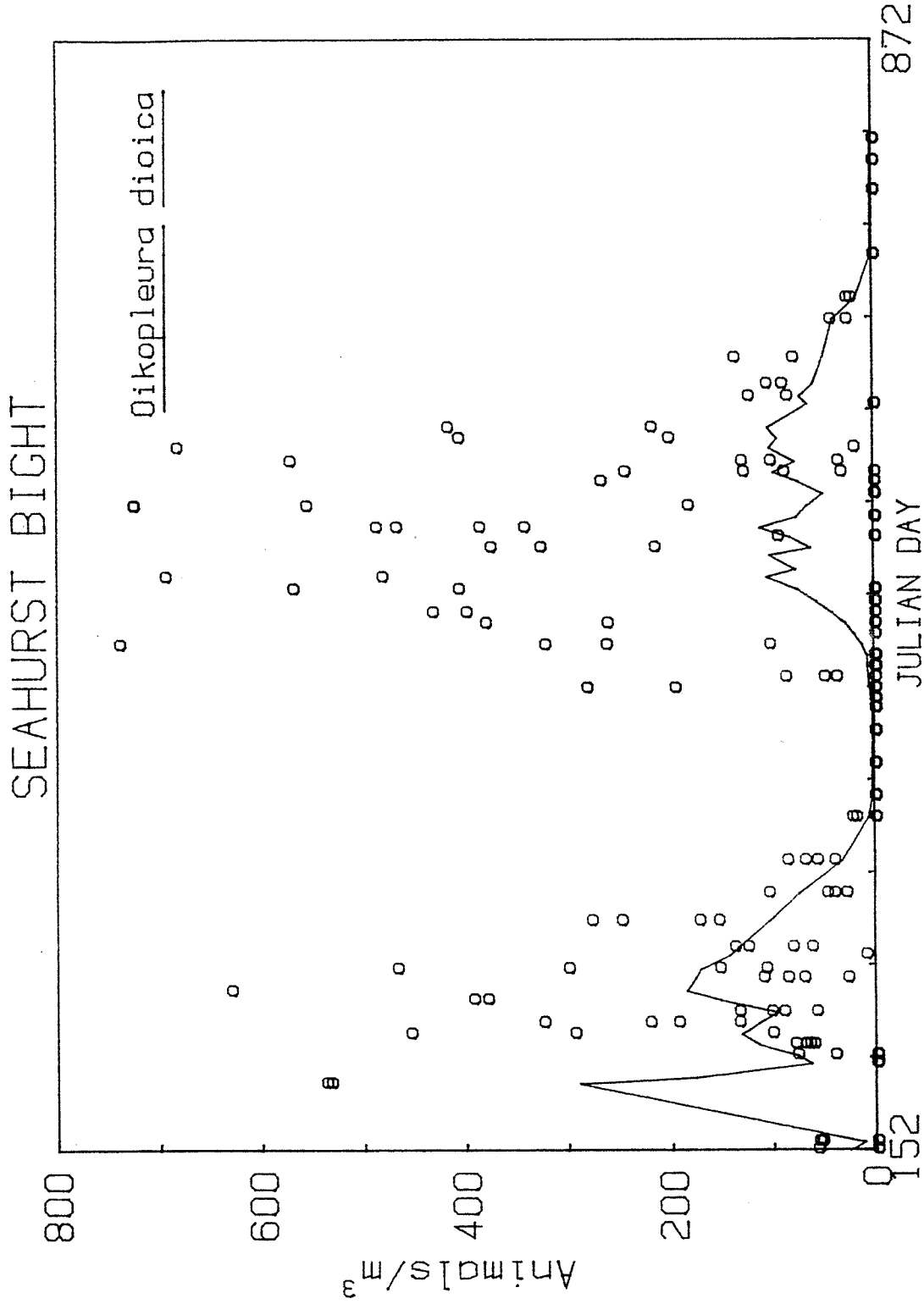

Figure 4.36a. Total numbers of Oikopleura dioica in Seahurst Bight with smooth distribution.

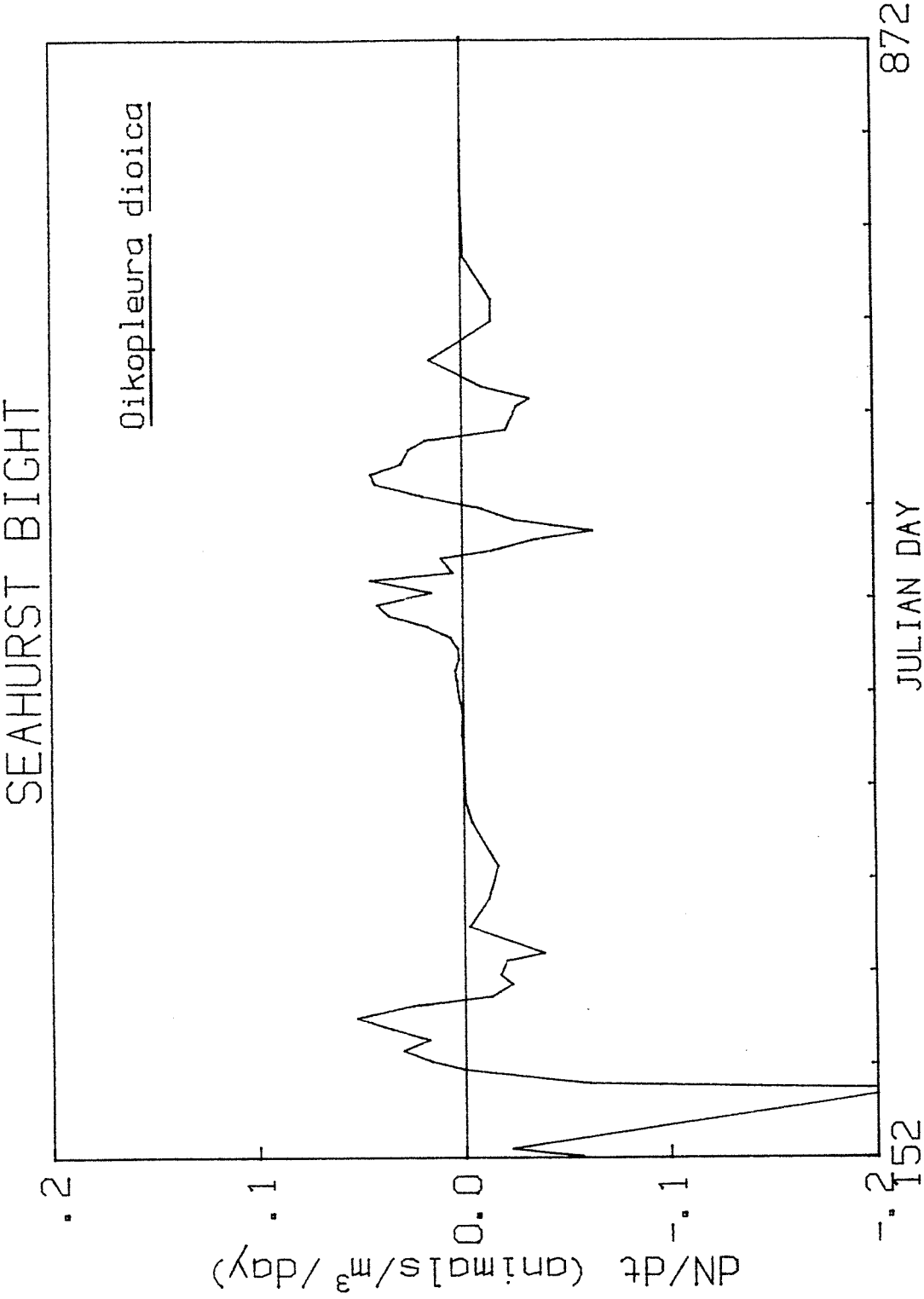

Figure 4.36b. Slope of smoothed distribution depicting rate of change of Oikopleura dioica numbers.

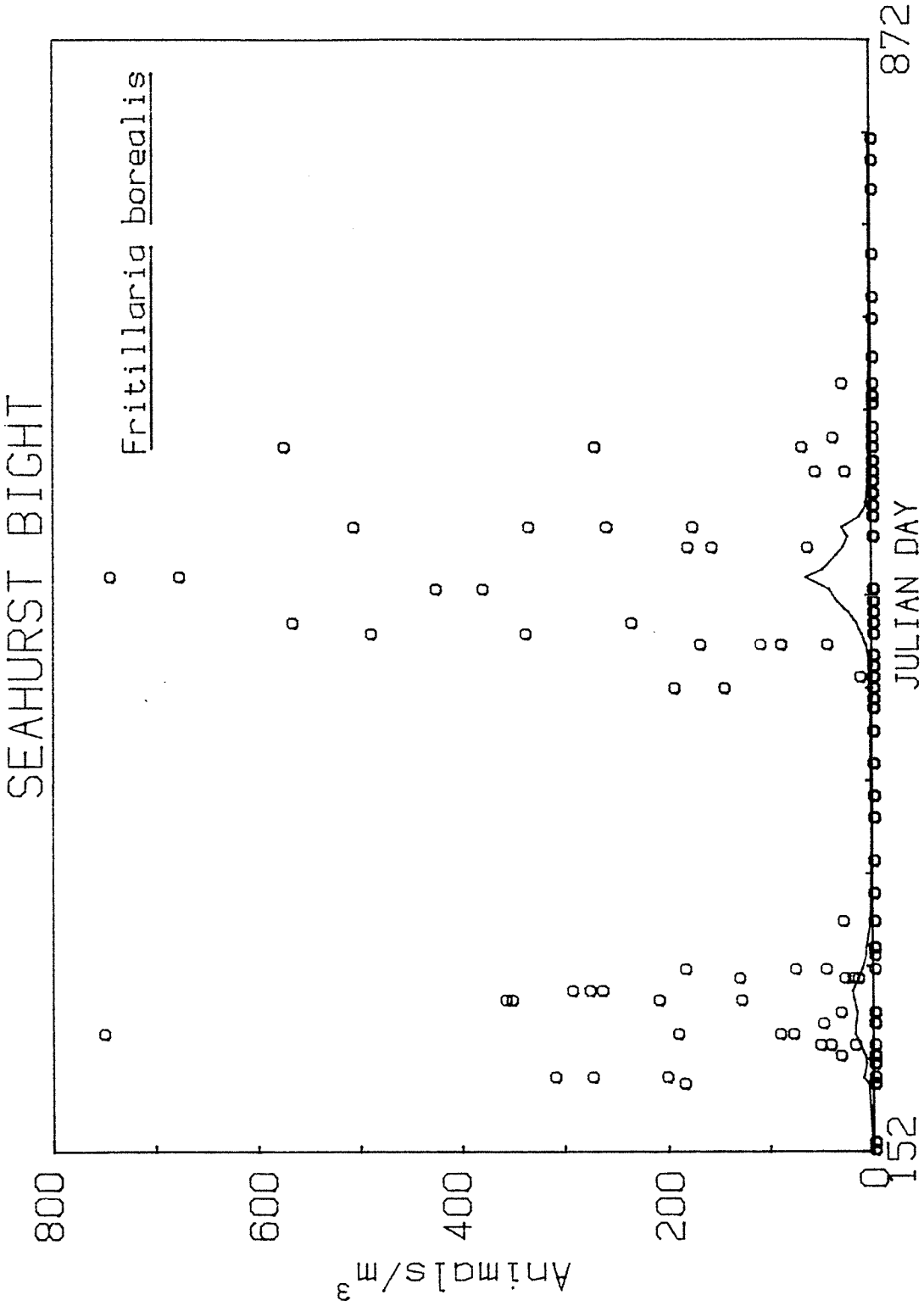

Figure 4.37a. Total numbers of Fritillaria borealis in Seahurst Bight with smooth distribution.

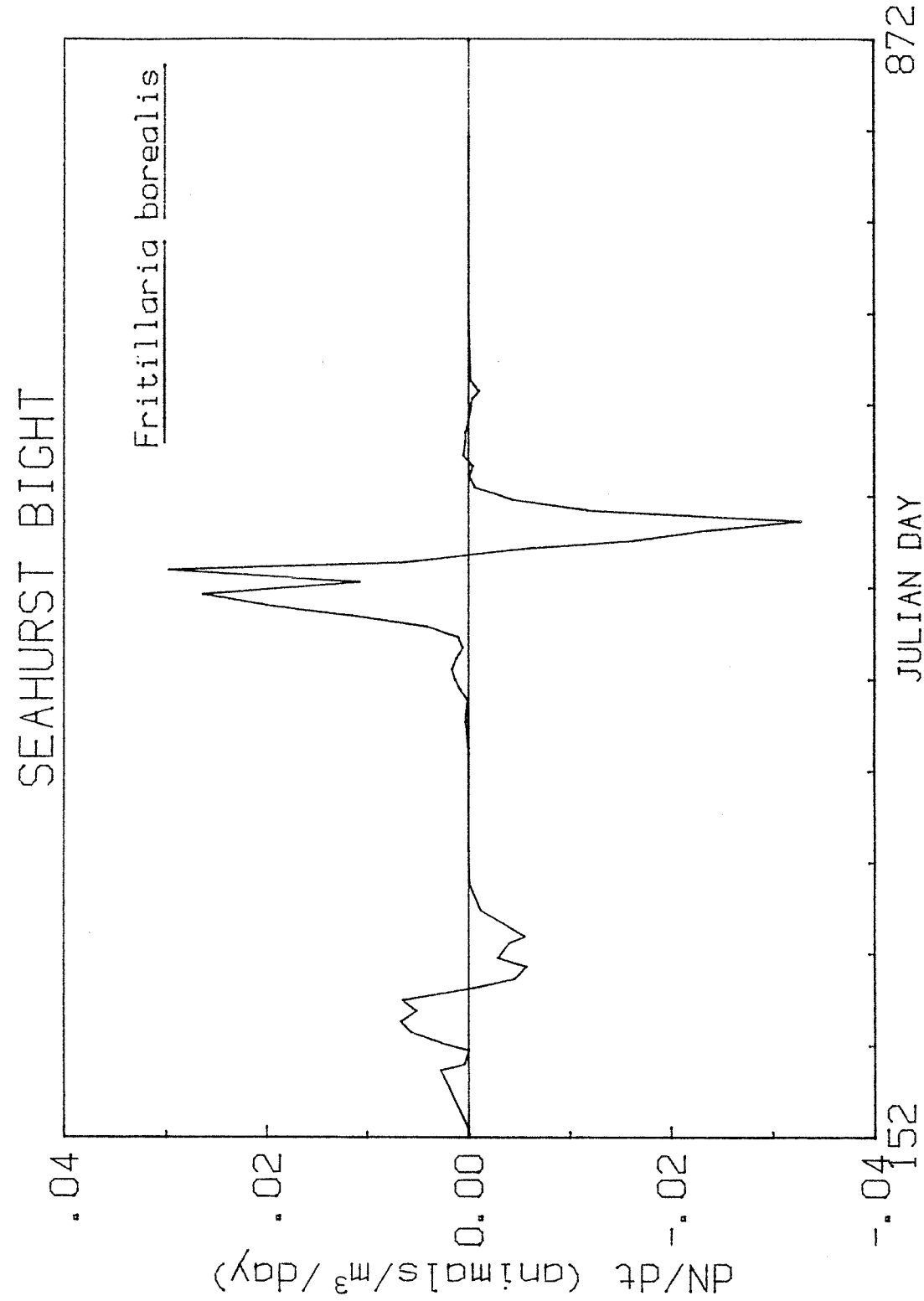

Figure 4.37b. Slope of smoothed distribution depicting rate of change of Fritillaria borealis numbers.

temporal variability was 44% and the spatial variability was 26% (Table 4.19).

In the shallow water of Seahurst Bight (station 10) Calanus pacificus levels decreased while the larvacean Oikopleura diocia increased (Figure 4.38). This trend may be the result of the shallow depth at station 10. Calanus late copepodid stages and adults prefer depth of 100 m or more (Marshall and Orr 1972; Daamker 1964). Larvaceans have a high intrinsic growth rate, short generation time and little locomotory ability (King 1981; Alldredge 1976). Their increases at station 10 may be due to favorable conditions or from the exclusion of other potential prey species.

4.4.1.4 Nutrients

The nutrients; phosphate, nitrate, and silicate, are required for phytoplankton growth and consequentially their seasonal cycles are the inverse of those for phytoplankton. Maximum concentrations of phosphate, nitrate and silicate in the photic zone occurred near the winter solstice and minimum values occurred near the summer solstice. Nitrate dropped below 3 mg-at/m 3 on five sampling data in spring 1983 and three times in summer 1982 (Figures 4.39a, 4.40a and 4.41a). Average values and equilibrium levels of the nutrients for equinox and solstice periods are given in Table 4.20.

The maximum rate of uptake of nutrients in the photic zone was near the vernal equinox. A net input of nutrients occurred between the summer solstice and mid-winter. In mid-summer of 1983 the net rate approached zero (Figures 4.39b, 4.40b and 4.41b). The maximum nutrient uptake rates were 0.3 mg-at/m^3/day for nitrate, 0.017 mg-at/m^3/day for phosphate and 0.6 mg-at/m^3/day for silicate. The resulting uptake ratios are 17.6 for a nitrate/phosphate ratio and 35 for the silicate/phosphate ratio. These ratios are similar to those given in Parsons and Takahashi (1973).

Nitrite in the photic had a unique seasonal distribution with minimum

Table 4.19. Relative variability of zooplankton species and dry weight from Seahurst Bight as computed according to Section 4.6.3.10.

Species	Temporal variability	Spatial variability
Dry weight	0.44	0.29
Calanus pacificus	0.90	0.42
Paracalanus sp.	0.63	0.28
Pseudocalanus spp.	0.97	0.49
Microcalanus sp.	0.74	0.42
Corycaeus anglicus	0.76	0.27
Oithona similis	0.47	0.25
Oikopleura dioica	1.72	0.46
Fritillaria borelis	1.18	0.50

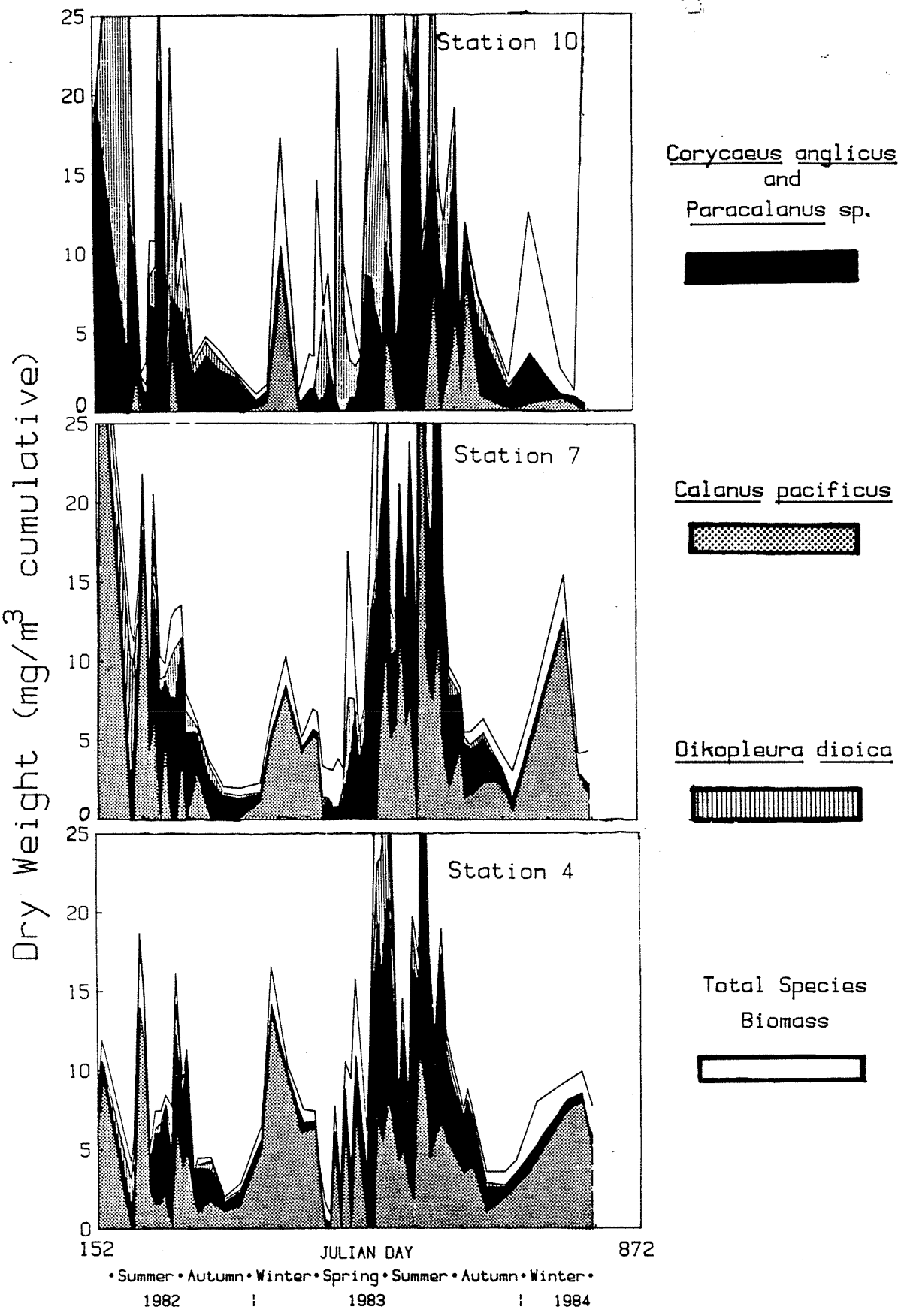

Figure 4.38. Zooplankton species dry weight over time at Seahurst Bight near shore (10), intermediate (7) and off shore (4) stations.

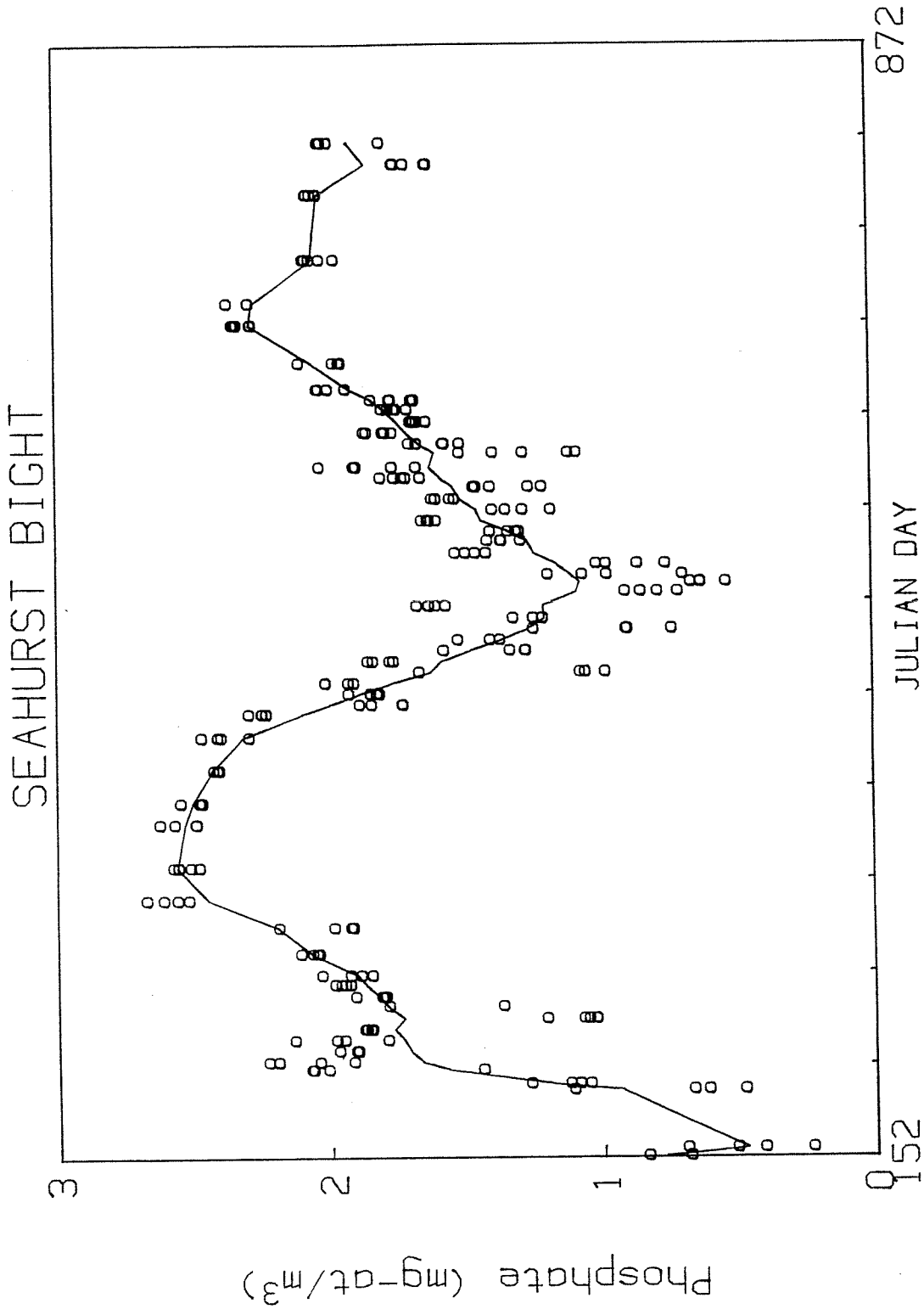

Figure 4.39a. Phosphate concentration in Seahurst Bight photic zone with smoothed distribution.

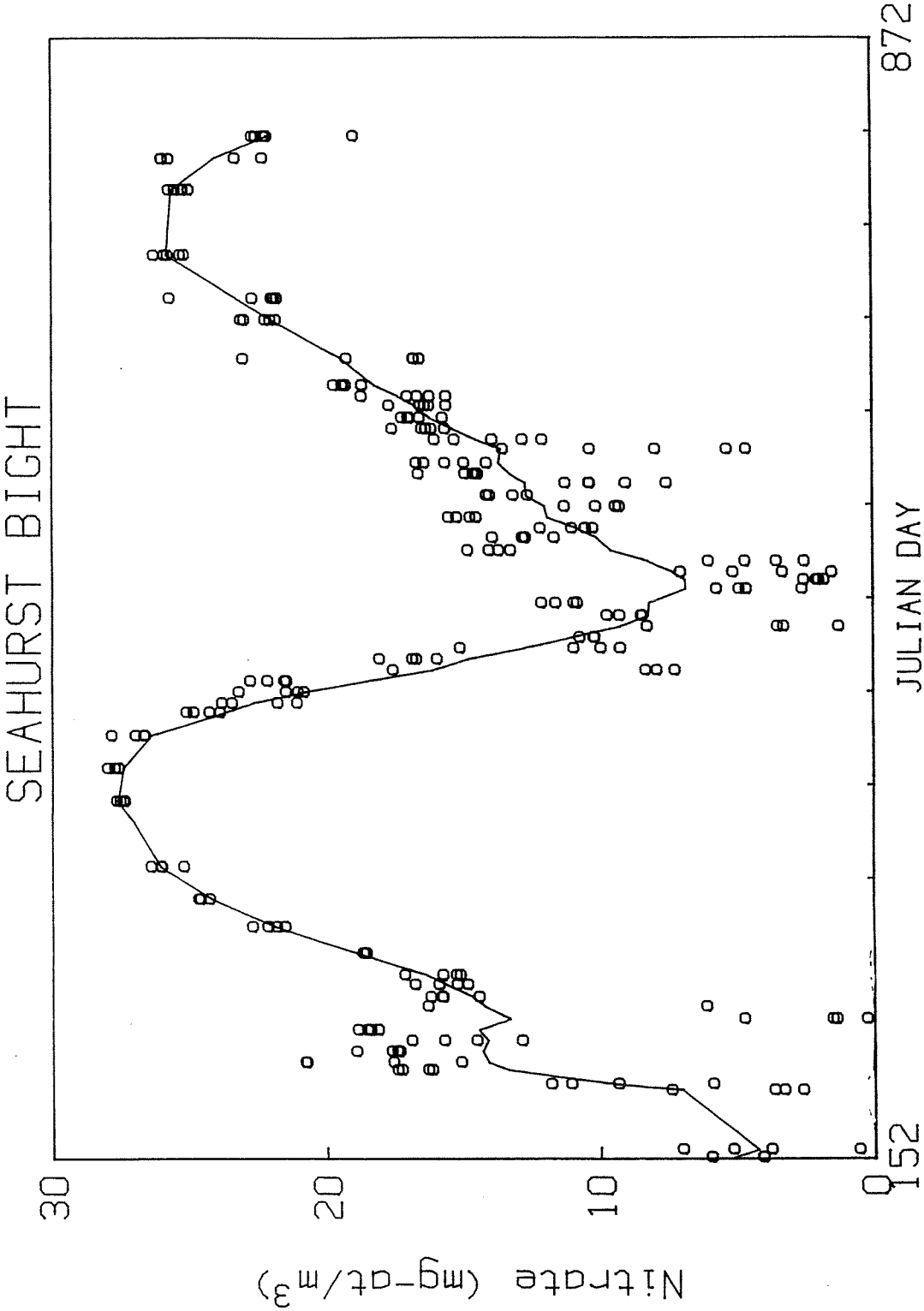

Figure 4.40a. Nitrate concentration in Seahurst Bight photic zone with smoothed distribution.

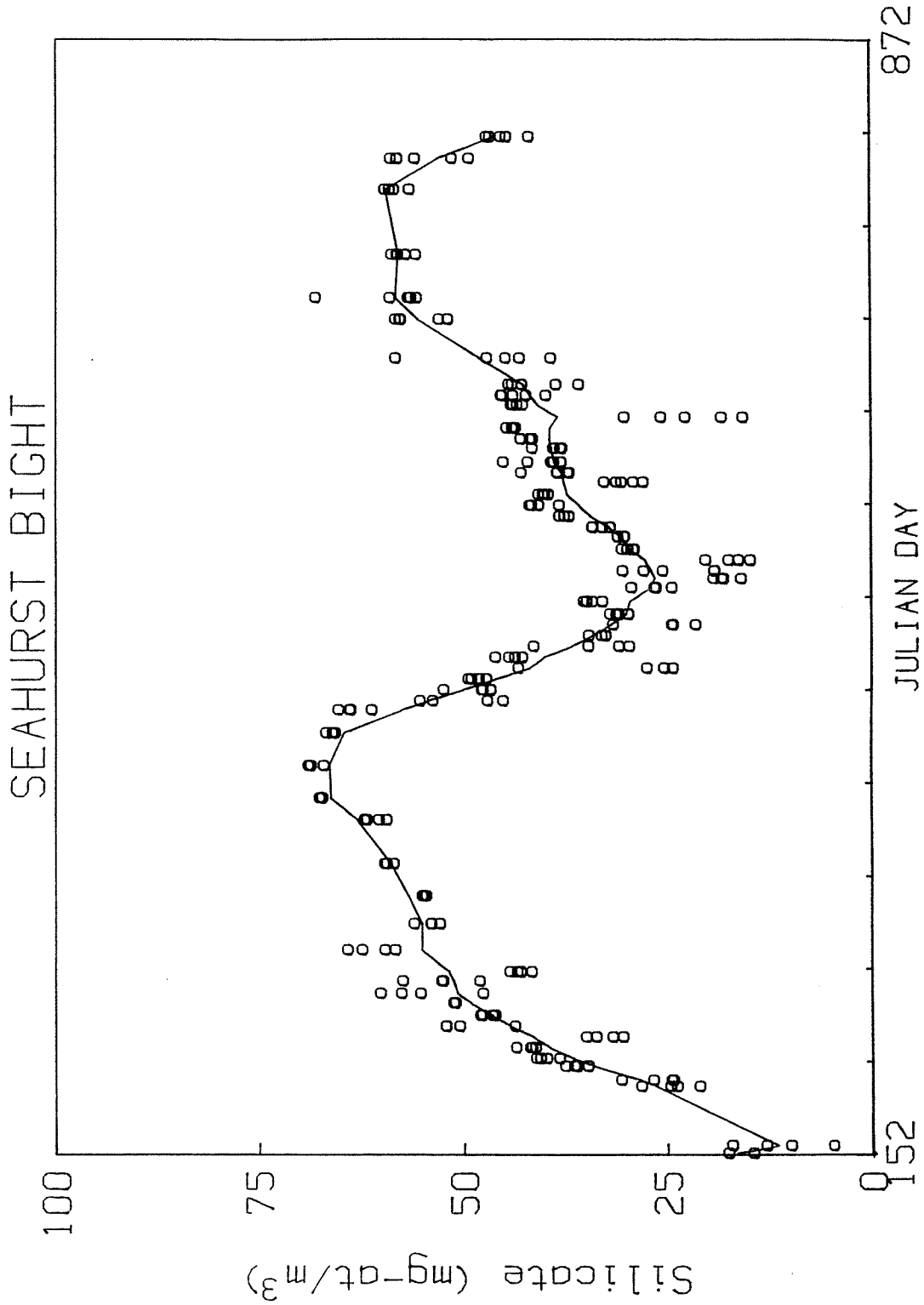

Figure 4.41a. Silicate concentration in Seahurst Bight photic zone with smoothed distribution.

Table 4.20. Gamma mean and 90% gamma confidence interval for photic zone integrated average nutrients in the Seahurst Bight. Units in mg-at/m^3. Data grouped in 6 week intervals about equinox and solstice dates. Significantly higher years marked by *.

Period	Phosphate	Silicate	Nitrate	Nitrite	Ammonia
Summer solstice 1982	0.63 (0.50-0.77)	17.9 (13.5-22.4)	4.5 (3.3-5.7)	0.23 (0.19-0.27)	1.28* (0.96-1.60)
Summer solstice 1983	1.07* (0.98-1.20)	26.2* (24.2-28.6)	7.3* (6.2-9.1)	0.25 (0.22-0.28)	0.58 (0.49-0.70)
Autumnal equinox 1982	1.76 (1.62-1.93)	52.2* (49.7-54.9)	13.4 (11.2-15.6)	0.52* (0.40-0.64)	1.30* (0.95-1.66)
Autumnal equinox 1983	1.70 (1.64-1.78)	39.8 (37.2-42.00)	15.5 (14.3-16.9)	0.34 (0.32-0.36)	0.49 (0.41-0.59)
Winter solstice 1982	2.54* (2.51-2.57)	63.0* (60.9-65.1)	26.8* (26.2-27.4)	0.13 (0.12-0.15)	0.25* (0.20-0.31)
Winter solstice 1983	2.22 (2.14-2.30)	57.9 (56.3-59.7)	23.7 (22.9-24.6)	0.12 (0.11-0.14)	0.14 (0.12-0.16)
Vernal equinox 1982	1.92 (1.76-2.10)	51.6 (47.2-56.0)	21.4 (19.0-24.3)	0.23 (0.21-0.25)	0.51 (0.43-0.58)

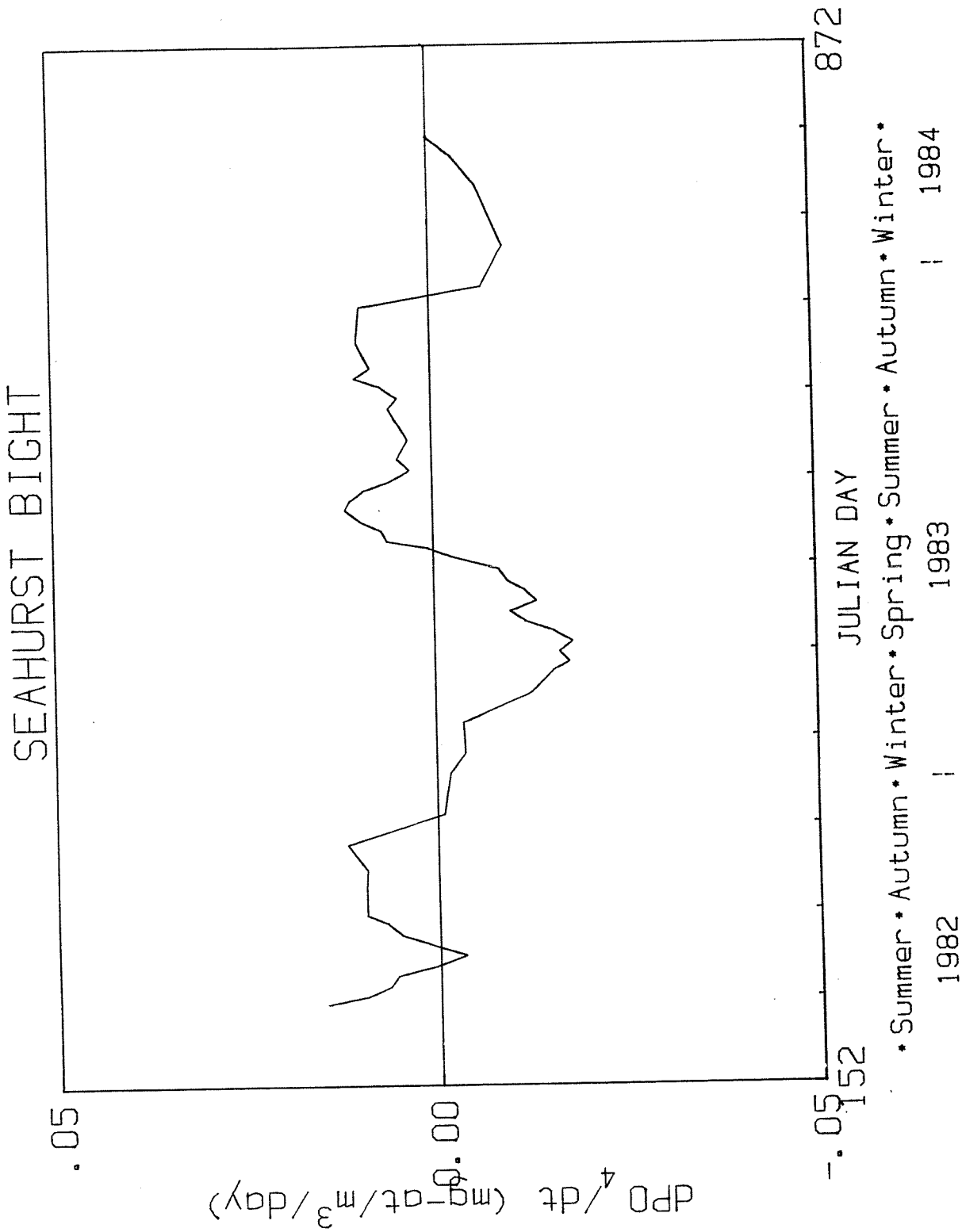

Figure 4.39b. Slope of smoothed distribution depicting rate of change of phosphate concentration.

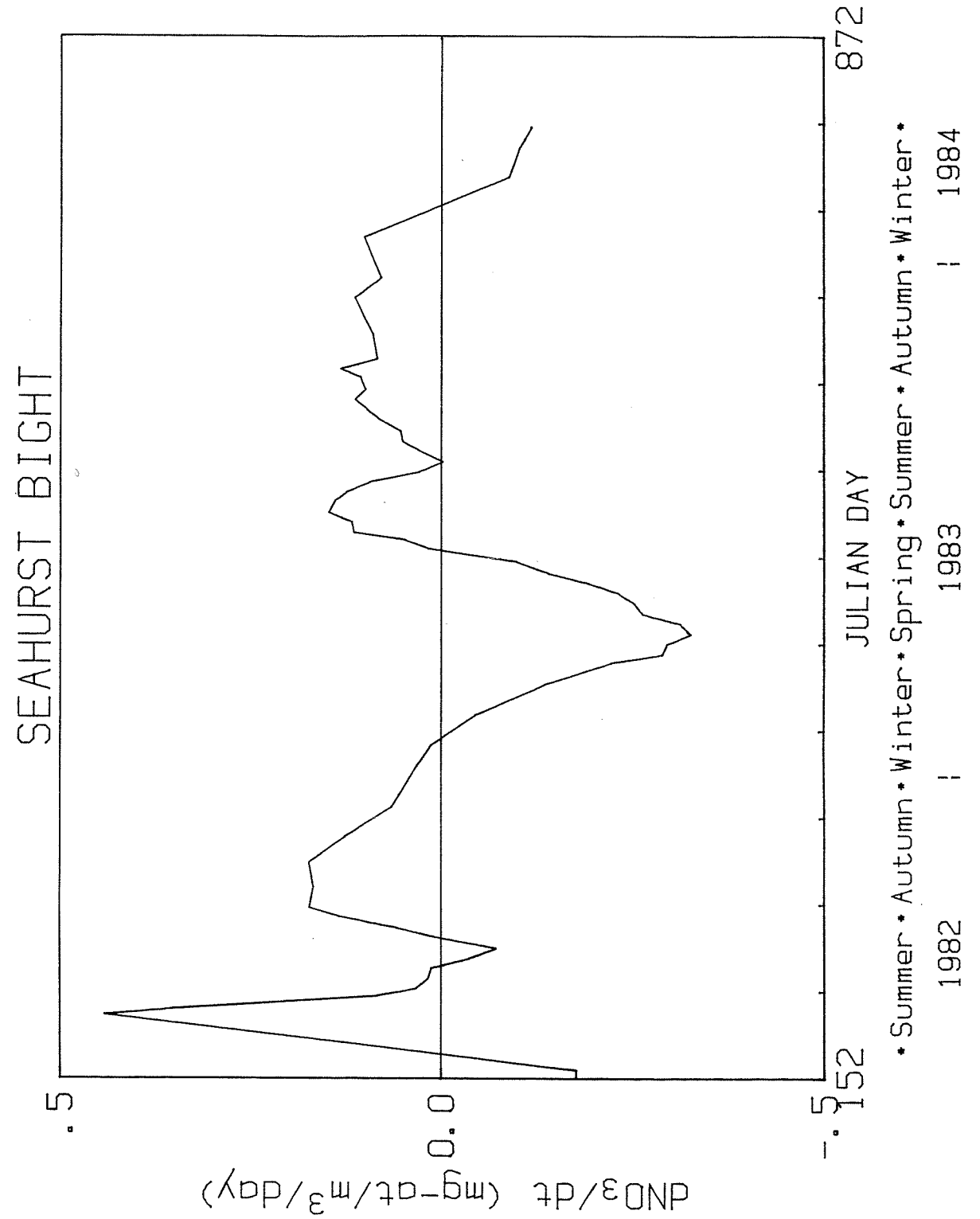

Figure 4.40b. Slope of smoothed distribution depicting rate of change of nitrate concentration.

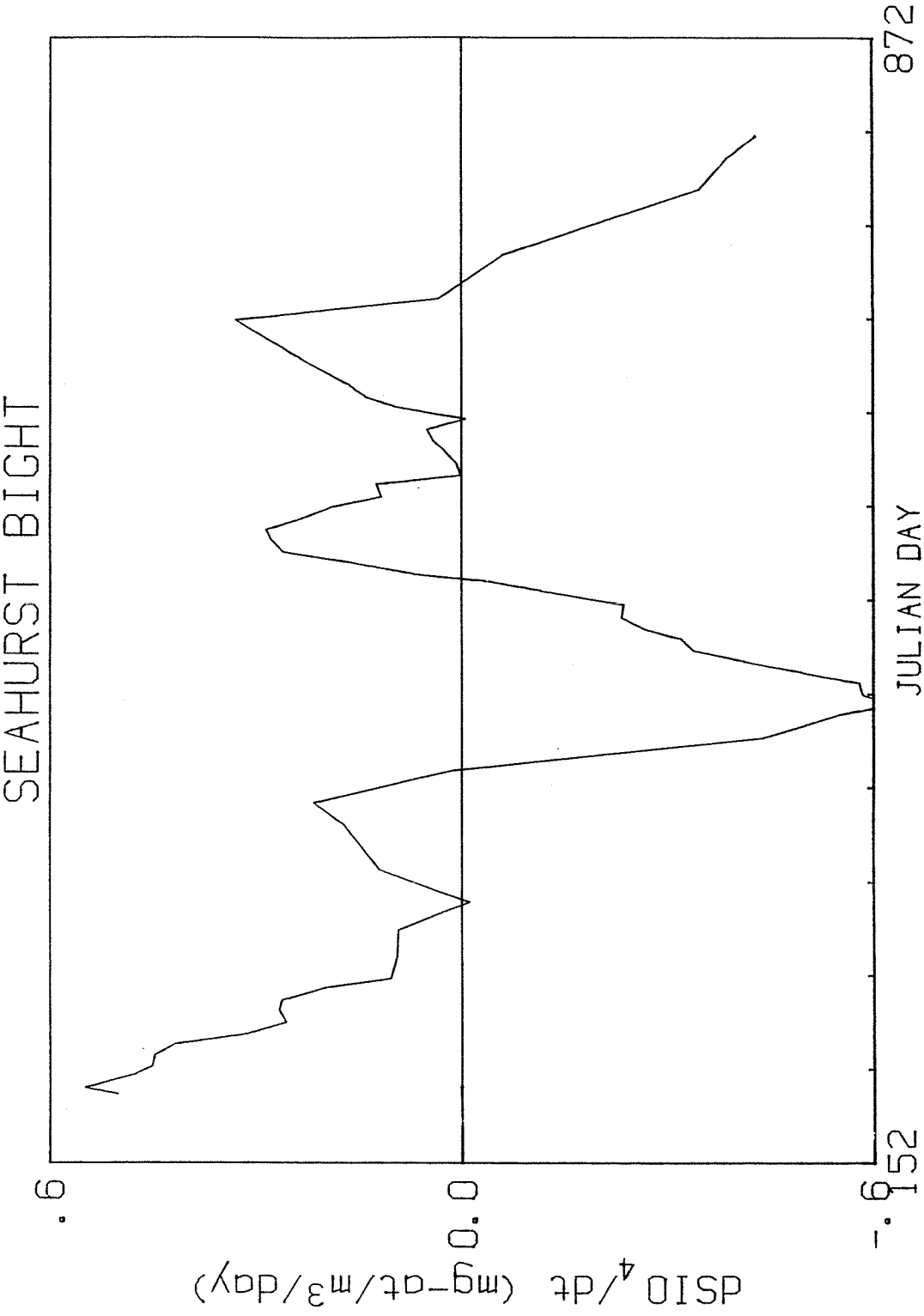

Figure 4.41b. Slope of smoothed distribution depicting rate of change of silicate concentration.

values near the winter solstice and maximum values in mid-spring and autumn (Figures 4.42a and 4.42b). The concentration at the 1982 autumnal equinox was larger than at the 1983 autumnal equinox (0.5 vs. 0.3 mg-at/m^3) (Table 4.20).

Ammonia exhibited a weak seasonal cycle with minimum values about the winter solstice and high values throughout the spring and summer (Figure 4.43a). The duration of a net input or loss of ammonia appeared to extend for several months (Figure 4.43b).

Normal probability distributions of photic zone integrated average nitrate and ammonia about the summer and winter solstices in 1982 and 1983 are illustrated in Figures 4.44 and 4.45 (see Appendix 4.D).

The spatial and temporal variability of the nutrients was lower than observed in the plankton measures. In general, the spatial variability was 60% of the temporal variability. Phosphate and silicate variability were lowest, nitrate and nitrite variability were intermediate, and ammonia variability was the largest (Table 4.21).

4.4.2 Main Basin

The goal of study in the Main Basin of Puget Sound was to compare and contrast the principal water column nutrient and plankton properties. In general the nutrient and plankton differences between stations 1 through 4 were small and seasonal patterns were similar to those in Seahurst Bight.

4.4.2.1 Physical and Meteorological

Stations 1, 3, and 4 extend from north to south down the deep water passage of the Main Basin. The net surface flow is to the south and the deep water flow is to the north. The mixed layer depth follows the seasonal pattern described for the Seahurst Bight. Station 2 in Colvos passage is different because of the greater vertical mixing in the passage compared to the main channel. At station 2 both the surface and deep water flows are to

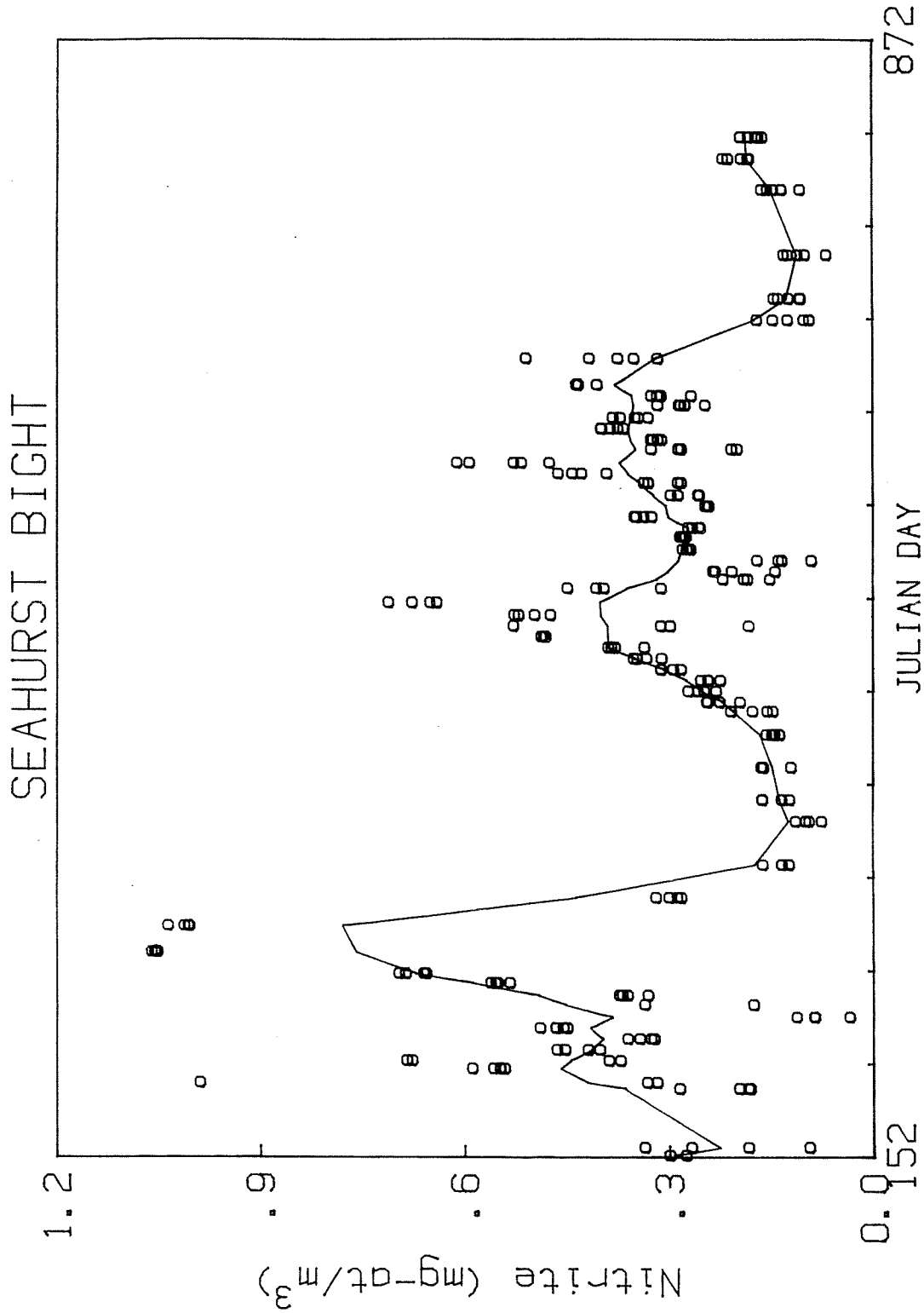

Figure 4.42a. Nitrite concentration in Seahurst Bight photic zone with smoothed distribution.

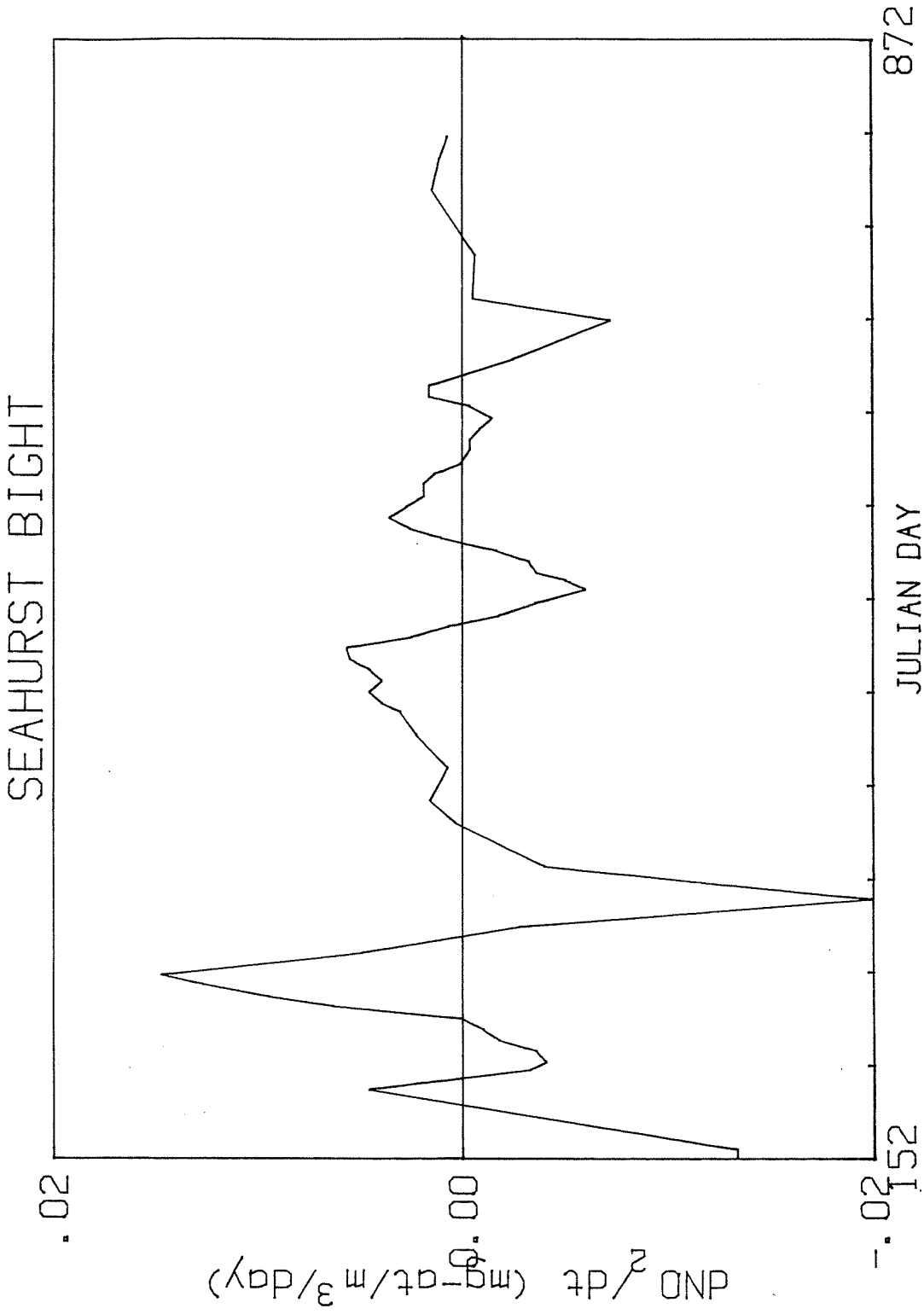

Figure 4.42b. Slope of smoothed distribution depicting rate of change of nitrite concentration.

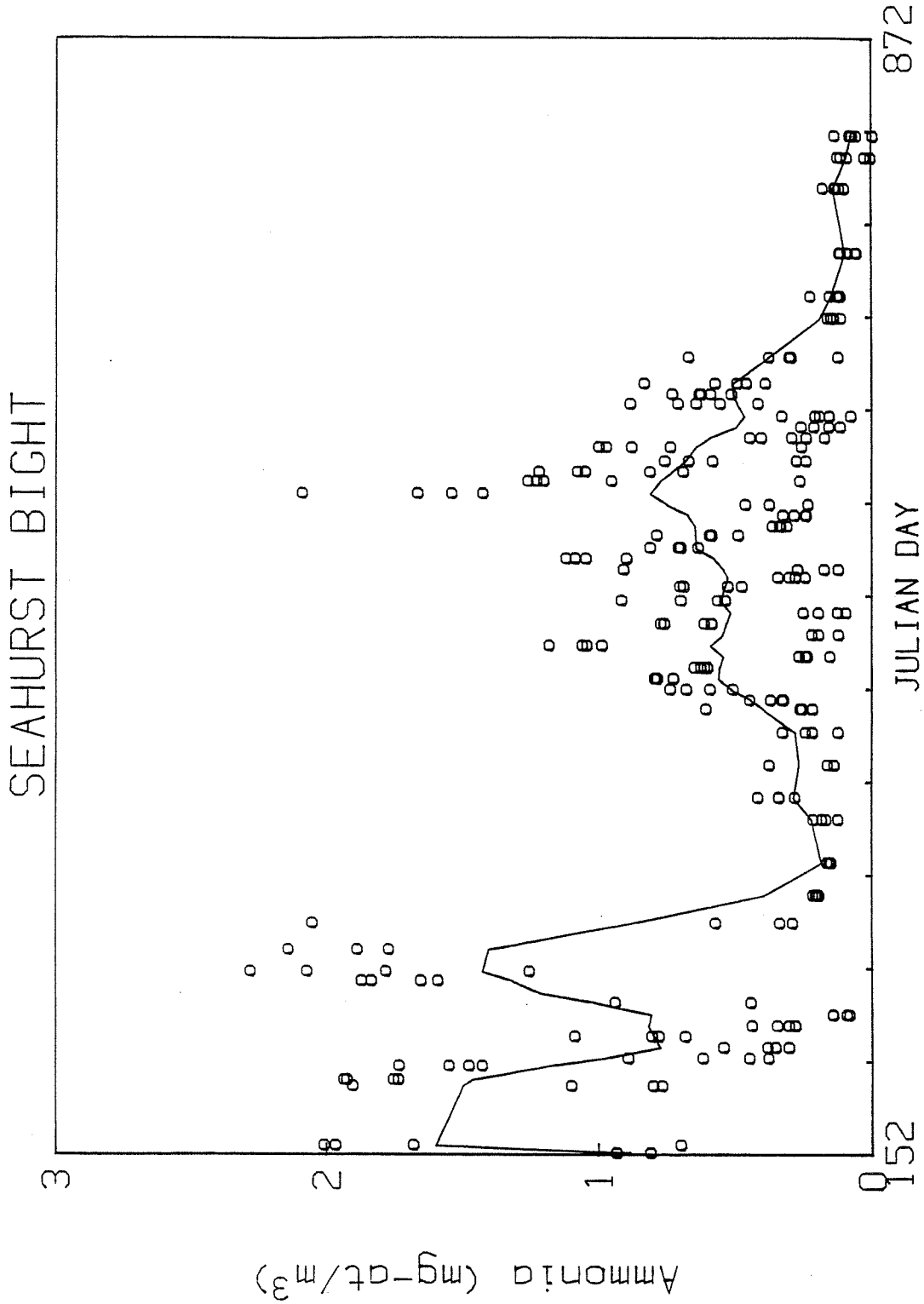

Figure 4.43a. Ammonia concentration in Seahurst Bight photic zone with smoothed distribution.

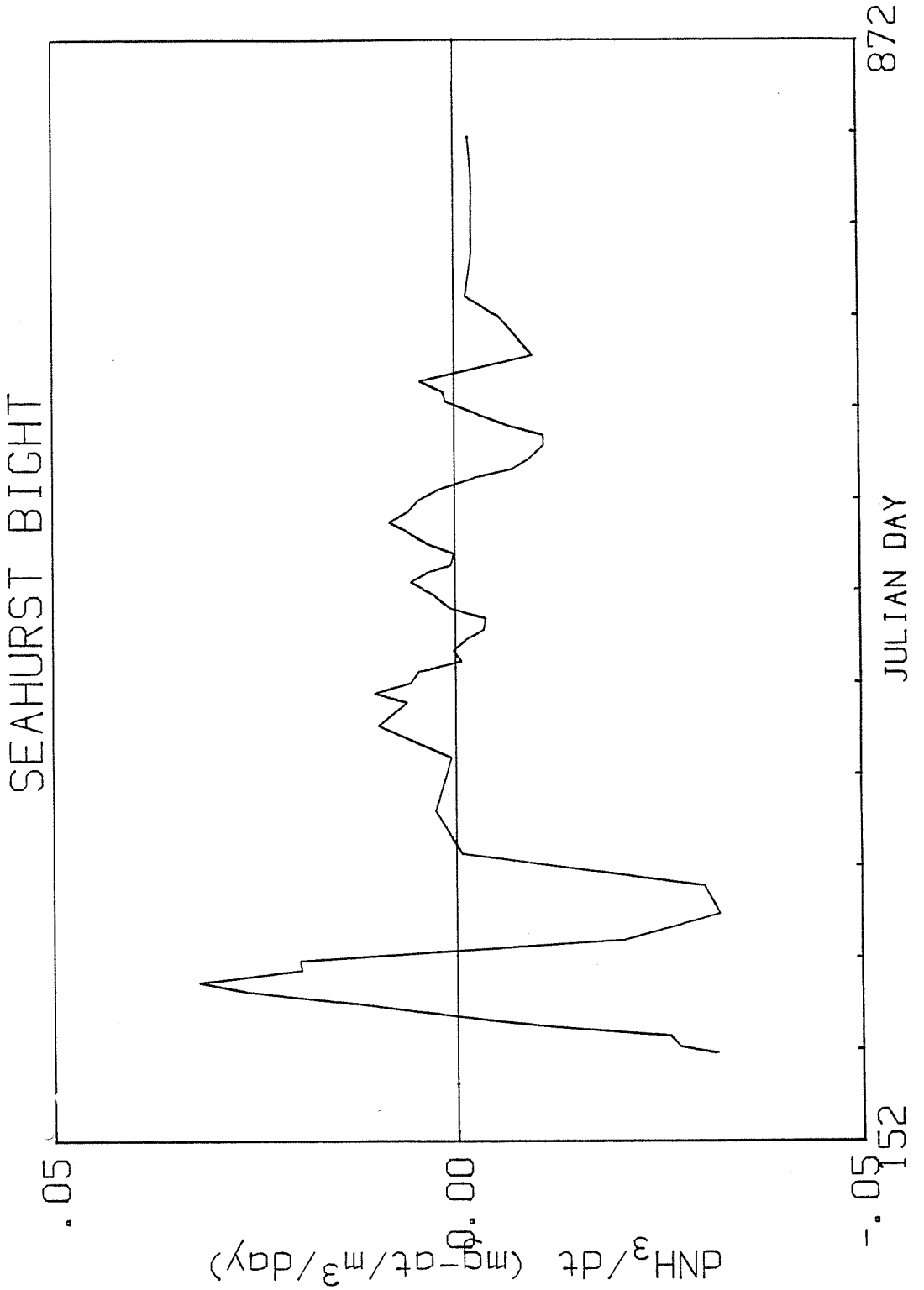

Figure 4.43b. Slope of smoothed distribution depicting rate of change of ammonia concentration.

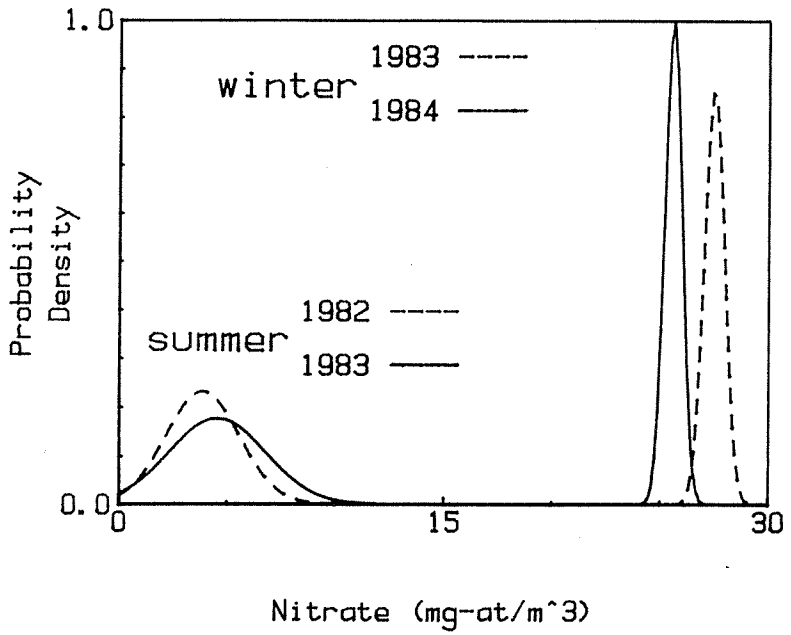

Figure 4.44. Normal probability distributions for Seahurst Bight photic zone nitrate concentration for summer 1982-1983, and winter 1983-1984.

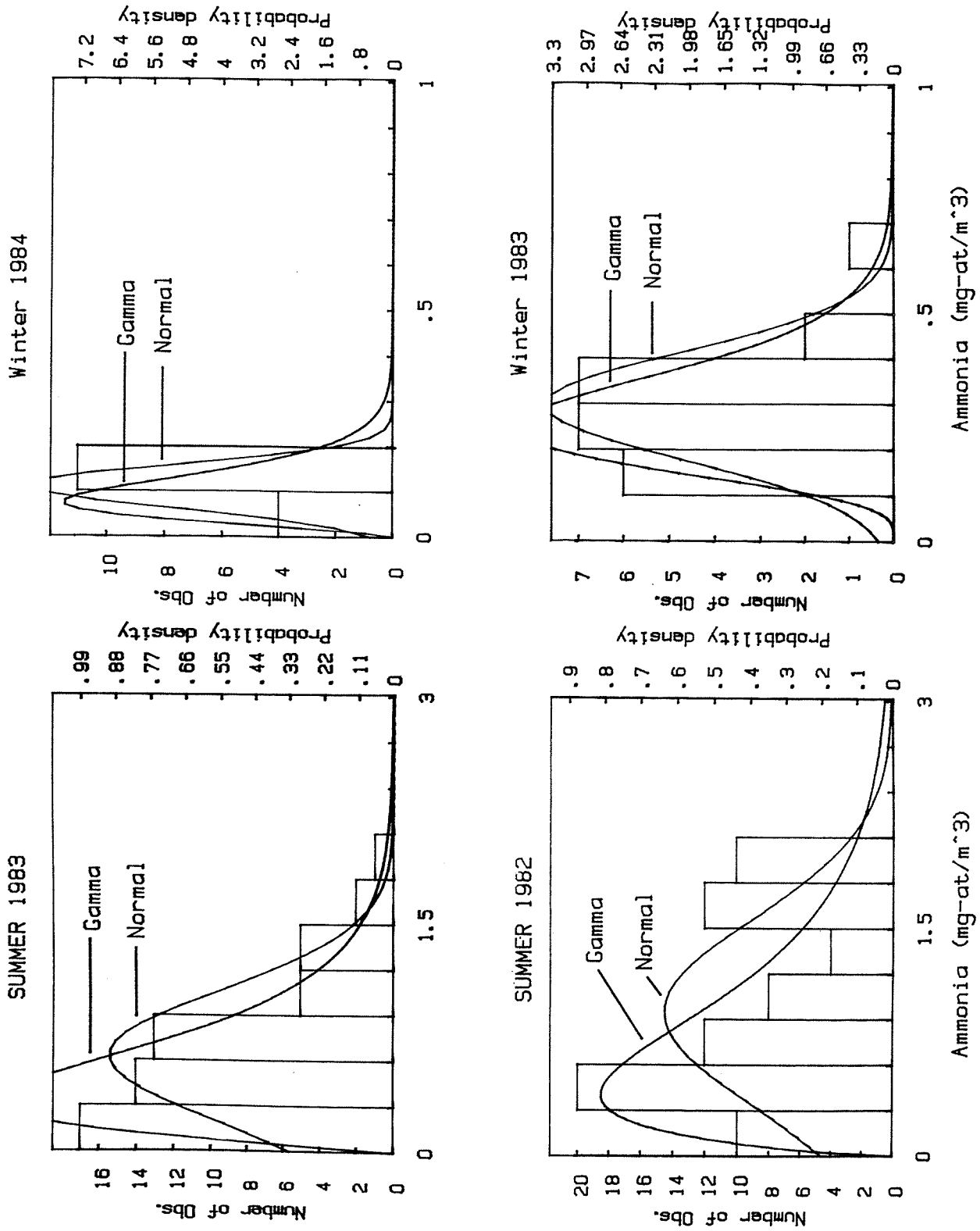

Figure 4.45. Normal probability distributions for Seahurst Bight photic zone ammonia concentration for summer 1982-1983, and winter 1983-1984.

Table 4.21. Relative variability of photic zone depth integrated average nutrients in the Seahurst Bight as computed according to Section 4.6.3.10. Number of observations between 110 and 254.

Nutrient	Temporal variability	Spatial variability
Phosphate	0.16	0.09
Silicate	0.14	0.09
Nitrate	0.27	0.21
Nitrite	0.28	0.16
Ammonia	0.47	0.30

the north. Station 3 off Browns Point has a freshwater lense in the upper few meters due to the presence of Puyallup River water. This feature is discussed in section 4.4.4. The study did not identify meteorological difference between the main basin stations but little difference was expected.

4.4.2.2 Phytoplankton

The seasonal distribution of chlorophyll at main basin stations followed the pattern observed in Seahurst Bight. Higher chlorophyll levels were observed in 1983 than in 1982 (Figure 4.46). The onset of the spring bloom near the spring equinox, the low at the summer solstice, and the mid-summer bloom occurred at all stations. Lower chlorophyll concentrations in Colvos Passage (station 2) were probable because of the stronger vertical mixing at this station. Average integrated chlorophyll in the summer of 1982 was significantly lower than in the summer of 1983. For both summers chlorophyll at station 2 was lower than at stations 1, 3, and 4 (Table 4.22). The phaeopigments exhibited a similar seasonal pattern but with more variability in the magnitude of the peak values (Figure 4.47 and Table 4.23).

The temporal varability of chlorophyll and phaoepigments about the seasonal pattern are illustrated in Figure 4.48 and 4.49. The smooth seasonal lines were obtained with the smoothing algorithm (section 4.3.4.9) using T = 75 days, Te = 15 days and Te = 3 days.

The relative temporal variability is about a factor of 3 greater than the spatial variability (Table 4.24), indicating that the random weekly variations were greater than the variations between stations.

The phytoplankton species were similar between main basin stations and the seasonal pattern was similar to that in Seahurst Bight. Smoothed plots of the main genera illustrate diatoms dominated on a carbon basis while dinoflagellates and microflagellates were of secondary importance (Figure

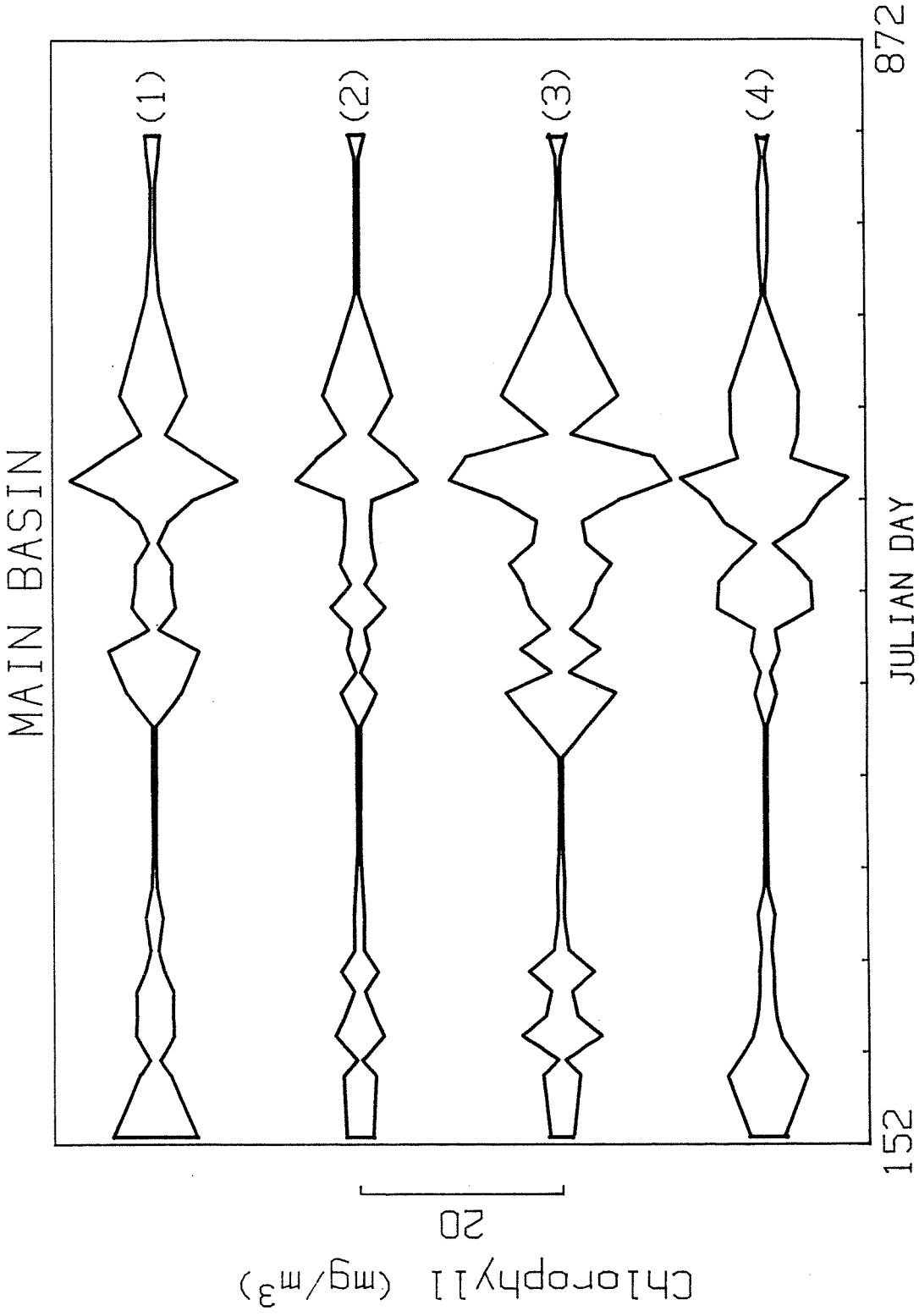

Figure 4.46. Photic zone chlorophyll concentrations over time at main basin stations 1 to 4. Scale on left depicts 20 mg Chl/m^3.

Table 4.22. Carrying capacities and 90% gamma confidence interval for phytoplankton chlorophyll (mg/m^3) for summer and winter seasons stations 1 to 4 in main basin. Significantly higher level for a season marked with *.

Station	1	2	3	4
Summer 1982	2.8 2.4 - 3.7	2.6 1.9 - 4.2	3.9 2.8 - 6.2	3.1 2.0 - 5.6
Summer 1983	6.4* 4.5 - 12.0	4.9 3.6 - 7.7	10.4* 7.4 - 17.3	8.2* 6.1 - 12.4
Winter 1983	0.3 0.3 - 0.4	0.3 0.3 - 0.4	0.4 0.3 - 0.6	0.2 0.2 - 0.3
Winter 1984	0.9* 0.6 - 1.5	0.6 0.4 - 1.0	1.0 0.6 - 1.7	0.7* 0.5 - 1.2

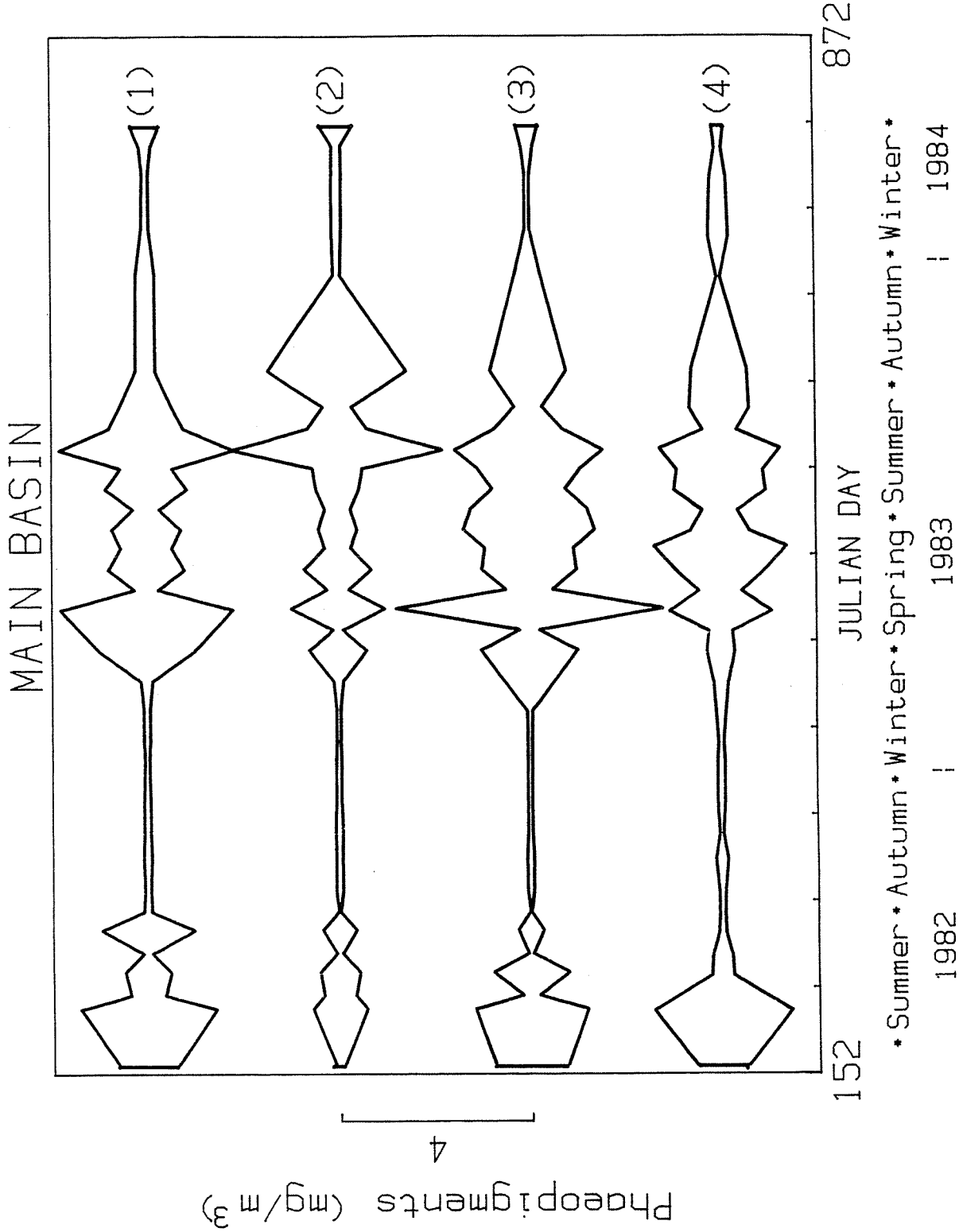

Figure 4.47. Photic zone phaeopigment concentrations over time at main basin stations 1 to 4. Scale on left depicts 20 mg Pha/m^3.

Table 4.23. Gamma mean values and 90% gamma confidence interval for phaeopigment (mg/m^3) for summer and winter seasons stations 1 to 4 in main basin. Significantly higher level for a season marked with *.

Station	1	2	3	4
Summer 1982	1.1 0.7 - 2.2	0.5 0.4 - 1.2	0.7 0.5 - 2.2	0.7 0.4 - 2.3
Summer 1983	1.4 1.0 - 2.4	1.9* 1.5 - 2.5	1.5 1.2 - 2.0	1.6 1.2 - 2.3
Winter 1983	0.1 0.1 - 0.1	0.1 0.1 - 0.2	0.1 0.1 - 0.2	0.2 0.1 - 0.2
Winter 1984	0.3* 0.2 - 0.5	0.3 0.2 - 0.5	0.3 0.2 - 0.5	0.2 0.2 - 0.4

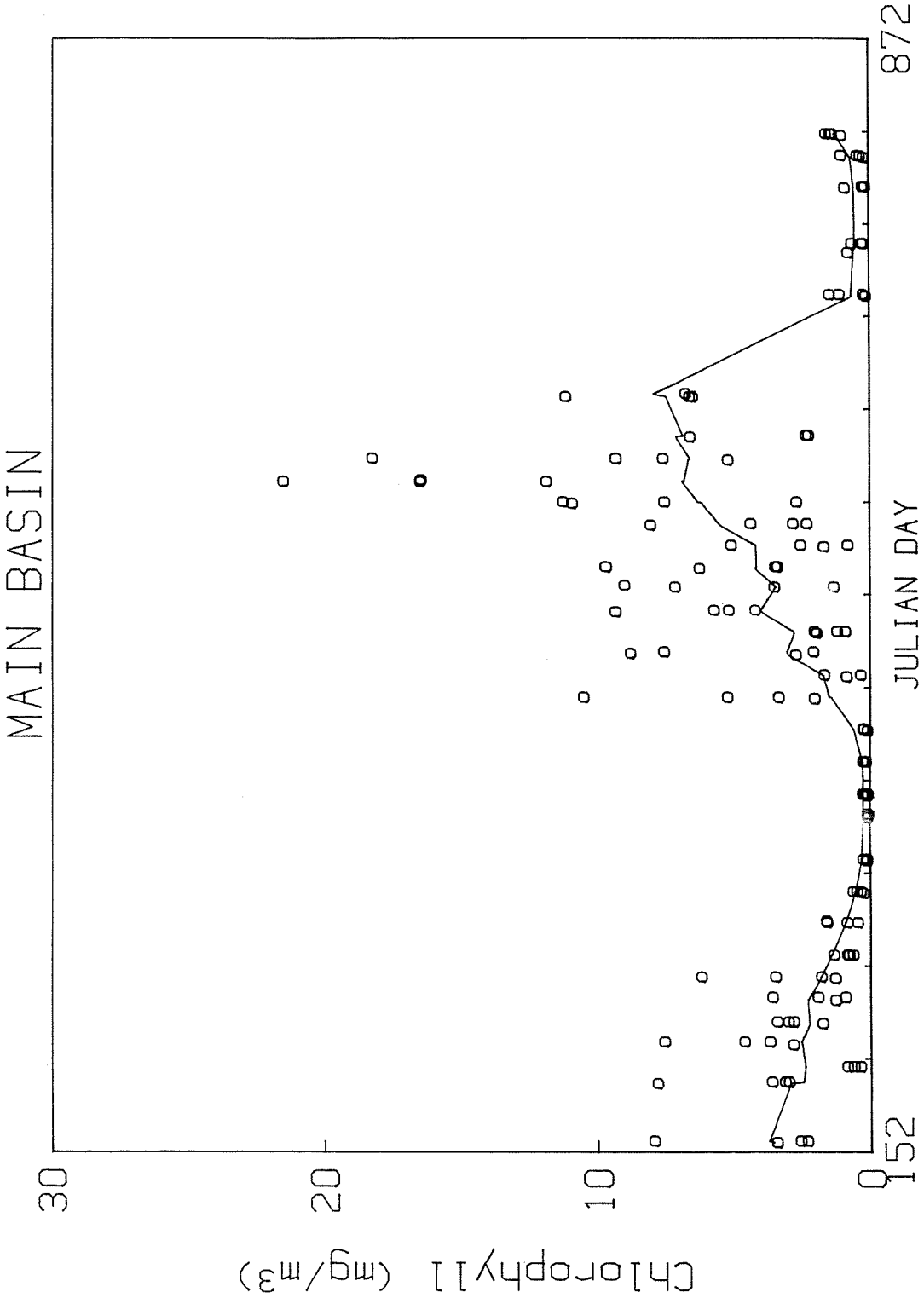

Figure 4.48. Chlorophyll photic zone concentration in main basin with smoothed distribution.

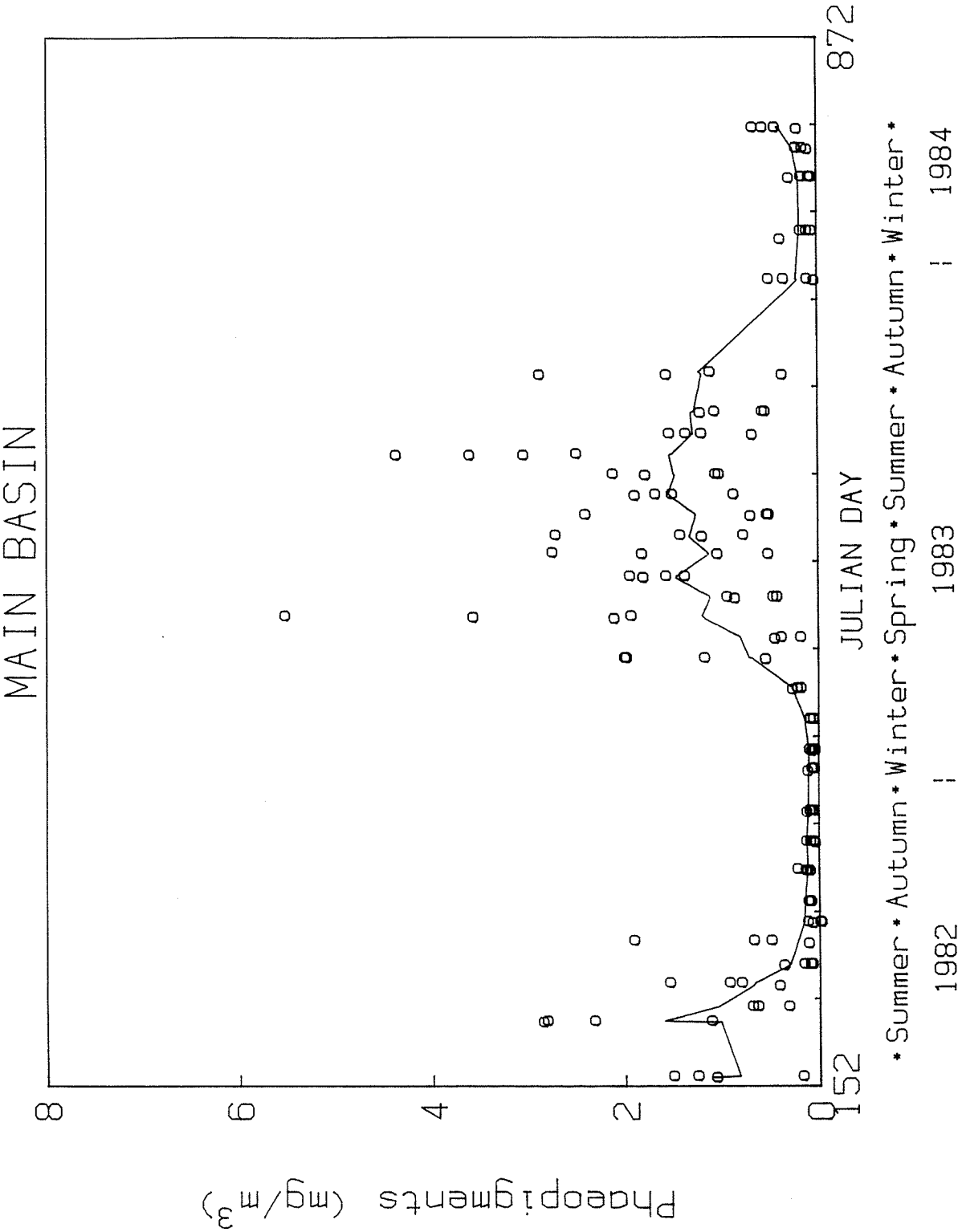

Figure 4.49. Phaeopigment photic zone concentration in main basin with smoothed distribution.

Table 4.24. Relative spatial and temporal variability of main basin phytoplankton carbon (mg/m^3). Measures calculated using section 4.6.3.10 with smoothing parameters T = 75 days, Te = 15 days, and Td = 3 days.

Property	Temporal variability	Spatial variability
Chlorophyll (mg/m^3)	0.89	0.36
Phaeopigment (mg/m3)	0.98	0.38
Dinoflagellates	2.36	0.35
Microflagellates	1.04	0.32
Diatoms	2.22	0.38

4.50). Dominant diatom species include: Thalassiosira sps., Chaetoceros debilis and other Chaetoceros species, and Skeletonema costatum (Figure 4.51). The variability of species carbon was less between stations than between weeks (Table 4.24).

To evaluate the long term trend in main basin phytoplankton chlorophyll integrated to the 1% light depth is compared for summer and winter seasons for the composite of years 1964 to 1966, and the years 1979, 1982, 1983, and 1984 (Table 4.25). Included for comparison are chlorophyll data from Seahurst Bight. Histograms and gamma probability distributions for the summer and winter periods of the years are illustrated in Figure 4.52. Only the summer of 1983 had significantly higher levels of chlorophyll.

4.4.2.3 Zooplankton

Zooplankton abundance followed the patterns observed in Seahurst Bight with high summer and low winter dry weight biomass as measured by weight of material captured in the plankton net per cubic meter of volume filtered (Figure 4.53). Biomass calculated from counts of the dominant species converted to biomass using Table 4.11 were a factor of 2 to 3 lower than the net dry weight but exhibited the same seasonal pattern (Figure 4.54). The smooth main basin dry weight biomass exhibited a mid-summer high in 1983 as illustrated in Figure 4.55. A comparison of summer and winter dry weight carrying capacities indicate that summer 1982 had significantly lower levels than the summer of 1983 while winter 1983 and 1984 levels were similar. Within the 90% gamma confidence limits stations were not significantly different within a season (Table 4.26).

The dominant zooplankton species identified in the Main Basin were the same as found in Seahurst Bight with Corycaeus anglicus, Paracalanus sp. Calanus pacificus and Oikpleura dioica accounting for the major portion of the

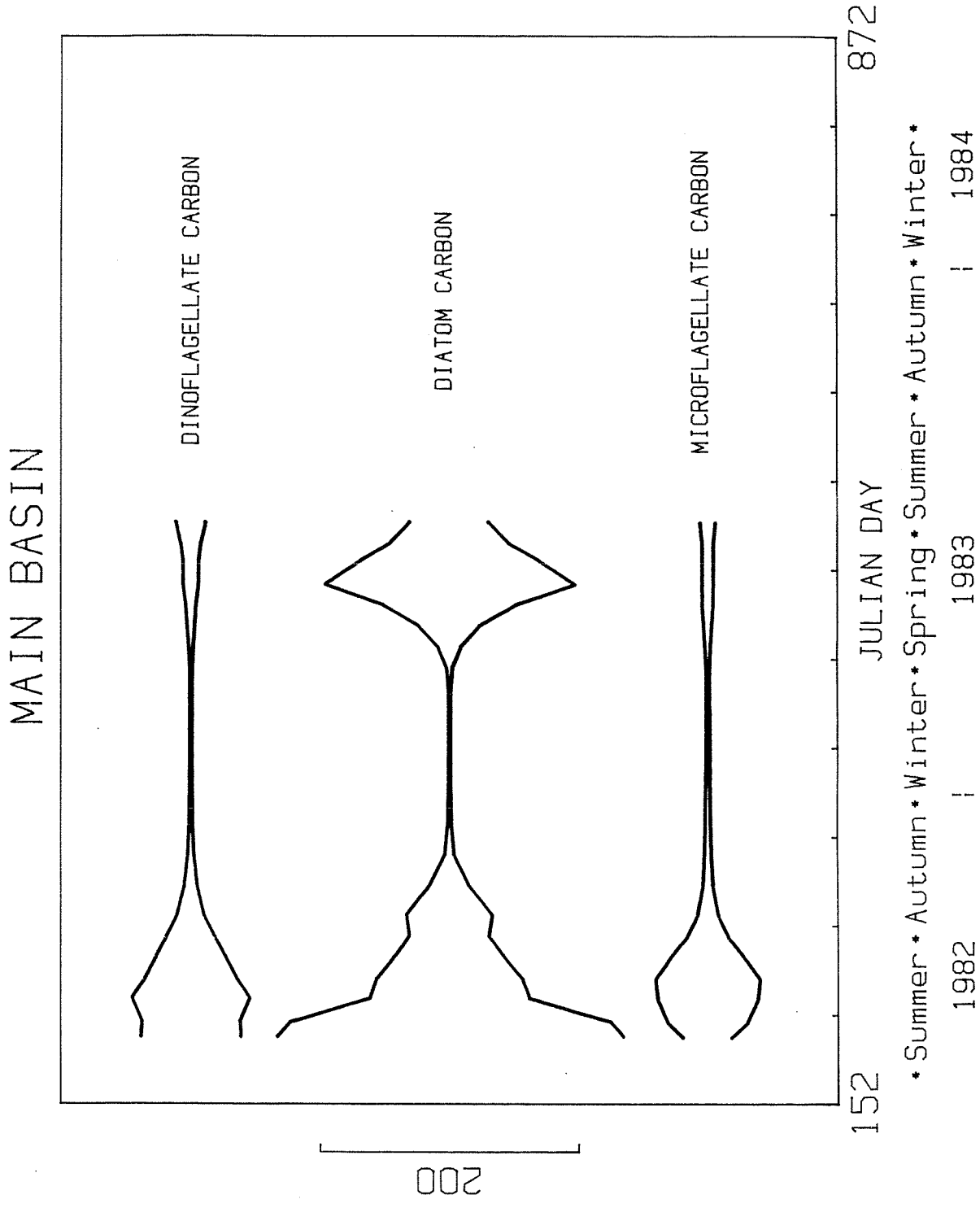

Figure 4.50. Photic zone major phytoplankton group numbers over time at main basin station 1. Scale on left depicts 200 cells/ml.

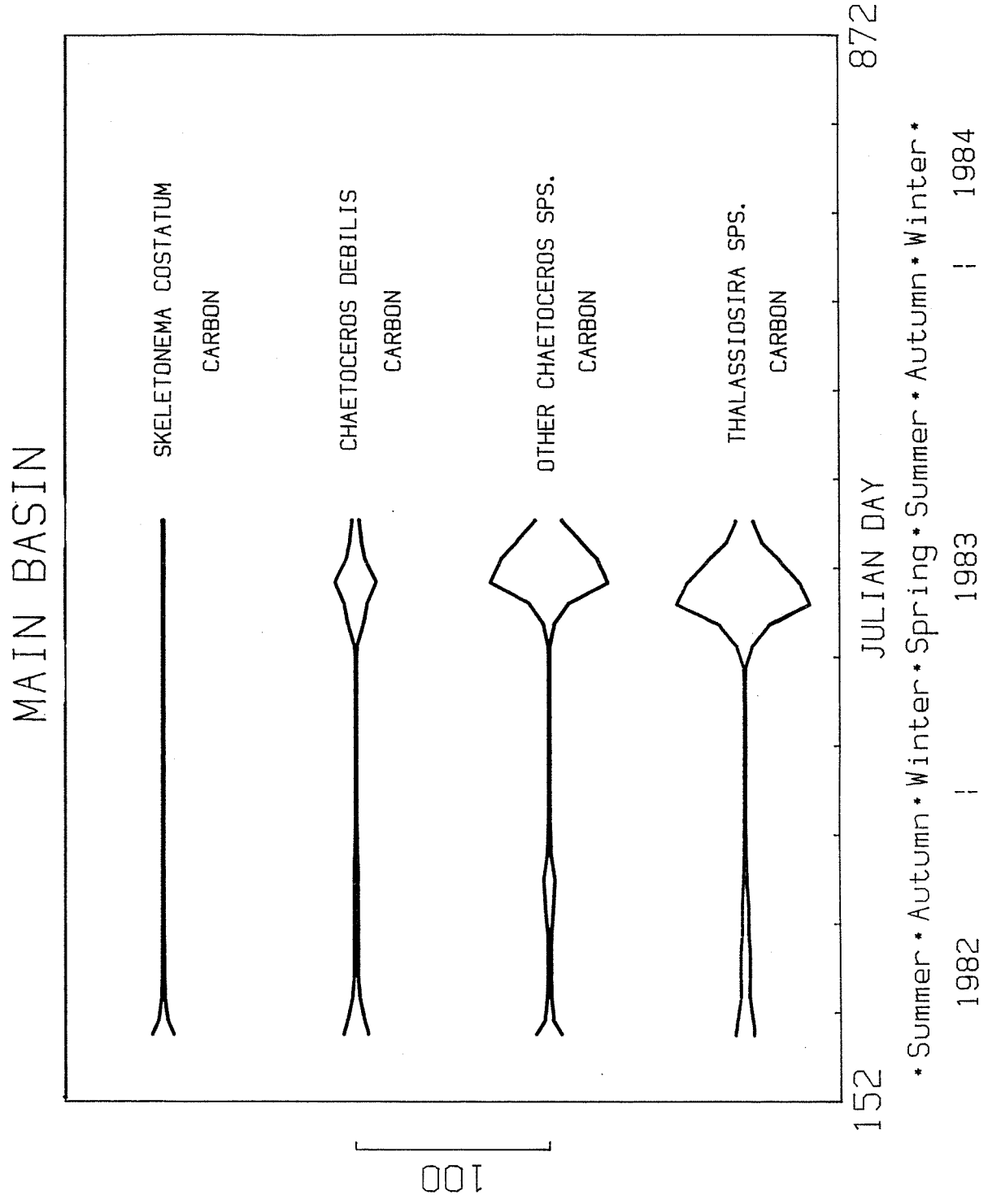

Figure 4.51. Photic zone major diatom species numbers over time at main basin station 1. Scale on left depicts 100 cells/ml.

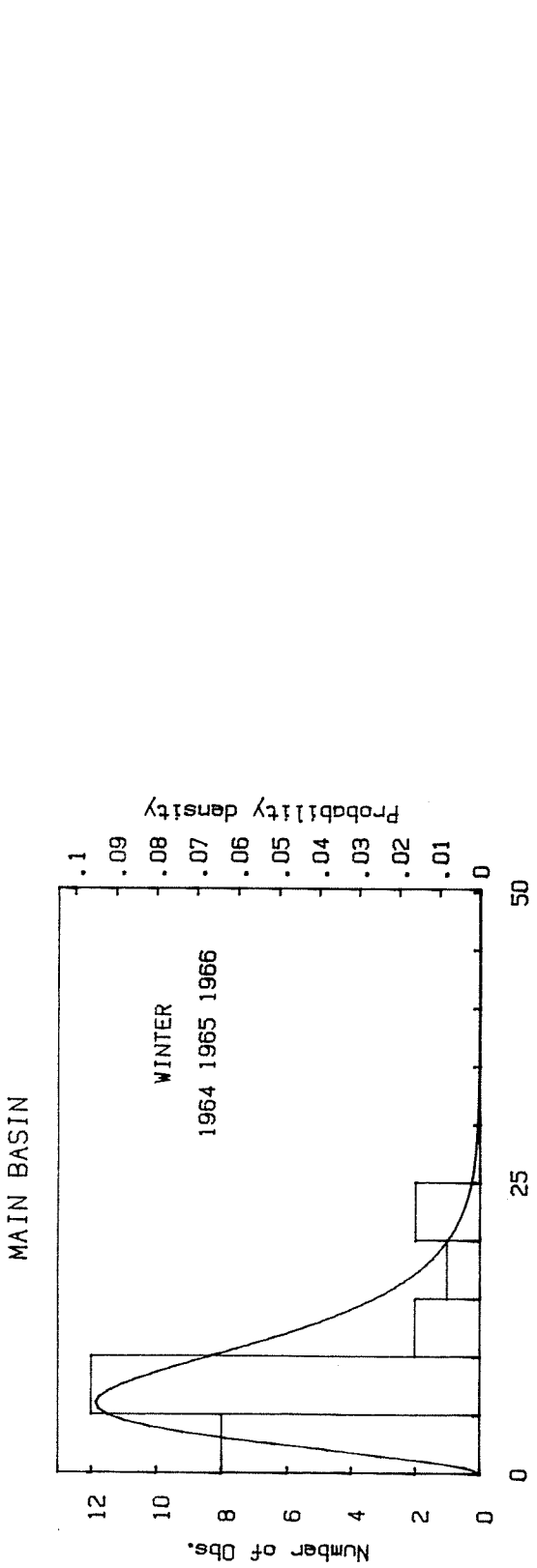

Figure 4.52. Gamma probability distributions of photic zone chlorophyll integrated to the 1% light depth for data near or at sta 1 in the main basin. Data grouped over winter and summer seasons for years 1964-1966, 1979, 1983, 1983, 1984.

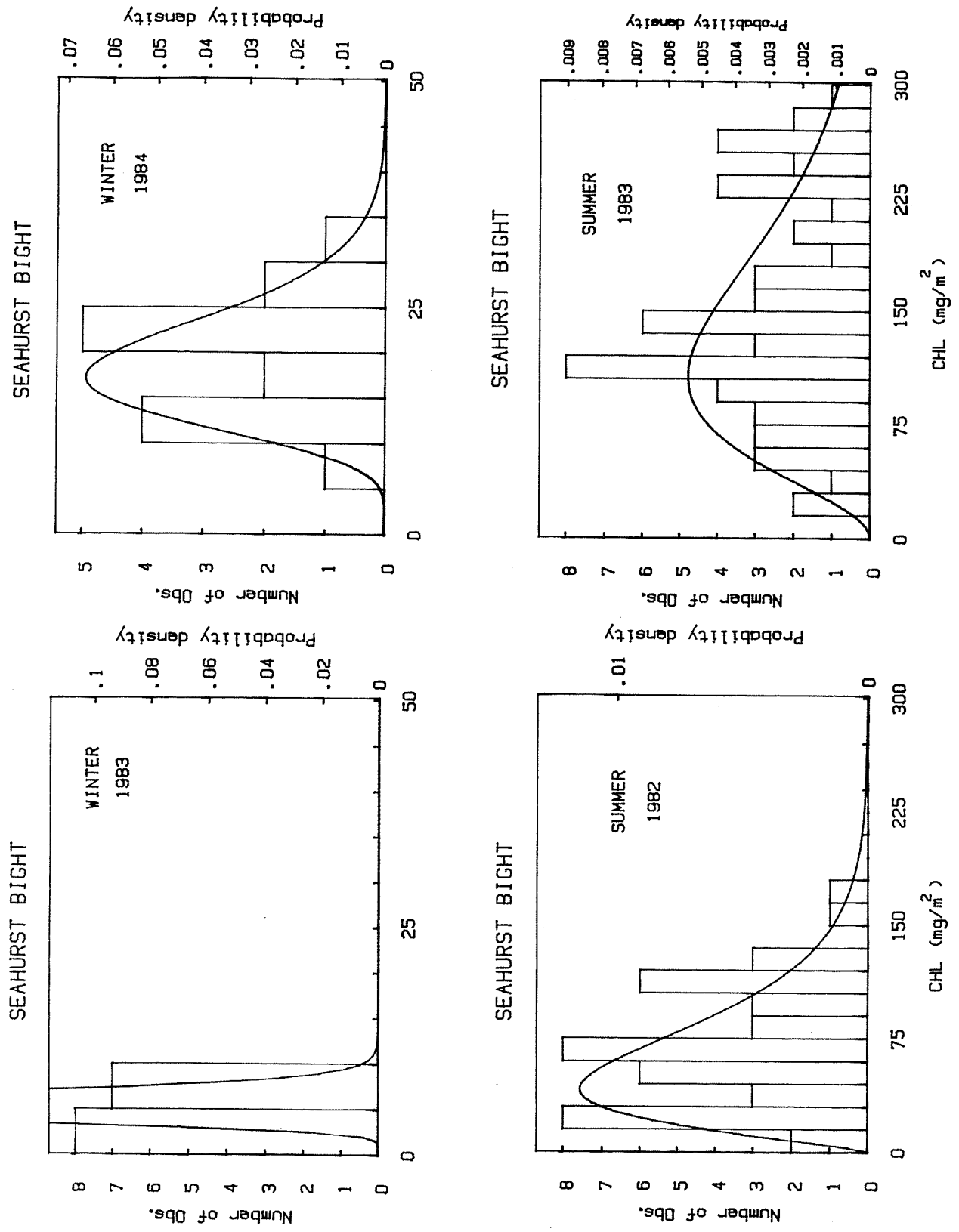

Figure 4.52. Continued

Table 4.25. Gamma mean values and 90% confidence limits for chlorophyll integrated to the 1% light depth (mg Chl/m^2) for summer and winter seasons. # is number of data points. Significantly higher year within season designated by *. Main basin location, station 1. Seahurst location, stations 4 to 13. Data for 1964-1966 from unpublished University of Washington Department of Oceanography report. Data for 1979 from J. A. Runge (1981).

Year	Location	Summer	#	Winter	#
1964-1966	main basin	61 51-78	19	9 7-11	25
1979	main basin	96 69-160	13		
1982	main basin	77 57-115	5		
1983	main basin	118 85-195	6		
1982	Seahurst	67 60-83	44		
1983	Seahurst	154* 140-180	59	5-6	15
1984	Seahurst			19* 17-23	15

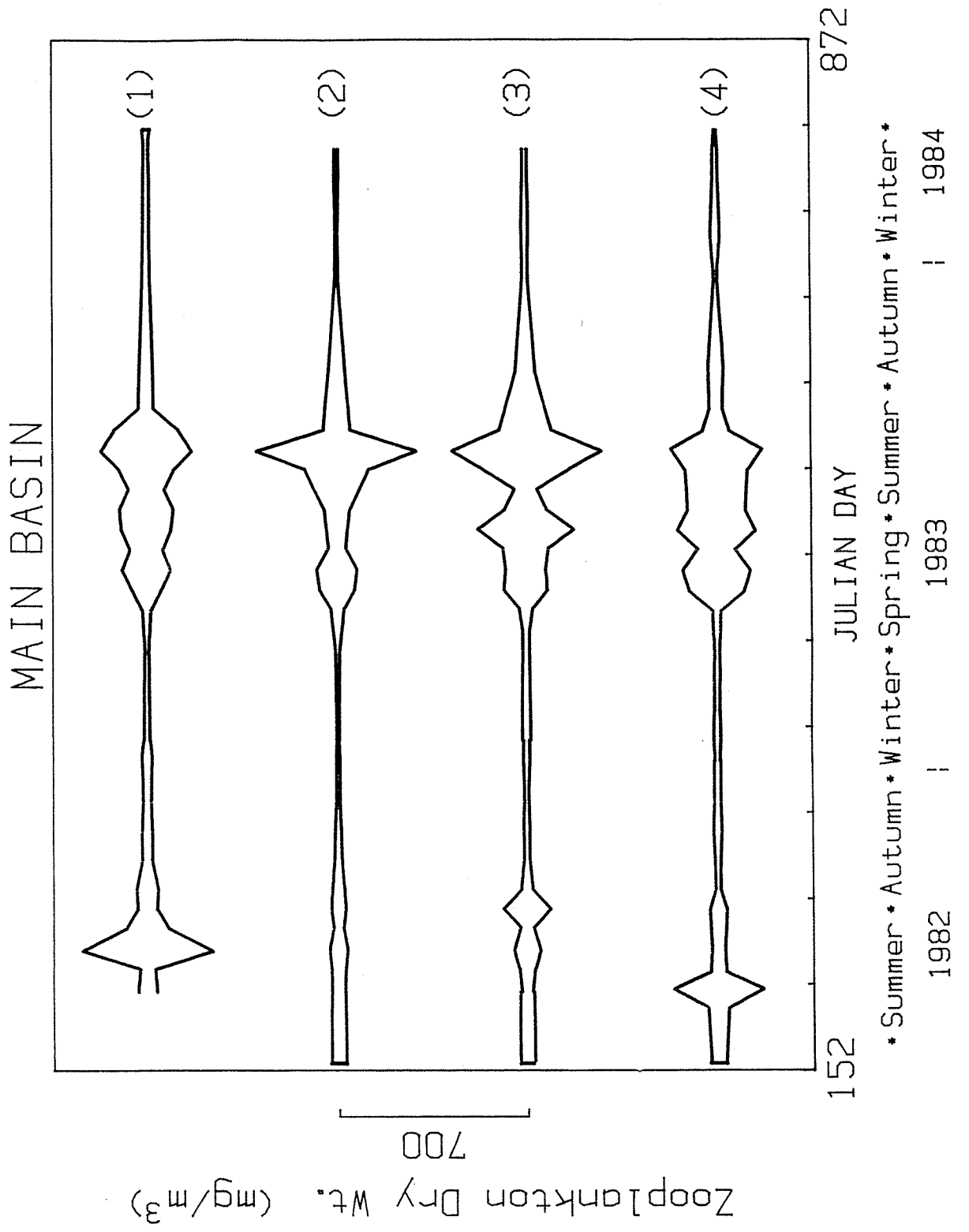

Figure 4.53. Total zooplankton dry weight over time at main basin stations 1 to 4. Scale on left depicts 700 mg/m^3 of zooplankton dry weight.

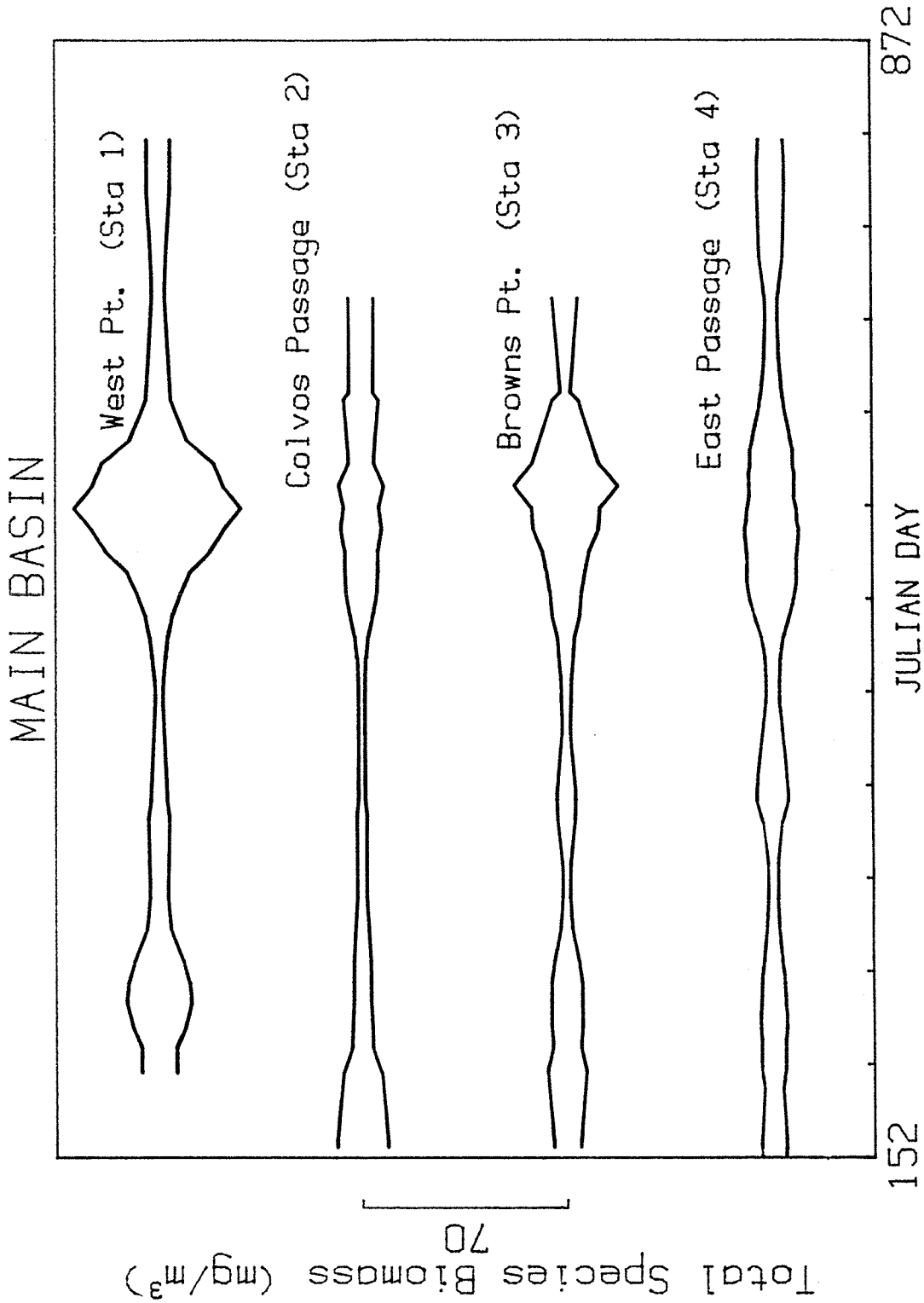

Figure 4.54. Total zooplankton species dry weight over time at main basin stations 1 to 4. Scale on left depicts 70 mg/m^3 of species zooplankton dry weight.

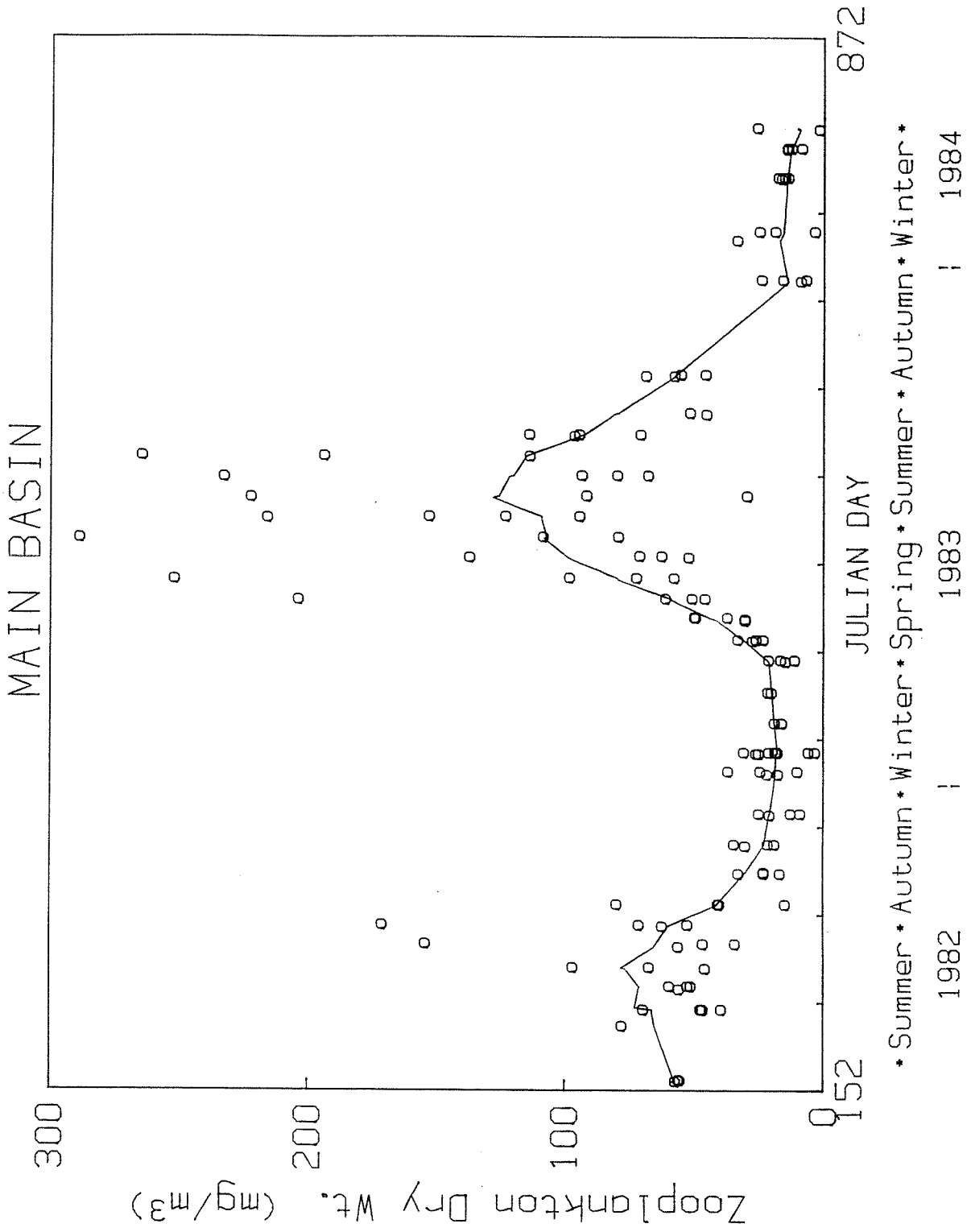

Figure 4.55. Zooplankton dry weight in main basin with smoothed distribution.

Table 4.26. Carrying capacities and 90% gamma confidence interval for zooplankton dry weight (mg/m^3) for summer and winter seasons stations 1 to 4 in main basin.

Station	1	2	3	4
Summer 1982	-	-	59 47-76	104 75-174
Summer 1983	95 81-114	-	106 73-178	192 144-284
Winter 1983	-	-	-	21 20-22
Winter 1984	-	-	-	-

biomass (Figure 4.56). Station 1 exhibited the highest total species biomass. This pattern was evident in both the summer of 1982 and 1983 and was the result of larger numbers of Calanus at station 1. The difference in numbers, which is significant at the 90% gamma confidence limits (Table 4.27), may be from the water column being deeper at station 1 than at stations 2, 3, or 4. This would favor the deeper living Calanus.

Corycaeus anglicus exhibited higher numbers in the summer of 1983 than in 1982. Station 1 in both years had higher numbers than were observed at stations 2, 3, and 4 (Table 4.28).

The temporal and spatial variability of the major species in the main basin fall into two categories with Paracalanus and Corycaeus having low spatial and temporal variability and the other species having high spatial and temporal variability (Table 4.29).

4.4.2.4 Nutrients

The concentrations of nutrients in the photic zone followed similar seasonal patterns at all stations (Figures 4.57, 4.58 and 4.59). Average concentrations integrated over the photic zone exhibited maximum values at the winter solstice and minimum values at the summer solstice (Figure 4.60, 4.61, and 4.62). Variability about the seasonally smoothed distributions was maximum at the summer solstice and minimum at the winter solstice, exhibited the greatest amount of variability of the primary nutrients followed by phosphate and silicate (Table 4.30).

For both the summer of 1982 and 1983 the mean photic zone concentrations of nitrate between stations were not significantly different within the 90% gamma confidence interval (Table 4.31).

Seasonal variations of nitrite exhibited a regular pattern at all stations (Figure 4.63). Maximum values occurred just after the autumnal

Table 4.27. Carrying capacities and 90% gamma confidence interval for Calanus pacificus (#/m^3) for summer and winter seasons, stations 1 to 4 in main basin. Stations with significantly higher levels marked *. NC designates species not counted because of low numbers.

Station	1	2	3	4
Summer 1982	271* 191-426	NC	145 111-204	80 56-141
Summer 1983	263* 218-394	130 76-482	176 121-342	68 55-89
Winter 1983	79 50-157	NC	52 33-113	69 54-99
Winter 1984	46 30-89	NC	NC	62 50-81

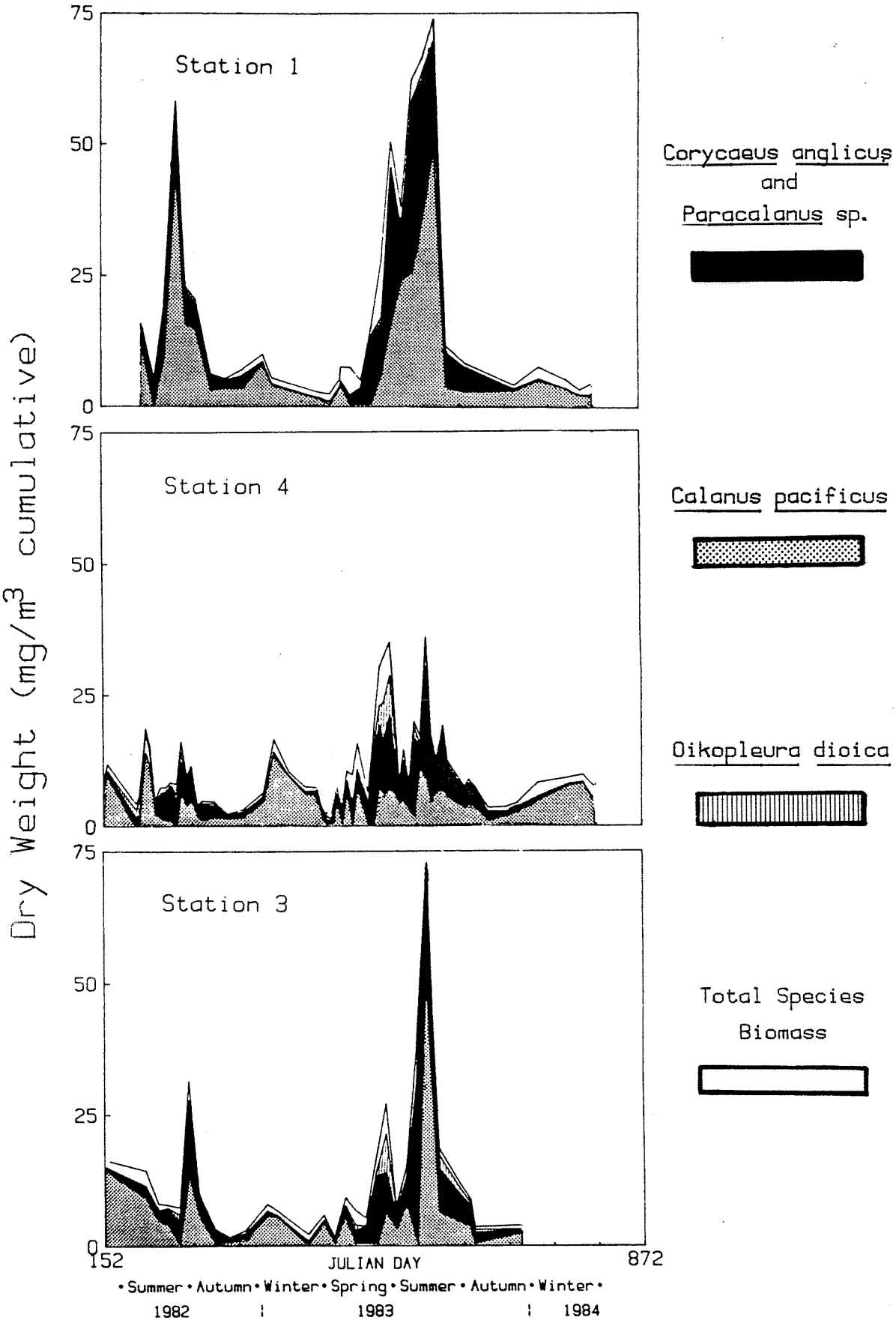

Figure 4.56. Zooplankton species dry weight over time at main basin stations 1, 4, 3 representing north to south locations.

Table 4.28. Carrying capacities and 90% gamma confidence intervals for Corycaeus anglicus (#/m^3) for summer and winter seasons, stations 1 to 4 in main basin. NC designates species not counted because of low numbers.

Station	1	2	3	4
Summer 1982	1009 853-1223	812 635-1172	692 602-813	746 618-939
Summer 1983	2771 2364-3457	1366 1068-1972	1972 1486-3769	1398 1081-2042
Winter 1983	194 138-324	172 140-251	148 120-194	114 101-139
Winter 1984	68 50-97	NC	NC	115 91-151

Table 4.29. Relative spatial and temporal variability of main basin zooplankton species. Measures described in section 4.6.3.10 using smoothing parameters T = 75 days, Te = 15 and Td = 10 days.

Property	Temporal variability	Spatial variability
Dry weight (mg/m^3)		
Calanus pacificus	1.20	0.60
Pseudocalanus sp.	1.13	0.52
Paracalanus sp.	0.70	0.43
Microcalanus sp.	0.95	0.53
Corycaeus anglicus	0.75	0.44
Oithona similis	0.72	0.40
Oikopleura dioica	1.1	0.56
Fritillaria borealis	0.87	0.44

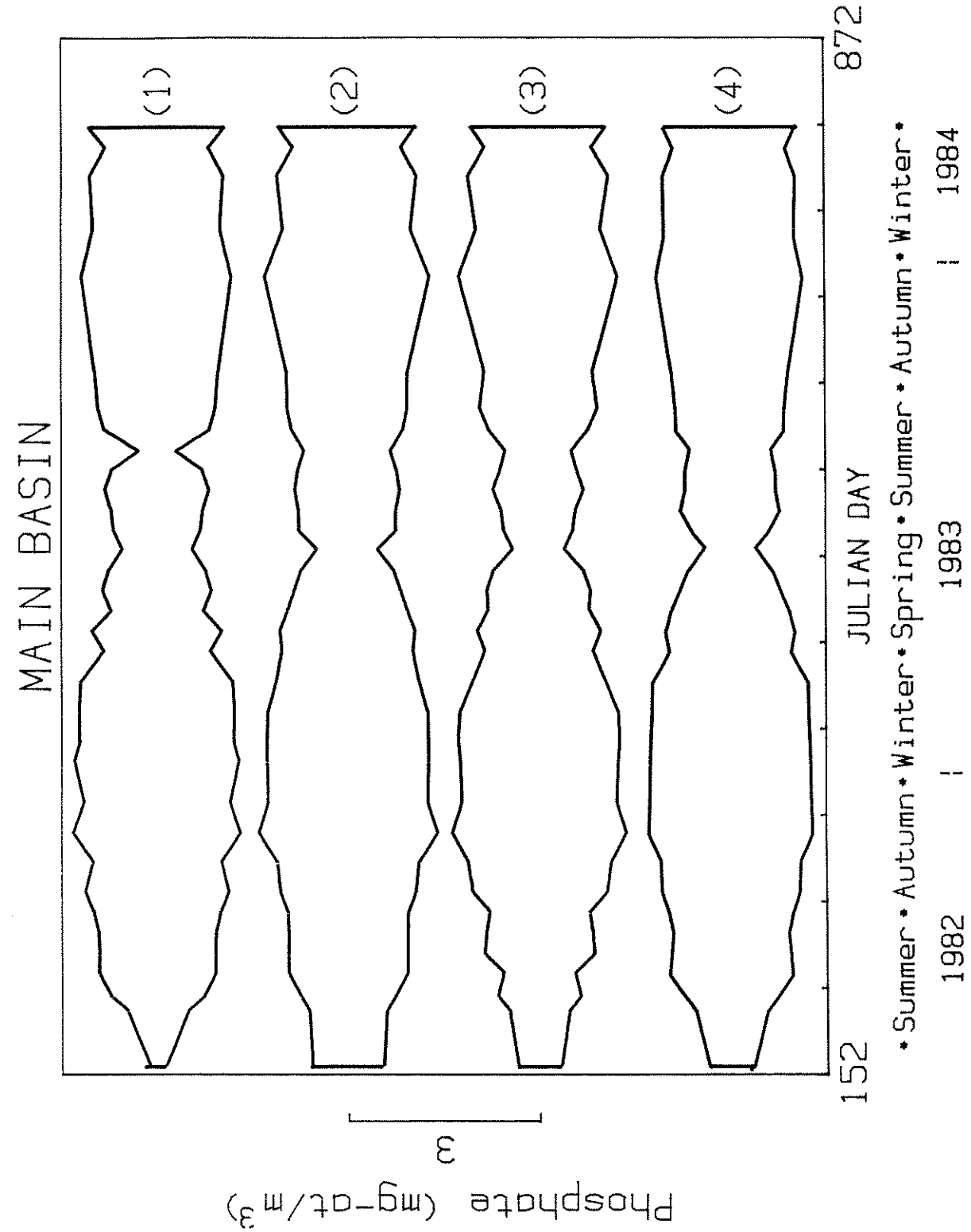

Figure 4.57. Photic zone phosphate concentrations over time at main basin stations 1 to 4. Scale on left depicts 3 mg-at/m^3.

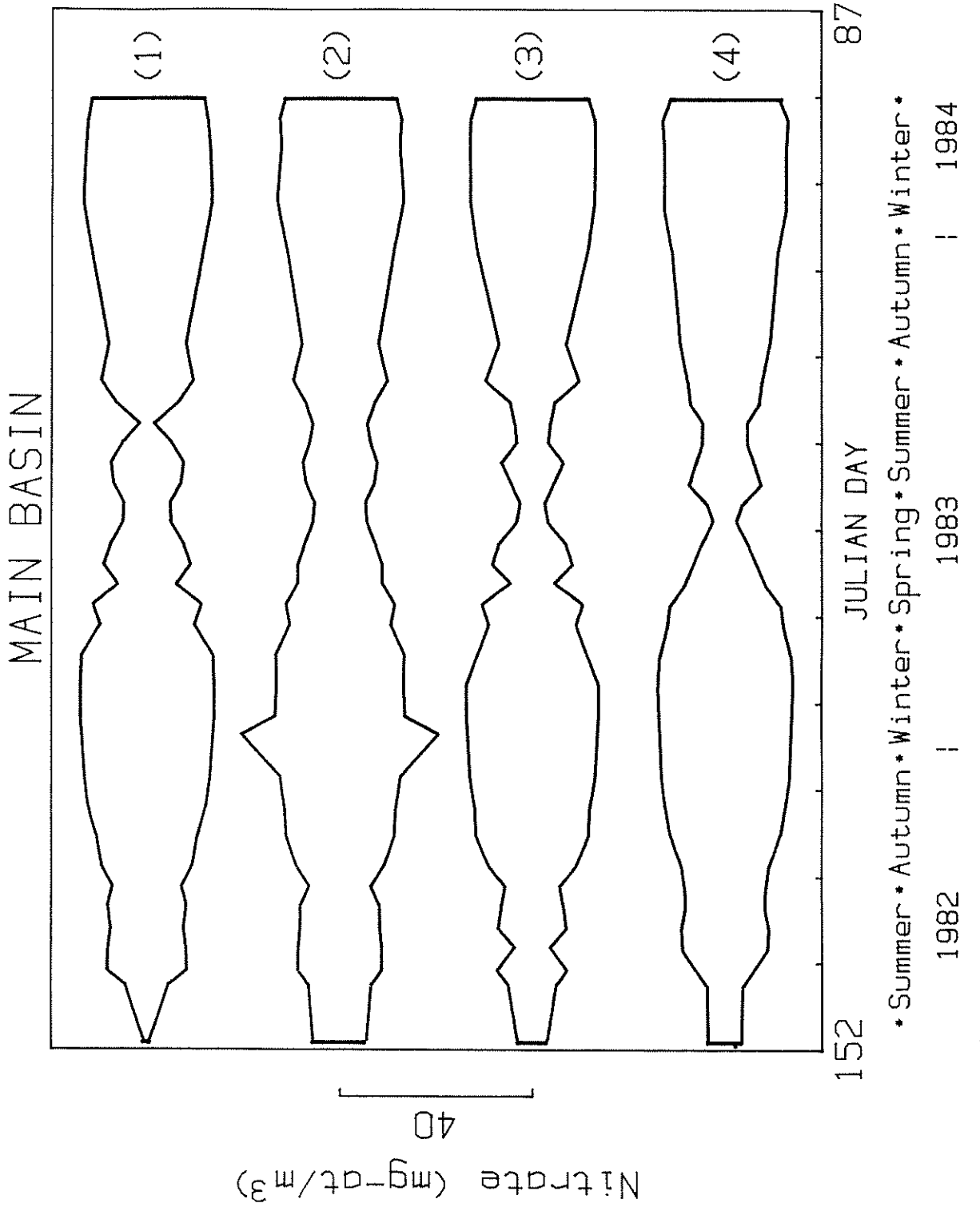

Figure 4.58. Photic zone nitrate concentrations over time at main basin stations 1 to 4. Scale on left depicts 40 mg-at/m^3.

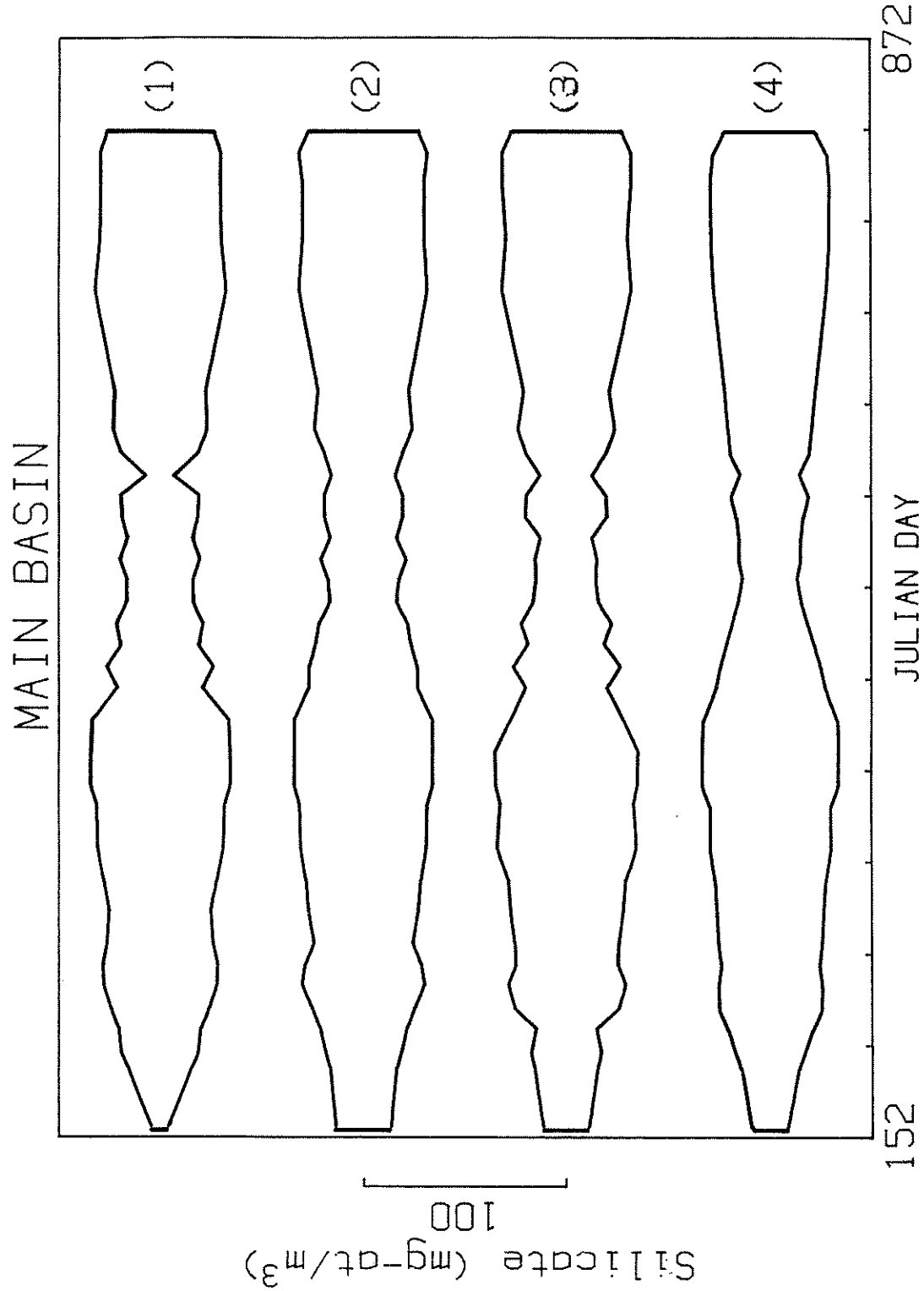

Figure 4.59. Photic zone silicate concentrations over time at main basin stations 1 to 4. Scale on left depicts 100 mg-at/m^3.

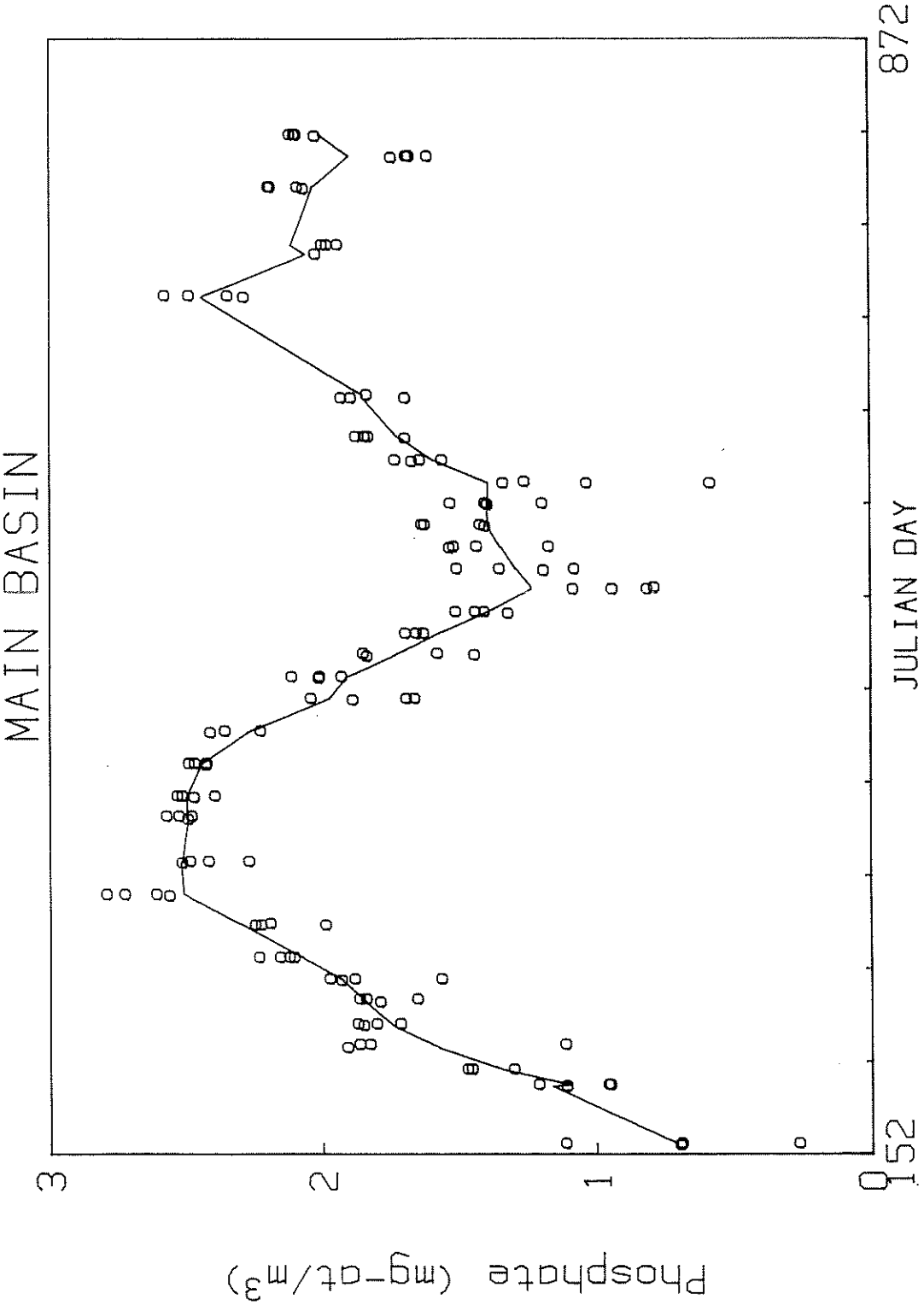

Figure 4.60. Phosphate concentration in the main basin photic zone with smoothed distribution.

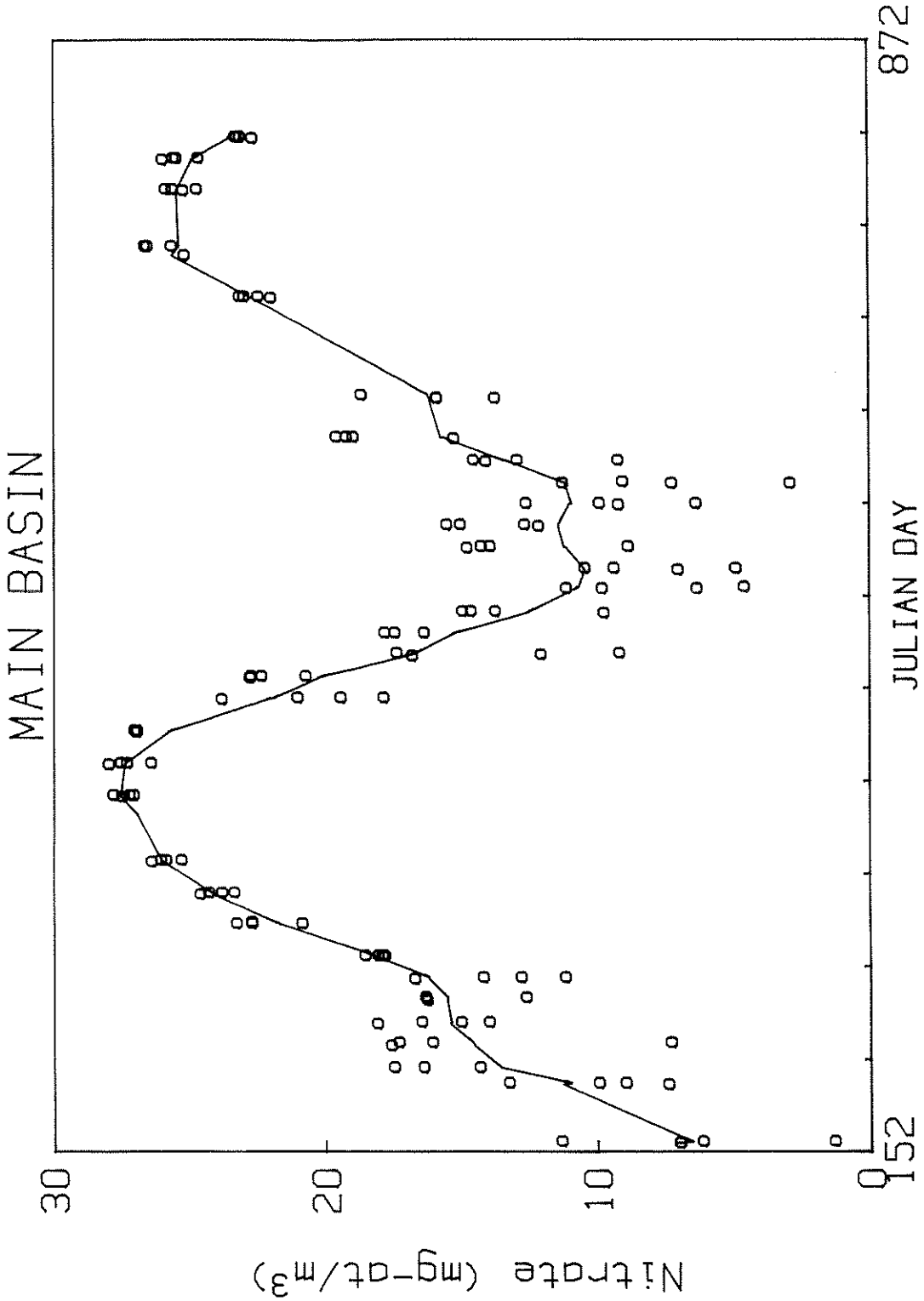

Figure 4.61. Nitrate concentration in main basin photic zone with smoothed distribution.

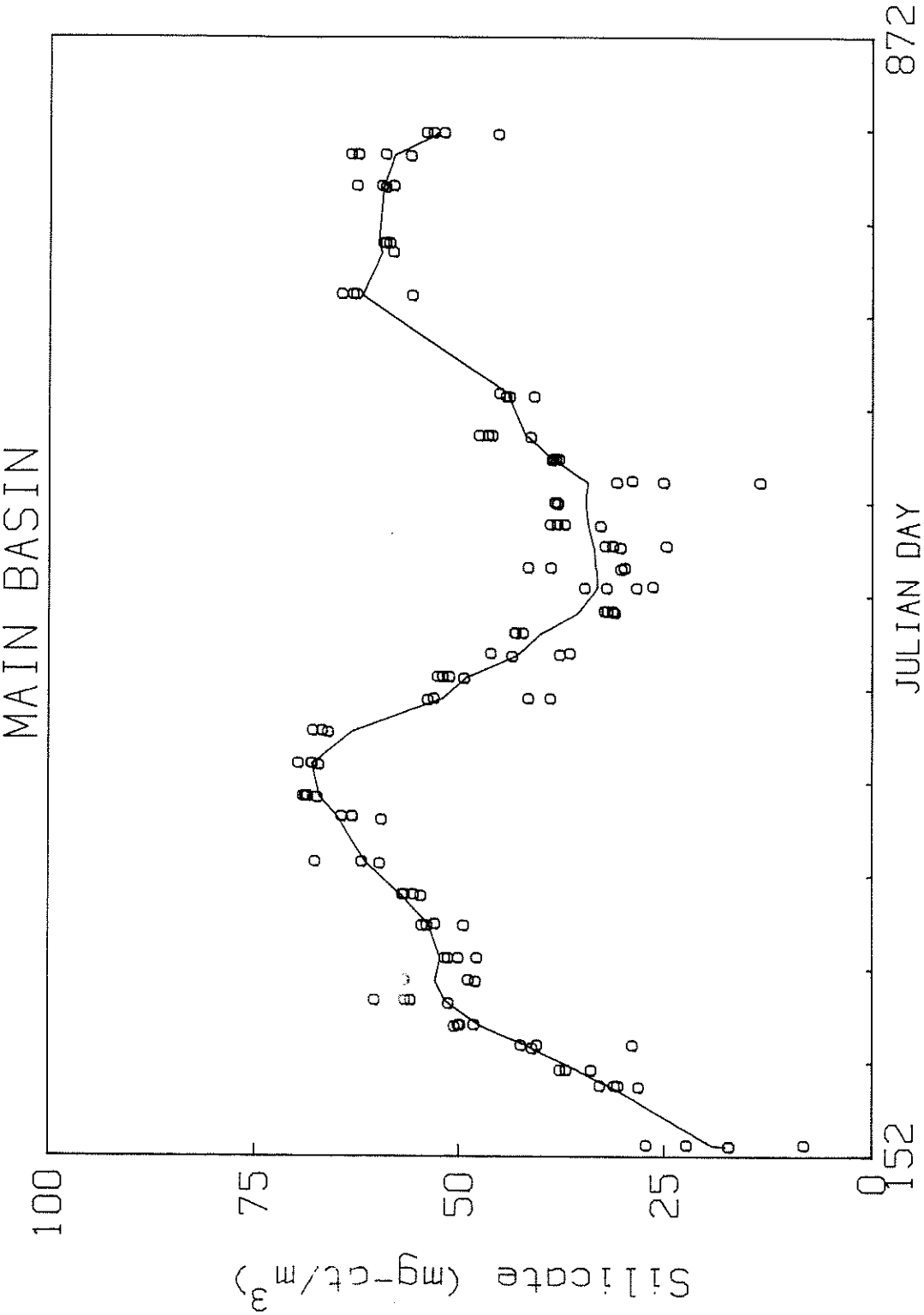

Figure 4.62. Silicate concentration in main basin photic zone with smoothed distribution.

Table 4.30. Relative spatial and temporal variability of main basin average depth integrated nutrients. Measures described in section 4.6.3.10 using smoothing T = 75 days and Te = 15 days.

Property	Temporal variability	Spatial variability
Nitrate	0.21	0.19
Phosphate	0.13	0.12
Silicate	0.12	0.10
Ammonia	0.42	0.28
Nitrite	0.24	0.17

Table 4.31. Mean value and 90% confidence interval for average depth integrated nitrate (mg-at/m^3) for summer and winter seasons, stations 1 to 4 in main basin.

Station	1	2	3	4
Summer 1982	14.6 12.6-17.4	16.2 15.2-17.6	11.7 9.9-14.2	15.3 12.4-19.6
Summer 1983	12.3 9.5-17.2	14.7 13.4-16.4	10.7 8.8-13.5	12.5 11.1-14.2

Table 4.32. Mean value and 90% confidence interval for average depth integrated ammonia (mg-at/m^3) for summer and winter seasons, stations 1 to 4 in main basin.

Station	1	2	3	4
Summer 1982	1.3 0.8-2.6	1.3 0.9-2.4	1.4 0.9-2.7	1.1 0.7-2.0
Summer 1983	0.5 0.4-0.8	0.5 0.4-0.7	0.4 0.3-0.5	0.5 0.4-0.7

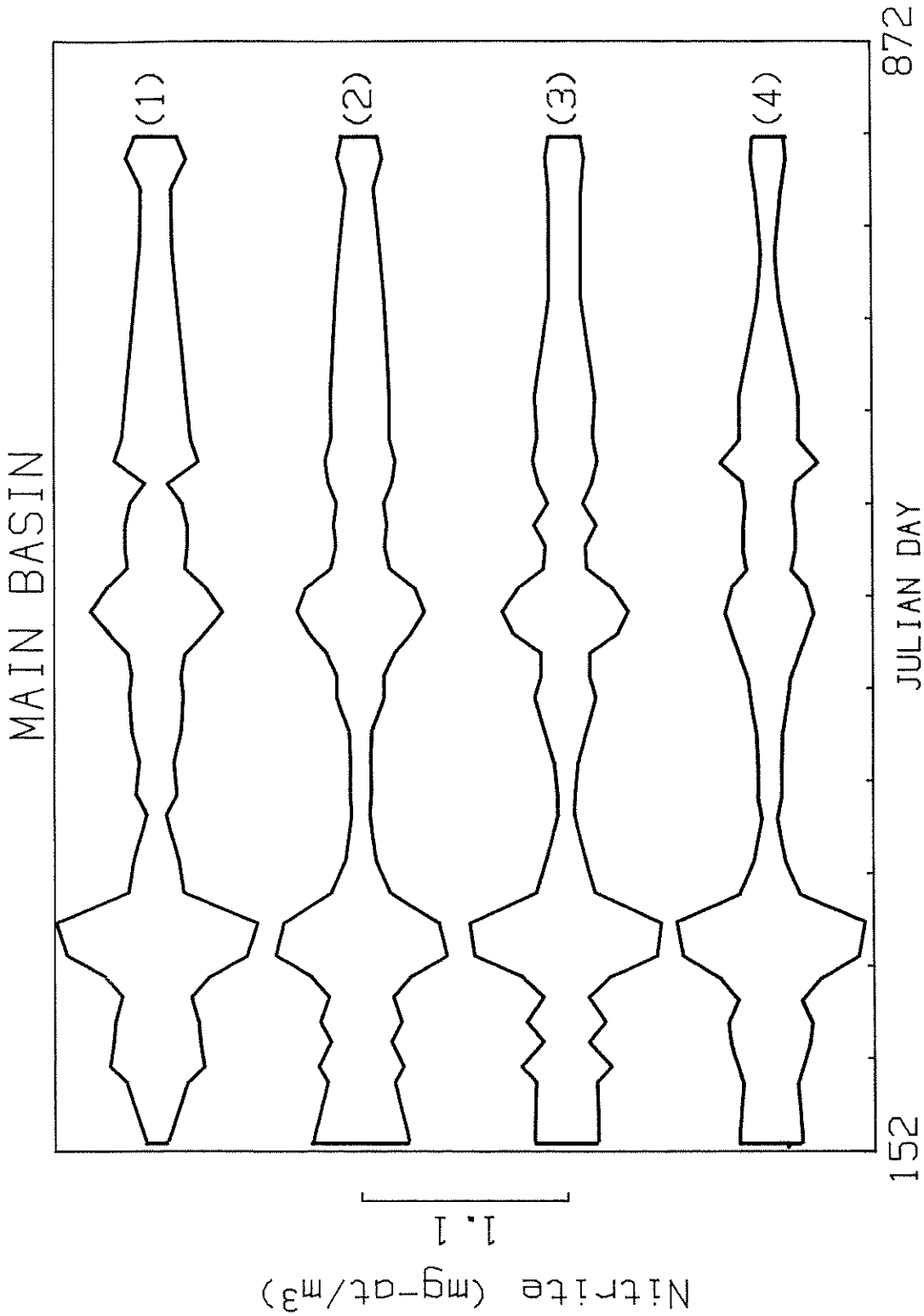

Figure 4.63. Photic zone nitrite concentrations over time at main basin stations 1 to 4. Scale on left depicts 1.1 mg-at/m^3.

equinox in 1982 and minimum values at the winter solstice. In 1983 nitrite was high in the spring. No sampling occurred near the autumnal equinox in 1983 so the autumn maximum was not observed (Figure 4.64). Temporal variability exceeded spatial variability for nitrite (Table 4.30).

Seasonal variations of average photic zone integrated ammonia were similar at all stations (Figure 4.65). Spring, summer and autumn concentrations in 1983 were about 0.6 mg-at/m 3. In 1982 ammonia levels were about 0.2 mg-at/m 3. Winter 1983 and 1984 levels were about 0.2 mg-at/m 3 (Figure 4.66). The reason for the differences in the ammonia levels between years is not known. The spatial and temporal variability of ammonia exceeded that for other nutrients (Table 4.30). Mean photic zone concentrations of ammonia between stations were the same within the 90% gamma confidence intervals for a given season. Higher levels in the summer of 1982 compared to 1983 (Table 4.32).

4.4.3 Seahurst Intertidal

Water samples for nutrients and chlorophyll collected from the Seahurst intertidal zone on a nearly daily basis had the same seasonal patterns as observed in the surface waters of the Seahurst Bight. This close correlation resulted from the daily tidal exchange of the intertidal water with the surface water of the Bight. The seasonal distributions of the properties were determined with the smoothing algorithms (Section 4.3.4.) with T = 75 days, Te = 15 days and Td = 3 days.

The Seahurst intertidal zone observations are compared with the surface water of the Bight and observations collected from an intertidal zone at Indianola Beach near Port Madison on the east side of the main basin across from Seattle. To assess the importance of tidal variability on the intertidal observations, intertidal samples collected every 1/2 hr on August 29, 1983

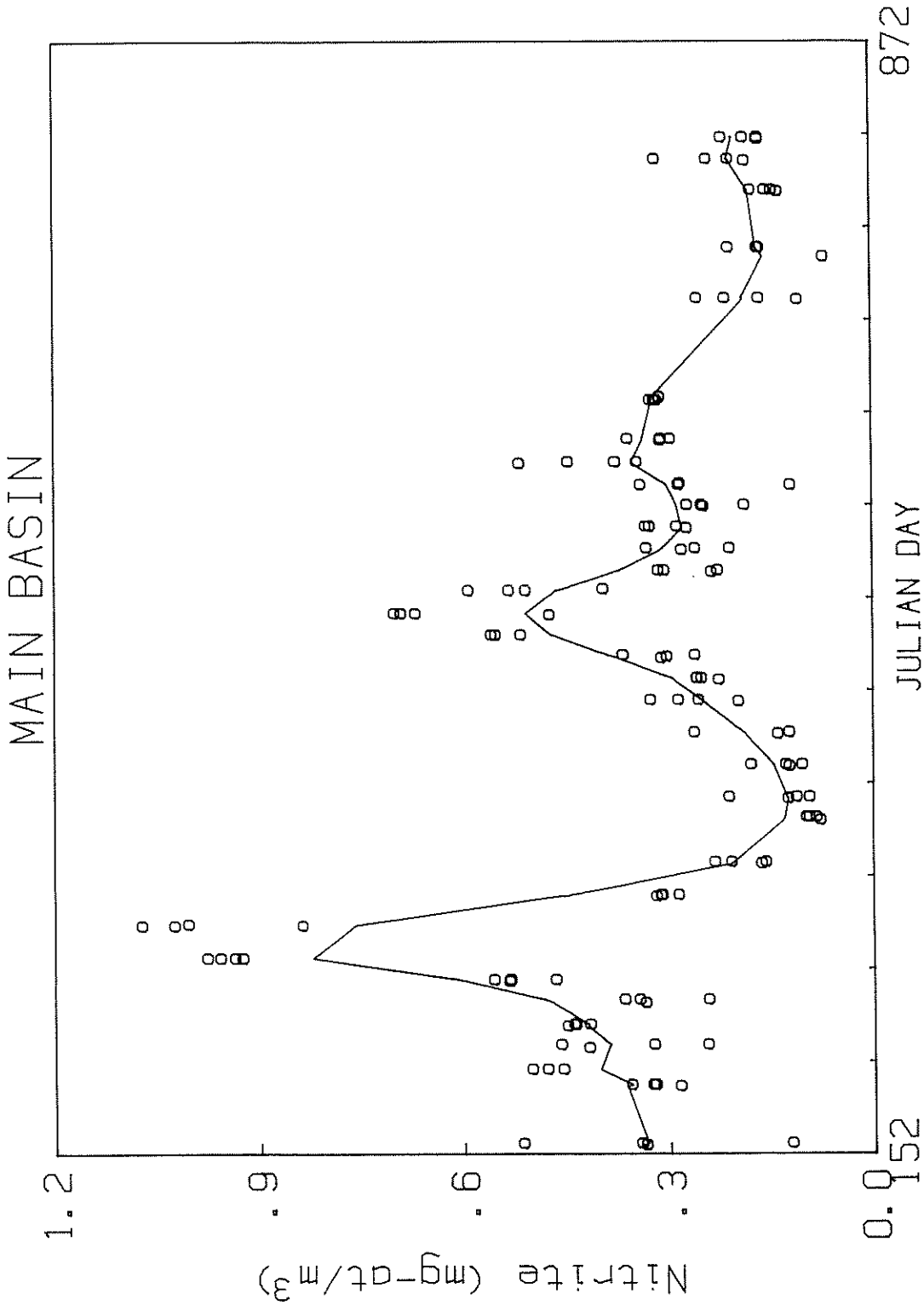

Figure 4.64. Nitrite concentration in main basin photic zone with smoothed distribution.

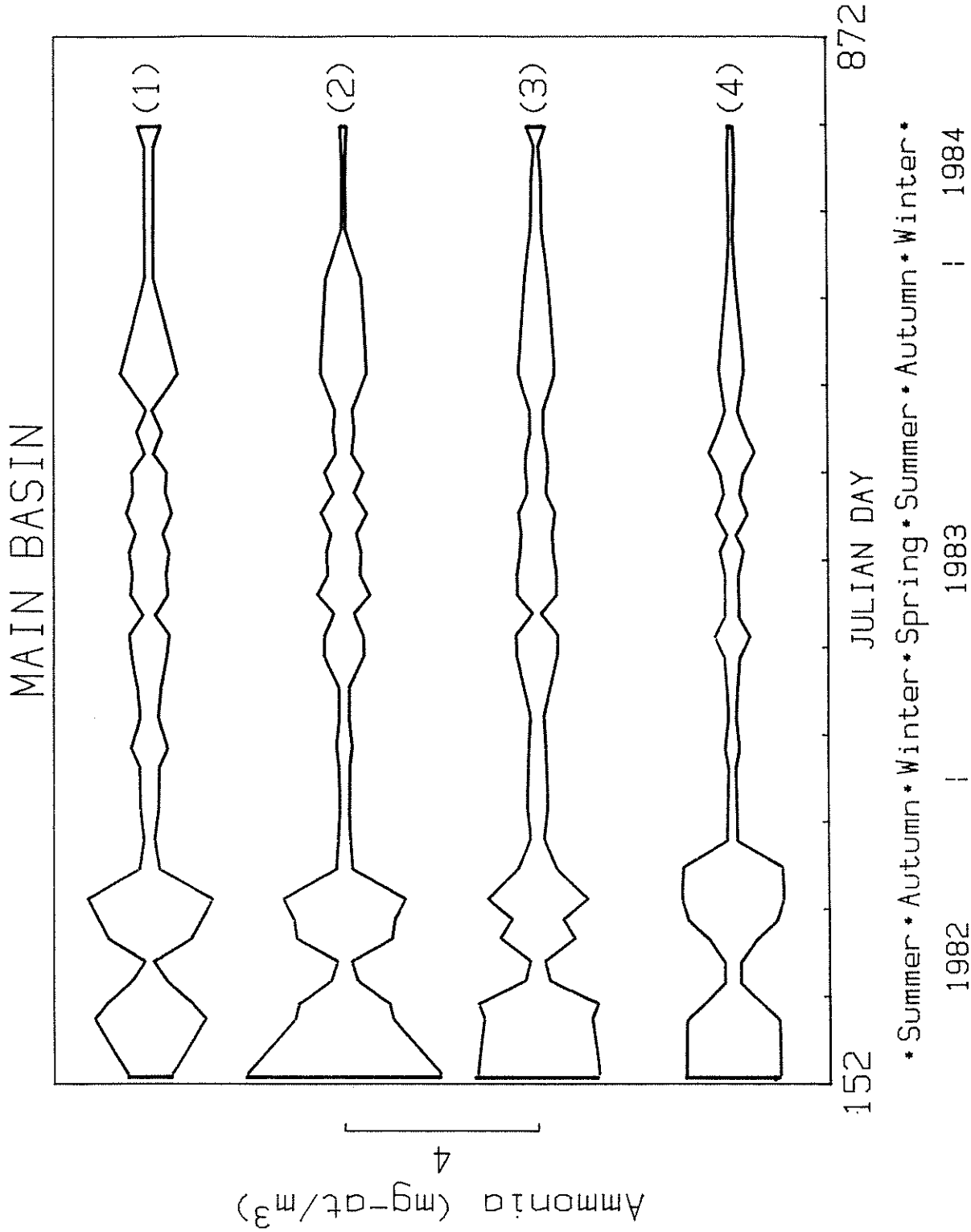

Figure 4.65. Photic zone ammonia concentrations over time at main basin stations 1 to 4. Scale on left depicts 4 mg-at/m^3.

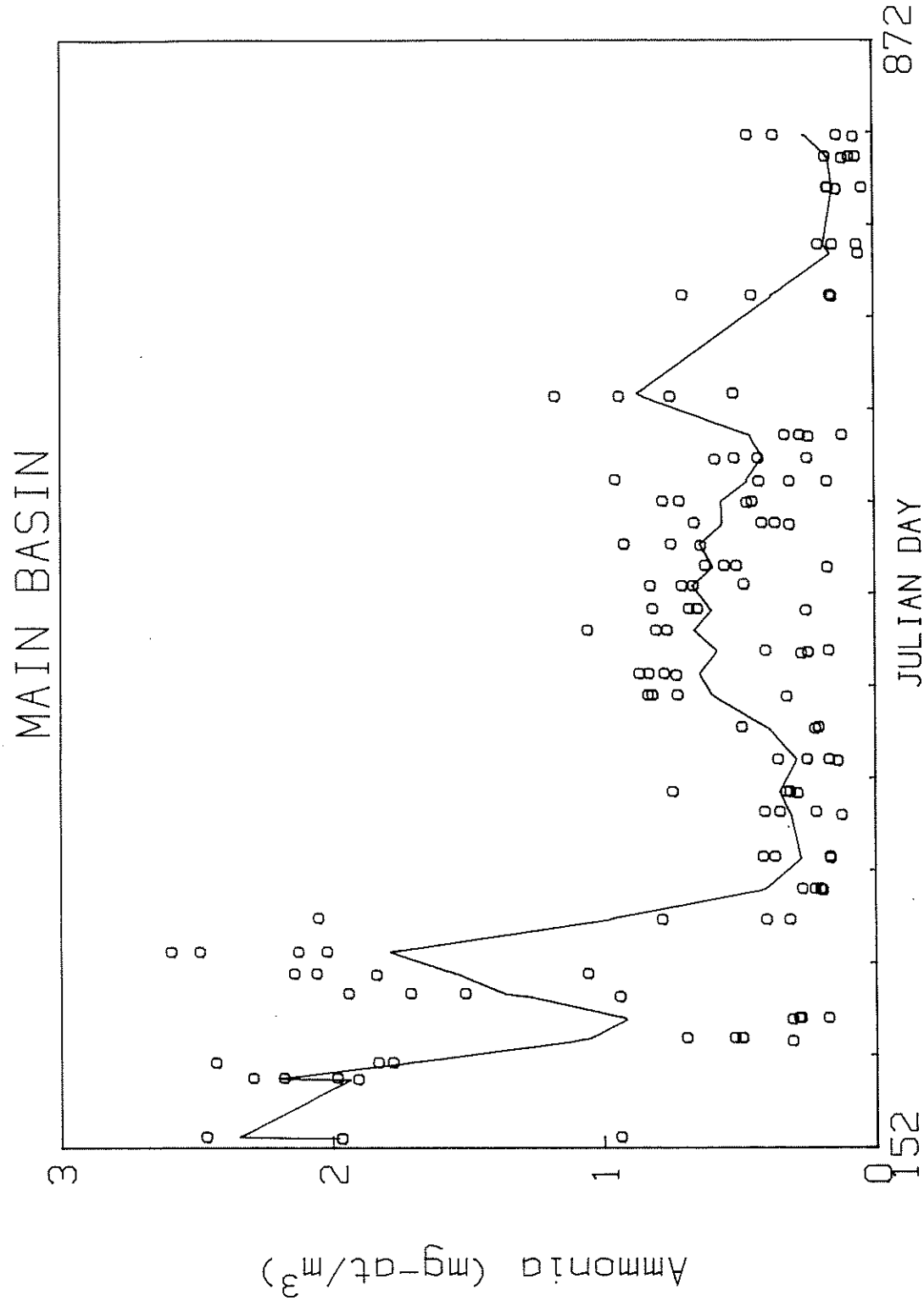

Figure 4.66. Ammonia concentration in main basin photic zone with smoothed distribution.

between 8 am and 9 pm are compared with the samples collected once a day.

4.4.3.1 Phytoplankton

The seasonal pattern of chlorophyll in the intertidal zone was similar to the pattern in the Seahurst Bight photic zone with a mid-summer maximum and winter minimum. Peak mid-summer seasonally smoothed chlorophyll concentrations were 4 mg/m^3 in 1982 and 7 mg/m^3 in 1983 (Figure 4.67a). Net production of chlorophyll occurred in 1983 from mid-winter to mid-summer. Net loss of chlorophyll occurred from mid-summer to mid-winter (Figure 4.67b). The magnitude of the changes were typically 0.05 mg Chl/m 3/day.

A comparison of the carrying capacity of chlorophyll at solstice and equinox dates for 1982 and 1983 indicates that the two years were not significantly different at the 90% gamma confidence interval with the exception of the winter solstice which in 1983 had twice the chlorophyll observed in 1982 (Table 4.33). A comparison with the intertidal chlorophyll at the Indianola Beach in 1983 indicates that the Seahurst levels were nearly twice as great at the summer solstice and autumnal equinox but the levels were essentially the same at the winter solstice (Table 4.33). The Seahurst Bight surface water chlorophyll was significantly higher than that of the intertidal zone at the vernal and autumnal equinoxes and the summer solstice. Winter values were not significantly different for 1983 and 1984.

Phaeopigments in the Seahurst intertidal water exhibited a seasonal cycle with a large amount of daily variability (Figure 4.68a). Net production of pigments occurred about the vernal equinox and in the later summer. Losses occurred in mid-summer and the winter (Figure 4.68b). In comparison to the Seahurst Bight surface waters and Indianola intertidal water, the Seahurst intertidal water had considerably higher phaeopigment levels. Levels in 1983 were also higher than in 1982 (Table 4.34).

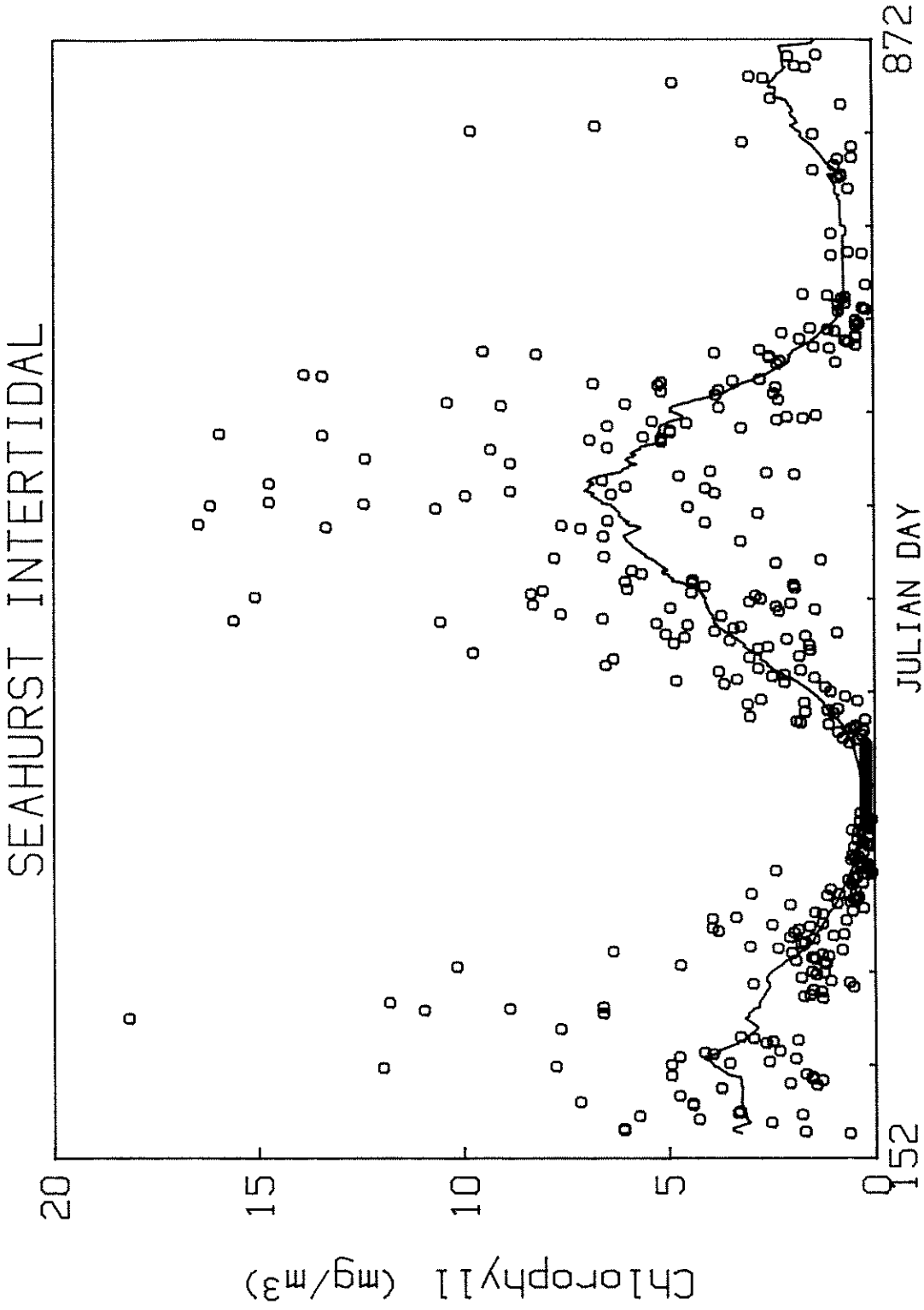

Figure 4.67a. Chlorophyll concentration in Seahurst intertidal zone with smoothed distribution.

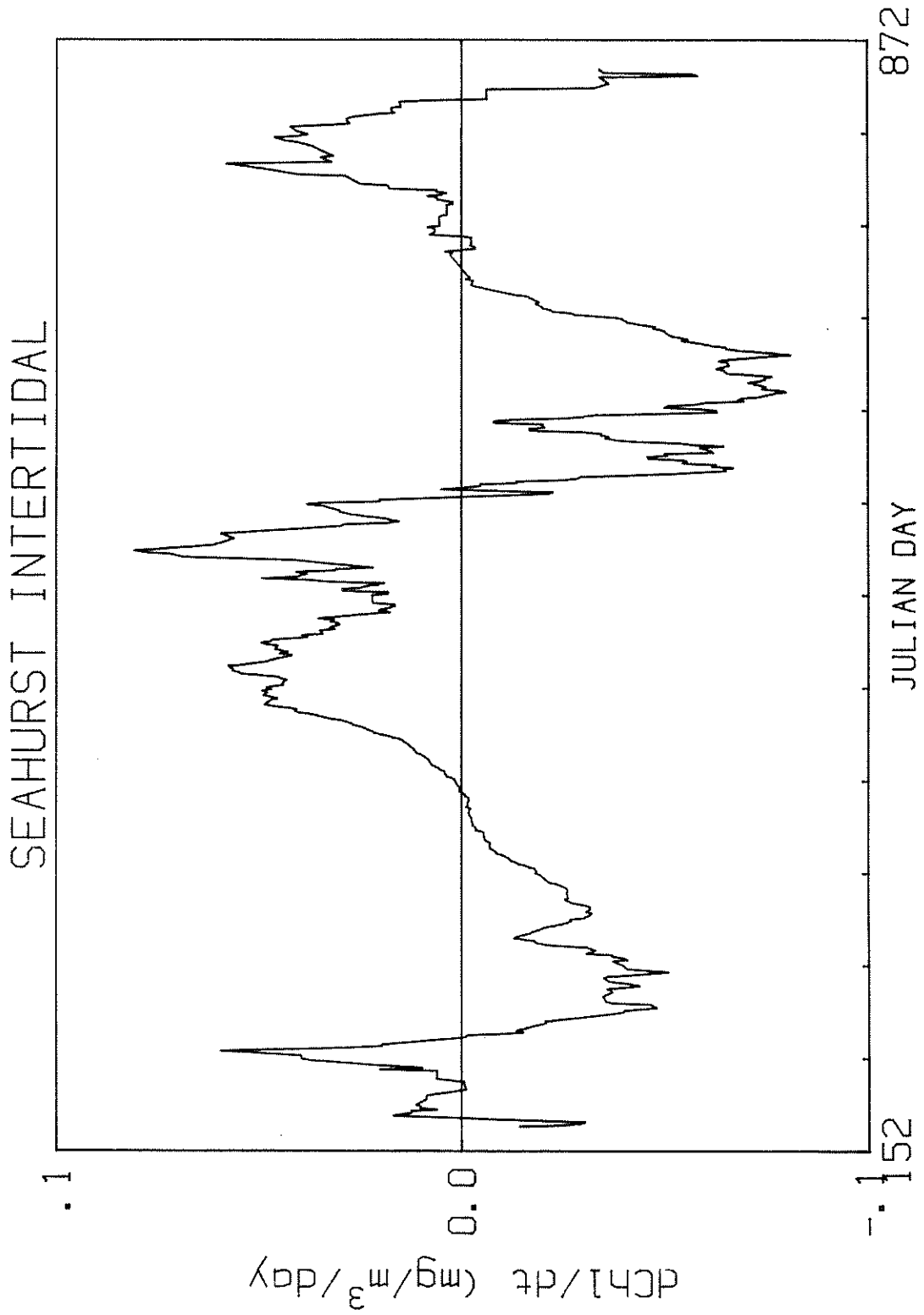

Figure 4.67b. Slope of smoothed distribution depicting rate of change of chlorophyll concentration.

Table 4.33. Carrying capacity and 90% gamma confidence interval for phytoplankton chlorophyll (mg/m^3) for Seahurst and Indianola intertidal zones and the surface water of Seahurst Bight. Data were collected from 6-week periods about the equinox and solstice dates for 1982 and 1983.

Period	Seahurst intertidal	Seahurst Bight, 0 m	Indianola intertidal
Summer solstice, 1982	4.9 (3.7-7.4)	6.3 (4.6-11.7)	
Summer solstice, 1982	5.3 (4.4-6.8)	8.3* (7.5-9.9)	3.3 (2.6-4.6)
Autumnal equinox, 1982	4.0 (3.4-6.6)	9.7* (8.9-15.6)	
Autumnal equinox, 1983	6.0 (5.1-7.7)	15.5* (13.6-21.0)	2.9 (2.5-3.5)
Winter solstice, 1982	0.4 (0.3-0.5)	0.4 (0.04-0.5)	
Winter solstice, 1983	0.8 (0.6-1.2)	1.2 (1.0-1.8)	1.3 (1.0-7.1)
Vernal equinox, 1982	1.7 (1.4-2.2)	4.4 (3.9-6.6)	

*Significantly higher level within period.

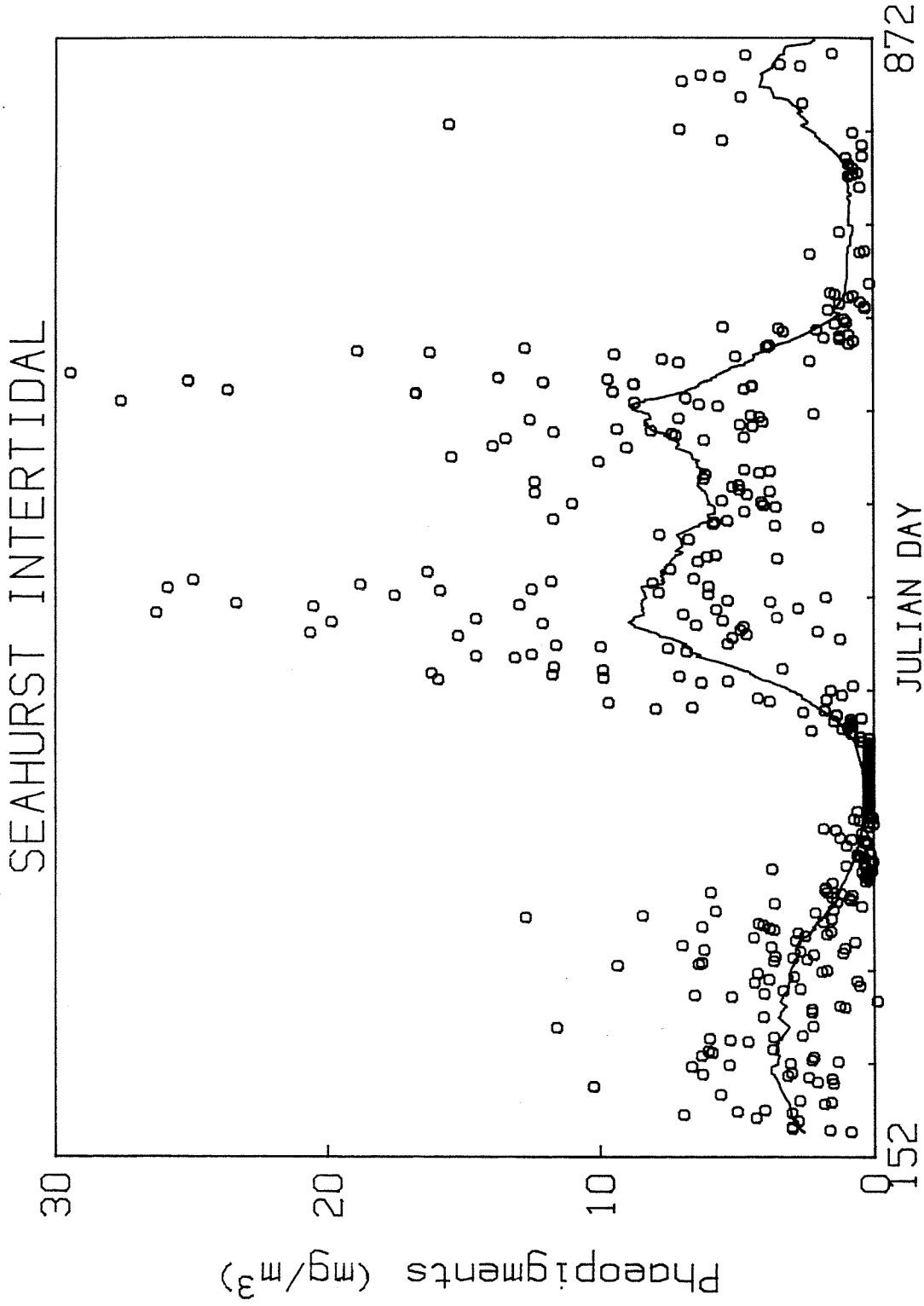

Figure 4.68a. Phaeopigment concentration in Seahurst intertidal zone with smoothed distribution.

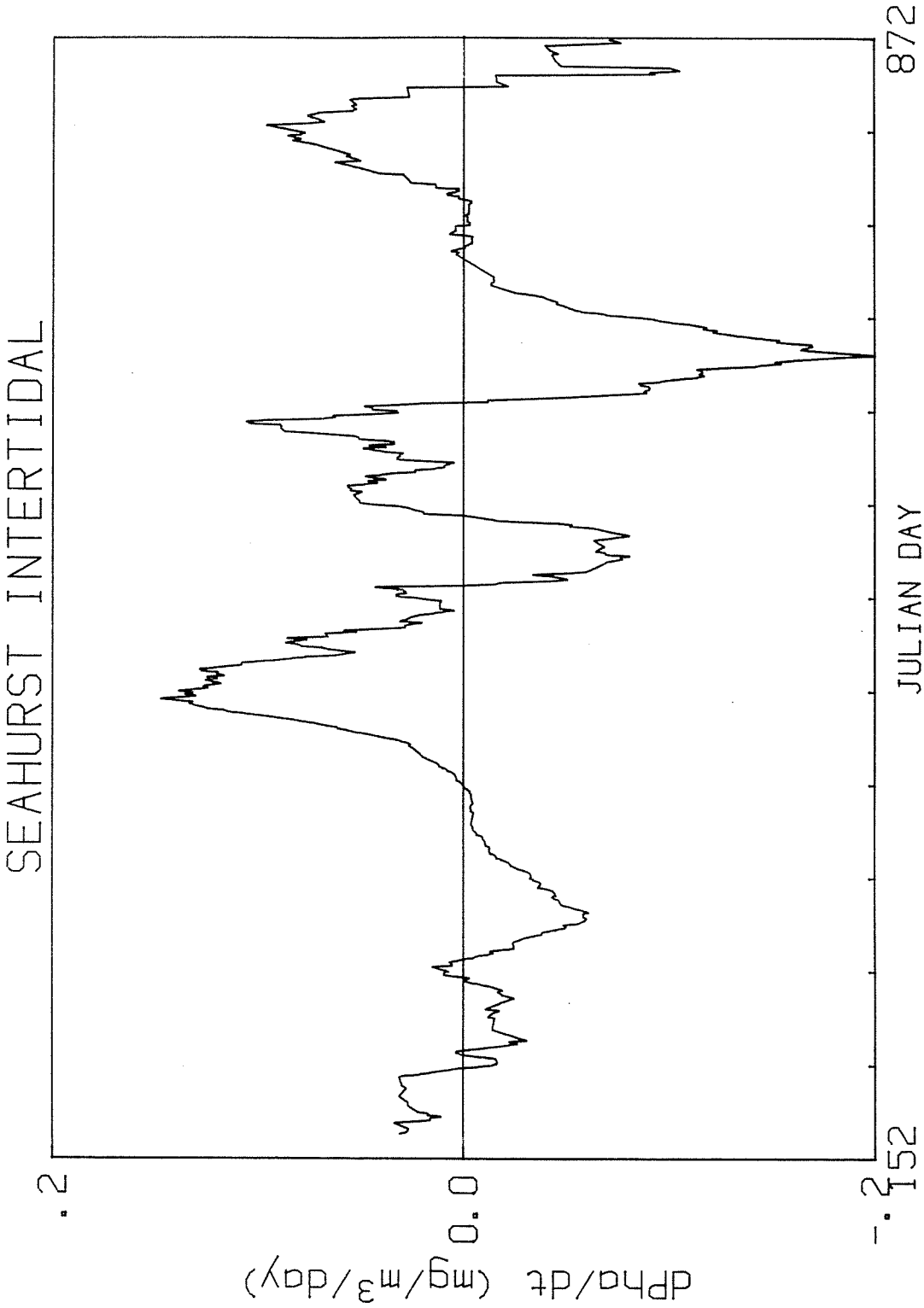

Figure 4.68b. Slope of smoothed distribution depicting rate of change of phaeopigment concentration.

Table 4.34. Carrying capacity and 90% gamma confidence interval for phaeopigments (mg/m^3) for Seahurst and Indianola intertidal zones and the surface water of Seahurst Bight. Data were collected from 6-week periods about the equinox and solstice dates for 1982 and 1983.

Period	Seahurst intertidal	Seahurst Bight, 0 m	Indianola intertidal
Summer solstice, 1982	4.9* (3.6-8.5)	2.9 (2.0-6.2)	
Summer solstice, 1982	10.2* (8.1-14.0)	2.5 (2.3-3.3)	2.1 (1.6-3.0)
Autumnal equinox, 1982	4.2* (3.5-5.9)	1.0 (0.9-1.8)	
Autumnal equinox, 1983	10.5* (8.9-14.0)	1.5 (1.3-2.5)	2.5 (1.8-3.6)
Winter solstice, 1982	0.7 (0.6-0.9)	0.1 (0.1-0.1)	
Winter solstice, 1983	1.0* (0.7-1.6)	0.3 (0.2-0.4)	1.3 (0.9-2.1)
Vernal equinox, 1982	4.2* (3.5-6.4)	1.3 (1.2-2.0)	

*Significantly higher level within period.

The relative temporal variability of chlorophyll and phaeopigment were similar. The relative variability observed in a day is also similar (Table 4.35), suggesting that, in the intertidal zone, the major pigment variability occurs on a diel scale. In comparison, the diel scale temporal variability of integrated average chlorophyll in Seahurst Bight was 0.27, this indicated that the variability in the Bight was on longer time scale.

4.4.3.2 Nutrients

The nutrients, nitrate, phosphate and silicate had maximum intertidal levels at the winter solstice and minimum levels at the summer solstice. The maximum levels at the winter solstice of 1983 were 85% of the levels in 1982 for the three properties. Summer solstice levels of phosphate and silicate were similar for 1982 and 1983, while 1983 nitrate levels were 40% below those of 1982 (Figures 4.69a, 4.70a, and 4.71a). The maximum nutrient increases occurred in mid-autumn and the maximum loss occurred close to the vernal equinox (Figure 4.69b, 4.70b, and 4.71b). The Seahurst intertidal nutrient concentrations were similar to the surface levels in the Bight and the Indianola intertidal zone. The pattern for nitrate at the solstice and equinox dates is representative of the other nutrients (Table 4.36).

Nitrite exhibited peaks in the spring and autumn of all years. Low values occurred in the winter and summer. The highest and lowest values occurred in 1982 (Figure 4.72a). The seasonal pattern and concentrations of nitrite in the intertidal zone, Seahurst Bight, and the main basin were similar. Typical rates of change were on the order of 0.05 mg-at/m^3/day (Figure 4.72b).

Ammonia levels in the intertidal zone were highly variable from day to day but a weak seasonal pattern was evident with low values occurring in the winter and high values in the spring (Figure 4.73a). The seasonal pattern had

Table 4.35. Relative temporal variability of properties on seasonal and diel scales in the Seahurst intertidal zone and bight. Intertidal zone diel scale includes samples collected August 29, 1983 between 8: a.m. and 9:00 p.m. Bight diel scale determined from average integrated water column values collected at bight stations between 10:00 a.m. and 4:00 p.m.

	Intertidal zone		Seahurst Bight	
Property	Seasonal scale	Diel scale	Seasonal scale	Diel scale
Chlorophyll	0.86	0.74	1.16	0.27
Phaeopigment	1.00	0.84	0.90	0.27
Phosphate	0.13	0.18	0.16	0.09
Silicate	0.14	0.27	0.14	0.09
Nitrate	0.33	1.00	0.27	0.21
Nitrite	0.33	0.43	0.28	0.16
Ammonia	0.43	0.45	0.47	0.30

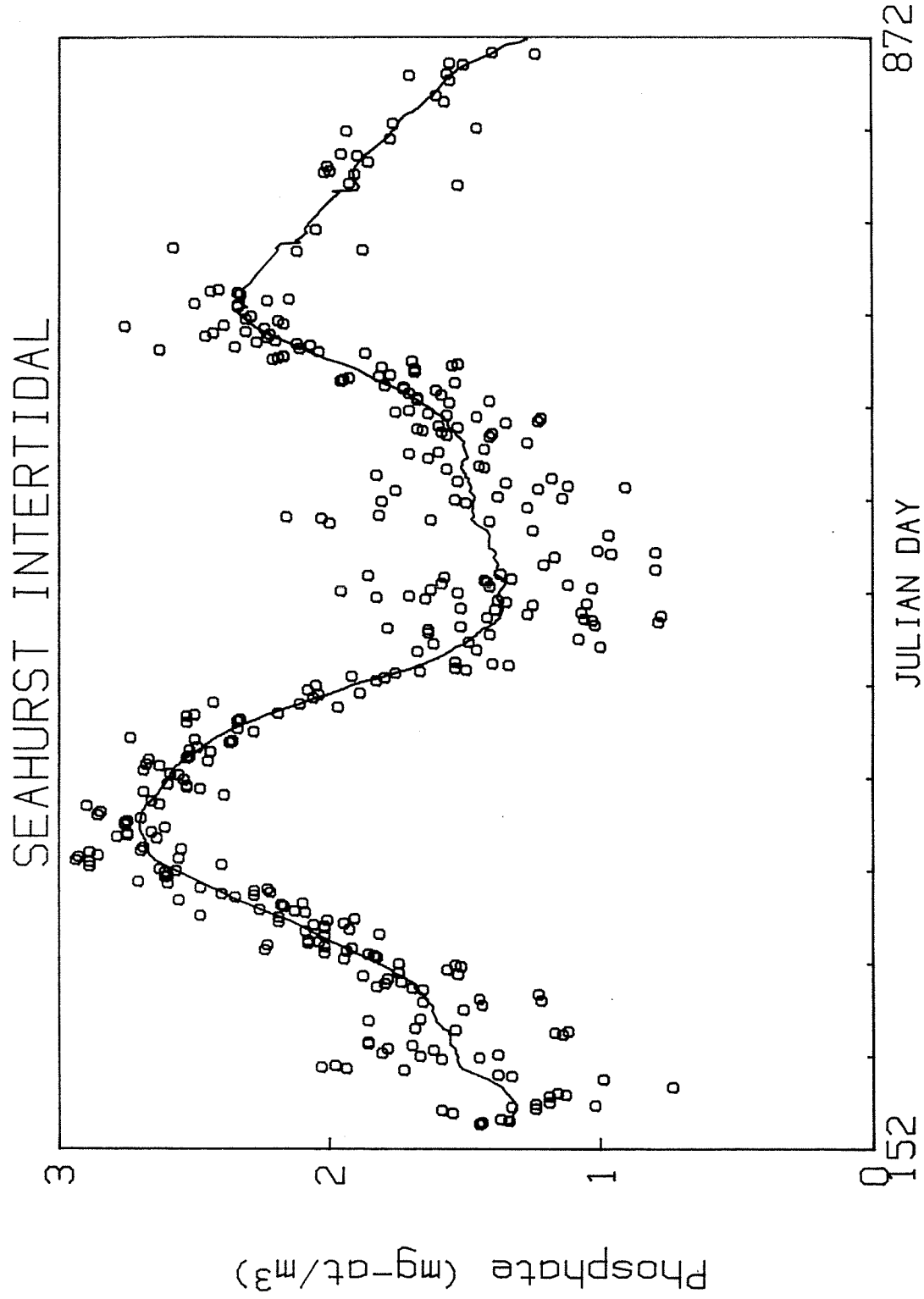

Figure 4.69a. Phosphate concentration in Seahurst intertidal zone with smoothed distribution.

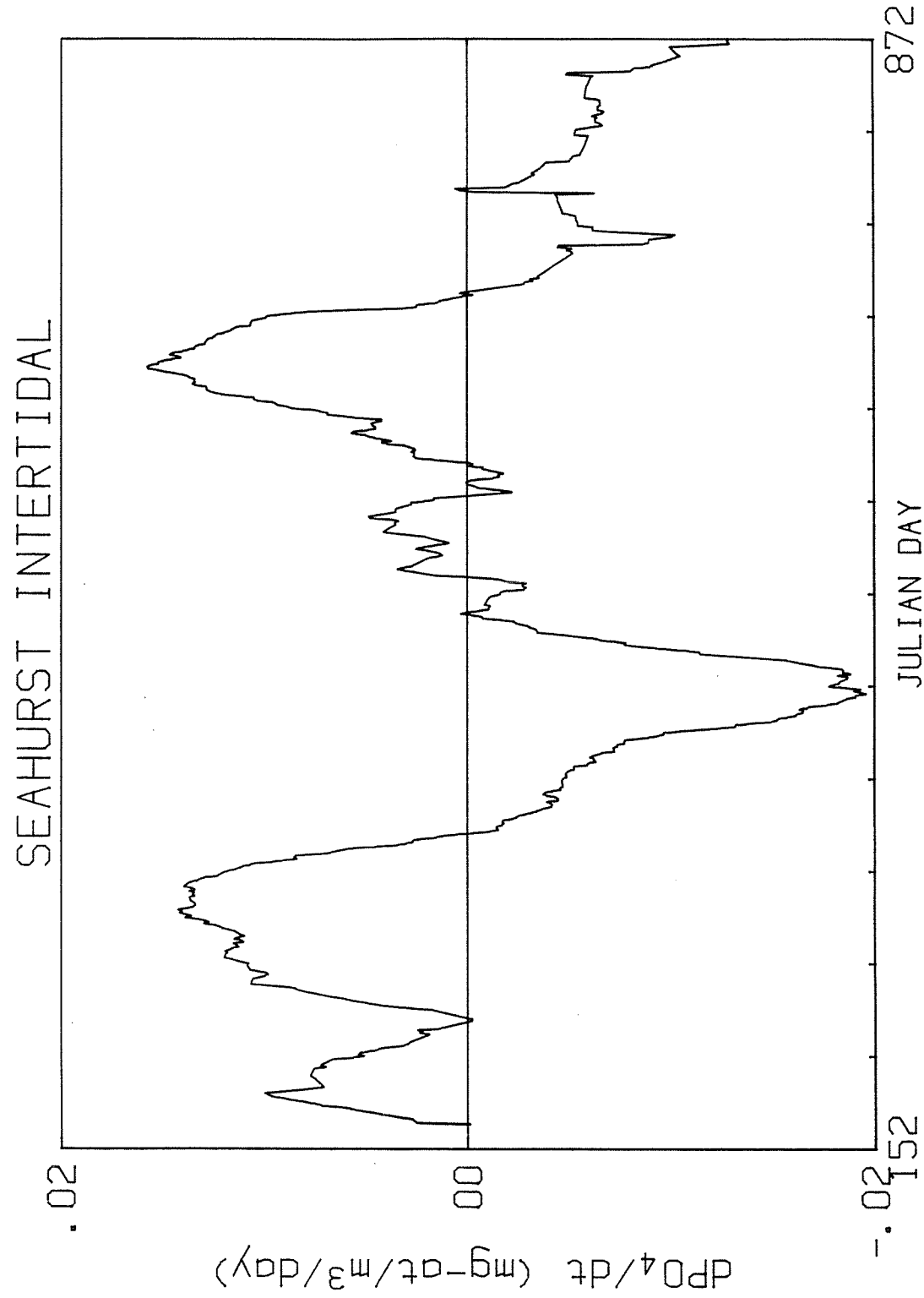

Figure 4.69b. Slope of smoothed distribution depicting rate of change of phosphate concentration.

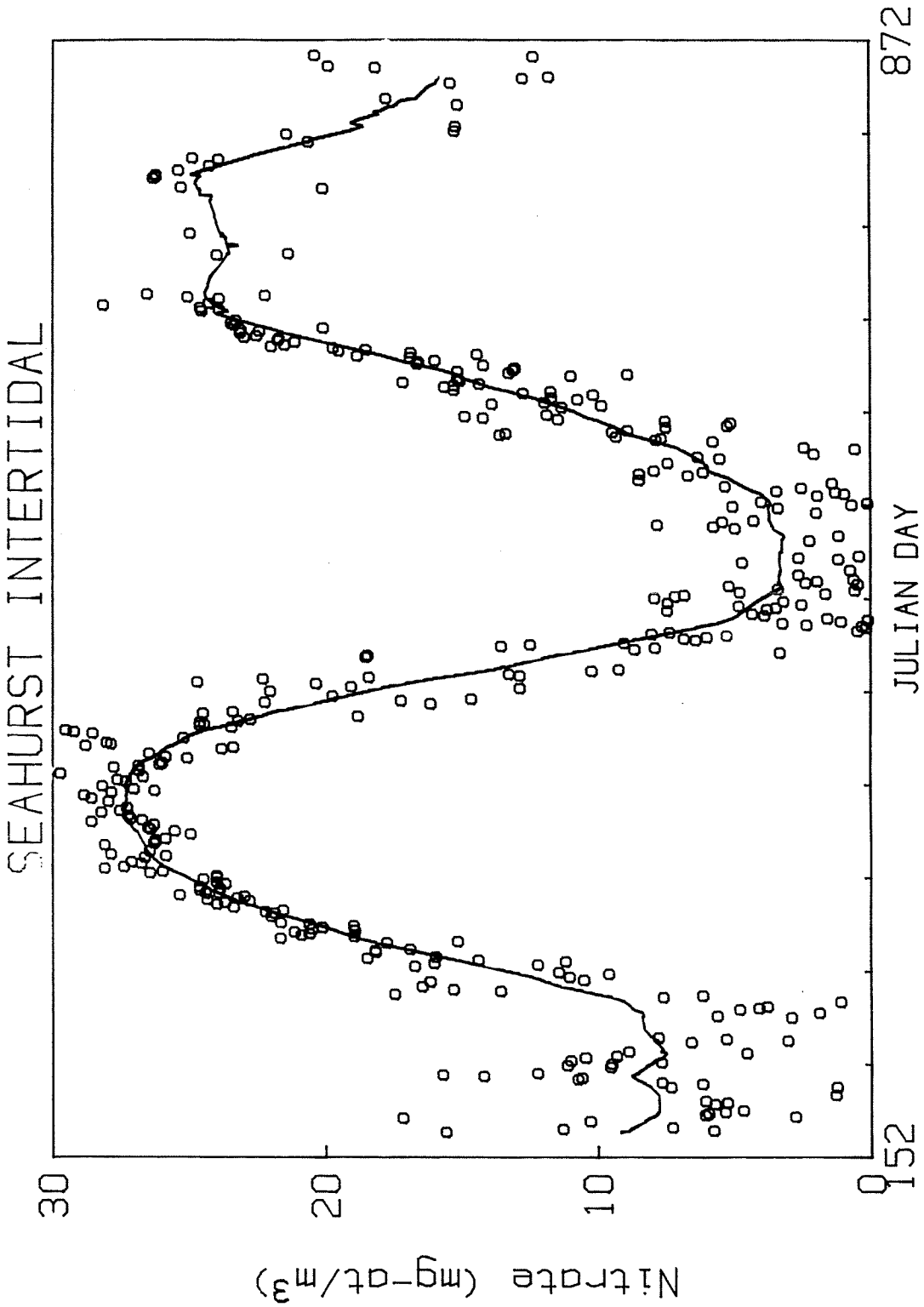

Figure 4.70a. Nitrate concentration in Seahurst intertidal zone with smoothed distribution.

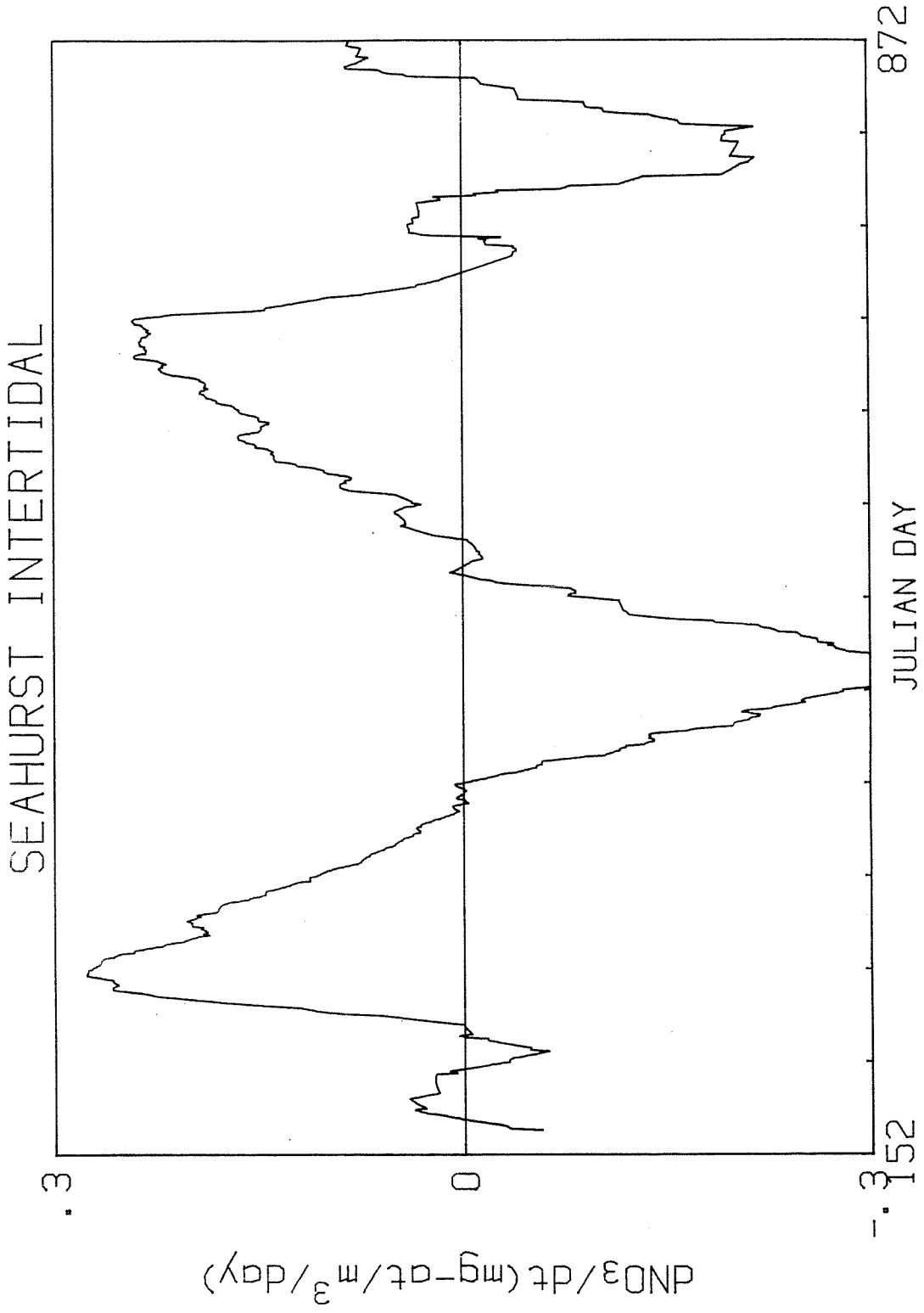

Figure 4.70b. Slope of smoothed distribution depicting rate of change of nitrate concentration.

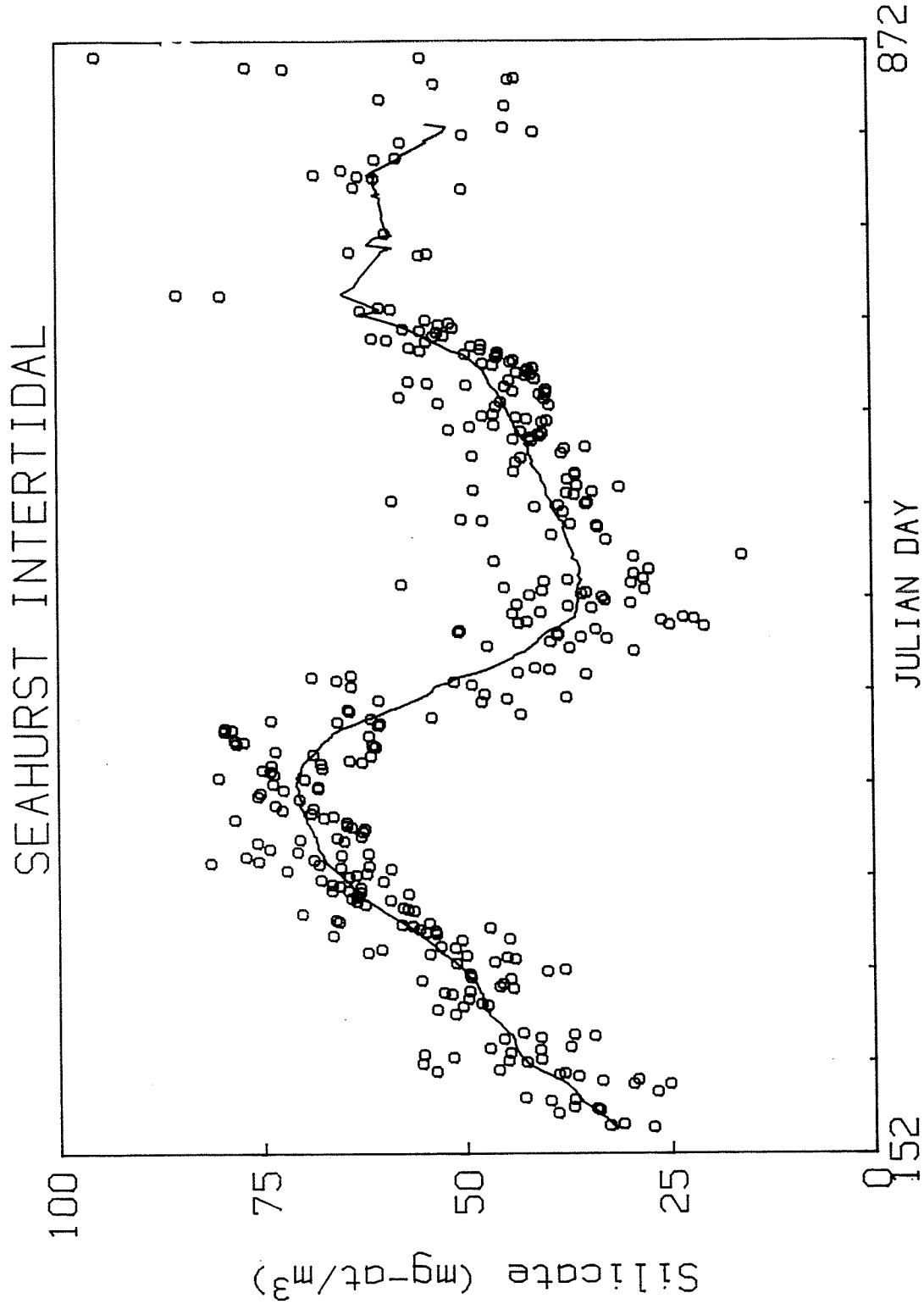

Figure 4.71a. Silicate concentration in Seahurst intertidal zone with smoothed distribution.

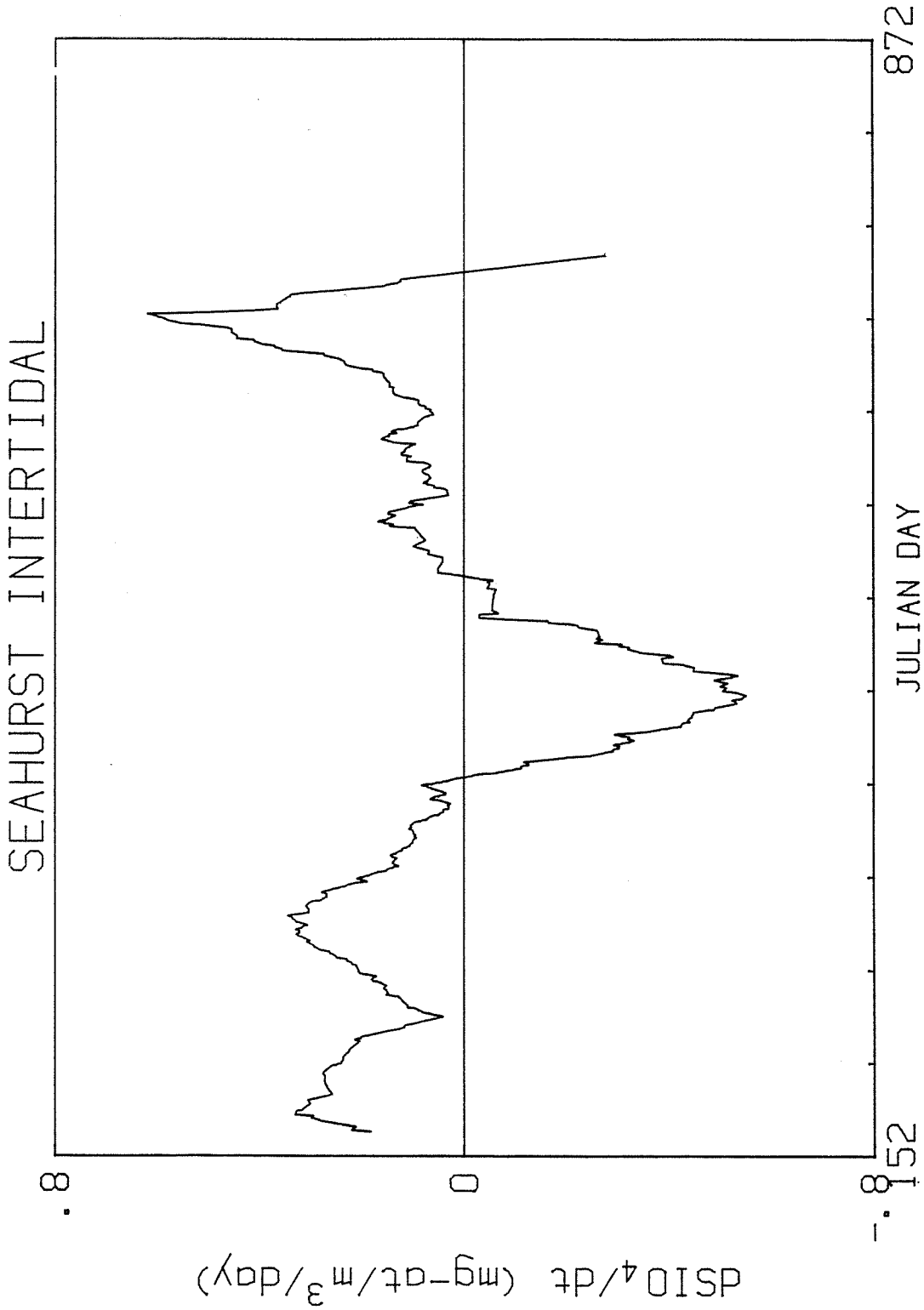

Figure 4.71b. Slope of smoothed distribution depicting rate of change of silicate concentration.

Table 4.36. Mean value and 90% confidence interval for nitrate (mg-at/m^3) for Seahurst and Indianola intertidal zones and the surface water of Seahurst Bight. Data were collected from 6-week periods about the equinox and solstice dates for 1982 and 1983.

Period	Seahurst intertidal	Seahurst Bight, 0 m	Indianola intertidal
Summer solstice, 1982	7.5* (6.6-8.3)	2.8 (0.9-4.7)	
Summer solstice, 1983	5.0 (1.8-8.2)	4.0 (2.9-5.0)	2.8 (2.1-4.9)
Autumnal equinox, 1982	13.4 (11.1-15.7)	9.4 (7.6-11.2)	
Autumnal equinox, 1983	10.5 (9.3-11.6)	12.6 (11.3-13.9)	9.9 (7.8-13.2)
Winter solstice, 1982	26.3 (25.3-27.5)	32.6 (28.3-32.6)	
Winter solstice, 1983	24.6 (25.5-27.7)	23.0 (21.8-24.3)	26.2 (25.5-26.8)
Vernal equinox, 1982	22.9 (20.6-25.2)	19.0 (17.3-20.7)	

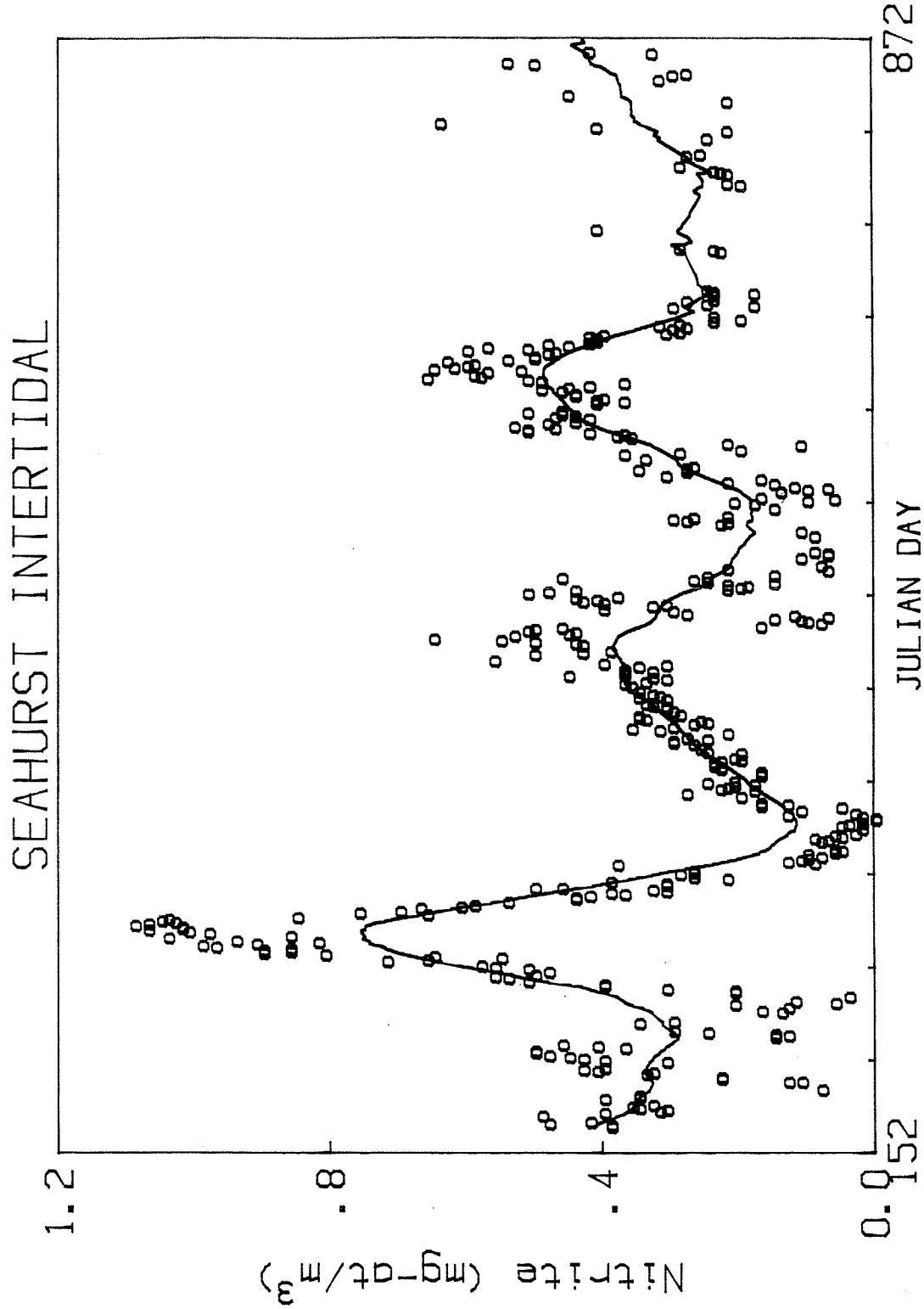

Figure 4.72a. Nitrite concentration in Seahurst intertidal zone with smoothed distribution.

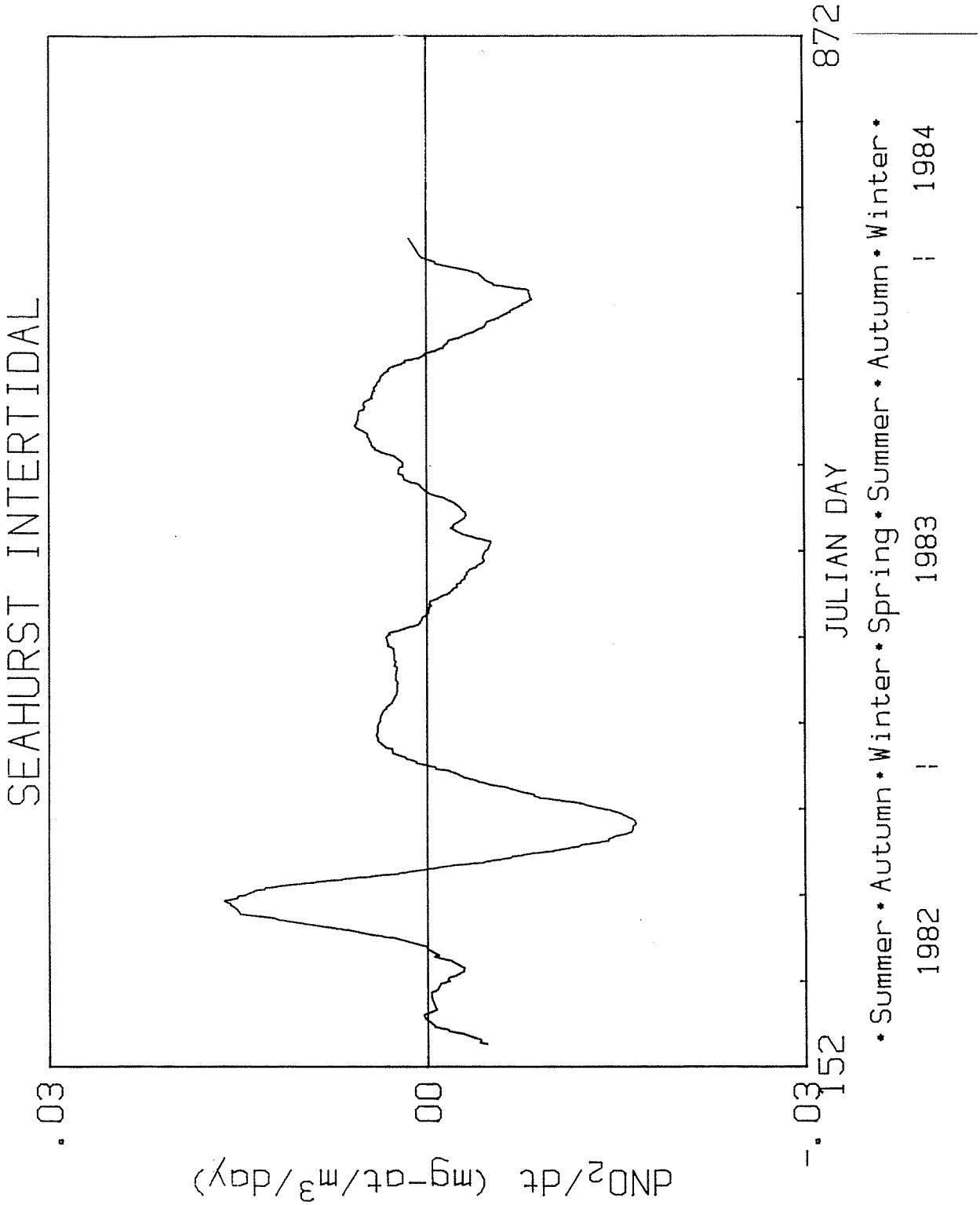

Figure 4.72b. Slope of smoothed distribution depicting rate of change of nitrite concentration.

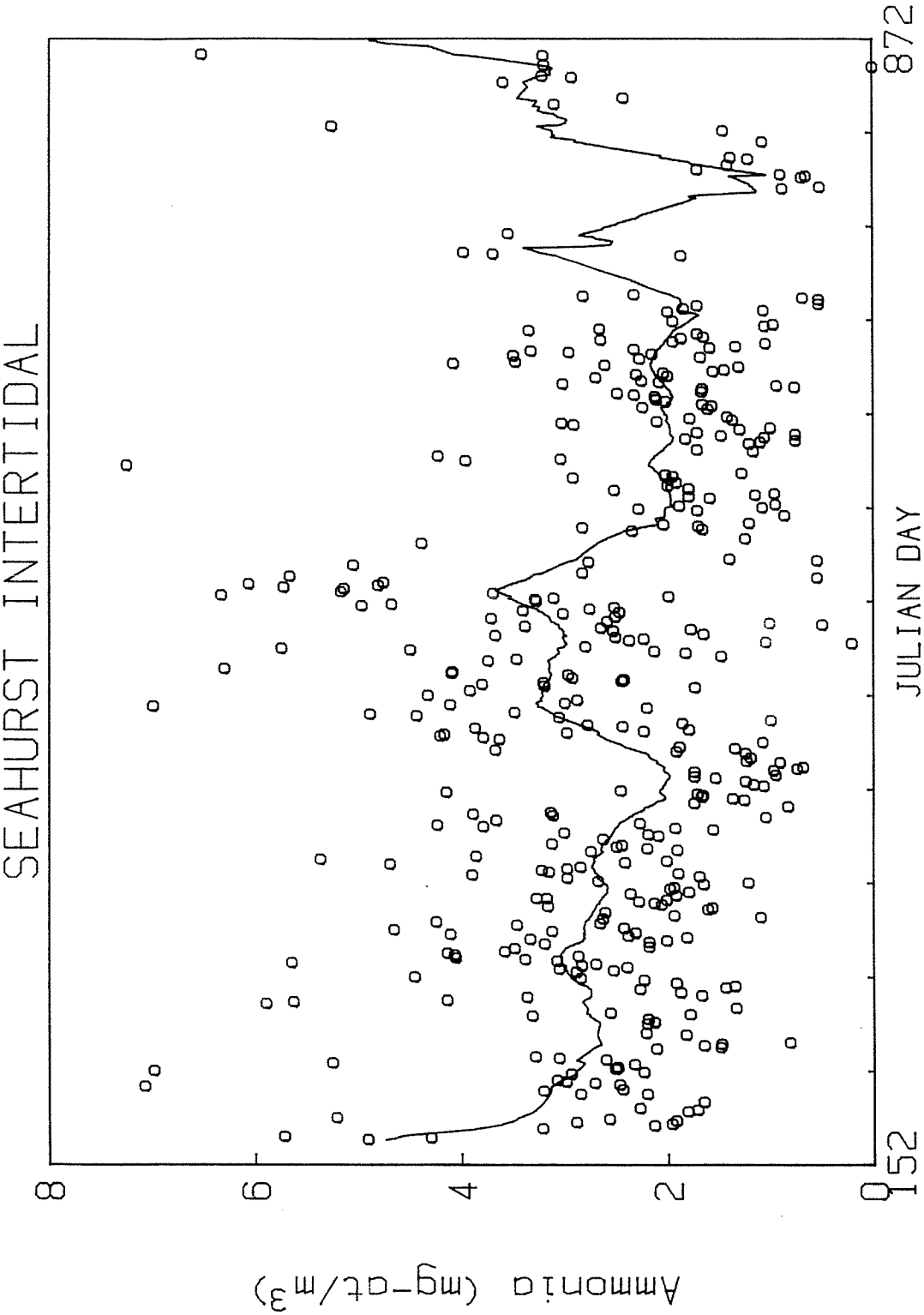

Figure 4.73a. Ammonia concentration in Seahurst intertidal zone with smoothed distribution.

a net rate on the order of 0.05 mg-at/m 3/day (Figure 4.73b). The ammonia levels were larger than those found in the surface waters of Seahurst Bight but were similar to those found in the intertidal waters of Indianola (Table 4.37).

The relative seasonal temporal variability of nutrients in the intertidal zone is of the same order as in the Seahurst Bight, with phosphate and silicate having the lowest levels followed by nitrate and nitrite, and ammonia having the highest level (Table 4.35). In comparing the diel variability in the two regions it is evident that the spatial variability in the Bight was lower while the diel variability in the intertidal zone was unusually high for nitrate and nitrite. This pattern suggests that most of the relative intertidal variability occurred on a diel scale. The anomolously large nitrate level may be an artifact of the sampling or from a diel cycle in the intertidal zone nitrate that was not observed in the daily sampling since samples were always collected in the daylight.

4.4.3.3 Diel Study

In a 24 hour period beginning 8 a.m. August 29, 1983 nutrient and chlorophyll samples were collected every 2 hours and 1/2 hour respectively in the Seahurst intertidal zone. Between 9 pm and 3 am heavy rain fell and the intertidal water became laddened with silt. Over this period all the properties experienced a considerable amount of variability. The relative variability before the rain was less than during the rainy period. In general the nutrients increased during the rain. Chlorophyll and phaeopigment were not affected as much by the rain. The results are shown in Figure 4.74. Smoothed distributions are calculated with a smoothing interval of T = 4 hr, Te = 4 hr and Td = 4.

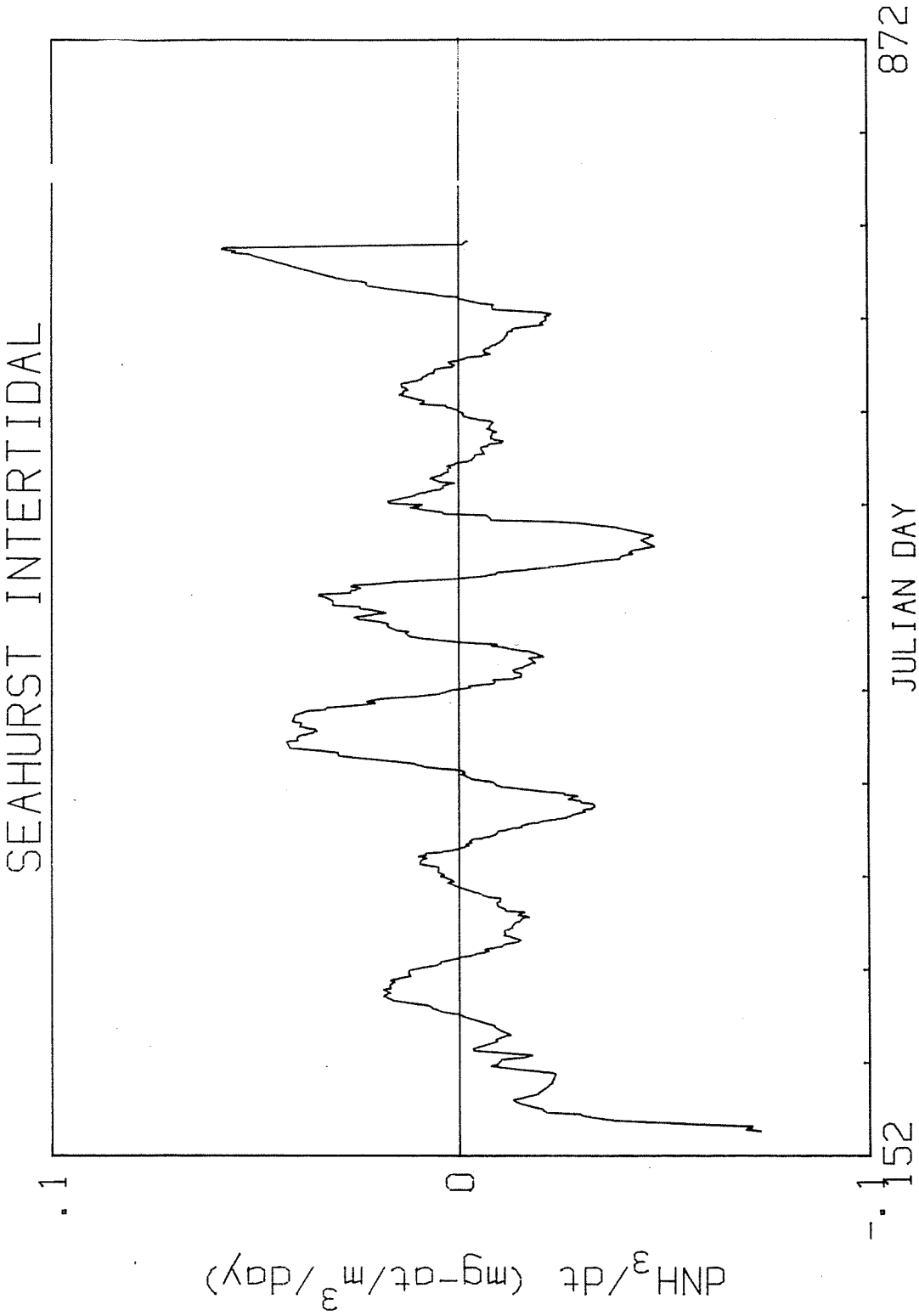

Figure 4.73b. Slope of smoothed distribution depicting rate of change of ammonia concentration.

Table 4.37. Mean value and 90% confidence interval for ammonia (mg-at/m^3) for Seahurst and Indianola intertidal zones and the surface water of Seahurst Bight. Data were collected from 6-week periods about the equinox and solstice dates for 1982 and 1983.

Period	Seahurst intertidal	Seahurst Bight, 0 m	Indianola intertidal
Summer solstice, 1982	3.4* (2.5-4.4)	0.9 (0.5-1.3)	
Summer solstice, 1982	4.0* (3.1-5.0)	0.4 (0.4-0.5)	2.8* (2.4-3.4)
Autumnal equinox, 1982	2.9* (2.6-3.4)	1.6 (1.0-2.2)	
Autumnal equinox, 1983	1.7* (1.5-1.9)	0.4 (0.4-0.5)	2.8* (2.5-3.2)
Winter solstice, 1982	2.8* (2.6-3.4)	0.3 (0.3-0.4)	
Winter solstice, 1983	2.0* (1.3-2.7)	0.2 (0.2-0.3)	2.5* (1.8-4.1)
Vernal equinox, 1982	3.3* (3.0-3.6)	0.5 (0.5-0.6)	

*Significantly higher level within period.

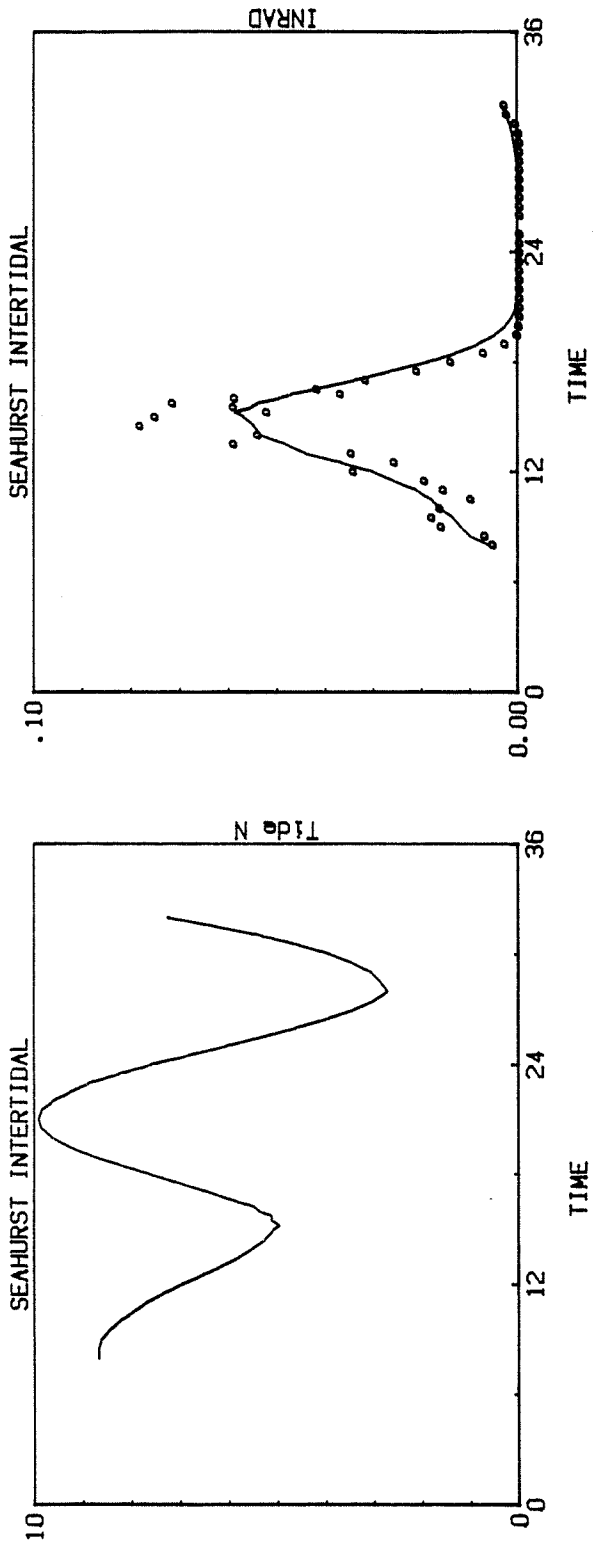

Figure 4.74. Results of the diel study at the Seahurst intertidal zone. Time in hours since midnight August 29 1983. Tide height in ft, INRAD is incident radiation in u einsteins/m^2/min. Nutrient concentrations in mg-at/m^3.

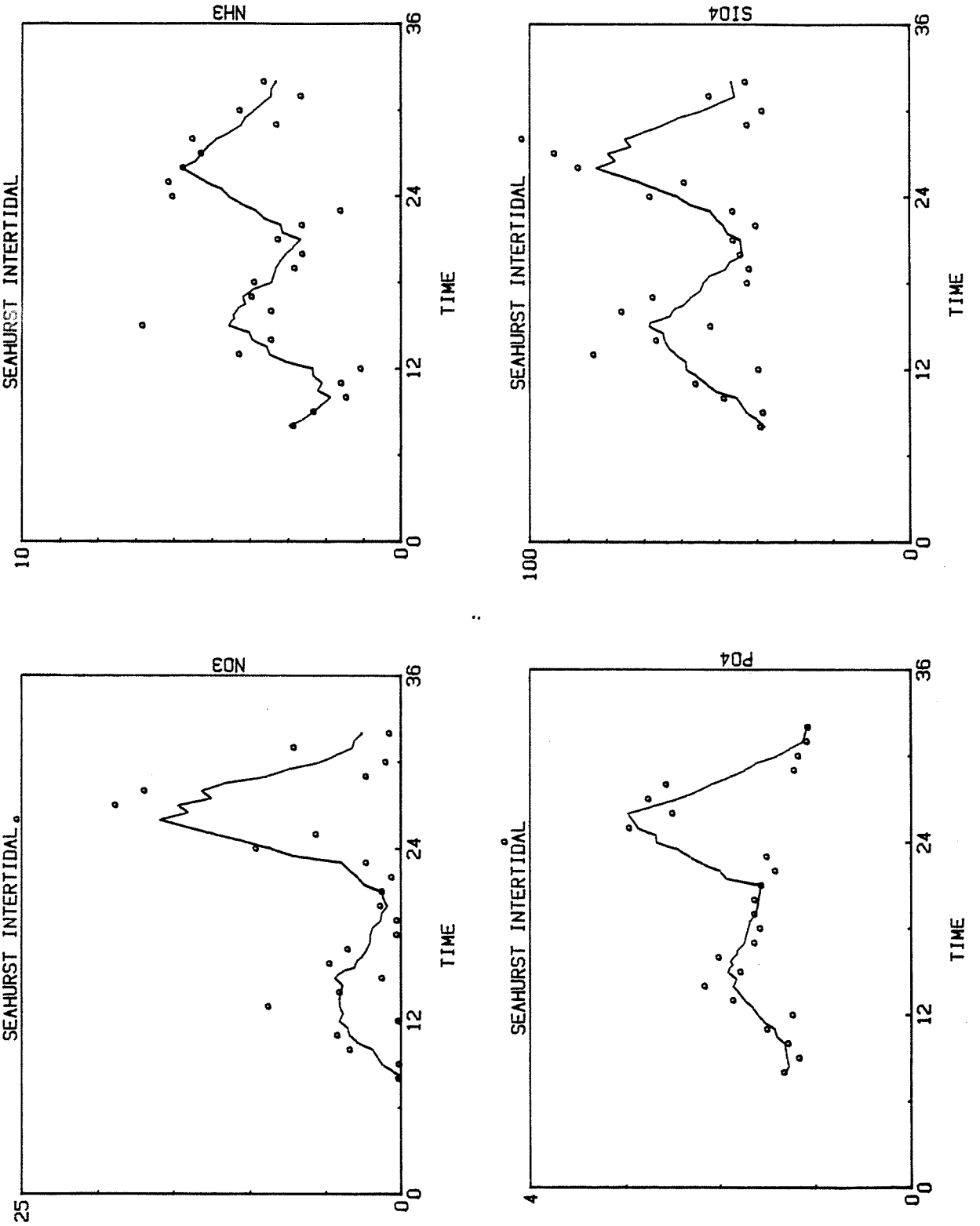

Figure 4.74. Continued

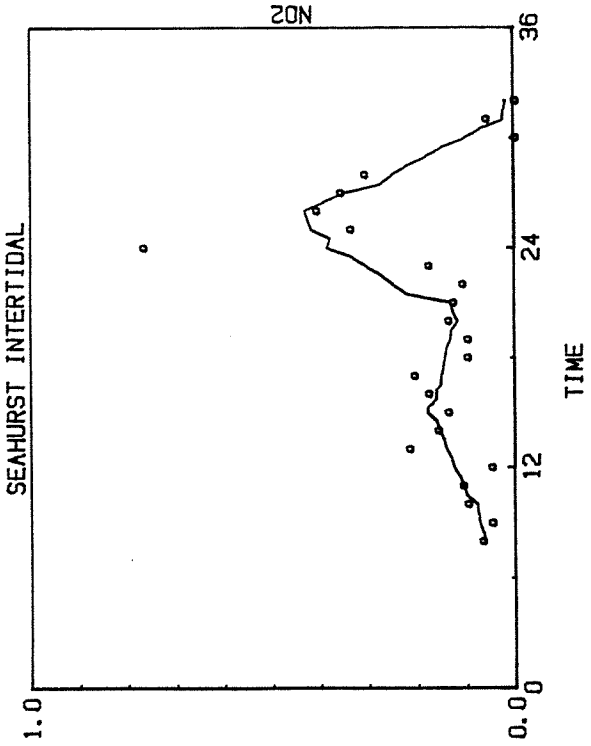

Figure 4.74. Continued

4.4.4 Freshwater Sources

4.4.4.1 Freshwater Sources in the Seahurst Area

A special underway cruise was carried out on January 10, 1984 to examine the distribution of nearshore freshwater from the Seahurst area to Brown's Point. The data was used to distinguish between local and Puyallup River influences, and to characterize freshwater sources.

The freshwater sources along the eastern shore of East Passage include a number of creeks, unnamed streams and sewage outfalls (Figure 4.75).

The creeks in the vicinity of Seahurst Park have not been gauged or monitored for water quality parameters. Estimates of their annual average discharge (Ebbesmeyer et al. 1982) suggest that they contribute only 0.5% of the freshwater entering the main basin, or about 1.4% of the discharge of the Puyallup River.

The cruise track (Figure 4.75) was divided into four parts designated "Seahurst," "Normandy-Des Moines," "North Poverty Bay" and "South Poverty Bay-Station 3." Temperature, salinity, turbidity, chlorophyll and ammonia data were collected in these regions and are plotted against distance (Figure 4.76).

A period of heavy precipitation prior to the cruise contributed large amounts of freshwater to the surface layer. The salinity decreased along the transect, from a maximum of 27.92 $^{o}/oo$ in the Seahurst region, to a minimum of 21.46 $^{o}/oo$ at station 3. A decrease in temperature and an increase in turbidity and ammonia were correlated with the salinity decrease. A chlorophyll maximum in the Normandy-Des Moines region had no correlation with salinity.

The salinity, temperature, turbidity and ammonia data suggests the presence of Puyallup River water at station 3. The features labeled B through

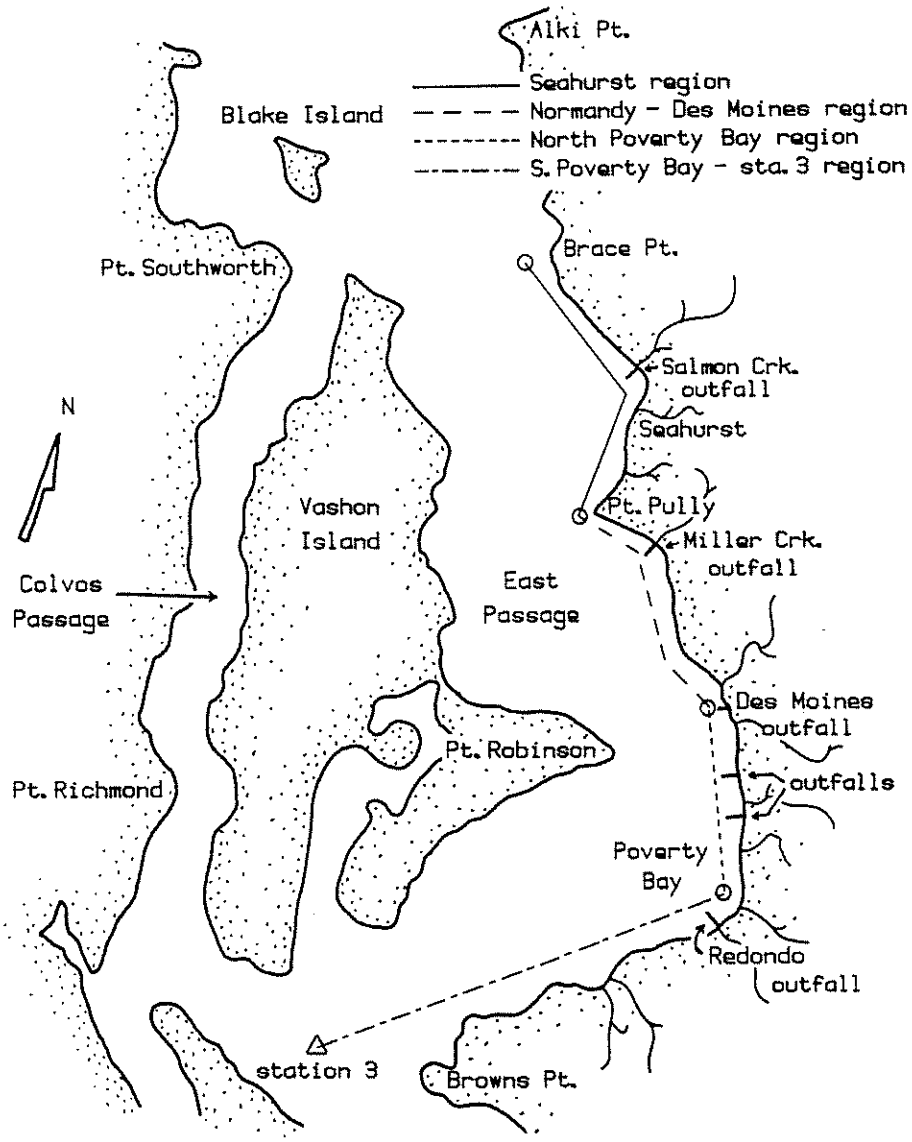

Figure 4.75. Cruise track for special cruise (1-10-84) to study fresh water sources in east passage. Cruise segments denoted by lines.

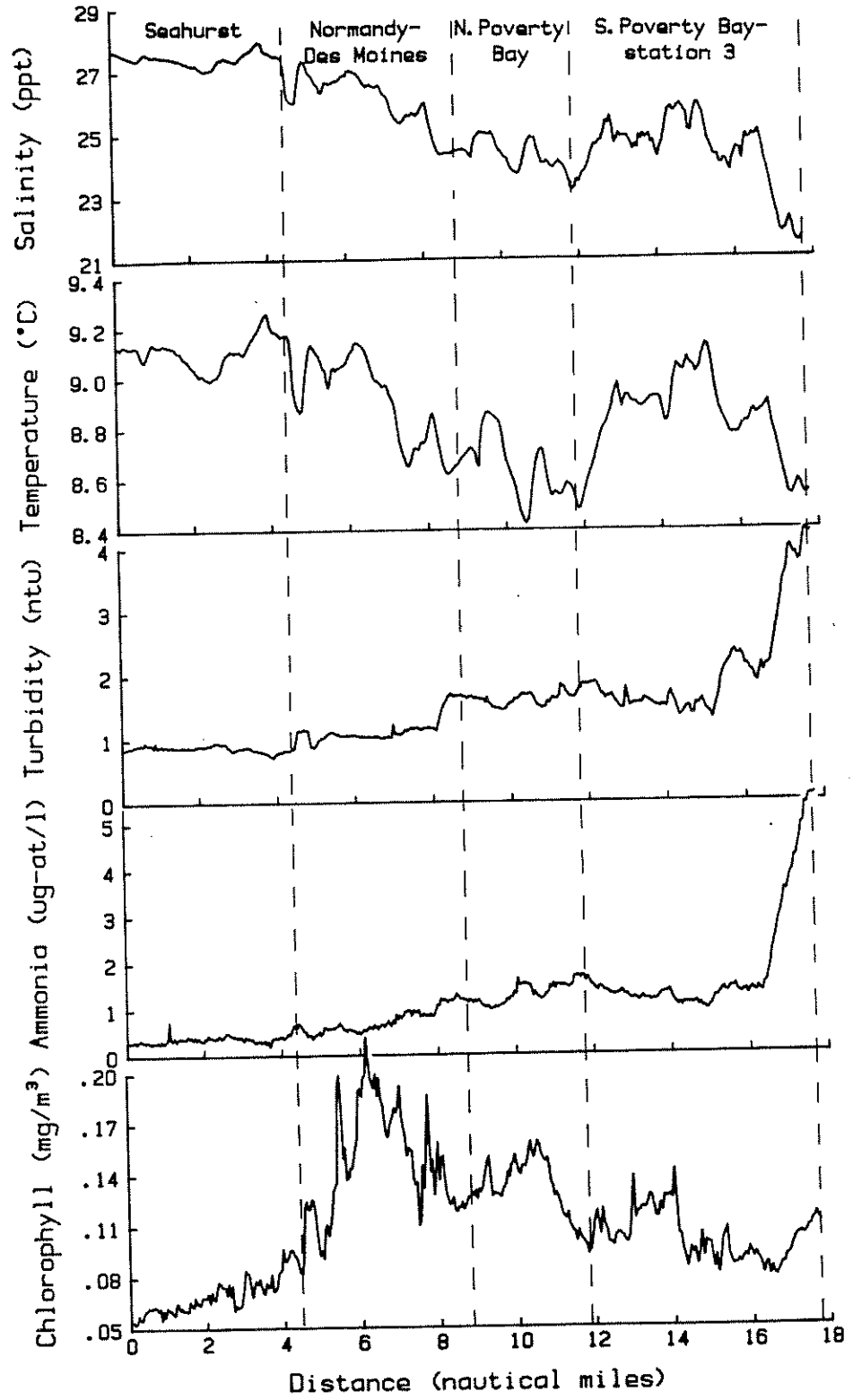

Figure 4.76. Results from special cruise (1-10-84). Cruise segments and distance from Brace Point denoted.

E in the salinity plot are associated with large decreases in temperature, and small increases in turbidity and ammonia. Feature F is associated with a smaller decrease in temperature, and large increases in turbidity and ammonia (Figure 4.76).

Plots of turbidity and ammonia versus salinity (Figures 4.77 and 4.78) show two distinct freshwater signatures-one of low turbidity and ammonia, and one of high turbidity and ammonia. At a salinity of 23 $^{o}/_{oo}$ the difference between turbidity and ammonia levels in these two water types (predicted from the regression equations in Figures 4.77 and 4.78) are 1.23 NTU and 1.74 mg-at/m^3, respectively. The data points falling along the low turbidity and ammonia lines include nearly all of the nearshore region (between 0 and 15 nautical miles in Figure 4.75, n=301). The points which fall along the high turbidity and ammonia lines include only the region near station 3 (between 15 and 18 nautical miles in Figure 4.75, n=49) where the effects of the Puyallup River are pronounced. This suggests that the low salinity water along the shore was from local sources, and that the Puyallup River influence was restricted to a relatively small area near station 3.

Table 4.38 summarizes the characteristics and possible sources of the salinity features labeled in Figure 4.75. In general, salinity changes due to local runoff were associated with large temperature decreases, and small turbidity and ammonia increases. Salinity changes due to Puyallup River water were associated with small temperature decreases and large turbidity and ammonia increases. (The temperature of local source and Puyallup River water is dependent on atmospheric conditions, and will change seasonally.) Chlorophyll showed no consistent relationship with salinity, regardless of freshwater origin.

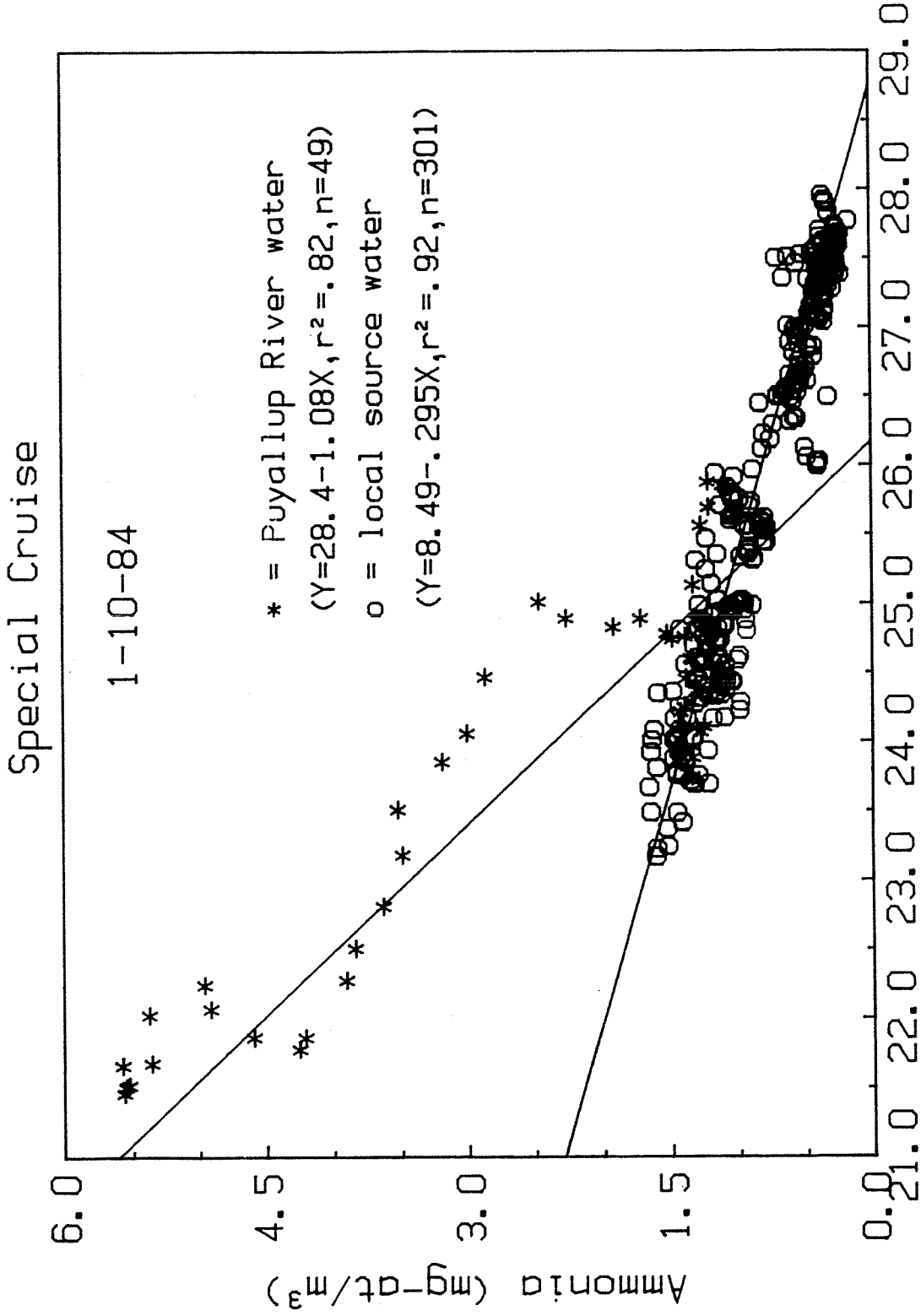

Figure 4.77. Ammonia salinity relationship for special cruise (1-10-84).

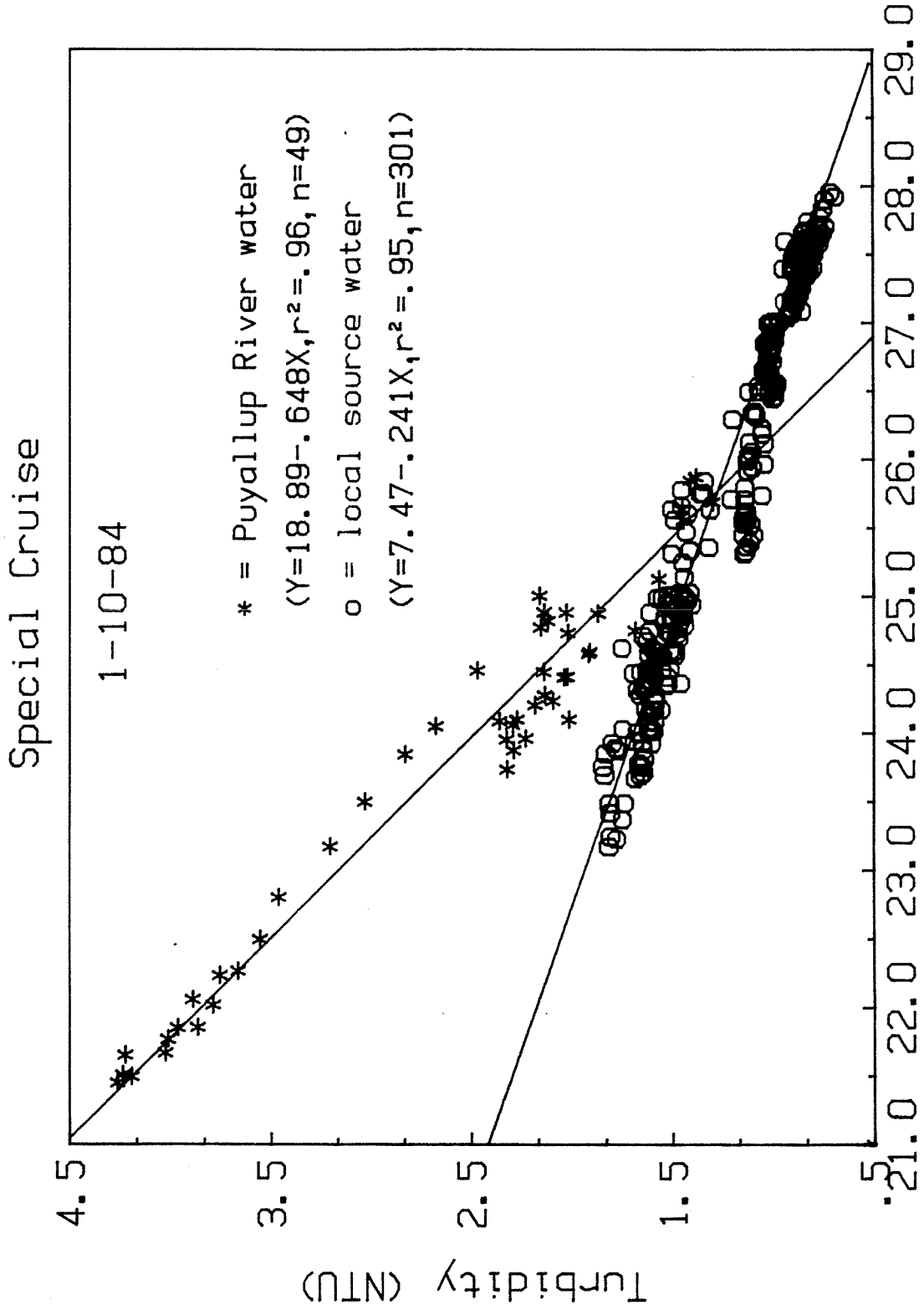

Figure 4.78. Turbidity salinity relationship for special cruise (1-10-84).

Table 4.38. Salinity, temperature, turbidity, ammonia and chlorophyll-a characteristics of the features labeled in Figure 4.2, and possible sources. Arrows indicate the magnitude and direction of change.

	-FRESHWATER PROPERTIES-					
LABEL	△SAL.	△TEMP.	△TURB.	△NH_3	△CHL-A	POSSIBLE SOURCES
A	↓	↓	⊘	⊘	⊘	Salmon Creek Salmon Creek sewer outfall
B	↓	↓	↑	↑	↑	Miller Creek Miller Creek sewer outfall
C	↓	↓	↑	↑	↓	Des Moines sewer outfall local streams (fig. 1)
D	↓	↓	↑	↑	↑	two sewer outfalls (fig. 1) local streams (fig. 1)
E	↓	↓	↑	↑	↓	Redondo sewer outfall local streams (fig. 1)
F	↓	↓	↑	↑	↑	Commencement Bay (Puyallup River)

4.4.4.2 Duwamish River Water

On January 10, 1984 a cruise was undertaken to characterize Duwamish River water with the underway sampling system. Continuous data was collected for salinity, temperature, turbidity, chlorophyll and ammonia on the transect shown in Figure 4.79.

With an annual average discharge of 39 m^3/s, the Duwamish River contributes about 15% of the runoff entering the main basin of Puget Sound (Ebbesmeyer et al. 1982). Upstream sources in the Duwamish River are responsible for over two-thirds of the total freshwater, sediment, iron, and mercury load reaching Elliott Bay, and may also be the major source of organic carbon and pesticide inputs (Harper-Owes 1983). The Renton Treatment Plant supplies nearly 80% of the total ammonia load, but contributes relatively negligible quantities of metal and organic toxicants (Harper-Owes 1983).

The salinity data (Figure 4.80) shows that the area was dominated by freshwater from the Duwamish River. The salinity difference between inner and outer Elliott Bay was approximately 12 °/oo with minimum values (17 °/oo) off the East Waterway. Moving shoreward, the first major decrease in salinity was detected directly off the West Waterway in leg 2 of the transect. Most of the freshwater encountered was along the eastern side of Elliott Bay (legs 2 & 3, Figure 4.79).

This pattern indicates a counter-clockwise circulation in the surface layer, with Duwamish River water flowing along the eastern shore and exiting to the north on an ebb tide. This is in agreement with existing data (Stober and Pierson 1984) which show that clockwise circulation occurs during flood tide, and counter-clockwise circulation occurs during ebb tide. Field data suggest that net flow is to the north (Stober and Pierson 1984).

In Legs 1, 2, and 3 of the transect there is a correlation between

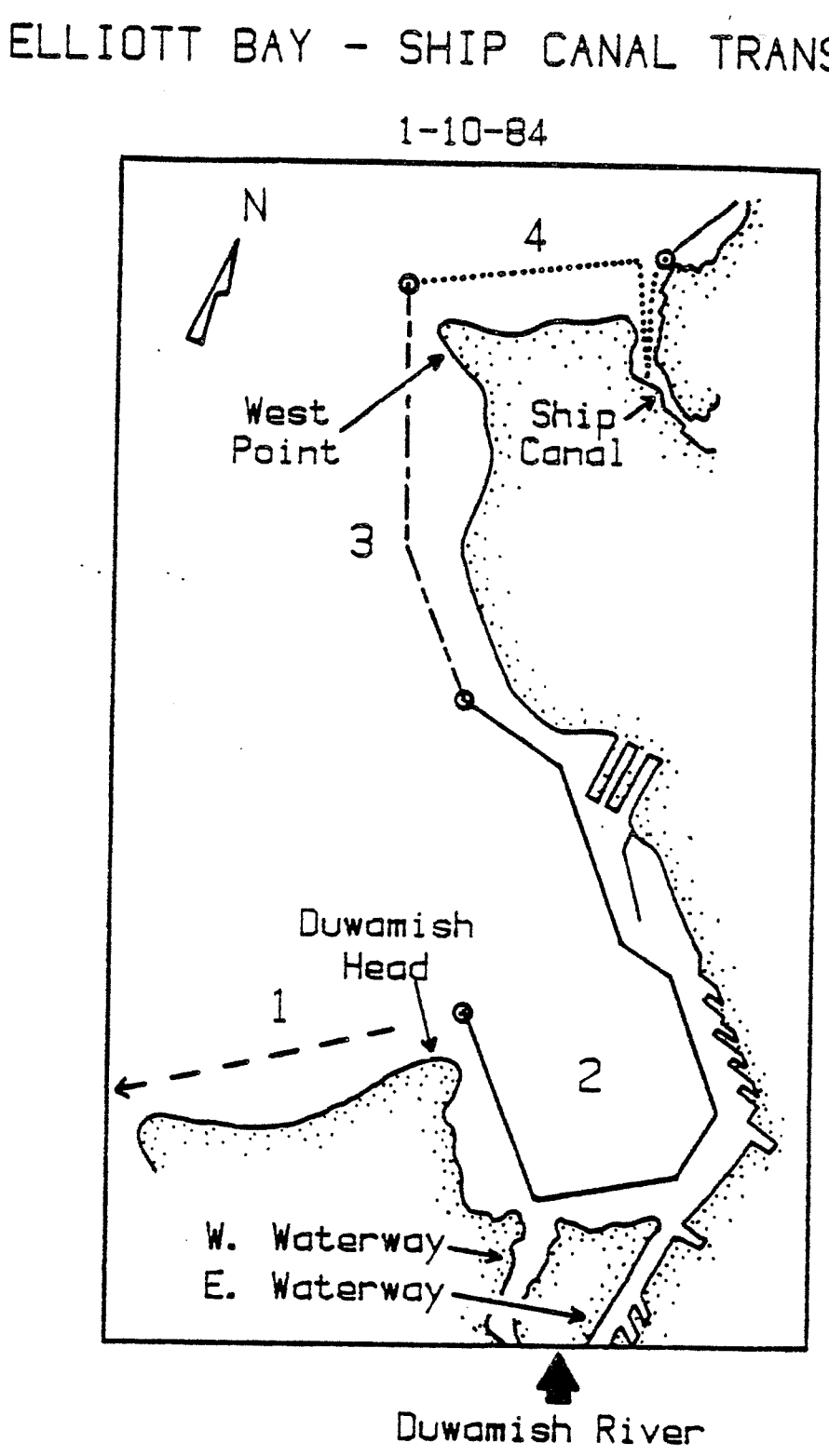

Figure 4.79. Cruise track for Elliott Bay cruise. Cruise segments denoted by lines.

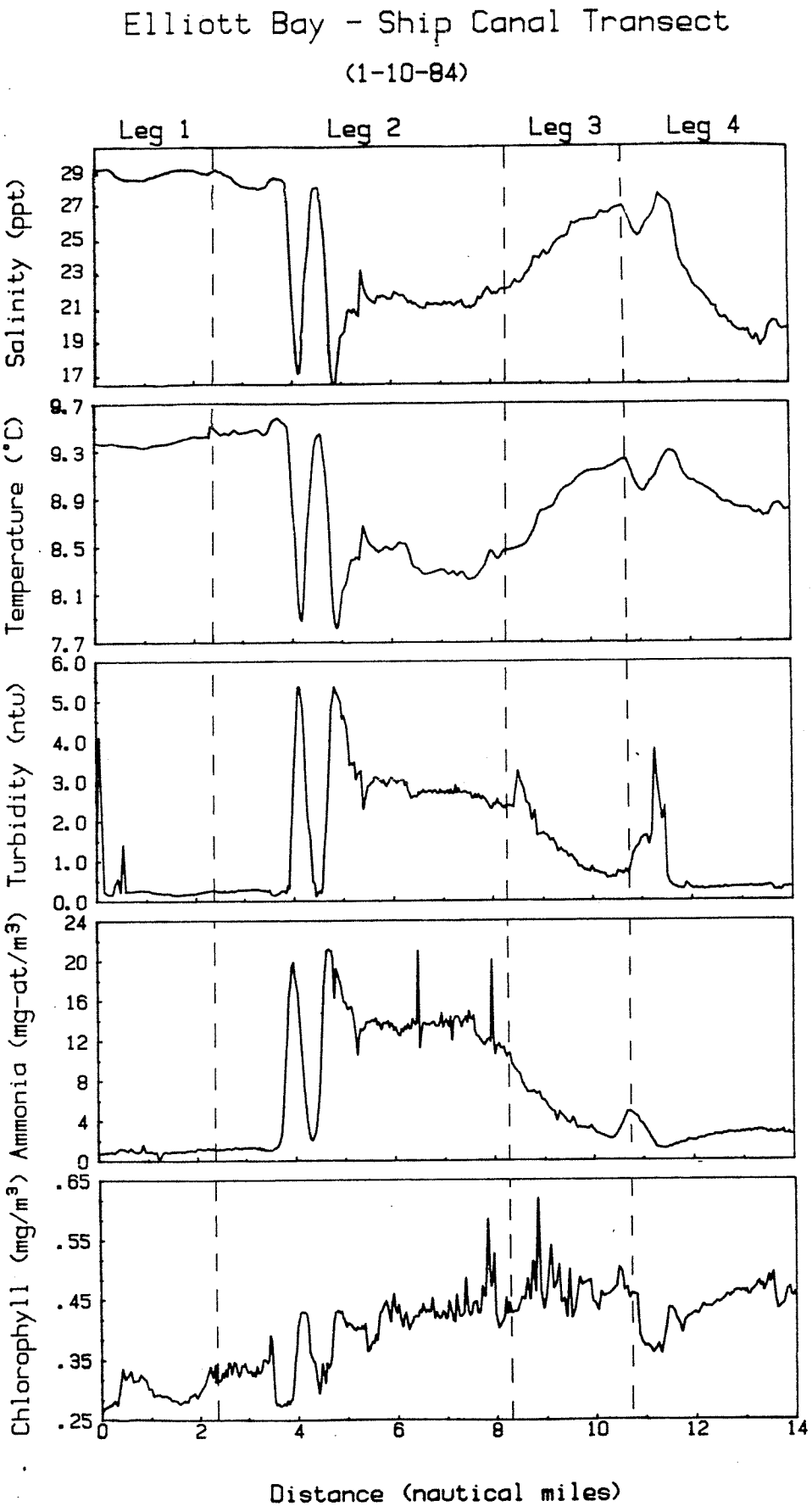

Figure 4.80. Results of Elliott Bay cruise. Distance measured from Alki Point.

salinity, temperature, turbidity and ammonia (Figure 4.80), indicating that the Duwamish River was primarily responsible for the concentrations observed. The river water was characterized by turbidity and ammonia levels higher than observed in the water of Elliott Bay. The levels were 5.0 NTU and 20 mg-at/m^3 higher for turbidity and ammonia, respectively, with maximum levels off the East and West Waterways of the Duwamish River.

The salinity decreased in the vicinity of the West Point sewage outfall. The characteristics of this water were similar to Duwamish River water, and it is not clear whether effluent from West Point or the Duwamish River was responsible. The majority of the freshwater in Leg 4 appeared to be of ship-canal origin, which was warmer, and lower in turbidity and ammonia.

The positive correlation between temperature and salinity shows that the freshwater sources were colder than the marine receiving waters.

Chlorophyll concentrations were generally low and variable throughout the transect (Figure 4.80). The correlation with salinity was low in Legs 1, 2 and 3, indicating that chlorophyll levels in Elliott Bay were dictated by factors other than the Duwamish River. Some river effects were apparent directly off the East and West Waterways in Leg 2 where decreases in chlorophyll were observed.

4.4.4.3 Puyallup River Water

On November 17, 1982 a cruise was undertaken to characterize Puyallup River water with the underway sampling system. Continuous data was collected for salinity, temperature, turbidity, chlorophyll, and ammonia (Figure 4.81).

The Puyallup River, which has an annual average discharge of 97 m^3/s, contributes 39% of the runoff entering the Main Basin of Puget Sound (Ebbesmeyer et al. 1982). Recent water quality studies (Dames and Moore 1981) have demonstrated that measurable amounts of toxic chemicals are entering the

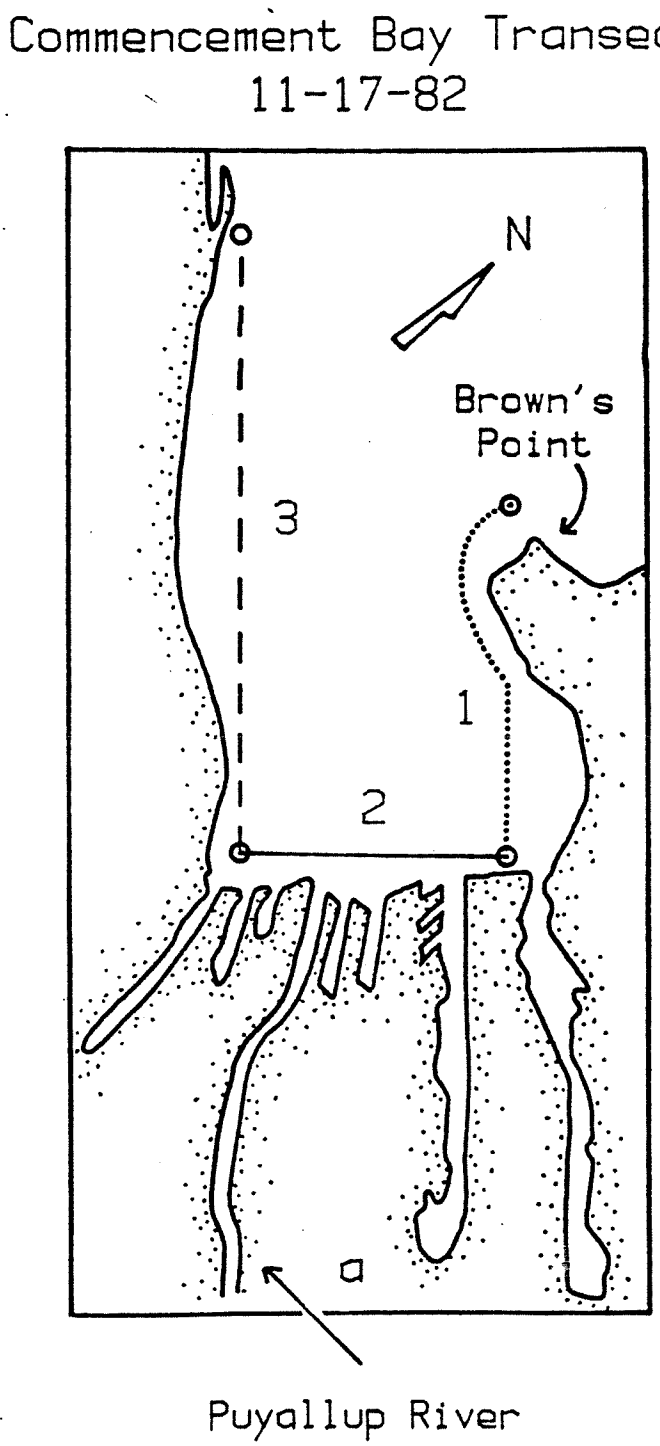

Figure 4.81. Cruise track for Commencement Bay cruise. Cruise segments denoted by lines.

freshwater and marine receiving waters of Commencement Bay where the Puyallup River is discharged. Sewage input is detectable in the form of increased ammonia levels.

Salinity measurements show that Commencement Bay is dominated by freshwater from the Puyallup River (Figure 4.82). The salinity difference between inner and outer Bay was approximately 18 $^{o}/oo$, with minimum values ($11^{o}/oo$) encountered directly off the river mouth. A strong correlation between salinity and the other observations (Figure 4.82) indicates that the Puyallup River was primarily responsible for the concentrations observed.

During the winter months, the river water is colder than the surrounding water, as shown by the temperature data (Figure 4.82) which is positively correlated with salinity.

Puyallup River water is characterized by high concentrations of suspended particulate matter and ammonia (Figure 4.82). Ammonia was largely the result of sewage input from the Tacoma Central Wastewater Treatment Plant which discharges into the river about 1.5 miles upstream from the mouth. The peak in ammonia (>32 mg-at/m^3) at the end of Leg 2 (Figure 4.82) was not associated with a salinity minimum, indicating the presence of other ammonia sources in the southeastern part of the bay.

The negative correlation between salinity and chlorophyll suggest that the river imports brackish and freshwater phytoplankton at concentrations above that of the marine receiving waters.

The effect of Puyallup River water in East Passage was determined using underway data collected between the channel buoy TA off Point Pully, and station 3 (Figure 4.4) for 24 cruises between July 16, 1982 and October 2, 1983. To contrast the plume with the surrounding water, the salinity channel was used to identify and define a front and a non-front, or "farfield" region

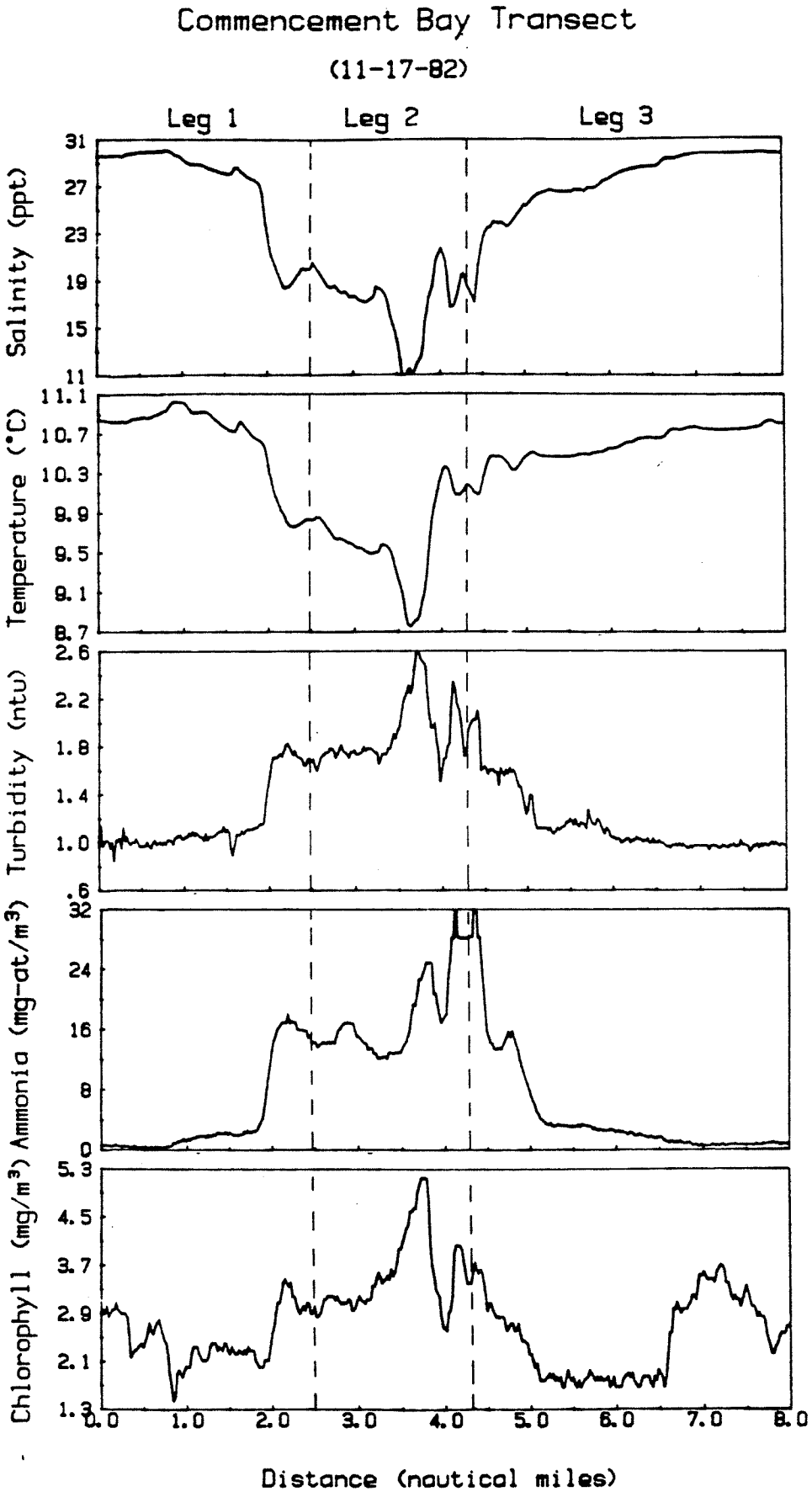

Figure 4.82. Results of Commencement Bay cruise. Distance measured from Browns Point

(Figure 4.83). Mean concentrations in these regions were calculated for temperature, salinity, turbidity, chlorophyll and ammonia for each of the 24 cruises and a paired sample analysis was performed (Table 4.39). The mean difference (d), and the percent mean difference (dp) for each channel was calculated as follows:

$$d = [\ \Sigma\ (F_i - f_i)]\ /n \qquad (44)$$

$$dp = [\ d/((\Sigma f_i)/n)]\ X\ 100 \qquad (45)$$

where f is the mean farfield concentration for cruise i, F is the mean frontal concentration for cruise i, and n is the total number of cruises.

On average, the front of Puyallup River water was less saline (-2^{o}/oo), warmer ($+0.5^{o}$C), more turbid (+0.7 NTU), and higher in ammonia (+1 mg-at/m^3) than the surrounding water. The mean difference in chlorophyll, however, was not significantly different from zero (α = .05), and the variation between cruises was high (S = 3.73). Frontal chlorophyll values ranged from 6.6 mg/m^3 lower to 8.5 mg/m^3 higher than those of the farfield (Appendix 4.F). The percent difference (dp) was relatively small (<10) for temperature and salinity. The average turbidity of the front, however, was about 40% higher than the farfield, and the average ammonia in the front was over 200% higher than the farfield. (Approximately 80% of the data points used to calculate means were collected between April and October of either 1982 and 1983. These are periods in which relatively strong fronts were encountered.

To examine the relative importance of the forces which determine the amount of Commencement Bay water in the southern reaches of East Passage multiple linear regression analysis was employed (Eq. 46). The dependent variable (Y) is the size of the freshwater lens observed in East Passage

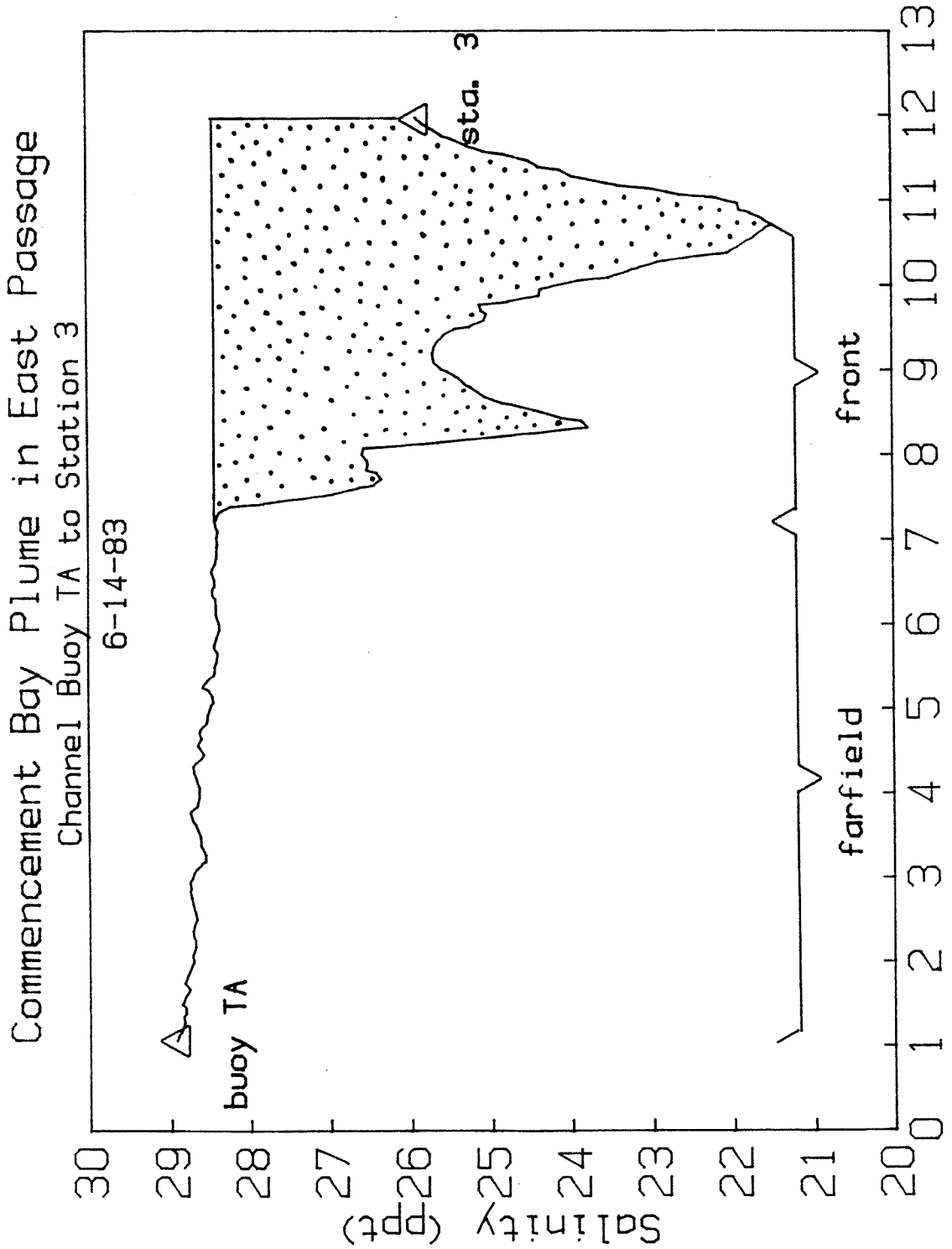

Figure 4.83. Effect of Commencement Bay plume in East Passage depicted by surface salinity vs distance meaured from bouy TA off Point Pully (See Fig. 4.4).

Table 4.39. Paired sample analysis on mean front and farfield concentrations. Negative values represent lower frontal concentrations.

Channel	#Obs. (n)	Mean diff. (d)	% Mean diff. (dp)	Std. dev. (Sd)
Salinity (^{o}/oo)	24	-2.0531*	-7.0667*	1.3787
Temperature (°C)	24	0.4520*	3.5763*	0.6264
Turbidity (NTU)	20	0.6722*	36.8935*	0.7200
Chla (mg/m^3)	23	0.2032	1.7167	3.7307
NH3 ($mg\text{-}at/m^3$)	19	1.1109*	220.8988*	0.9647

*significant at = .05

calculated from the salinity data. This is defined as the area over the curve between station 3 and the deflection point of the front (stippled region in Figure 4.83). The area was calculated for each of the 24 cruises between July 16, 1982 and October 2, 1983. The regression equation is

$$Y = 7.701 - 0.163X_1 - 1.026X_2 + 0.0024X_3 \quad (46)$$

where X_2 is tidal height in feet at the time of sampling, X_1 is the north-south component of the wind velocity (in knots) averaged over 48 hours prior to sampling (included are observations from both Point Robinson and Alki Point) and X_3 is the output of the Puyallup River (in ft^3/sec) averaged over four days prior to sampling. These intervals were chosen to maximize the significance of the regression after testing 48, 24, 9 and 3 hour intervals for wind and 4, 2, and 1 day intervals for river discharge.

Analysis of variance (Table 4.40) shows that the multiple linear regression is statistically signficant ($.001 > P > .0005$). Changes in wind velocity, tidal height, and river discharge account for about 60% ($r^2 = .57$) of the variation in the amount of Puyallup River water observed in East Passage. Tidal height, discharge, and wind account for about 30% ($r^2 = .30$), 15% ($r^2 = .15$) and 12% ($r^2 = .12$), of the change observed in the dependent variable, respectively, this suggests that tides are the principle force governing the movement of the plume in the southern reaches of East Passage.

A large fraction of the variation in Y is unaccounted for by this analysis. Considerations of Puget Sound oscillatory tidal transport (which is approximately 300 times the mean river flow) and the ratio of energy dissipation of tidal currents to wind (which is approximately 100 to 1) indicate that tidal forces are significant. The relative importance of tidal

Table 4.40. Analysis of variance of multiple linear regression (eq. 46).

Source	Deg. freedom	Sum Square	Mean Square	F-value
Total	22	1201.2893		
Regression	3	678.7308	226.2436	8.2261*
Wind	1	144.9331	144.9331	5.2697*
Tides	1	357.7555	357.7555	13.0078*
Discharge	1	176.0421	176.0421	6.4008*
Residual	19	522.5585	27.5031	

*significant at = .05

forces should be less significant in the surface layer than in the water column as a whole. The results found here indicate that the ratio of tidal effects to wind and river discharge are approximately 2:1:1, in the surface layer of East Passage.

4.4.5 Sediment Trap Studies

Two successful sediment trap deployment-recoveries were completed during the study. Deployment-recovery #1 occurred from November 25, 1982 until January 17, 1983, for a total trap exposure time of 52.5 days. Deployment-recovery #2 covered 29.1 days from February 14, 1983 to March 15, 1983. Subsamples from each sediment trap were analyzed (Table 4.41).

The traps were effective at catching fecal pellets, intact phytoplankton cells and detritus (Lorenzen et al. 1981). The fecal pellets contained phaeopigments produced by the degradation of phytoplankton chlorophyll in the guts of herbivorous zooplankton (Schuman and Lorenzen 1967). The flux of carbon and nitrogen can be used to estimate the quantity and quality of organic matter passing from phytoplankton to zooplankton (Copping 1982; Welschmeyer 1982).

There was no significant difference between a pair of sediment traps deployed together, as seen for pigment, CHN, or dry weight analysis ($\alpha = .05$). Significant differences in the flux of phaeopigment, carbon, nitrogen and total trap material (Table 4.42) were noted between deployments.

Microscopic analysis of trap material showed many dead cells in both January and March, largely diatoms (including Skeletonema costatum, Coscinodiscus sps., Melosira sp. and various pennates) and some dinoflagellates. A small number of live cells were seen in each set of traps, with more live cells occurring in March than in January. There were fecal pellets visible in both sets of traps, falling into three size classes: 20 x

Table 4.41. Analysis of sediment trap samples.

Type of Analysis	Reason for Analysis
Chlorophyll and Phaeopigments	measure of organic matter fallout and passage through the herbivore trophic level => calculate phaeopigment flux
CHN	organic content of material => calculate carbon flux, nitrogen flux
Dry weight	sedimentation rate of inorganic and organic portion => calculate flux of total material
Microscopic analysis	characterization of living/dead material

Table 4.42. Results of sediment trap deployment-recoveries, calculated as flux of phaeopigment, carbon, nitrogen and total material into the traps. Ratios of carbon to phaeopigment and carbon to total trap material provide qualitative information.

	Phaeopigment flux ($mg/cm^2/d$)	Carbon flux ($mg/cm^2/d$)	Nitrogen flux ($mg/cm^2/d$)	Total material flux ($mg/cm^2/d$)	C/phaeo.	C/total material
Deployment #1 (January)	$\bar{X}=6.44 \times 10^{-7}$ $S=3.31 \times 10^{-7}$	$\bar{X}=3.14 \times 10^{-3}$ $S=5.45 \times 10^{-4}$	$\bar{X}=3.26 \times 10^{-4}$ $S=9.28 \times 10^{-5}$	$\bar{X} = 12.13$ $S = 1.24$	4876	2.59×10^{-4}
Deployment #2 (March)	$\bar{X}=3.09 \times 10^{-5}$ $S=2.16 \times 10^{-6}$	$\bar{X}=1.22 \times 10^{-3}$ $S=2.67 \times 10^{-4}$	$\bar{X}=1.20 \times 10^{-4}$ $S=4.15 \times 10^{-5}$	$\bar{X} = 22.98$ $S = 1.03$	39.5	5.31×10^{-5}

90 um, 40 x 90 um and 70 x 140 um, probably produced by a small and large copepod (such as Pseudocalanus sp. and Calanus pacificus) and by an euphausiid, respectively (Shuman 1978). Many more fecal pellets were visible in the March recovery.

The significantly higher flux rates of phaeopigment into the traps, the presence of larger numbers of live cells and identifiable fecal pellets in March indicate that there were more algae present to serve as herbivore food than there had been in January.

Chlorophyll levels in the water column and primary productivity rates support this (see Section 4.4.1.2). The total material in the traps (as measured by dry weight) was double that for January, indicating an increased availability of both organic and inorganic matter. Flux rates for carbon and nitrogen into the traps were lower for March than for January.

In January, herbivorous zooplankton were also low in abundance and many were in overwintering stages which do not feed (Hebard 1956), causing a low phaeopigment flux into the sediment traps. By March, juvenile stages of copepods and other herbivorous zooplankton became abundant (Sections 4.7.1.3). Most of the algal cells were eaten voraciously by zooplankton and were seen as an increased load of fecal pellets in the sediment traps. Some excess algae which sank from the photic zone appeared as intact cells under the microscope. The quality of the material egested by copepods in March was low (as indicated by the low carbon/phaeopigment ratio - Table 4.42), as this was the period of fastest growth for juvenile animals and much of the organic matter ingested went to growth and to satisfy their increased metabolic rates. In January, the few feeding zooplankters needed energy only to support a slow metabolism, allowing them to egest fecal pellets containing excess of organic matter (higher C/Ph ratio - Table 4.42).

Greater inorganic sediment loading caused by early spring runoff accounts for the much larger dry weight (total trap content) found in March. The smaller carbon/total material ratio seen for March (Table 4.42) indicates a lower organic content.

The seasonal sedimentation rate and sediment quality patterns can not be determined from the limited sediment trap data but a comparison between winter (November-January) and early spring (February-March) conditions can be made. The results of these deployments are within the limits for material caught in sediment traps elsewhere in Puget Sound (Shuman 1978; Copping 1982) for the same times of year.

The sediment trap program was suspended following the loss of four strings of sediment traps and all the accompanying line, anchors, floats and hardware. In at least one case there is good evidence that US Navy minesweepers had been working in the area. Other losses were probably due to fishing boats. The nearshore area at Seahurst Park presented many problems for anchored deployment of gear, including the proximity to a populated beach and commercial fishery, and the steep bathymetry of the area.

4.4.6 Onshore Flow

An investigation to find a possible onshore bottom flow of water in the Seahurst Park area was carried out throughout the fall and early winter of Phase I. Temperature and salinity readings taken with a Beckman Induction Salinometer were calibrated against the Interocean CTD aboard the R/V Liberty. Figure 4.27 A and B were drawn from results of temperature taken on two separate dates (11/30/82 and 1/2/83) along the same transect (see Figure 4.2). Sampling stations were occupied on each transect with measurements taken every meter from the sea bottom to the surface. Contours were drawn through the isotherms. Figure 4.84a from November 1982, shows remnants of a vertically

stratified water column, due to residual thermal heating from the summer months. By January 1983 (Figure 4.84b), all semblance of vertical structure had disappeared, leaving a uniformly mixed water column. There was no evidence in these figures or in other data to indicate a shoreward lean of isotherms suggesting a movement of bottom water.

If a net movement of water towards the shore were present, it is to be expected that the coefficients of variation (s/x) for the near surface and bottom water would differ. Statistical analysis of the data for five sampling dates (Table 4.43) shows that the two coefficients of variation are not significantly different at the 8% level. CTD profiles from discrete sampling stations likewise show no indication of onshore bottom water flow.

All evidence gathered here leads to the conclusion that there is no onshore movement of bottom water. Weekly CTD traces will continue to be examined for evidence to the contrary. On that basis, the investigation using the Induction Salinometer was discontinued.

4.5 Correlations

The temporal variations of nutrients, phytoplankton and zooplankton show no correlations on time scales of weeks but the properties are correlated on a seasonal scale. The rate of change of sunlight associated with the change in day length over the year is the most important determinant of the net rate of change of chlorophyll which in turn affects the rates of change of zooplankton and nutrients. The concentrations of properties are determined by the time integration of the rates. Consequently, deviations in the rates from the main relationships with sunlight are additive in terms of concentration so that the correlation of concentration measures are not well defined.

The correlations are most evident in terms of the time constants. A time

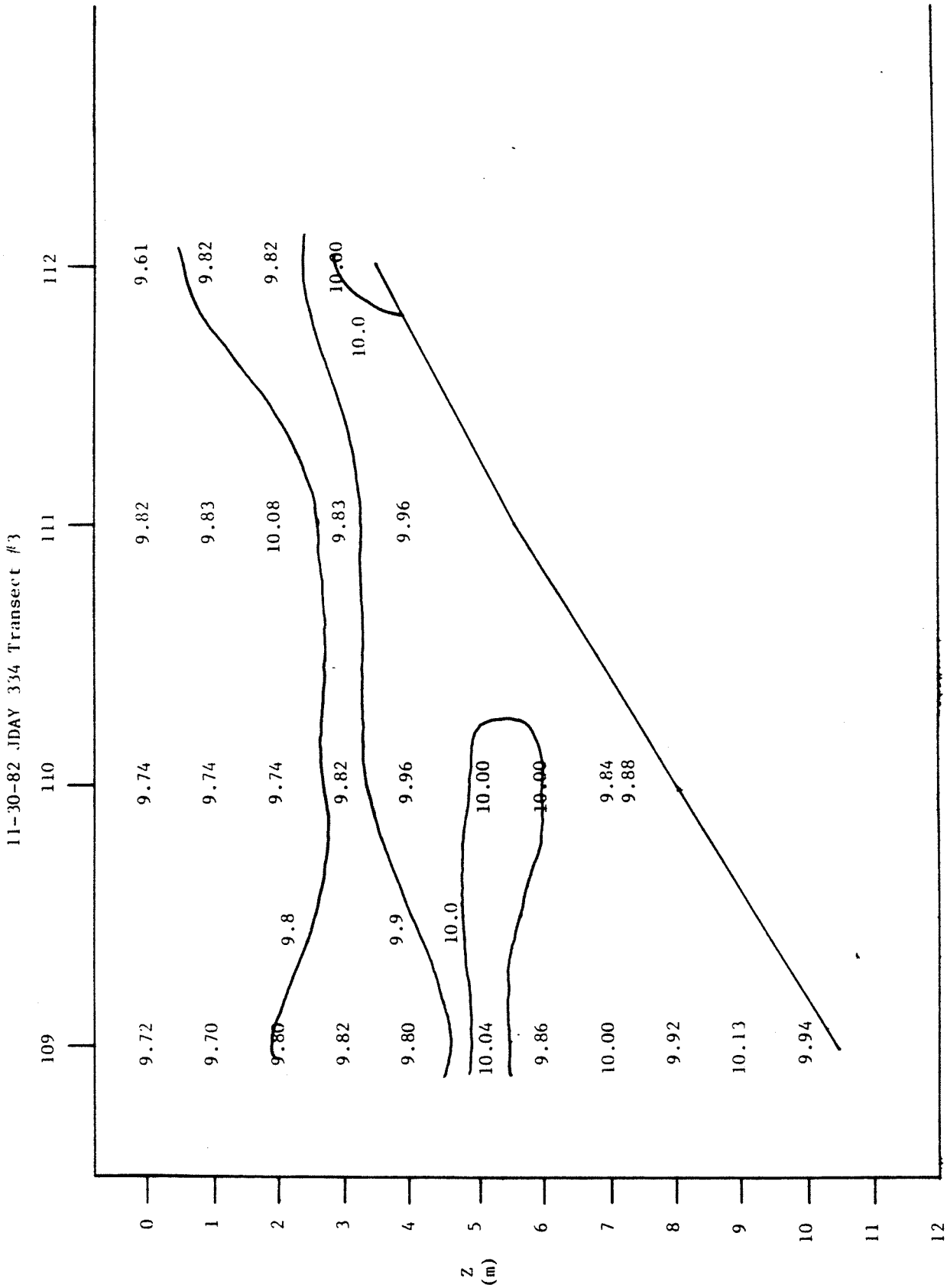

Figure 4.84a. Near shore temperature in Seahurst Bight at transect 3 (See Fig. 4.5) on November 30 1982.

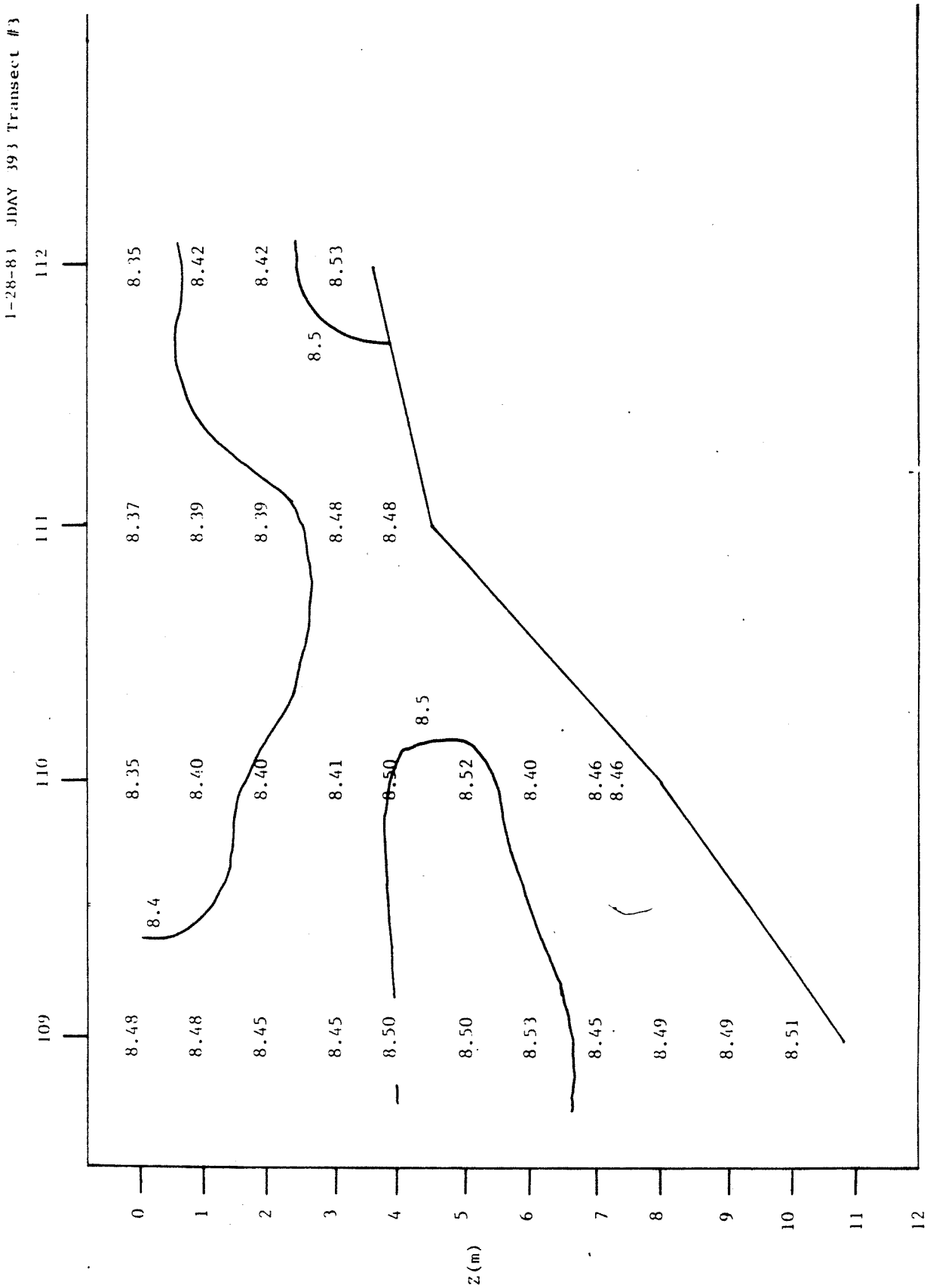

Figure 4.84b. Near shore temperature in Seahurst Bight at transect 3 (See Fig. 4.5) on January 28 1983.

Table 4.43. Statistical analysis of Seahurst Inshore studies temperature data. Temperature in degrees centigrade.

		2 Meter Water			Bottom Water		
Date	Transect	Mean	Variance	Coef. Var.	Mean	Variance	Coef. Var.
10/19/82	1	11.39	.109	.0096	11.40	.040	.0035
	2	11.45	.049	.0043	11.40	.025	.0022
	3	11.39	.030	.0026	11.41	.060	.0053
	4	11.44	.039	.0034	11.40	.050	.0044
11/30/82	1	9.80	.048	.0049	9.98	.047	.0047
	2	9.73	.068	.0070	9.94	.013	.0013
	3	9.86	.130	.0132	9.95	.043	.0043
	4	9.83	.094	.0096	10.03	.161	.0161
1/11/83	1	8.82	.032	.0036	8.87	.034	.0038
	2	8.76	.040	.0046	8.84	.026	.0029
	3	8.82	.044	.0050	8.84	.034	.0038
	4	8.71	.128	.0147	8.82	.068	.0077
1/20/83	1	8.40	.057	.0068	8.47	.043	.0051
	2	8.33	.167	.0200	8.48	.050	.0059
	3	8.34	.025	.0030	8.49	.059	.0069
	4	8.34	.072	.0086	8.50	.043	.0051
1/28/83	1	8.54	.030	.0035	8.50	.048	.0056
	2	8.48	.037	.0044	8.53	.043	.0050
	3	8.42	.023	.0027	8.50	.027	.0032
	4	8.46	.030	.0035	8.53	.022	.0026

constant of a rate is defined as the rate of change of a smoothed property divided by its concentration. Three correlations were evident for the Seahurst Bight data. The time constant for the rate of change of chlorophyll had a linear trend with the time constant for the rate of change of incident radiation (Figure 4.85), the time constant for zooplankton dry weight rate of change had a linear trend with the chlorophyll time constant (Figure 4.86), and the time constant for the nutrient rate of change had a linear trend with the chlorophyll time constant (Figure 4.87). Chlorophyll and nutrient data from the Seahurst intertidal site had the same patterns (Figures 4.88 and 4.89). Zooplankton data was not collected at the intertidal site. The correlations between time constants are significant in all examples and can be fit with linear regressions. The nutrient vs. chlorophyll time constant regression had the highest correlation coefficient and the light vs. chlorophyll time constant regression had the lowest (Table 4.44). In none of the examples is it apparent that a more complicated nonlinear regressio would provide a better fit to the data. Multiple linear regressions including stratification and other properties did not significantly improve the simple linear regressions.

To investigate the significance of the linear trends in the time constants, their dynamics have been investigated. Following along the lines of Appendix (4.1) a general equation for the rate of change of a water column property x is written

$$dx/dt = r \times G(x/K) \qquad (47)$$

where r is a rate constant and G(x/K) is an unspecified saturation function that describes the rate of change of x relative to its equilibrium value K.

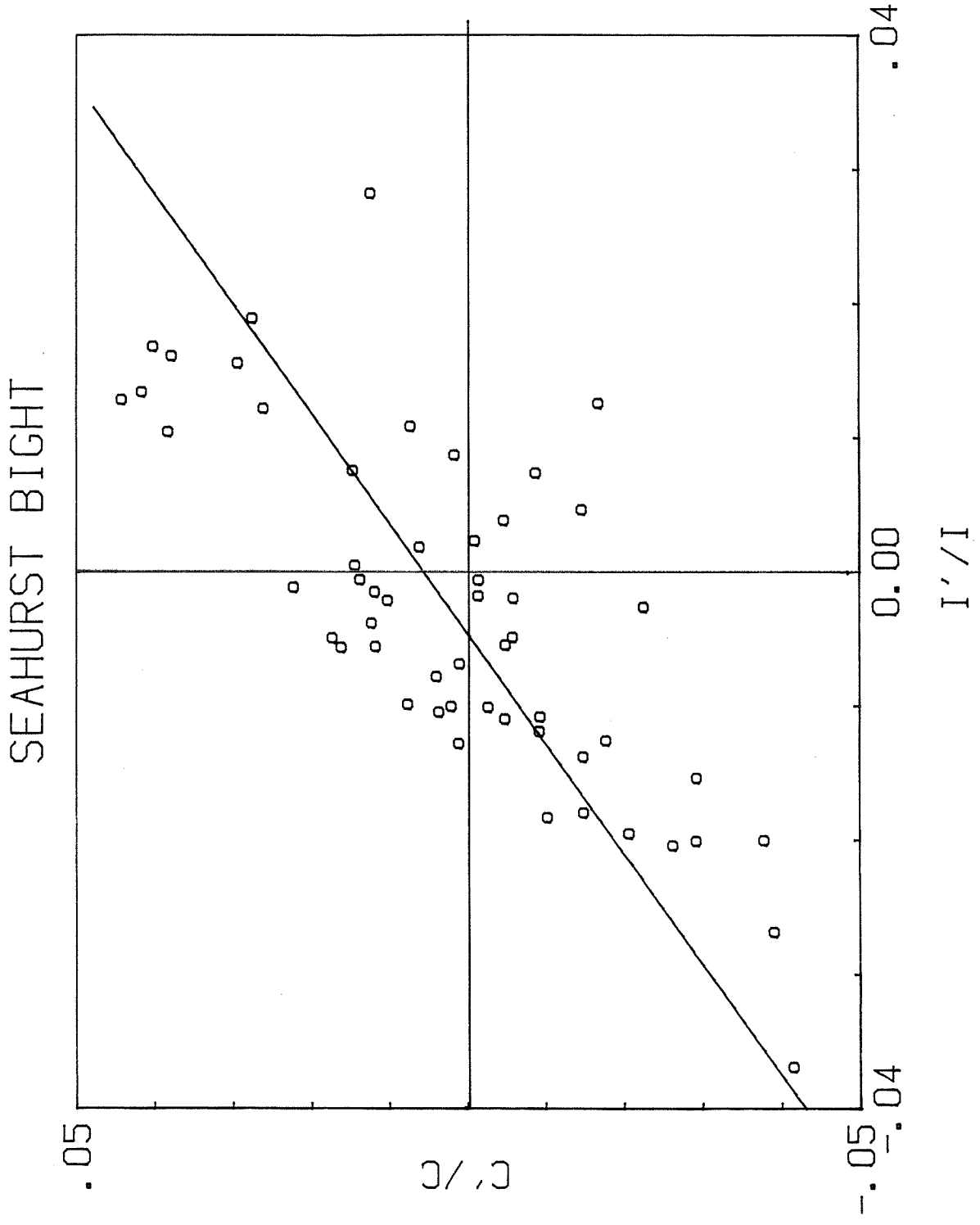

Figure 4.85. Correlation between incident radiation time constant I'/I and chlorophyll time constant C'/C for the Seahurst Bight photic zone. Time constant units (1/day).

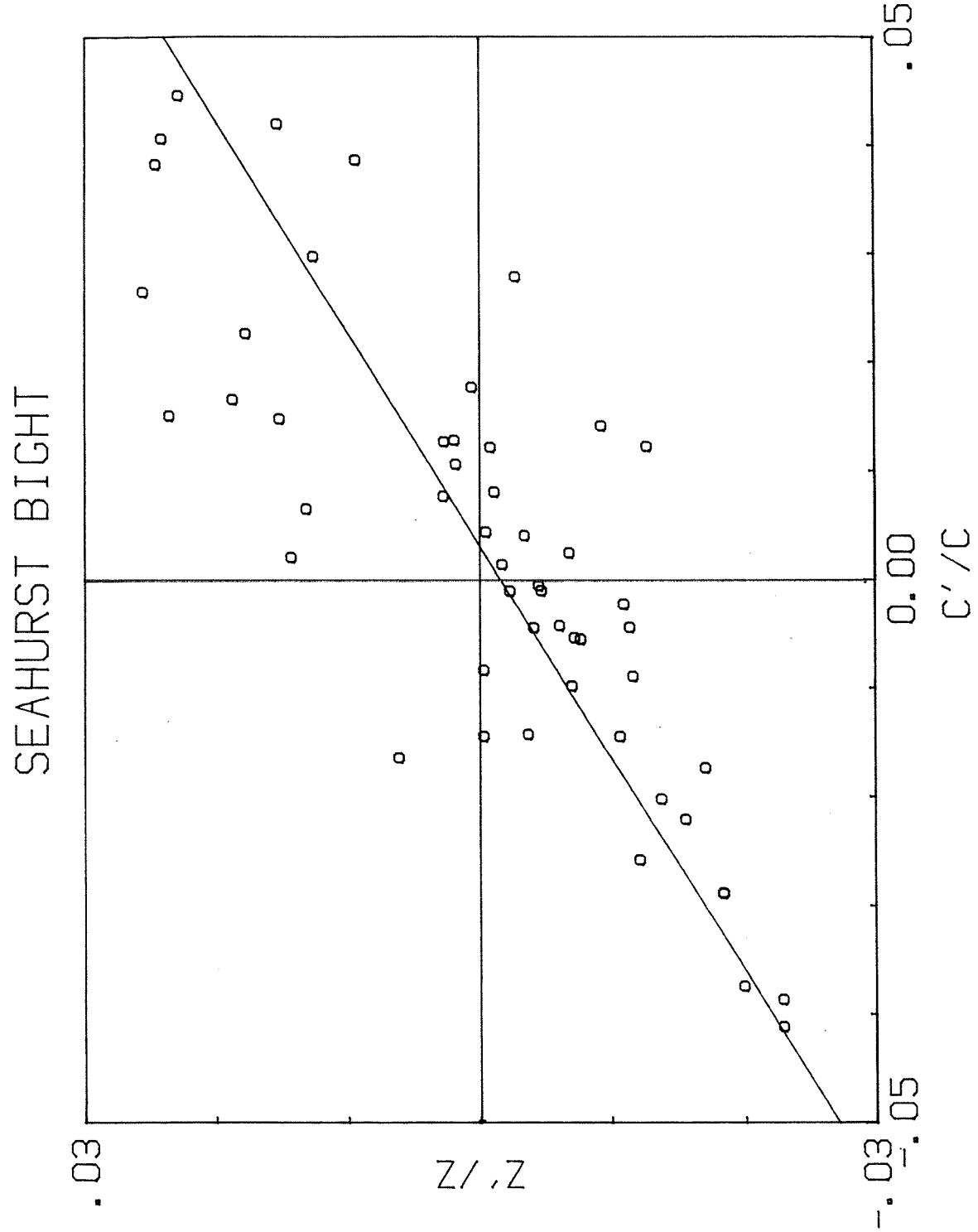

Figure 4.86. Correlation between chlorophyll time constant C'/C and zooplankton dry weight time constant Z'/Z for the Seahurst Bight photic zone. Time constant units (1/day).

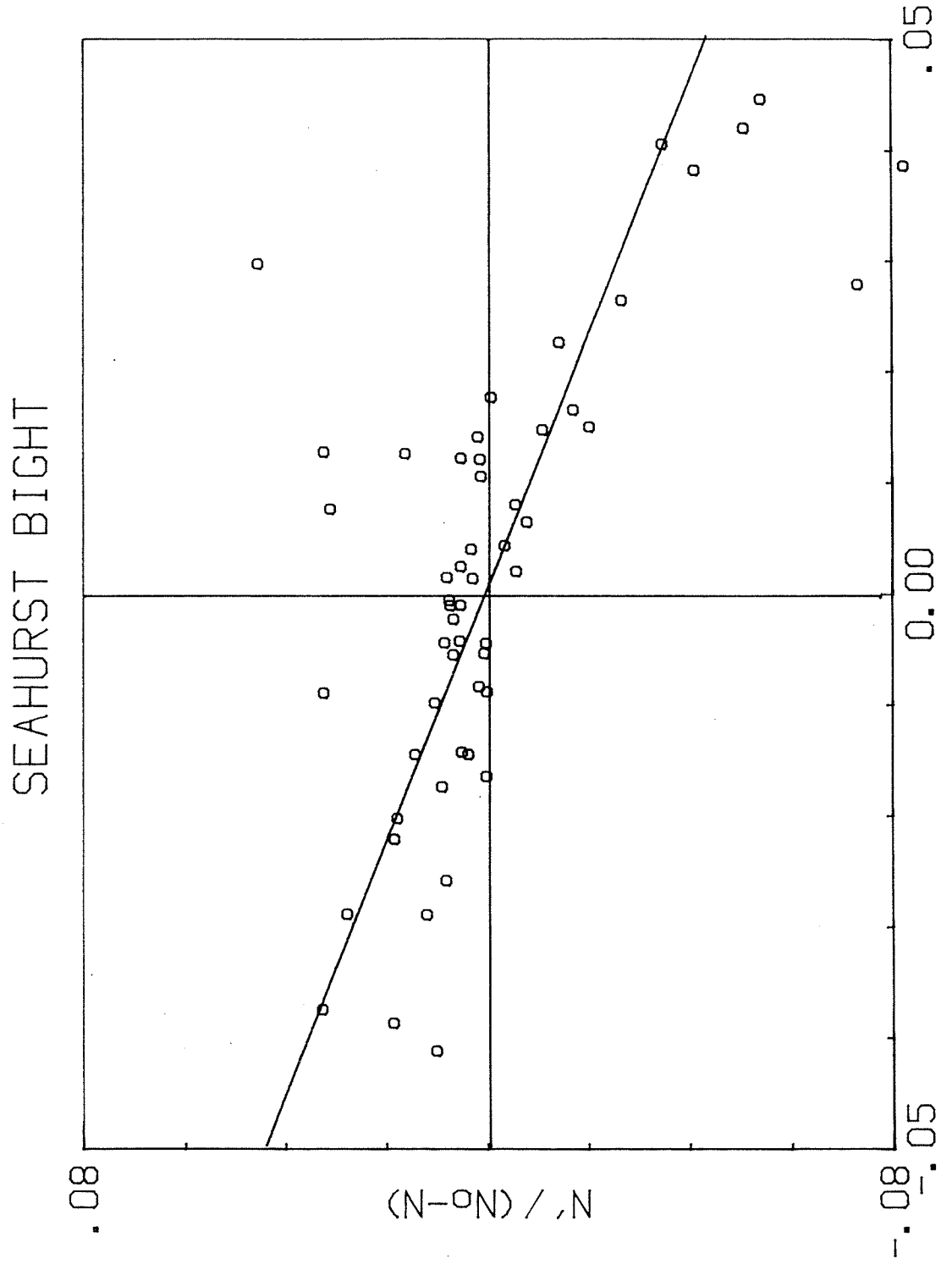

Figure 4.87. Correlation between chlorophyll time constant C'/C and nitrate time constant N'/(No-N) for the Seahurst Bight photic zone. Time constant units (1/day).

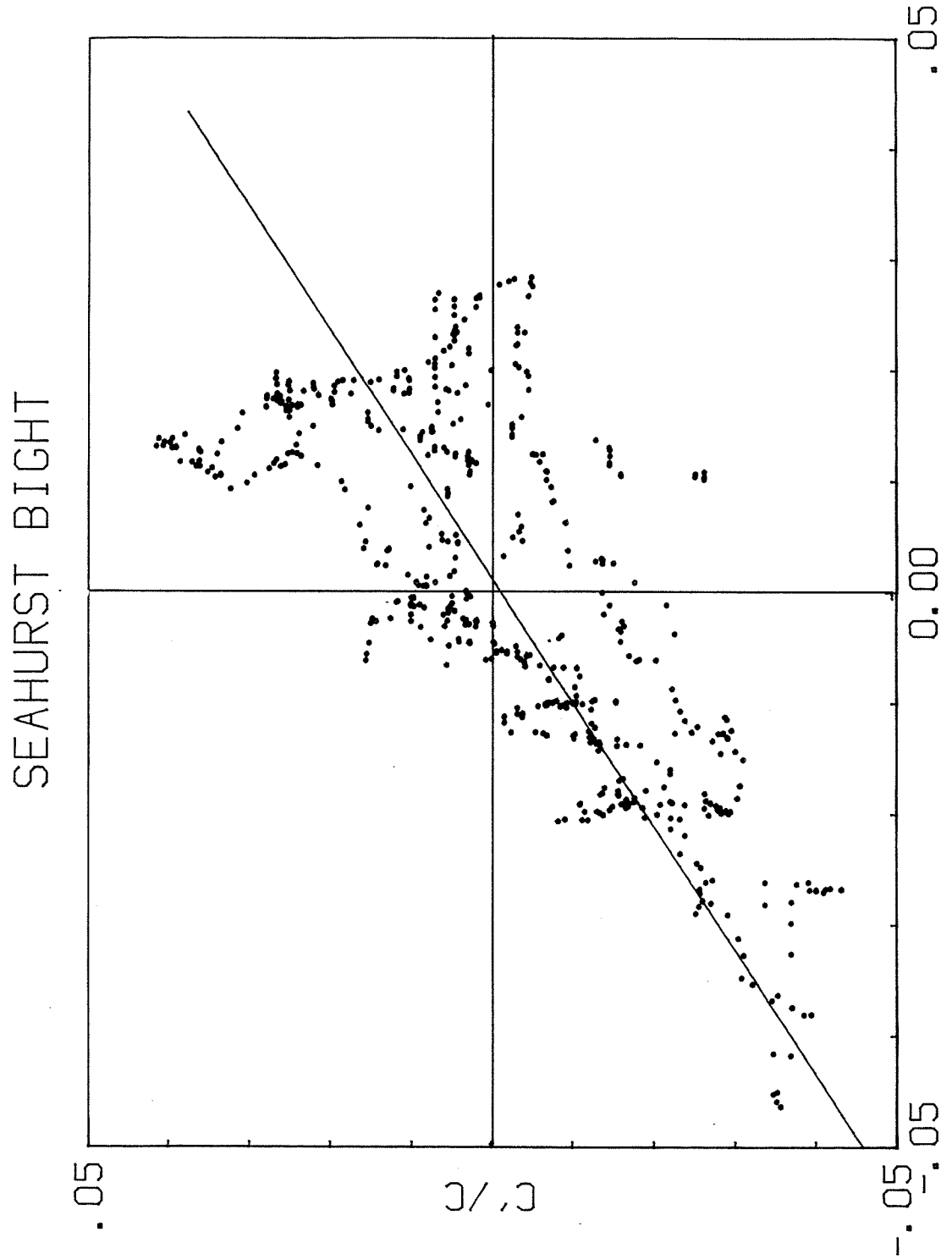

Figure 4.88. Correlation between incident radiation time constant I'/I and chlorophyll time constant C'/C for the Seahurst intertidal zone. Time constant units (1/day).

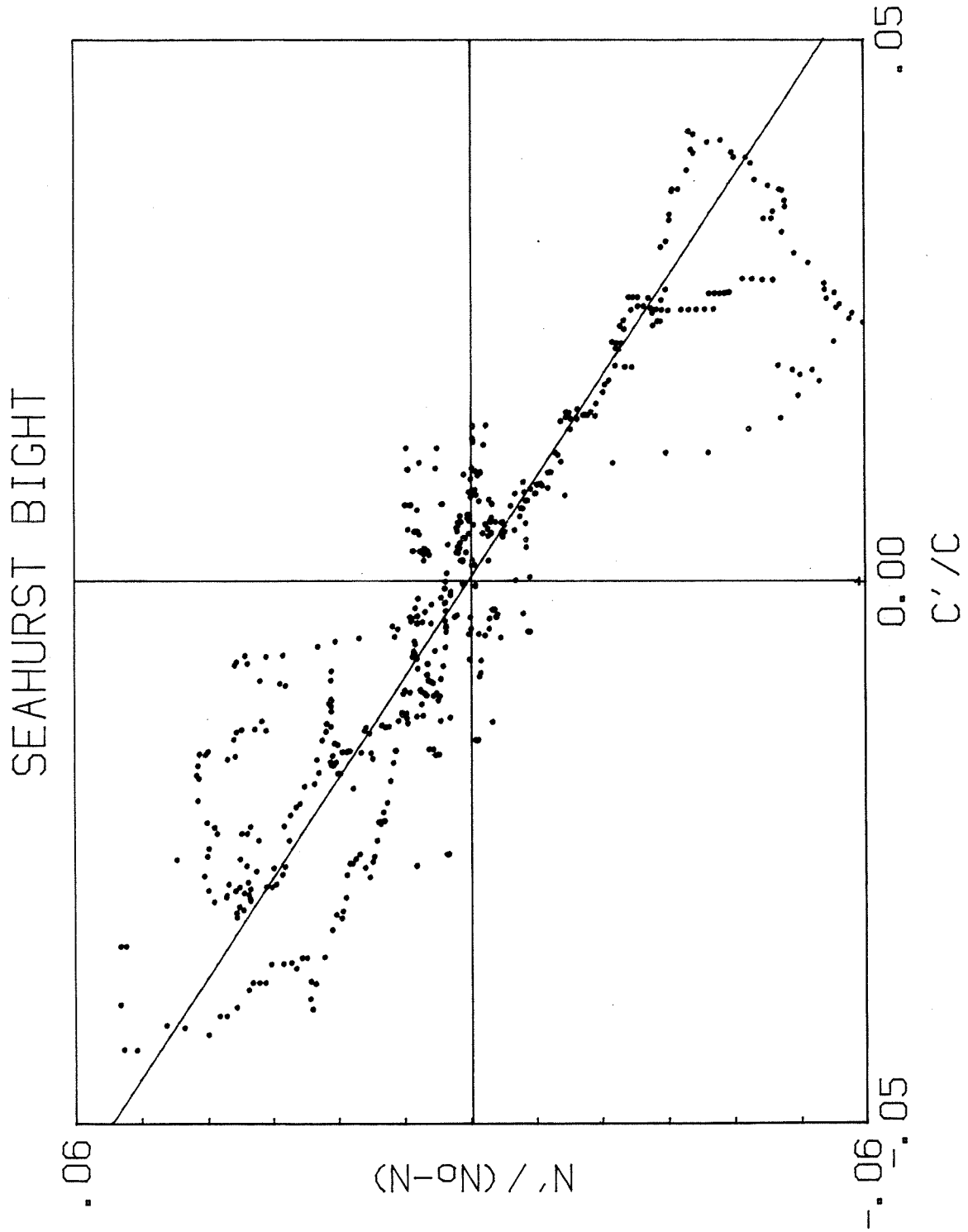

Figure 4.89. Correlation between chlorophyll time constant C'/C and nitrate time constant N'/(No-N) for the Seahurst intertidal zone. Time constant units (1/day).

Table 4.44. Results of the water column property time constant regressions using the equation y = a + bx. C'/C designates the chlorophyll time constant, 1'/1 the solar radiation time constant and Z'/Z the zooplankton time constant. Units are in (1/day). r^2 is the correlation coefficient, df denotes degrees of freedom and F is the F statistic value.

LOCATION	x	y	a	b	r^2	df	F
Bight	I'/I	C'/C	0.005	1.2	0.57	53	69
Intertidal	I'/I	C'/C	-0.001	0.9	0.56	569	729
Bight	C'/C	N'/N*	0.00047	-0.9	0.56	52	65
Intertidal	C'/C	N'/N*	0.00002	-1.1	0.80	569	1000
Bight	C'/C	Z'/Z	-0.002	0.5	0.67	52	102

The basic characteristics of G(x/K) are

$$G(0) = 1 \qquad (48a)$$

$$G(1) = 0 \qquad (48b)$$

$$dG(x/K)/dx < 0 \qquad (48c)$$

$$dG(x/K)/dK > 0 \qquad (48d)$$

For systems that are not close to extinction, that is were $x > 0$, the criterion of eq. 48a is not important and an equation for the saturation term that fulfills characteristics 48b-d is the log function

$$G(x/K) = -\ln(x/K) \qquad (49)$$

To investigate the essential features of x when K changes over time an equation for the rate of change of the equilibrium can be defined. For illustrative purposes a first order equation is sufficient where

$$dK/dt = cK \qquad (50)$$

and c is the rate coefficient for the change in the equilibrium value over time. The solution of eq(50) is

$$K = \exp(ct) \qquad (51)$$

and the resulting equation for x is

$$x = \exp[ct - (1-\exp(-rt))r/c] \qquad (52)$$

In general the rate coefficient c of eq(50) is much smaller than the rate coefficient r of eq(47), that is, the change in the equilibrium is lower than the time required to attain the equilibrium. The important result of r >> c is that the second derivative of x reduces to

$$x'' = c^2 \exp(ct - r/c) \qquad (53)$$

where x" is the second derivative of x with respect to time. Equation (53) implies x" is close to zero and x changes as the equilibrium K changes.

Differentation of eq(47) with respect to time using eq(48) to define G yields

$$x'' = -r\ln(x/K)x' - rx' + rxK'/K \qquad (54)$$

where the superscript (1) is the first derivative of the property with respect to time. From the assumption that r >> c and if c is small it follows that ln(x/K = 0 and x" = 0 and the time constant of the rate of change of x is related to the time constant of the equilibrium K by the relationship

$$x'/x = K'/K \qquad (55)$$

Thus, the investigation of what factors control the time constant of x reduces to an investigation of the factors that control the time constant of the equilibrium K. Using eq(55) as a starting point three simple models have been developed that produce the linear correlations of the time constants shown in Figures 4.85 to 4.89.

A phytoplankton model that yields the linear relationship between the

chlorophyll and solar radiation time constants is based on the equation

$$dC/dt = C(aI^m - bC^n \qquad (56)$$

where the production of chlorophyll C is dependent light I according to a photosynthesis relation proposed by Cosby. Hornberger and Kelly (1984) and a loss rate that is concentration dependent. The equilibrium condition, dC/dt = 0, is at

$$K = (a/b)^(1/n) \quad I^(m/n) \qquad (57)$$

and from eq(55) the chlorophyll time constant is related to the solar radiation time constant by the relation

$$C'/C = (m/n) \quad I'/I \qquad (58)$$

The slope of the line in Figure 4.85 and 4.88 are defined by the ratio m/n. The regressions (Table 4.44) yield a slope of about 1 and with m = 0.5 (Cosby et al. 1984). The loss coefficient exponent is n = 0.5.

The linear relationship between the zooplankton time constant and the phytoplankton time constant requires an equation of the form

$$dZ/dt = Z\ C(a - b\ Z^m/C^n) \qquad (59)$$

where Z is zooplankton dry weight, C is chlorophyll, a is a growth rate coefficient, b is a loss rate coefficient, and m and n are exponents defining how the loss rate is related to zooplankton and phytoplankton levels. The

loss term incorporates the feature that omnivorous zooplankton food items included juvenile of their own species, other species, and phytoplankton. The loss function increases with zooplankton as the zooplankton feed upon each other, and decreases with an increase in phytoplankton since zooplankton presumably then encounter and consume more phytoplankton than zooplankton. The equilibrium relationship between zooplankton and phytoplankton is defined by the equation

$$K = (1/b)^{(1/m)}\ C^{(n/m)} \qquad (60)$$

and the relationship between the time constants is

$$Z'/Z = (n/m)\ C'/C \qquad (61)$$

The regression of the Seahurst Bight data (Table 4.44) yields n/m = 0.5 which implies that the zooplankton equilibrium increases with the square root of the phytoplankton concentration.

The linear regression between nutrient and chlorophyll time constants can be developed from the equation

$$dN/dt = aNo - bC^m - aN \qquad (62)$$

where the nutrient concentration is N, the concentration of nutrient being mixed into the region is No, the mixing coefficient is a, the rate coefficient for the uptake of nutrient by phytoplankton is b, and the m is an exponent of the uptake relation with chlorophyll C. The equilibrium level is

$$K = No - b/a\ C^m \qquad (63)$$

Defining the difference between the equilibrium and input concentration as

$$N^* = No - K \qquad (64)$$

the time constant relationship becomes

$$N'/N - mN^*/(No-N^*)\ C'/C \qquad (65)$$

Since the system is near equilibrium, N = K and taking No as the concentration at the bottom of the thermocline the time constant relation reduces to

$$N'/N^* = m\ C'/C \qquad (66)$$

Using No = 28 mg-at/m^3 for nitrate the regression of N'/N* vs. C'/C for the the Seahurst Bight and the Seahurst intertidal zone data yields a slope of m = 1 (Table 4.44).

The three models provide a basis for understanding the linear relationships between time constants of properties but they succeed to varying degrees. the chlorophyll nutrient model gave a high regression coefficient suggesting that the principle nutrient dynamic is the balance between a seasonally varying uptake of nutrient in phytoplankton growth and a constant input of nutrient from deep water. The relationship between zooplankton and chlorophyll suggests a strong coupling between the two trophic levels that is based in part on the the trade off of zooplankton for phytoplankton in grazing and in part on phytoplankton food limitation in zooplankton growth.

Cannibalism may be an important factor controlling zooplankton levels in the autumn when chlorophyll levels are decreasing. The relationship between the light and chlorophyll time constants has the lowest regression coefficient and the linear relationship is best approximated in periods when the daily average light gradient is negative. This corresponds to the summer and autumn seasons when the days are progressively shorter. In the winter and spring, days are progressively longer and the linear relationship breaks down but the general correlation still holds.

This analysis indicates that the timing of the spring bloom, the summer maxima and the autumnal decline in plankton are primarily determined by the seasonal minima, maxima and zero points in rate of change of sunlight energy flux to the water column trophic community.

Secondary factors that effect the rate dynamics have not been included inthe correlation modesl but in many cases they are included indirectly since many secondary factors are themselves related to sunlight. For example stratification, which affects the intensity of vertical mixing, has a well defined pattern with seasonal sunlight intensity (Figure 4.90). In a similar manner river runoff and the intensity of tidal mixing also have seasonal cycles correlated with sunlight. Thus, in general, sunlight is the major factor affecting the water column plankton and nutrient distributions. The analysis presented in this section provides a theoretical basis for the correlations of the timings of water column properties and the seasonal cycle of sunlight.

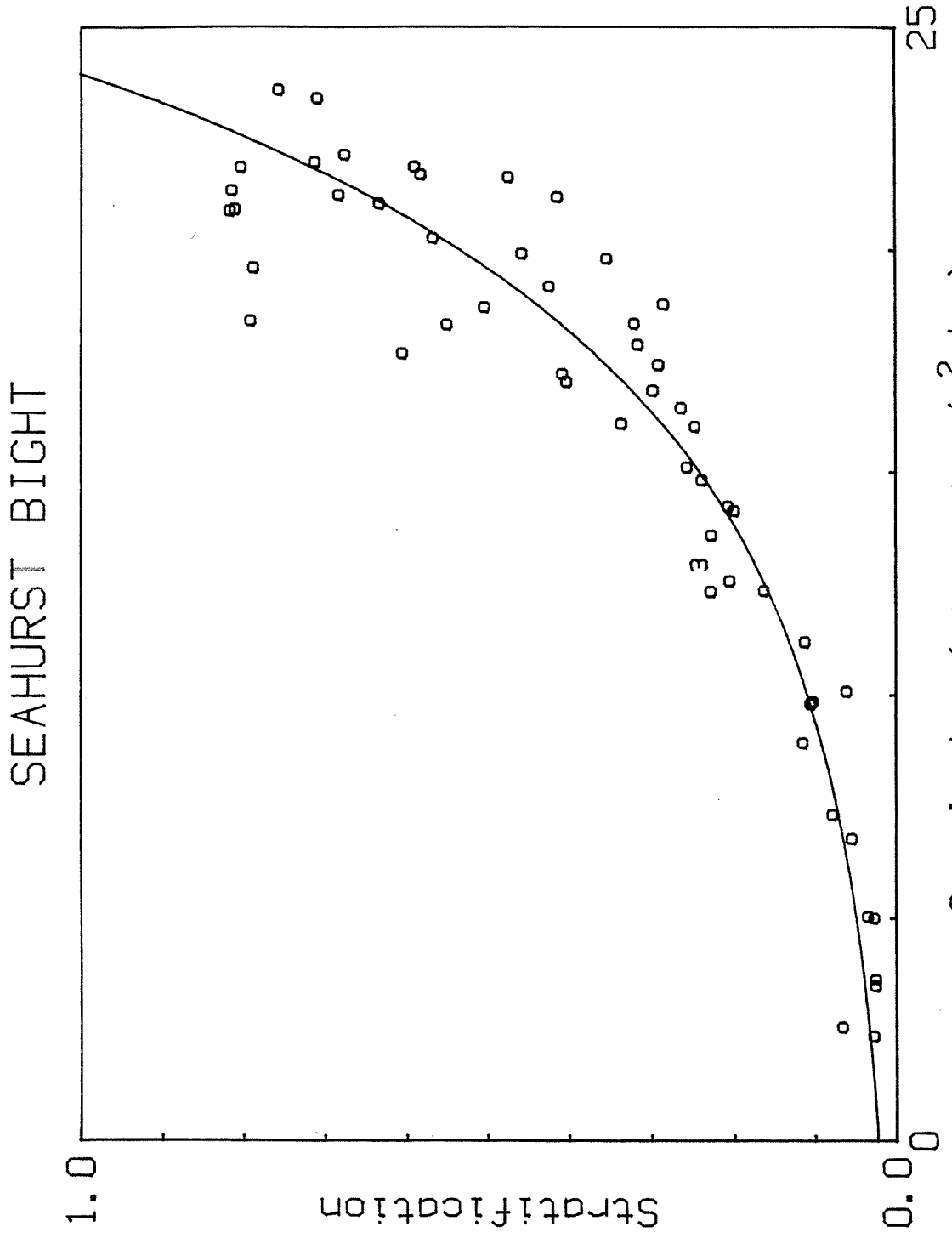

Figure 4.90. Correlation between smoothed incident radiation and stratification in Seahurst Bight. Stratification is the density difference between 25 m and the surface. Regression equation is STRAT = 0.022*EXP(0.158*I). Correlation coefficient r^2 = .092.

4.6 Summary

1. The basic seasonal levels of plankton and nutrients in the photic zone were related to the seasonal cycle of sunlight. Chlorophyll essentially followed the sunlight cycle and nutrients and zooplankton followed the chlorophyll cycle. The cycles were coupled in terms of the rates of change of the properties. The phytoplankton rate of change was positive in the spring during the day length rapid increase in day length and negative in the autumn during the day length rapid decrease in day length. Phytoplankton levels were minimum near the winter solstice and maximum near the summer solstice. The rate of change of zooplankton followed the rate of change of chlorophyll with a large positive rate in the spring and a large negative rate in the autumn. Maximum abundance was observed about the summer solstice and minimum abundance was observed about the winter solstice. The rate of change of nutrients were inverse to the chlorophyll rate resulting in maximum nutrient concentrations about the winter solstice and minimum concentrations about the summer solstice.

2. Plankton and nutrient levels exhibit a large amount of variability about the seasonal pattern. The variation between stations sampled on a given day, which is a measure of spatial variability, was about 15% for nutrients, 30% for plankton biomass measures, and 40% for plankton species abundance measures. The variability from one sampling time to the next, which includes temporal and spatial variability, was about 2 to 3 times larger than the spatial variability. Thus, the total variability about the seasonal smoothed averages was about 15 to 30% for nutrients, 100% for

plankton biomass measures, and 150 to 200% for plankton species measures.

3. The change of observing a high level of photic zone chlorophyll (10 mg chl/m^3 or greater) was larger in the summer of 1983 (15%) than in the summer of 1982 (7%). In general it appeared that 1983, the only year for which a complete set of measurements was obtained, had unusually high plankton levels. During the summer of 1983 chlorophyll levels were about twice that observed in any year over the last decade. A major El Nino affected the waters of the Northeast Pacific in 1983 and resulted in an average water column temperature increase of about 1°C in Puget Sound. It is possible that the El Nino had a positive effect on phytoplankton growth in Puget Sound during the spring and summer seasons of 1983. A similar positive effect on phytoplankton growth was observed in the Gulf of California during the same period (Lara-Lara, Valdez-Holguin and Perez 1984). The cause of the doubling in the chlorophyll level in the Sound is not understood and appeared as an anomaly in the chlorophyll-light relationship in the spring of 1983.

4. The dominant phytoplankton species in Puget Sound were diatoms, which had maximum rates of growth in the spring. Dinoflagellates were the second most abundant type of phytoplankton with maximum numbers in midsummer. Toxic dinoflagellates were infrequently observed in the samples and only in small numbers. The dominant zooplankton observed in the main basin and Seahurst Bight were Paracalanus sp. and Corycaeus angilicus. Calanus pacificus was not numerically abundant but because of its large size it was important in terms of biomass.

The Puyallup River and several small streams along the eastside of East Passage contributed freshwater, ammonia and silt to the surface waters of East Passage. A combination of an ebb tide and northerly winds favord northward intrusion of Puyallup River water into East Passage. The Duwamish River water plume was not observed in East Passage.

5. Bottom water intrusion into the shallow waters of Seahurst Bight was theoretically possible because of the curved shape of the Bight. The presence of an intrusion was investigated with detailed temperature measurements in the shallow waters of the Bight. No evidence of a deep water intrusion was found.

6. To investigate the effect of ammonia on phytoplankton growth chlorophyll levels were compared in areas with high and low levels of ammonia. Ammonia concentrations were high in the intertidal waters of Seahurst and Indianola (5 mg-at/m^3), and in the river water (30 mg-at/m^3). Levels were relatively low in the surface waters of the Seahurst Bight and main basin of Puget Sound (1 mg-at/m^3). The chlorophyll levels in the intertidal waters were not significantly different from the surface water chlorophyll levels in Puget Sound. Chlorophyll was elevated above the background surface water level in the Puyallup River plume and was depressed below the background in the Duwamish River plume.

7. Sediment trap studies in January and March 1982, indicated a flux of fecal pellets, intact phytoplankton cells, and inorganic material through the water column. The total flux of material was twice as large in March as in January and the flux of degraded phytoplankton pigments in fecal pellets increased by a factor of 50.

4.7 Conclusions and Recommendations

The water column study provides to date the most complete seasonal description of plankton and nutrients in Puget Sound. In total, it extended over two years and included sampling on daily and weekly intervals. To analyzed the data new integrated statistical procedures were developed that have first principle biological foundations. The data and the analysis techniques should prove highly valuable for the monitoring and assessment of the changes in Puget Sound well into the 21st century.

From the study several important conclusions have been reached on how the pelagice food chain operates and what impact the input of sewage into the Sound may have on the food chain. The study has also clarified several important questions that are critical to the immediate and long-term monitoring of Puget Sound.

The time averaged sunlight flux is the most important factor that determines the seasonal level of phytoplankton in Puget Sound. Zooplankton, which are a principle food source of juvenile fish, have growth rates that follow the phytoplankton growth rate. The level of nutrients follow the phytoplankton levels in an inverse manner. Ammonia, associated with sewage and river runoff, has no clear pattern with chlorophyll and the evidence suggests that on seasonal time scales ammonia does not affect phytoplankton growth in the Sound. The El Nino, which was responsible for unusually warm water in the Sound in 1983, was also coincident with extremely large spring and summer phytoplankton levels. How the El Nino affected the phytoplankton is not understood so an accurate prediction of phytoplankton levels from meteorological conditions can not be made at this time.

From the study it is clear that any realistic assessment of the significance of pollution on the productivity of the Sound must be evaluated

in terms of how pollution alters the productivity from natural levels determined by seasonal and large scale weather cycles. This means that a biological model must be developed that is based on the seasonal sunlight flux and correctly deals with natural anomalies such as the El Nino. The problem requires a long-term point of view, since a gradual warming of the atmosphere from the effects of carbon dioxide is predicted up into the 21st century. This study and others suggests that anomalies of the water temperature can significantly affect pelagic productivity. The long-term warming is likely to evolve at a rate similar to the increase of pollutants in Puget Sound. Thus it is critical to evaluate separately the effects of pollution and weather since one can be mediated, at great expense, while the other can not.

A specific recommendation is to carry out a long-term, but limited, plankton study. The success of the Seahurst beach daily sampling program indicates that frequent long-term observations of water column properties from a suitable pier or dock would be a significant cost effective way to monitor a region and obtain a data set for the development of a sunlight-plankton mdoel. The type of program that has been typically conducted in the past, consisting of short-term sampling with closely spaced station locations, is of limited value for monitoring and understanding the long-term trends and dynamics of Puget Sound biological communities.

4.8 References

Alldredge, A. 1976. Appendicularians. Sci. Amer. 235:94-102.

Anderson, J. J. and A. Okubo. 1984. Zooplankton probability distributions: everything is coming up gamma. Abstract Ocean Sciences Meeting New Orleans, Louisiana. Ja. 23-27, 1984.

Campbell, S. A., W. K. Peterson and J. R. Postel. 1977. Phytoplankton production and standing stock in the main basin of Puget Sound. Final Report to the Municipality of Metropolitan Seattle. Council Resolution No. 2203. M77-5 pp. 132.

Carpenter, J. H. 1965. Chesapeake Beay Institute technique for the Winkler dissolved oxygen method. Limnol. Oceanogr. 10:141-143.

Copping, A. E. 1982. The distribution and passage of organic matter in the marine good web, using nitrogen as a tracer. Ph.D. Thesis, Univ. Washington, Seattle. 155 pp.

Cosby, B. J., G. M. Hornberger and M. G. Kelly. 1984. Identification of phytosyntesis-light models for aquatic systems. II. Application toa macrophyte dominated stream. Ecol. Modelling, 23:25-51.

Damkaer, D. M. 1964. Vertical distributions of Copepoda in Dabob Bay, December, 1960. M.S. thesis, Univ. Washington, Seattle. 84 p.

Grice, J. V. and L. J. Bain. 1980. Inferences concerning the mean of the gamma distributions. J. Amer. Stat. Assoc. 75:929-933.

Ebbesmeyer, C. C., C. A. Coomes, J. M. Cox and J. M. Helseth. 1982. Historical oceanographic data in East Passage and approaches. Prepared for the Municipality of Metropolitan Seattle.

Engelhardt, M. and L. J. Bain. 1978. Technometrics 20:485-489.

Goel, N. S. and N. Richter-Dyn. 1974. "Stochastic Models in Biology."

Academic Press, New York, pp. 269.

Harper-Owens. 1983. Water quality assessment of the Duwamish estuary, Washington. Submitted to Municipality of Metropolitan Seattle (METRO). 193 p. + App.

Hebard, J. F. 1956. The seasonal variation of zooplankton in Puget Sound. M.S. Thesis, University of Washingotn, Seattle, Washington. 64 p.

King, K. R. 1981. The quantitative natural history of Oikopleura dioica (Urochordata: Larvacea) in the laboratory and enclosed water columns. Ph.D. Thesis, University of Washington, Seattle, Washington. 152 p.

Lara-Lara, J. R., J. E. Valdez-Holguin and L. C. J. Perez. 1984. Plankton studies in the Gulf of California during the 1982-1983 El Nino. Trophical Ocean-Atmos. Newsletter 28:16-17.

Lorenzen, C. J., F. R. Shuman and J. T. Bennett. 1981. In situ calibration of a sediment trap. Limnol. Oceanogr. 26:580-585.

Lovegrove, T. 1966. The determination of the dry weight of plankton and the effects of various factors on the values obtained. (pp. 429-467 in) Some Contemporary Studies in Marine Science, H. Barnel (ed. George Allen and Urwin Ltd. London).

Lund, J. W. G., E. D. LeCren, and C. Kiping. 1958. The inverted microscrope method of estimating algal numbers and the statistical basis of estimation by counting. Hydrobiologica. 11:143-170.

Marshall, S. M. 1973. Respiration and feeding in marine copepods. Adv. Mar. Biol. 11:57-120.

Marshall, S. M. and A. P. Orr. 1972. The biology of a marine copepod. 2nd ed., Springer Verlag, Berlin. 188 p.

Nakanishi, M. and M. Monji. 1965. Effect of variation in salinity on photosynthesis of phytoplankton growing in estuaries. J. Fac. Sci.,

Univ. Tokyo, Sec. III Botany, 9:219-246.

Nisbet, R. M. and W. S. C. Gurney. 1982. "Modeling Fluctuating Populations." Academic Press, New York, pp. 542.

Parson, T. R. and M. Takahashi. 1973. Biological Oceanographic Processes. Pergamon Press, Oxford. pp. 186.

Runge, J. R. 1981. Egg production of Calanus pacificus Brodsky and its relationship to seasonal changes in phytoplankton availability. Ph.D. Thesis, University of Washington, pp. 116.

Shuman, F. R. and C. J. Lorenzen. 1975. Quantitative degradation of chlorophyll by a marine herbivore. Limnol. Oceanogr. 20:580-586.

Shuman, F. R. 1978. The fate of phytoplankton chlorophyll in the eupthotic zone - Washington coastal waters. Ph.D. Thesis, Univ. Washington, Seattle. 243 pp.

Stober, Q. J. and K. B. Pierson. 1984. A review of the water quality and marine resources of Elliott Bay, Seattle, Washington. Final Report to Municipality of Metropolitan Seattle, FRI-UW-8401.

Strathmann, R. R. 1967. Estimating the organic carbon content of phytoplankton from cell volume of plasma volume. Limnol. Oceanogr. 12:411-418.

Strickland, J. D. H. and T. R. Parsons. 1972. A practical handbook of seawater analysis. Fish. Res. Bd. Canada Bull. 167, pp. 311.

4A.0 ENRICHMENT EFFECTS ON PHYTOPLANKTON IN BIOASSAYS

E. B. Welch and N. Messner

Department of Civil Engineering

4A.1 Introduction

Effluent from secondary treated sewage is high in dissolved nitrogen, especially ammonia-N. Renton plant effluent contains ammonia at about 15 mg l^{-1} (1.1 mg - at l^{-1}). Puget Sound contains more phosphorus than nitrogen, relative to the requirements of phytoplankton, and therefore N tends to be depleted before P, leaving N as the limiting nutrient. Treated sewage effluent is also high in dissolved organics, which could serve as complexers of toxic metals, and therefore may stimulate the growth of phytoplankton. Increased phytoplankton growth, and subsequently biomass, is a potential effect of continual and increased addition of treated sewage effluent to marine waters (Waldichuck 1983). The purpose of this study was to evaluate the potential effect of a secondary treated effluent discharged off Seahurst Park into Puget Sound.

Five in vitro bioassays were conducted during spring and summer of 1982 using the natural phytoplankton species assemblage (Ehlers 1983). Phytoplankton biomass increased in proportion to the increasing concentration of N; P was added in a constant amount. An observed low N:P ratio and the near depleted ambient NO_3 content in Puget Sound surface waters on two of the twelve cruises, indicated that N was the limiting nutrient. Use of the natural species assemblage gave poor results when ambient nitrogen content was lowest, however, this is the most critical time to determine if phytoplankton growth rate could be stimulated by N addition. When N content was low, phytoplankton biomass was high, which provided an initial biomass that was too

large. Much of the biomass at the peak of the bloom was senescent and was an inappropriate inoculum to determine response. To counteract that problem, a single species was used in 1983. Natural phytoplankton cells were removed by filtration and a constant inoculum of a unialgal culture was used in each of seven bioassays. That organism was found to be abundant in the natural phytoplankton mixed assemblage during 1982.

The objectives in the 1983 work were to: 1) determine if N was the limiting nutrient (a constant addition of P was omitted), 2) determine if the growth rate of a representative test alga was reduced during blooms when ambient N content is low, and 3) determine if there is an inhibitory effect of treated sewage effluent, or a stimulatory effect in excess of that due to N.

4A.2 Methods and Materials

Each bioassay consisted of inoculating a known concentration of algae into filtered Puget Sound water. A known concentration of nitrate or a dilution of RTP effluent was added to duplicate flasks, and algal growth and nutrient uptake were determined for the 7 to 10 day length of each assay. The diatom Skeletonema costatum was used in the last assay. The assays were conducted from 19 April through 10 August 1983, in an attempt to span the period during which the phytoplankton bloom and nutrients decline in Puget Sound.

Water was collected at stations 10 and 4 (Figure 4A.1), kept cool, and filtered through 0.45 um GF/C filters the same day upon return to the laboratory. Assays were either initiated the same day or the filtered water was stored at 5°C and the assay begun the next day. All glassware was initially autoclaved, and acid washed between assays. The initial volume in 1000 ml flasks was 600 ml, which was reduced to about 500 ml by the end of the

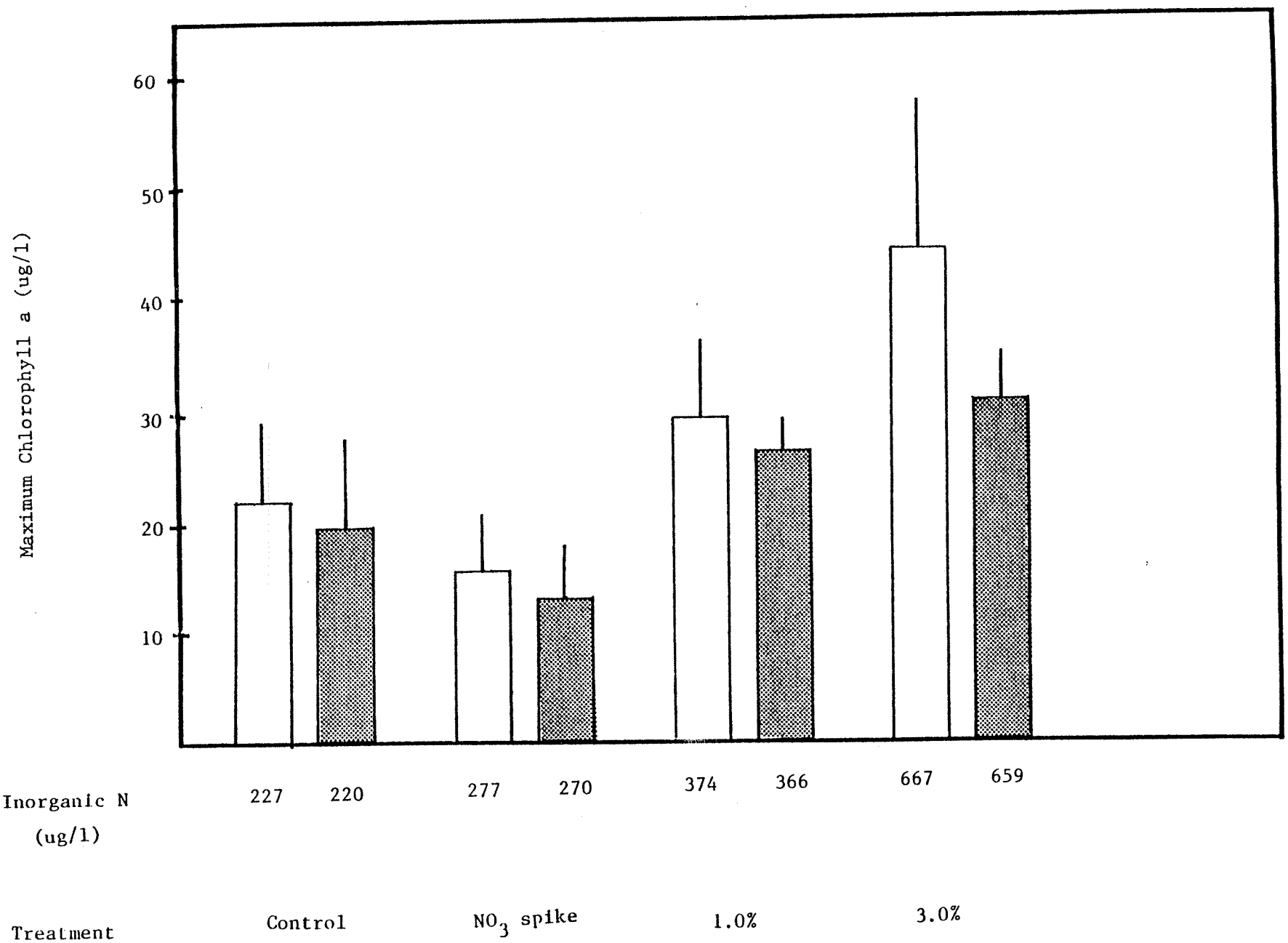

Figure 4A.1. Bioassay conducted 19 April - 26 April 1983. Chlorophyll a levels are means of the two highest readings for all replicates. Error bars are standard deviations. Inorganic nitrogen levels are initial concentrations: the sum of ambient and additions. White bars = assays with Station 10

assay. Assays were conducted in an incubation chamber at constant light (100-150 u Einsteins M^{-2} s^{-1}) provided by banks of cool-white fluorescent lights at a constant temperature of 12°C. Assay flasks were assigned positions in the incubator randomly.

Algae was grown in a modified IMR medium (Eppley et al. 1967) which contained 1% of the nitrate and 10% of the phosphate called for in the original medium. Algal cultures were transferred on a regular basis and algal inocula for experiments were tkane from cultures in the log growth phase. The initial concentration in each assay was about 1000 cells ml^{-1}. Inoculum volume was usually 1 to 2 ml.

Each treatment was done in duplicate or triplicate. Treatments consisted of a series of dilutions of effluent from RTP, plus one treatment with a known concentration of NO_3 added, and a control. Dilutions varied with the different assays, but ranged from 0.25% to 3% effluent. A spike of carbon-14 was added to each culture to bring the activity to approximately 5 uC 1^{-1}.

Every 24 hours, aliquots were removed from each flask for chl a and C-14 analyses. Samples for chlorophyll a were analyzed according to the fluorometric procedure of Strickland and Parsons (1972). Samples for C-14 were filtered through 0.45 um Millipore filters, and the filters placed in an acid fumer for 15-30 seconds, then in a filter-fluor, and stored in a dark cool area. All vials were read on a Beckman LS-8000 scintillation counter at the conclusion of each experiment. Nitrate concentrations on the first, third and final day of the assays were determined with an Autoanalyzer for the second and third assays. Ammonia was determined for the final three assays, using the Solorzano (1969) method.

Chl a maxima were determined as the mean of the two highest chl a levels in all replicate flasks. Growth rates were determined from plots of the log

transformation of the chl a or C-14 values versus time and were calculated as the slope of the linear portion of the curve.

4A.3 Results and Discussion

4A.3.1 Nutrients

Nitrate-N averaged 104 ± 81 and 120 ± ug 1^{-1} (7.4 and 8.6 ug-at 1^{-1}) at stations 10 (nearshore) and 4 (offshore), respectively, for the seven collections from April to August. Ammonia averaged about 10 ug 1^{-1}, (0.7 ug-at 1^{-1}) and is included for all estimates of N content in bioassay media. On one instance (June 14, 1983) nitrate was undetected and ammonia was 12 ug 1^{-1} (0.9 ug-at 1^{-1}). The N:P ratio averaged 3.3, clearly indicating that N exists in shorest supply and is therefore, the limiting nutrient in Puget Sound waters.

4A.3.2 Biomass Response

Results from three of the seven experiments are shown in Figures 4A.1-3 and results from all seven are shown in Tables 4A.1 and 4A.2. The three illustrated results represent high, low, and medium ambient nitrogen content, respectively. Maximum chl a attained during the six-day experiments was similar at both stations 10 and 4. This is contrary to 1982 results when chl a maximums were consistently higher at station 4, offshore. Care was taken to avoid surface film collections in 1983 and well mixed surface waters were obtained. Thus, there is no difference in response to water from stations 10 and 4 as had been suspected in 1982 samples.

The limiting nutrient and the presence of inhibitors can be detected by the degree to which the biomass yield after 5 to 6 days is related to the concentration of nutrient initially available. While there is a trend of increasing chl a with increasing N in all three experiments, the most

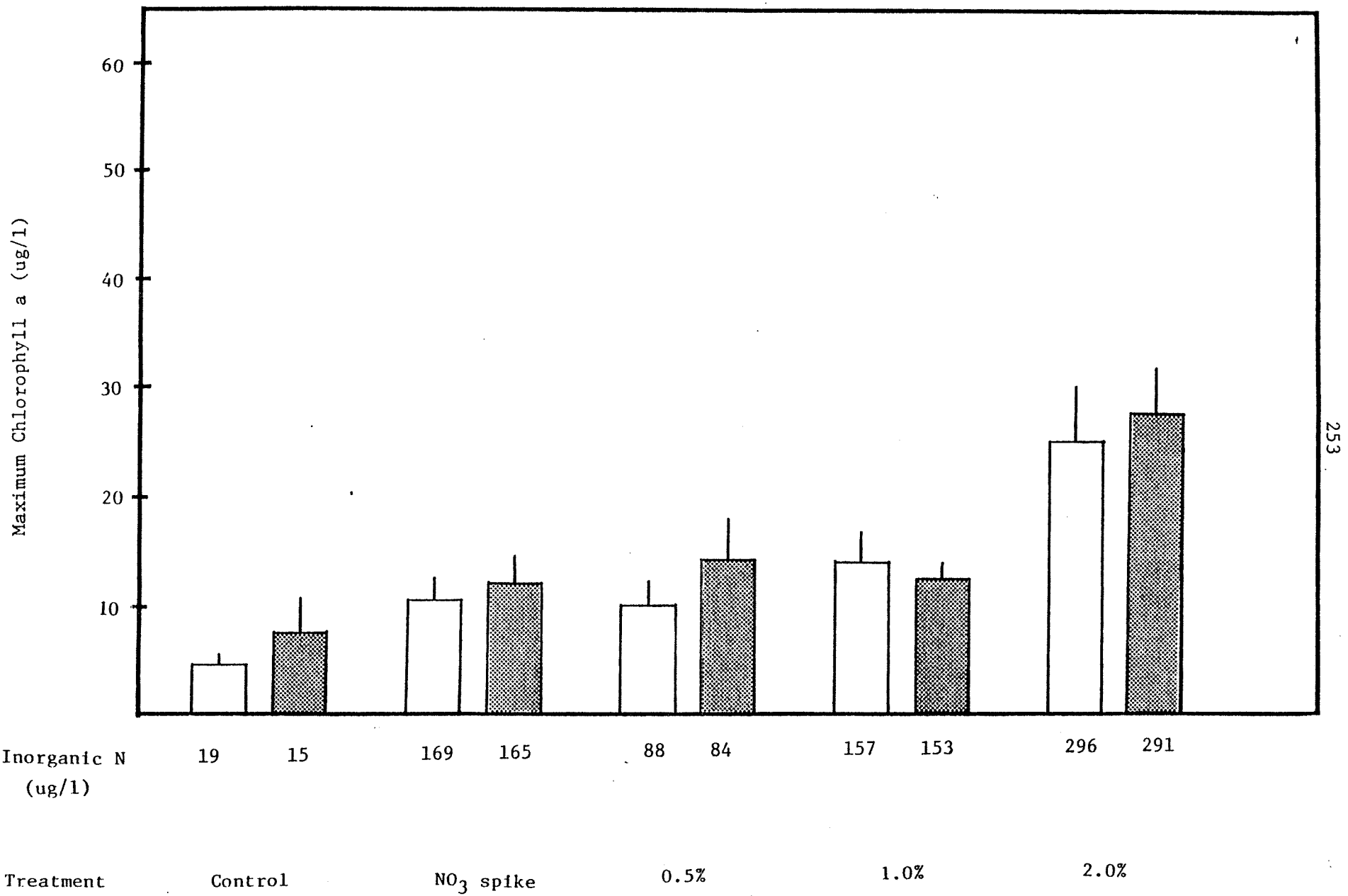

Figure 4A.2. Bioassay conducted 14 June - 21 June 1983. See description for Figure 1.

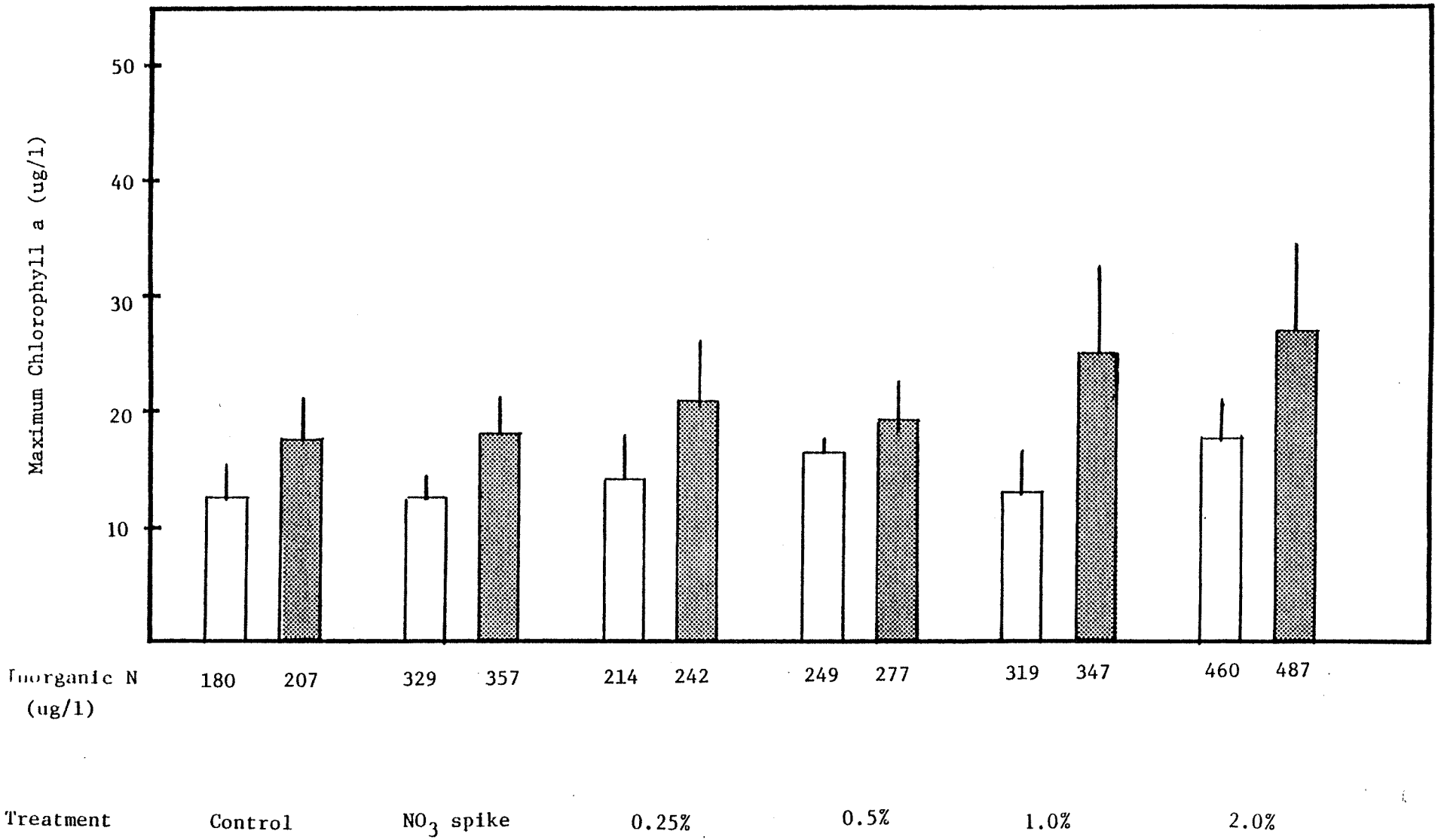

Figure 4A.3. Bioassay conducted 19 July - 25 July 1983. See description for Figure 1.

Table 4A.1. Maximum chl *a* in µg l^{-1} (SD) in bioassays conducted during 1983 using *Skeletonema costatum* (*Gymnodinium* in Aug. assay) in water, from stations in Puget Sound with % effluent and NO_3 additions.

	Control	0.25%	0.5%	0.7%	1%	2%	3%	NO_3	[NO_3-add]
					Station 10				
19-26 April	21.9 (7.03)				29.1 (7.07)		44.3 (13.16)	19.8 (5.84)	50 µg l^{-1}
10-18 May	5.0 (0.91)				11.3 (2.29)		11.6 (2.47)	10.1 (3.68)	500 µg l^{-1}
24-30 May	8.9 (0.80)		11.3 (1.55)	11.92 (1.31)	10.90 (3.09)	19.6 (11.63)		12.0 (2.55)	150 µg l^{-1}
14-21 June	4.5 (0.99)		10.0 (2.10)		13.9 (2.91)	24.9 (5.21)		10.6 (1.94)	150 µg l^{-1}
6-14 July	27.8 (6.05)	25.5 (8.98)	34.2 (9.17)		40.7 (5.04)	56.0 (23.97)		28.3 (4.58)	150 µg l^{-1}
19-25 July	12.4 (2.65)	14.2 (3.53)	16.3 (1.16)		12.8 (3.68)	17.8 (3.41)		12.4 (1.70)	150 µg l^{-1}
1-10 Aug.	24.8 (3.51)	22.7 (11.18)	36.6 (4.22)		43.6 (9.60)	63.7 (3.82)		37.8 (11.73)	150 µg l^{-1}
					Station 4				
19-26 April	19.6 (6.48)				26.2 (2.71)		30.6 (4.02)	13.0 (3.18)	50 µg l^{-1}
10-18 May	5.9 (0.38)				8.5 (0.81)		12.0 (3.13)		
24-30 May	4.6 (0.21)		8.4 (3.10)	10.7 (2.82)	7.2 (1.59)	16.6 (9.27)		6.4 (2.02)	150 µg l^{-1}
14-21 June	8.8 (1.97)		14.3 (1.82)		12.2 (1.00)	27.7 (4.06)		12.1 (2.31)	150 µg l^{-1}
6-14 July	12.4 (2.65)	24.9 (8.70)			27.2 (4.89)	42.3 (17.92)		27.1 (9.12)	150 µg l^{-1}
19-25 July	17.5 (3.51)	20.7 (5.37)	18.6 (4.04)		25.1 (7.23)	26.7 (7.84)		18.1 (2.96)	150 µg l^{-1}
1-10 Aug.	32.1 (6.35)	24.9 (13.76)	22.7 (12.13)		38.8 (25.08)	55.3 (9.44)		39.1 (10.41)	150 µg l^{-1}

Table 4A.2. Initial inorganic N ($\mu g\ l^{-1}$) concentrations in seven bioassays conducted during 1983 with % effluent and NO_3 additions.

	Control	0.25%	0.5%	0.7%	1%	2%	3%	NO_3
Station 10								
1) 19 April	227				374		667	277
2) 10 May	31				167		440	531
3) 24 May	157		227	251	297	442		307
4) 14 June	19		88		157	296		169
5) 6 July	72	115	157		242	412		222
6) 19 July	179	214	249		319	460		329
7) 1 Aug	164	208	252		341	519		314
Station 4								
1) 19 April	220				366		659	270
2) 10 May	74				211		484	574
3) 24 May	143		213	237	283	428		293
4) 14 June	15		84		153	291		165
5) 6 July	90	133	175		260	430		240
6) 19 July	207	242	277		347	487		357
7) 1 Aug	191	235	280		369	546		341

consistent trend is in Figure 4A.2, which shows results when ambient N was at the lowest observed concentration. Station 4 water with 0.5% effluent, and the controls, attained more chl a than expected from the N apparently available.

In some instances NO_3 addition produced less chl a than did similar quantities of NO_3 (as NH_4) in sewage effluent (1% in Figures 4A.2 and 4A.3). However, because of variability between replicates, the difference is not significant. On eight occasions, flasks with the NO_3 addition had similar initial N concentrations as those with sewage effluent addition. The mean N contents for the standard additions and sewage effluent additions were 260 $\pm$ 72 and 257 $\pm$ 71 ug l^{-1} (1.86 and 1.84 ug-at l^{-1}), respectively, while the mean chl a yields were 15.9 $\pm$ 8 and 18.8 $\pm$ 11 ug l^{-1} (1.1 and 1.3 ug-at l^{-1}), respectively. From these results, the organics, trace elements or other substances in treated effluent are apparently neither stimulatory nor inhibitory to Skeletonema, which is an abundant diatom species in Puget soudn. Effluent collected prior to dechlorination was markedly inhibitory, producing a biomass decrease at 3% and reduced growth at 1% effluent (Table 4A.2).

To evaluate how closely the maximum yield of chl a was related to the initial concentration of N available, all data were plotted together in Figure 4A.4. Except for the 10 high chl a values from the July 6 bioassay (large circles) the remaining data points conform reasonably well to the least squares regression shown ($r = 0.55$). That regression line represents a yield ratio of 1 ug chl a per 30 ug N available. That yield ratio is similar to the ratio of chl a to particulate N contained in fast growing S. costatum cells cultured in chemostats by Conway (1973) and therefore may indicate that yield in these experiments was optimum for the N available. This is corroborated by observations of N content in culture flasks which showed that N was

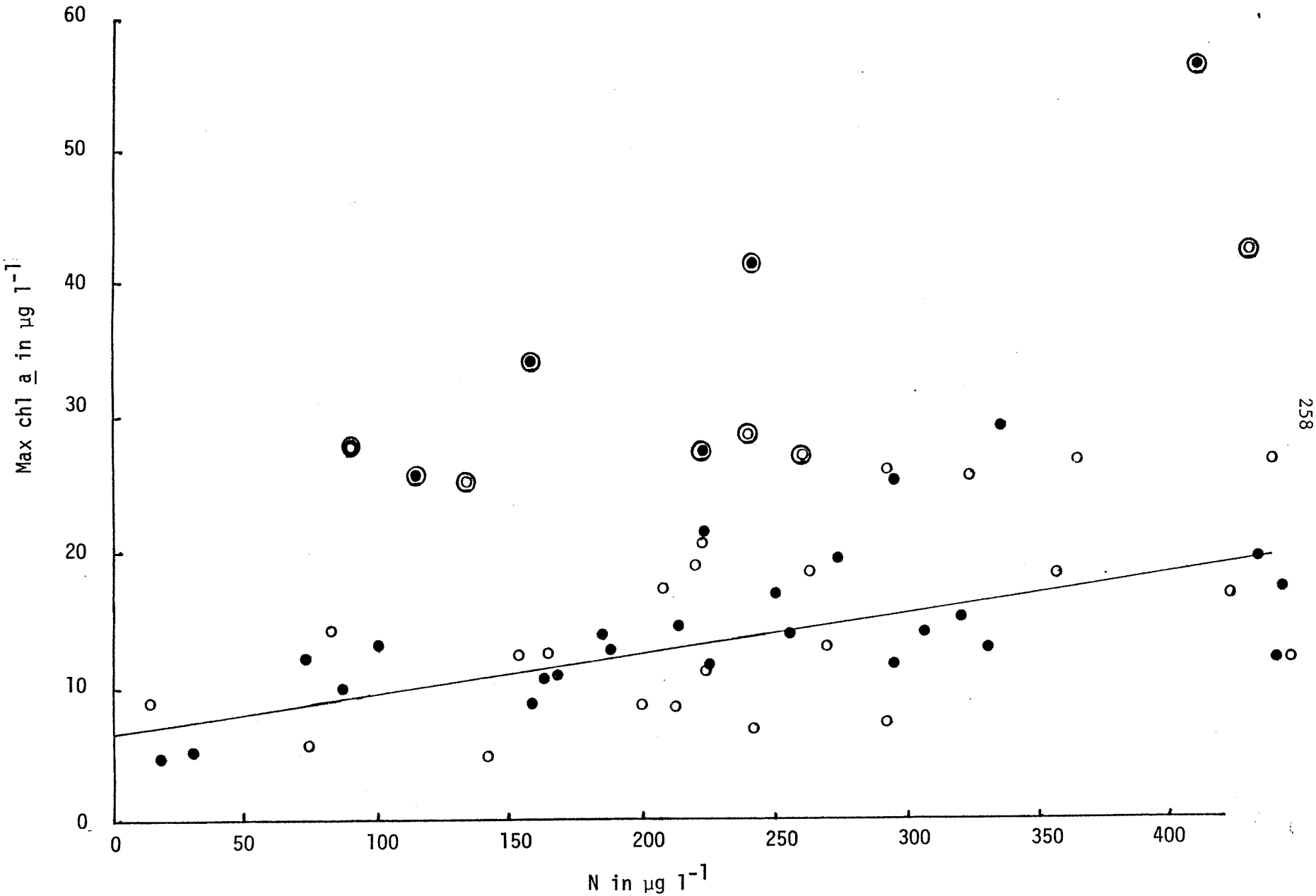

Figure 4A.4. Maximum chl a versus initial N content is all samples except 3 where P could have limited growth (see text). Line is the best least squares fit for data except the 10 highest chl a values (large circles). Equation for calculated line is chl a = 6.96 + 0.03 N and r = 0.55. Closed

efficiently depleted during the six-day experiments (Figure 4A.5).

P could have been limiting only in the control or NO_3 spiked samples at N concentrations over about 500 ug l^{-1} (e.g., 3% effluent in Figure 4A.1). The high concentrations of P in effluent (N:P = 3.1) precluded the possibility of P limitation in the other samples. There were 3 samples where P may have been limiting and these were eliminated from Figure 4A.4.

The high yields of chl a per unit N (10 large circles in Figure 4A.4) are difficult to explain. Conway (1973) found Chl a: particulate N ratios greater than 1/10 in slow growing S. costatum. The July cultures were the fastest growing (mean 0.074 $\pm$0.01 hr^{-1}) of all the experiments (Table 4A.3) and they also showed the highest yield ratio. The high yield ratio was a result of average chl a in that experiment being double that from all other experiments (31.5 $\pm$11 ug l^{-1} versus 15.4 $\pm$ 4 ug l^{-1}). A difference in growth rates is consistent with the distinctly different yields.

The high yields of chl a per unit N added and the high growth rates in the July 6 experiments may indicate an effect of dissolved constituents in the water other than N. Ambient chl a levels were low in the July 6 samples, following the bloom, which may indicate that inhibitory metabolites were also low.

A reasonably good correlation exists between chl a and N (r = 0.55) if the July 6 points, and the three where P could have been limiting are excluded, although the line does not go through the origin. Nevertheless, the relationship illustrates the dependence of phytoplankton biomass on nitrogen concentration in Puget Sound waters regardless of the source of N (i.e., from sewage as ammonia, ambient water or added as NO_3).

4A.3.3 Growth Rate

Although the data on chl a yield show the significance of N as a limiting

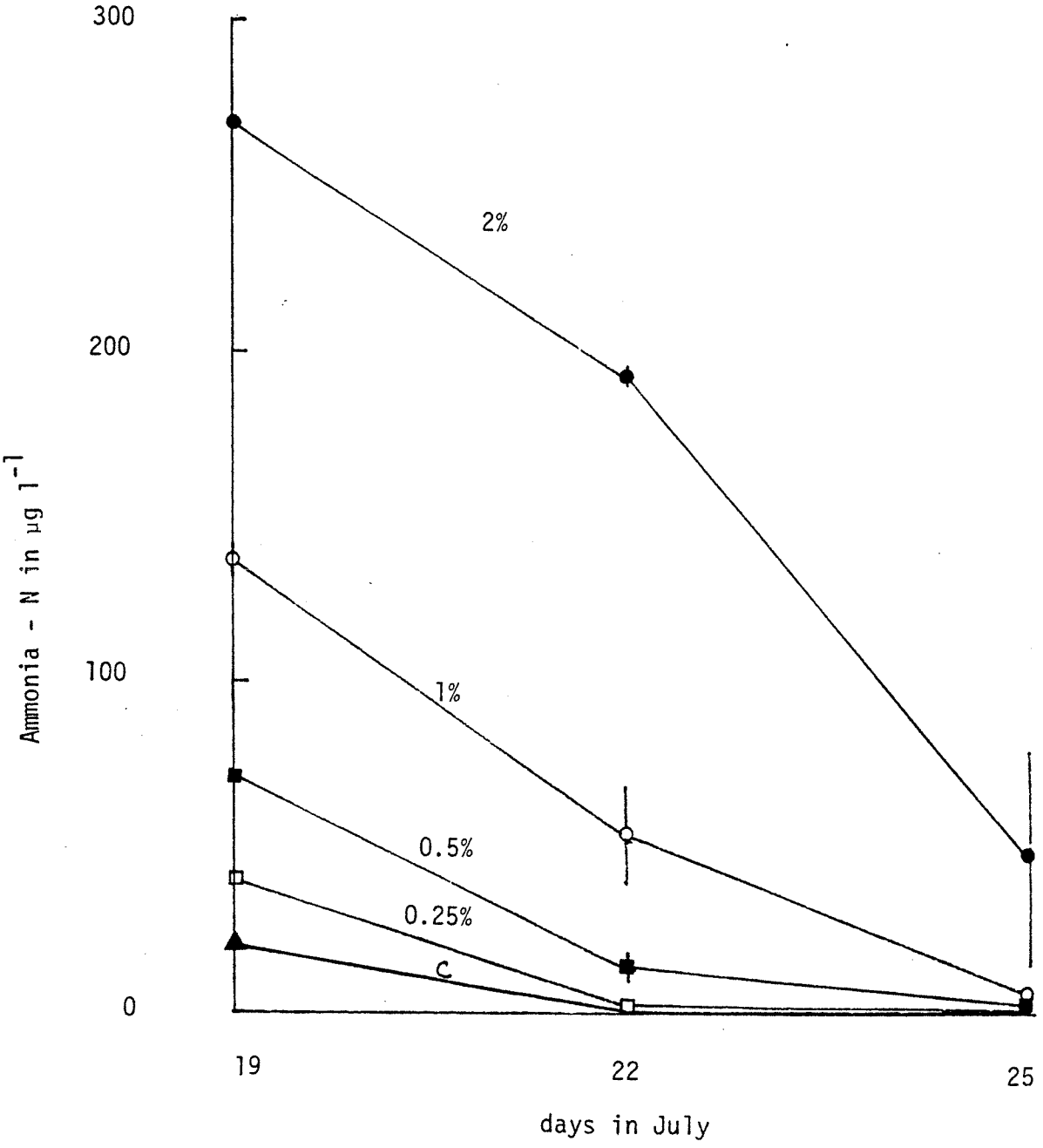

Figure 4A.5. Depletion of ammonia - N during a six-day bioassay using Skeletonema beginning July 19, 1983 (from same bioassay as Figure 3). Ambient ammonia - N concentrations were 11 and 13 µg l^{-1} at station 10 and 4, respectively; effluent contained 14,270 µg l^{-1}.

nutrient compared with other nutrients, the actual concentrations of chl *a* represent a potential biomass, not an absolute estimate of the level that would result from increased nitrogen in Puget Sound. The loss factors of grazing, sinking and advection reduce the population to a level below the potential biomass yield, even if all the limiting nutrient is utilized. The other important factor preventing the nutrient from being completely utilized is light, which limits phytoplankton growth much of the time, because the depth of mixing frequently exceeds the critical depth (depth where respiration exceeds phytosynthesis). However, the limiting nutrient may be depleted to growth-limiting levels during periods of a stable water column, which increases the availability of light. At that time, increasing the content of nitrogen could increase the growth rate and result in more phytoplankton biomass, assuming that the loss rates stay constant. The time when that is most likely to occur is during a bloom when biomass is highest and nitrogen is depleted. Additional nitrogen in Puget Sound at that time might increase bloom maxima. It must be shown, however, that growth rate is reduced during blooms when low nitrogen content occurs and that growth rates could be increased by raising the nutrient concentration in experimental cultures.

Results of analyses of growth rates, taken as the maxium slope of the chl *a*-time relationship, showed that *S. costatum* grew at an expected rate in these experiments (Table 4A.3). The means for the two stations 4 and 10 were 0.064 $\pm$0.014 and 0.063 $\pm$0.024 hr^{-1} for 1% effluent, respectively. *Skeletonema*, therefore, grew rather consistently at a rate of about 0.06 hr^{-1}. Dortch (1980) reported a range of 0.02 - 0.07 hr^{-1}. *Gymnodinium* grew at a much slower rate than *Skeletonema* (Table 4A.3).

Rates determined by the C-14 technique in 1983 averaged 0.040 $\pm$ 0.02 hr^{-1} in controls and 0.048 $\pm$0.02 hr^{-1} in 1% effluent in the first four experiments

Table 4A.3. Growth rates (μ_e in hr^{-1}) and generation times (t in hr) determined from chl a versus time plots in bioassays during 1983 using Skeletonema costatum (Gymnodinium in Aug. Assay) in water from two stations in Puget Sound with % effluent and NO_3 additions.

	Control	0.25%	0.5%	0.7%	1%	2%	3%	NO_3		
				Station 4						
19-26 April										
μ_e	0.061				0.067		0.066	0.048		
t	0.47				0.43		0.43	0.61		
10-18 May										
μ_e	0.068				0.053		0.050			
t	0.42				0.55		0.58			
24-30 MAY										
μ_e	0.059		0.063	0.069	0.062	0.066		0.063		
t	0.49		0.46	0.42	0.47	0.44		0.46		
14-21 June										
μ_e	0.042		0.059		0.045	0.058		0.043		
t	0.69		0.49		0.64	0.50		0.67		
6-14 July										
μ_e	0.065		0.071		0.074	0.070		0.066		
t	0.44		0.41		0.39	0.41		0.43		
19-25 July										
μ_e	0.076	0.080	0.078		0.083	0.080		0.078		
t	0.38	0.36	0.37		0.35	0.36		0.37		

1-10 Aug										
μ_e	0.034	0.047	0.025		0.026	0.034		0.033		
t	0.84	0.61	1.15		1.12	0.84		0.86		
				Station 10						
19-26 April										
μ_e (hr^{-1})	0.061				0.067		0.067	0.057		
T(hr)	0.47				0.43		0.43	0.51		
									- Cl_2 -	
									3%	1%
10-18 May										
μ_e	0.049				0.054		0.051	0.049	-0.030	0.046
T	0.59				0.53		0.57	0.59	-1.47	0.63
24-30 May										
μ_e	0.050		0.057	0.057	0.068	0.064		0.057		
T	0.58		0.51	0.51	0.42	0.45		0.50		
14-21 June										
μ_e	0.037		0.058		0.021	0.053		0.050		
T	0.78		0.50		0.59	0.55		0.58		
6-14 July										
μ_e	0.077	0.077	0.081		0.082	0.077		0.076		
T	0.38	0.37	0.36		0.35	0.37		0.38		
19-25 July										
μ_e	0.070	0.079	0.078		0.085	0.078		0.076		
T	0.42	0.37	0.37		0.34	0.37		0.38		

1-10 Aug										
μ_e	0.031	0.028	0.032		0.034	0.038		0.028		
T	0.94	1.04	0.88		0.84	0.76		1.03		

at both stations. Chl a determined rates for comparable experiments averaged 0.053 $\pm$0.01 hr^{-1} in controls and 0.055 $\pm$0.02 hr^{-1} in 1% effluent (Table 4A.3). Rates determined by chl a were higher than C^{-14} rates but were similarly consistent.

The lowest chl a growth rate determined in 1983 in the controls averaged 0.04 hr^{-1} and for the two stations occurred coincident with the lowest ambient N content (15 ug l^{-1}, 1.1 ug-at l^{-1}). Rates using C^{-14} for that date in the control were not the lowest, however. Furthermore, the chl a rates in the controls were not that different from other rates on that date with effluent or N added. In fact, differences in growth rates were greater among sampling dates than with enrichment level. The average of growth rates for Skeletonema at all N concentrations for that sample period (June 14-21) was less than for other periods. This was not true for C^{-14} determined rates, however. Thus, these data do not show any consistent and significant decrease in growth rate at low N concentrations in Puget Sound waters.

4A.3.4 Nutrient Limitation Summary

Neither bioassay results or field observations indicate that nitrogen limited growth rate existed in the Seahurst area in 1983. Although nitrate-N persisted at low levels (between 2 and 5 ug l^{-1}) for two to three weeks in June, ammonia-N content was approximately 5-10 ug l^{-1} (0.36-0.71 ug-at l^{-1}). Thus, the bioassay conducted with water collected June 14, during minimum ambient nitrate, (see Appendix Figures) showed no significant stimulation of Skeletonema growth rate with ammonia-N increases above the 15 ug l^{-1} (1.1 ug-at l^{-1}) ambient level of N and specific productivity (mg C mg chl^{-1} l^{-1}) in the water column was high. Although field observations of chl a showed minimum values on July 6 following the nitrate minimum (see Appendix Figures), Skeletonema grew satisfactorily in filtered water from that date (July 6) at

all nitrogen concentrations. The yield in chl a per unit N utilized in that assay was double that of any other experiment. There were, however, observations of low chl a content on other dates during the productive period in June and July when nitrate was relatively abundant, suggesting that other factors (hydrographic) were important.

The fact that bioassays did not indicate nitrogen limitation of growth rate, and specific productivity was relatively high when nitrate was at a minimum, supports the theory that nutrients do not limit phytoplankton growth in Puget Sound. These observations indicate that the growth rate of the phytoplankton (such as Skeletonema) is probably saturated at very low N concentrations and therefore added N would not be expected to increase growth rate and biomass. However, these results are inconsistent with values reported by Eppley et al. (1969). They determined Michaelis-Menten half saturation constants for S. costatum that averaged 24 ug l^{-1} (1.7 ug-at l^{-1}) ammonia. At that concentration the growth rate should be one-half the maximum and at 216 ug l^{-1} (15.4 ug-at l^{-1}) the growth rate should be 90% of the maximum. Yet, in the experiments reported here the growth rate was not less at ambient than at enriched concentrations even when the ambient level was as low as 15 ug l^{-1} (1.1 ug-at l^{-1}), which is less than the reported half saturation constant. Results from growth kinetics experiments are quite variable (95% confidence for the above half-saturation constants averaged greater than $\pm$50%). The data base from the experiments reported here is probably insufficient to convincingly document an effect of ammonia change on growth rate at such low concentrations. Nutrient concentration changes might cause changes in species composition, however. For example, Eppley et al. (1969) reported a half saturation constant of 77 ug l^{-1} (5.5 ug-at l^{-1}) for Gonyaulax polyedra. Species with high half-saturation constants could be

favored at increased ammonia concentrations. Such an effect would not be detected by studying one species only. Results reported here using Gymnodinium simplex did not show an effect on growth rate from changes in ammonia content.

4A.4 Summary

4A.4.1 N was determined to be the limiting nutrient for phytoplankton growth in Puget Sound. This was shown by a direct relationship between initial N available and maximum chl a attained as well as a low ambient ratio of N:P (3.3).

4A.4.2 Variability in the relationship between N and chl a was thought to be due to substances, possibly excretory metabolites from phytoplankton, in Puget Sound water rather than due to organics, trace elements or other stimulants/inhibitors in treated effluent. This effect was particularly evident in the July 6 experiment when chl a yield per N added was double the yield from other dates, growth rate was higher and ambient phytoplankton concentration was low.

4A.4.3 Skeletonema grew at an expected rate and was consistent in unialgal cultures in 1983. The chl a determined growth rate in control samples at the time of lowest ambient N content was about two thirds that of experimental rates, suggesting growth-rate limitation. However, this was not the case for C-14 determined rates. Although lower growth rates may have been expected based on published growth kinetic values, the data may be too few to detect such an effect. Differences in growth rate were greater among sampling dates than with enrichment level.

4A.4.4 From field observations of specific productivity and chl a and from

bioassay results, phytoplankton growth rate was not shown to be limited at minimum ambient nitrogen concentrations and, therefore, added ammonia from effluent at those critical times would probably not lead to increased biomass. However, this is based on results with S. costatum and does not preclude the possibility of a selection for species with high nitrogen requirements in the event of increased concentrations of ammonia.

4A.5 REFERENCES

Conway, H. L. 1973. The uptake and assimilation of inorganic nitrogen by Skeletonema costatum (Grev.) Cleve. Ph.D. Dissertation, Univ. of Washington, 125 pp.

Dortch, F. Q. 1980. Nitrate and ammonium uptake and assimilation in three marine diatoms. Ph.D. Dissertation, Dept. of Oceanrg., Univ. of Washington.

Ehlers, H. R. 1983. Nitrogen limitation bioassays: An assessment of a proposed marine outfall. Paper for MSE, Dept. of Civil Engineering, University of Washington, 84 pp.

Eppley, R. W., R. W. Holmes, and J. D. H. Strickland. 1967. J. Mar. Biol. Ecol. 1:191-208.

Eppley, R. W., J. N. Rogers and J. J. McCarthy. 1969. Half-saturation constants for uptake of nitrate and ammonium by marine phytoplankton. Limnol. and Oceanogr. 14:912-920.

Solorzano, L. 1969. Determination of ammonia in natural waters by the phenolypochlorite method. Limnol. and Oceanogr. 14:799-801.

Strickland, J. D. H. and T. R. Parsons. 1972. A practical handbook of seawater analysis. Bull. Fish. Res. Bd. Canada, No. 167 (2nd ed.), 310 pp.

Waldichuck, M. 1983. Pollution in the Strait of Georgia: a review. Can. J. Fish Aquat. Sci. 40:1142-1167.

Appendix of water column nitrate, ammonia, chl *a* and specific productivity at Seahurst

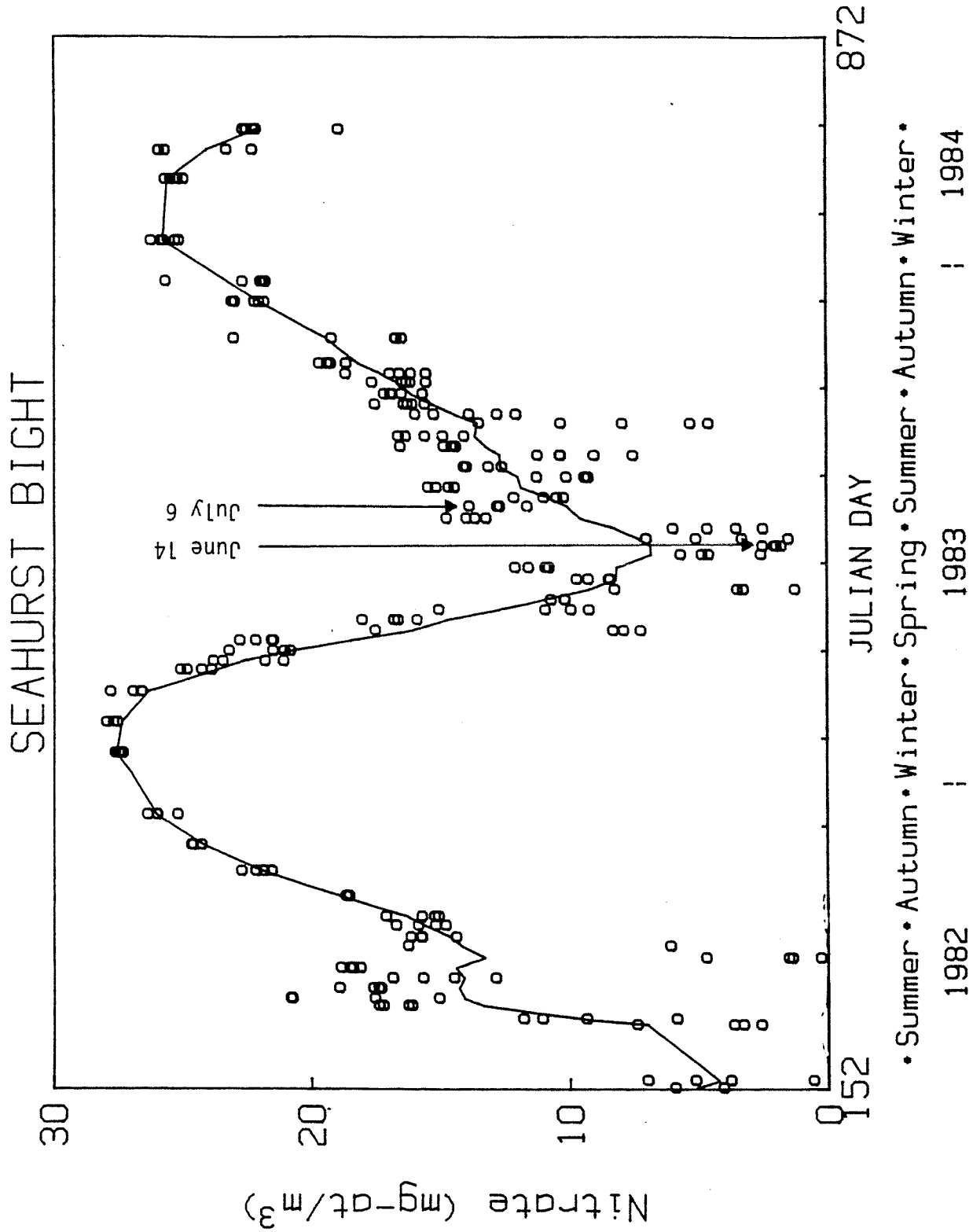
SEAHURST BIGHT
Nitrate (mg-at/m3)
30
20
10
0
152
872
JULIAN DAY
July 6
June 14
•Summer•Autumn•Winter•Spring•Summer•Autumn•Winter•
1982
1983
1984

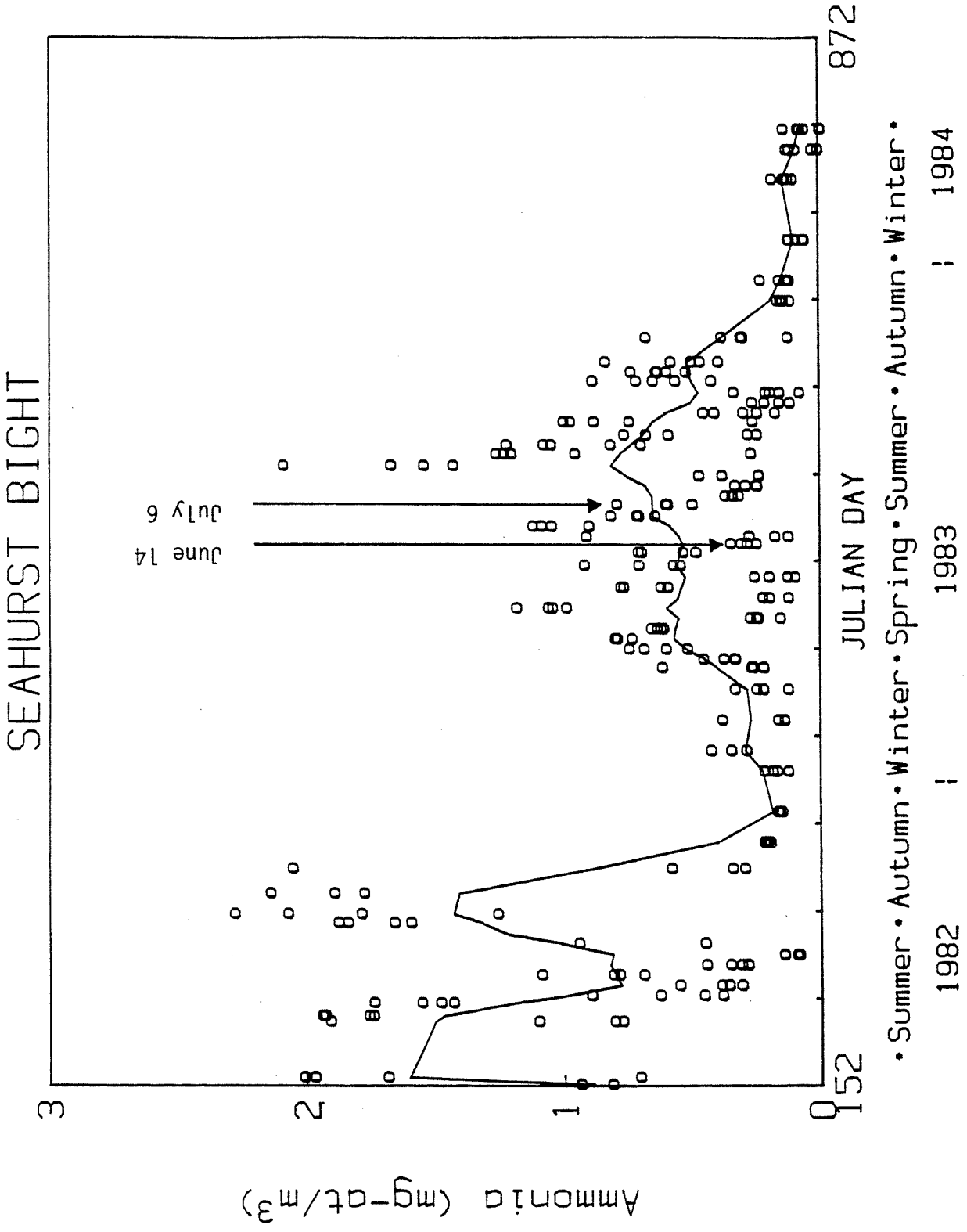
SEAHURST BIGHT
Ammonia (mg-at/m3)
3
2
1
0
152
872
JULIAN DAY
June 14
July 6
•Summer•Autumn•Winter•Spring•Summer•Autumn•Winter•
1982
1983
1984

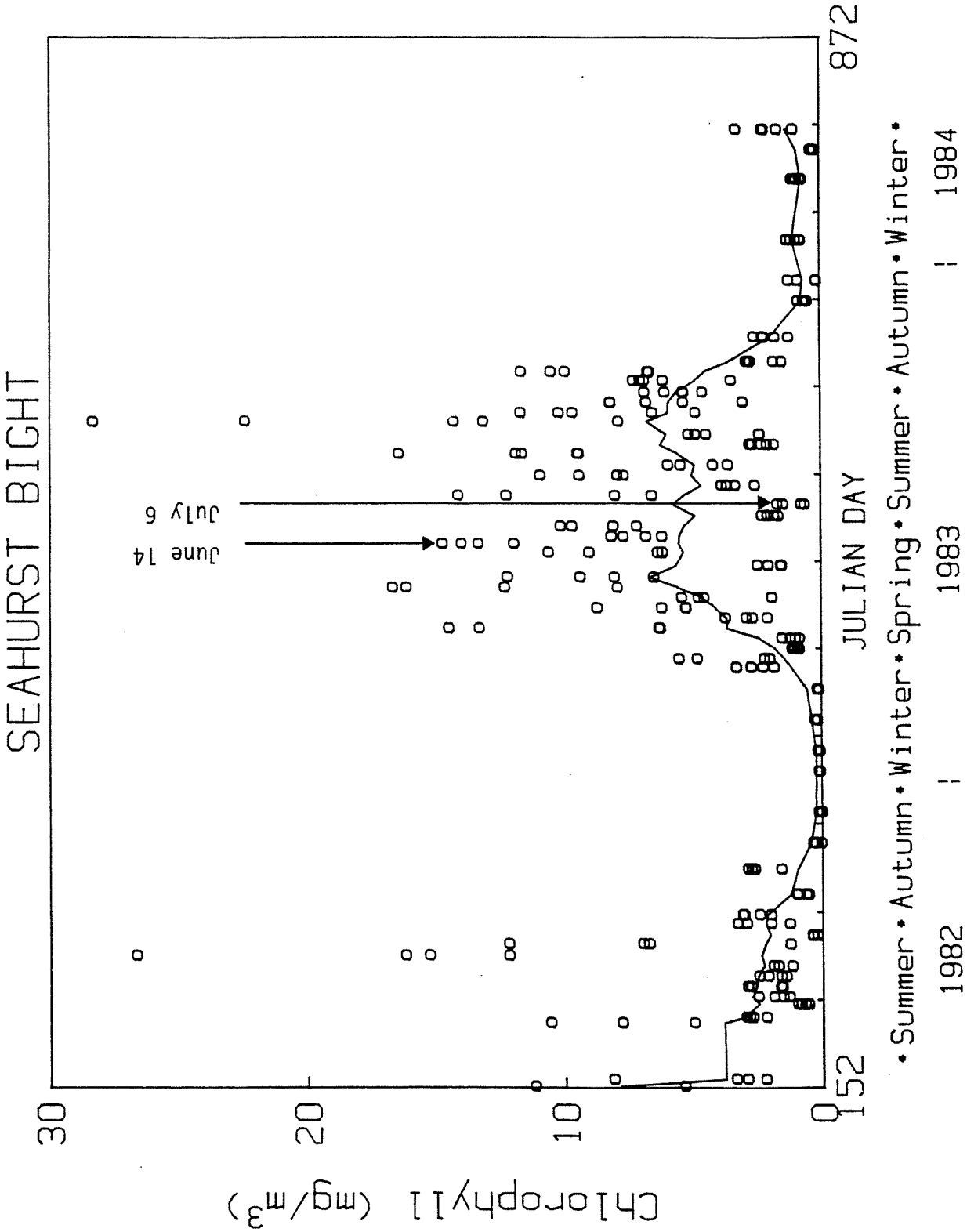
SEAHURST BIGHT
Chlorophyll (mg/m³)
30
20
10
0
152
872
JULIAN DAY
July 6
June 14
• Summer • Autumn • Winter • Spring • Summer • Autumn • Winter •
1982
1983
1984

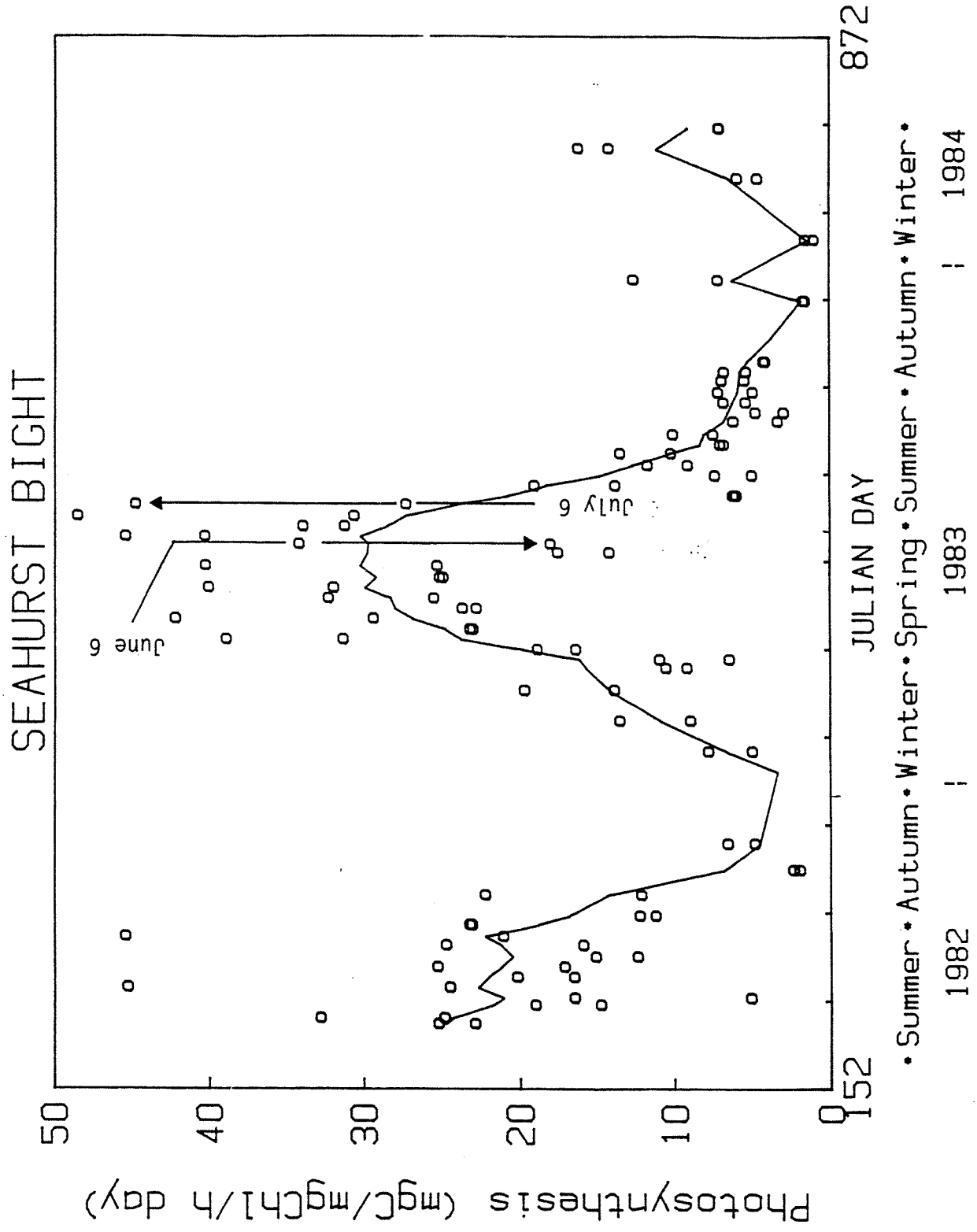
SEAHURST BIGHT
Photosynthesis (mgC/mgChl/h day)
50
40
30
20
10
0
152
872
JULIAN DAY
June 6
July 6
• Summer • Autumn • Winter • Spring • Summer • Autumn • Winter •
1982
1983
1984

Appendix 4.A

WHY LOG TRANSFORMATIONS OF POPULATION DATA HAVE NORMAL FREQUENCY DISTRIBUTIONS

by

James Jay Anderson

Fisheries Research Institute
University of Washington
Seattle, WA 98195

Submitted to
Journal of Theoretical Biology

It is common practice in biology to normalize skewed frequency distributions of population data by taking a logarithmic transformation. In this manner the variance of the transformed data is distributed symmetrically about the mean, and statistical methods requiring normal distributions can be used to compare data sets. This paper develops a model to explain why the log transformation successfully normalizes data and relates the statistical properties of the data to basic parameters of growth dynamics.

The model assumes that the rate of change of population number x over time t is described by a deterministic rate that changes in a predictable manner with population and a stochastic rate that changes randomly and accounts for the undefined and variable factors that control growth. The stochastic dynamic equation is

$$dx/dt = rxG(x/K) + fxi(t) \tag{1}$$

rate of change = deterministic rate term + stochastic rate term

The deterministic term contains an intrinsic growth rate r and a saturation inducing term G(x/K) that describes how the birth rate and the death rate change with the density of the population relative to the equlibrium level or carrying capacity K. The minimum characteristics on the saturation function are

$$G(0) = 1 \tag{2a}$$

$$G(1) = 0 \tag{2b}$$

$$dG(x/K)/dx < 0 \tag{2c}$$

Equation (2a) implies that at very low population levels the effects of density are minimum and the net growth rate approaches the maximum growth rate of an individual in the population. Equation (2b) implies that as the population approaches the carrying capacity K the birth rate and death rate balance each other so that the total population does not change. Equation (2c) implies that the net growth rate decreases in a smooth fashion as the population increases. In general the saturation effect is positive for populations below the carrying capacity and negative above the carrying capacity. The region of the function G(x/K) is illustrated in Fig. 4.A.

The stochastic term models population fluctuations caused by changes in the birth and death rate that are rapid compared to the rate of change of the population from the deterministic term. The stochastic term contains a white noise component, i(t) that rapidly fluctuates with a unit variance about a mean value of zero. The intensity of the fluctuations are quantified by f and are proportional to x. The term f has units $\text{time}^{(-1/2)}$ and f^2 is essentially a rate constant for the fluctuating processes. An important term in the model is the ratio of the stochastic and deterministic rate coefficients. This will be designated the rate variability coefficient

$$R = f^2/r \tag{3}$$

With the stochastic term eq(1) does not have an exact solution at any time and x is described by a probability density function that gives the frequency distribution of observing x. This can be determined by solving the Fokker-Planck equation or the forward Kolmogorov diffusion equation (see Goel and Richter-Dyn 1974 or Nisbet and Gurney 1982 for examples). At steady state, the probability density function is constant in time although x fluctuates between the boundaries 0 and ∞. Assuming that the population will not go to extinction then the general steady state probability density function for eq(1) is

$$P(x,\infty) = h(x)/\int h(x)dx \qquad (4a)$$

where

$$h(x) = [f^2 x^2 \exp\{-2\frac{r}{f^2}\int(G(x/K)/x^2)dx\}]^{-1} \qquad (4b)$$

Goel and Richter-Dyn (1974, p.131-143) have investigated a solution of (4) for a general form of G(x/K). A salient feature of their analysis is that the modal value is less than the average value so that the frequency distribution for a variety of forms of the saturation term are positively skewed in the same way that frequency distributions of populations are skewed.

Now the question of why population data approximates a normal distribution when log transformed can be considered in two steps. First we write the stochastic differential that has a normal probability density function and second we determine under what conditions of G(x/K) a log transform of eq(1) approximates the equation.

The appropriate stochastic differential equation with a normal probability distribution defines what is known as the Ornstein-Uhlenbeck process (Uhlenbeck and Ornstein 1930) and can be written

$$dz/dt = - rz + fi(t) \tag{5}$$

When the process is unrestricted so $-\infty < z < \infty$ then the probability distribution of z is the normal distribution

$$P(z,\infty) = (\pi R)^{(-.5)} \exp(-z^2/R) \tag{6}$$

where R is the rate variability coefficient of eq(3).

To show how the log transform of eq(1) can be approximated by eq(5) note that dx/x = dlnx = dln(x/K). Then with z = ln(x/K) so that x/K = exp(z) eq(1) is transformed to

$$dz/dt = rG(\exp(z)) + fi(t) \tag{7}$$

The success of the transform approximating a normal distribution is determined by how well eq(7) is approximated by eq(5) and this depends on G. The approximation is exact if

$$G(\exp(z)) = - z \tag{8a}$$

which can also be expressed

$$G(x/K) = - \ln(x/K) \tag{8b}$$

The position of $-\ln(x/K)$ in the allowable region of $G(x/K)$ is illustrated in Fig4.A. The important feature is that the approximation is very close for a population near the carrying capacity where $x/K = 1$. For populations much smaller than K, so $x/K \ll 1$, the log function is a poor approximation of G. In a qualitative sense this analysis suggests that any population which fluctuates about its carrying capacity or equlibrium will have an approximate normal probability distribution when the data is log transformed.

The carrying capacity and rate variability coefficient can be estimated without knowning the form of G if the log transform approximates a lognormal distribution. To illustrate this note that $z = \ln(x/K) = \ln(x) - \ln(K)$. Then the normal distribution can be written

$$P(y\text{-}yo,\infty) = (\pi R)^{(-.5)} \exp(-(\ln(x)-\ln(K))^2/R) \qquad (9)$$

Putting eq(9) into the standard form of a normal distribution then $\ln(K)$ is the distribution expected value and the variance is 2R. The carrying capacity and rate variability coefficient are thus defined

$$K = \exp(E\{\ln(x)\}) \qquad (10a)$$

$$R = 2\mathrm{Var}\{\ln(x)\} \qquad (10b)$$

When eq(8) holds the exact probability function of x is the lognormal distribution. Thus the mode of the x can be approximated with the lognormal distribution giving

$$xm = K \exp(-R/2) \qquad (11)$$

This analysis shows that when a population is fluctuating about its equlibrium or carrying capacity a log transform of the data should have a frequency distribution that is approximately normal. The closeness of the approximation is dependent on 1) the rate of the fluctuations being linear with the population level, and 2) the saturation function being similar to a log function near $x/K = 1$. Under these conditions the population dynamics can be described by two very basic parameters: the equilibrium level K and the ratio of random and deterministic rates R. Since K and R are independent of the form of the growth equation their values can be estimated by the statistics of the log transformation.

To evaluate the suitability of the log transformation the estimations of K, R and xm can be compared to estimations using a better approximation of G. The simplest improvement on eq(8) is a linear saturation function of the form

$$G(x/K) = 1 - x/K \qquad (12)$$

Equation (12) was first proposed by Verhulst (1845) in what is known as the logistic growth equation. It satisfies eq(2) and defines the center of the region of G(x/K) (Fig.4.A) The steady state probability density function of eq(1) with G defined by eq(12) is the standard gamma density function (Goel and Richter-Dyn 1974)

$$P(x,) = \frac{(x/a)^{(b-1)}}{a\Gamma(b)} \exp(-x/a) \tag{13}$$

where $\Gamma(b)$ is the gamma function, the scale parameter is $a = KR$ and the shape parameter is $b = 2/R$. From the method of matching moments the expected value and variance of the gamma distribution are $E\{x\} = ab$ and $Var\{x\} = a^2b$. The model parameters can be estimated

$$K = E\{x\} \tag{14a}$$

$$R = \frac{2Var\{x\}}{E(x)^2} \tag{14b}$$

The mode of the distribution is

$$xm = K(1-R) \tag{15}$$

If the probability boundary conditions are set at $-\infty$ and $+\infty$ the gamma shape parameter would become $b = 2/R-1$. In this case the carrying capacity is related to both the mean and the variance. This second formulation has been discussed by May (1974). It is not used in this paper because it allows for negative populations and the results are not in agreement with the results of the log transform method.

Estimates of K, R and xm from the gamma and log transform methods are compared for phytoplankton data in Table 4a Biomass measured as chlorophyll was collected on a nearly daily basis from an intertidal zone in a Puget Sound (Seahurst Park Beach). In general the log method gives lower estimates of the carrying capacity and higher estimates of

the mode of the distribution. The gamma method sometimes gives negative mode estimates that are the result of inaccurate estimates of R. Using an optimal unbiased inference procedure of Engelhardt and Bain (1978) more accurate estimates of the R and the confidence intervals about the parameters can be obtained. For this set of data the chi square fit of the transformed data to the normal distribution is better than the fit of the untransformed data to the gamma distribution.

The log transformation has been commonly used in analysis of biological data for more than 50 years (Bartlett 1935, Barns 1952) although the underlying meaning of the transform has not been precisely defined in terms of growth dynamics. Using a general stochastic growth model, the mean and variance of the log transformed data can be related to general growth parameters; the carrying capacity K and a rate variability coefficient R. The assumed underlying distribution in the log transform method is the lognormal distribution. This is compared to a second model based on a logistic equation which yields a gamma probability distribution. The models yield similar estimates of R and K but unless special procedures are taken to estimate the gamma parameters the lognormal distribution and the log transform method provide a better fit to the data and more realistic parameter estimates.

Recently a number of papers have suggested that the gamma distribution provides a general model of population data (Dennis and Patil 1984; Costantino and Desharnais 1981; May 1974). The models have an indeterminancy in the type of calculus that is appropriate to describe

the variability. Depending on the calculus (Ito or Stratonovich) a population may or may not have a steady state probability density function. The choice also determines how K and R are related to the mean and variance. The log transform avoids this problem since the stochastic term is independent of x so that both types of calculus yield the same stochastic differential equation.

The log transform method, because of the boundary conditions of eq(5), implies that x is confined in the region $0 < x < \infty$. Thus the probability of extinction can not be investigated.

In general the log transform method provides the simplest estimates of the two basic population parameters, K and R and since it is an approximation it is essentially independent of the form of the saturation function that maintains a population about its carrying capacity. Other models may provide better estimates of the confidence intervals about K and R but as with the gamma model the estimations of model parameters may require more complicated procedures.

ACKNOWLEDGMENTS

This work was supported by Municipality of Metropolitan Seattle contract "Renton Sewage Treatment Plant Project: Seahurst Baseline Study," and is Contribution No. ___ from the School of Fisheries, University of Washington, Seattle, WA 98195.

Table 4.A R, K and xm estimated by log transform and gamma statistics. Data grouped in summer (June 21-Sept 21) and winter (Dec 21-March 21) for years 1982 through 1984. K and xm in mg chl/m^3. R is dimensionless, Chi Sq and DF designate chi square goodness of fit test and degrees of freedom.

Method	Parameter	Eq. no.	Summer 82	Winter 82-83	Summer 83	Winter 83-84
log	K	10a	3.6	0.6	6.3	0.1
gamma	K	14a	5.2	0.8	7.5	0.1
log	R	10b	1.3	1.3	0.7	0.3
gamma	R	14b	2.7	1.4	0.7	0.2
log	xm	11	1.8	0.3	4.4	0.09
gamma	xm	15	-8.6	-0.2	2.2	0.07
log	Chi Sq		21.9	12	8	2.6
	(DF)		(15)	(13)	(10)	(3)
gamma	Chi Sq		13	13	26	6.5
	(DF)		(15)	(7)	(14)	(5)
number of data points			54	33	41	13

LITERATURE CITED

Barnes, H. 1952. The use of transformations in Marine Biological Statistics. J. Cons. Explor. Mer. 18:61-71.

Bartlett, M.S. 1935. The use of transformations. Biometrics, 3:39-53.

Costantino, R.F. and R.A. Desharnais. 1981. Gamma distributions of adult numbers for 'Tribolium' populations in the region of their steady state. J. of Anim. Ecol. 50:667-681.

Dennis, B. and G.P. Patil. 1984. The gamma distribution and weighted multimodal gamma distributuions as models of population abundance. Math. Bioscience 68:187-212.

Englhardt, M. and L.J. Bain. 1978. Construction of optimal unbiased inference procedures for the parameters of the gamma distribution. Technometrics 20:485-489.

Goel, N.S. and N. Richter-Dyn. 1974. Stochastic Models in Biology. Academic Press, New York. 269 pp.

May, R.M. 1974. Randomly fluctuating environments. Pages 109-139 in R. M. May (ed.). Stability and Complexity in Model Ecosystems. Monographs in Population Biology No. 6. Princeton, New Jersey. Second Edition.

Nisbet, R.M. and W.S.C. Gurney. 1982. Modelling Fluctuating Populations. Wiley and Sons, Chichester. 379 pp.

Uhlenbeck, G.E. and L.S. Ornstein. 1930. On the theory of Brownian motion. Phy. Rev. 36:823-841.

Verhulst, P.F. 1845. Recherches mathematiques sur la loi d'accroissement de la population. Mem. Acad. Roy. Belg. 18:1-38.

FIGURE CAPTION

Figure 4.A. Saturation function G(x/K) in relation to population x normalized to carrying capacity K. Unlined areas depict allowable region of function. Saturation function for lognormal distribution designated log. Saturation function for gamma distribution designated gamma.

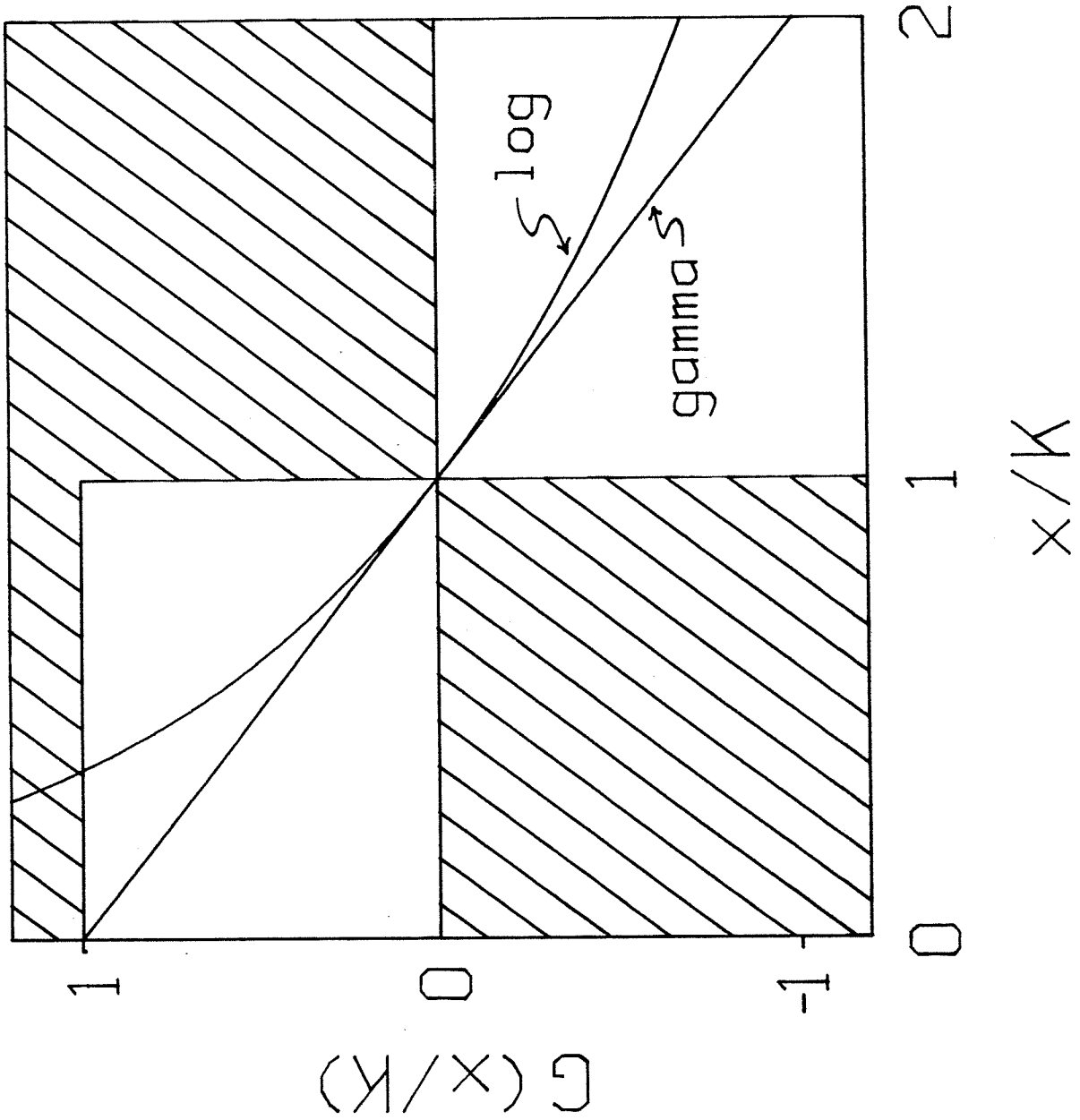
G (x/K)
1
0
-1
0
1
2
x/K
log
gamma

Appendix 4.B

Abstract of paper given at the Ocean Sciences Meeting
January 23-27, 1984, New Orleans, Louisiana

Zooplankton Probability Distributions: Everything is Coming Up Gamma

JAMES JAY ANDERSON, (School of Fisheries,
University of Washington, Seattle Wa. 98195)
AKIRA OKUBO (Marine Sciences Research Center,
State University of New York, Stony Brook
N.Y. 11974)

Zooplankton are not distributed uniformly random over time or space. Often the standard deviation is of the same order as the mean value, and a histogram frequency distribution is skewed positively. Ecologists often take the log of data to obtain a symmetrical frequency distribution which can then be analyzed using normal statistics. Our approach is to analyze data with a skewed frequency distribution; the gamma probability function that is obtained from the stochastic equation, $dx/dt = ax - bx^2 + c(t)x$, where x is zooplankton abundance, a and b are determinisitic parameters, and c(t) is a random parameter. Over short time intervals zooplankton distributions may be controlled by swarming dynamics therefore a and b can be interpreted as swarm fission and encounter rates. Over long time intervals growth dynamics are also important and the parameters might be interpreted as growth and mortality rates. In both models c(t) accounts for the undefined variability in the rates. These models suggest that probability distributions of zooplankton abundance should be similar in both the short term, where variability from swarming is important, and the long term where growth dynamics are important. To support this conclusion we compare zooplankton dry weight observations collected in Puget Sound at weekly intervals for over one year and observations published by Maranda and Lacroix (1983) that were collected at one-half hour intervals for one week.

Appendix 4.C

THE NORMAL PROBABILITY DISTRIBUTION AND NUTRIENTS IN AQUATIC ENVIRONMENTS

by

James Jay Anderson
Fisheries Research Institute
University of Washington
Seattle, WA 98195

and

Patrick J. Sullivan
Center for Quantitative Sciences in Fisheries
University of Washington
Seattle, WA 98195

ABSTRACT

A model for the steady-state probability distribution of nutrients in aquatic environments is developed. A stochastic equation balancing mixing and uptake of a nutrient yields a normal probability distribution in which the mean and variance can change independently. Analysis of nutrient data from an intertidal zone suggests that the mean is controlled by plankton uptake while the variance is controlled by stochastic factors.

This article presents a model that describes the statistical distributions of nutrient type observations in the aquatic environment. The model is based on the stochastic differential equation

$$dx/dt = u - vx + f\ i(t) \tag{1}$$

where the concentration of property x has a rate of change dx/dt that is determined by deterministic zero and first order rate terms u and vx, and a stochastic rate term f i(t).

The zero order rate represents the difference between the input of x into the region by diffusion and advection, and a concentration independent 'in situ' rate, which is typically associated with the uptake of nutrient by phytoplankton. The expression is

$$u = wX - rB \tag{2}$$

where w is the mixing rate coefficient into the region and X is the concentration of nutrient that is mixed into the region. The uptake of nutrient is assumed to be proportional to the plankton biomass B times a rate coefficient r that may be time dependent.

The first order rate represents the loss of x from the region by mixing and any 'in situ' rate processes that are dependent on concentration. The first order term can be written

$$vx = (w + q)x \tag{3}$$

where q represents the concentration dependent rate coefficient. With this formulation the diffusion of material into and out of the region is modeled as a linear mixing process w(X-x).

The third term is a stochastic rate that represents the random variability in the process. It contains two terms. The frequency of the random processes is described by i(t) and the magnitude of the processes is described by f. The frequency term is referred to as Gaussian white noise (Goel and Richter-Dyn 1974). It fluctuates rapidly compared to the time scales defining the changes in x. The mean value of i(t) is zero and it has a unit variance. The stochastic term represents the high frequency variations in the system. For nutrient dynamics in an aquatic environment these processes are associated with tidal, wind, and eddy mixing, spatial patchiness in plankton and nutrients, and temporal variation in the uptake and release of nutrients by plankton. These processes all vary significantly on time intervals of hours and thus they can be considered as high frequency noise when compared to the seasonal rate of change of nutrients.

The probability distribution of x varying according to eq(1) can be described by the Fokker-Planck or forward probability diffusion equation of the form

$$dP/dt = -d(u-vx)P/dx + (1/2)f^2d^2P/dx^2 \qquad (4)$$

where P is the probability of x as function of time t. A description of the Fokker-Planck equation can be obtained from a number of texts

including Goel and Richter-Dyn (1974), Karlin and Taylor (1975), and Nisbet and Gurney (1982).

Boundary conditions are built into the solution by requiring that the probability is confined within the space $0 \leq x < \infty$. This implies that x will not assume negative values and x = 0 is an imposed reflecting boundary according to the classification of Goel and Richter-Dyn (1974).

Under stochastic steady state conditions u and v are constant in time and x fluctuates about a mean value E{x} and a variance Var{x}. In this condition dP/dt = 0 and with the imposed reflecting boundary eq(4) can be solved for the steady state conditions. The appropriate expression (Table 3.10 in Goel and Richter-Dyn (1974)) is

$$P(x) = \{b\ Q(X) \int_0^{\infty} (b\ Q(y))^{-1}\ dy\}^{-1} \qquad (5)$$

where $b = f^2$ and $Q(x) = \exp\{-2 \int^{x} (u-vy)/b\ dy\}$. Integrating Q(x) and completing the square $Q(x) = C \exp\{(x-m)^2/s^2\}$ where $s^2 = f^2/v$ and $m = u/v$. Integrating eq(5) the steady state probability density function is

$$P(x) = \frac{2\ \exp\{-(x/m)^2/s^2\}}{s\quad (1+\mathrm{erf}(m/s))} \qquad (6)$$

where erf( ) is the error function. The mean value of x is obtained by integrating the equation

$$E\{x\} = \int_0^{\infty} x\,P(x)\,dx = \int_0^{\infty} (x-m)P(x)dx + \int_0^{\infty} mP(x)dx \tag{7}$$

which yields

$$E\{x\} = m + G(s,m) \tag{8}$$

where

$$G(s,m) = \frac{s\,\exp\{-(m/s)^2\}}{(1 + \text{erf}\ (m/s))} \tag{9}$$

The variance is defined $\text{Var}\{x\} = E\{x^2\} - E\{x\}^2$. To obtain the square term we note $E\{x^2\} = E\{(x-m)^2\} + 2mE\{x\} - m^2$. The term $E\{(x-m)^2\}$ is

$$E\{(m-x)^2\} = \int_0^{\infty} (m-x)^2P(x)dx \tag{10}$$

Integrating by parts eq(10) becomes

$$E\{(m-x)^2\} = m\,G(s,m) + s^2/2 \tag{11}$$

Using eq(8) and (11) the variance can be expressed

$$\text{Var}\{x\} = s^2/2 - m\,G(s,m) - G(s,m)^2 \tag{12}$$

The model parameters s and m can be evaluated by iteration of the equations

$$\begin{aligned} m_{i+1} &= E\{x\} - G(s_i,m_i) \\ s_{i+1} &= (2(\text{Var}\{x\} + m\,G(s_i,m_i) + G(s_i,m_i)^2))^{.5} \end{aligned} \tag{13}$$

For the first approximation $m_1 = E\{x\}$, $s = 2\text{Var}\{x\}$.

When the coefficient of variation $Var\{x\}/E\{x\} < 0.5$ the term G9s,m) is small and the model parameters can be approximated within 90% by the relationship

$$E\{x\} = m = u/v$$
$$2\ Var\{x\} = s^2 = f^2/v \tag{14}$$

In this case the term $m/s > 1.4$ and $erf(m/s) > 0.95$ so that eq(6) can be approximated by the normal probability density function where s and m are defined by eq(14).

To consider how the mean and variance of x can change with the model parameters eq(14) is written

$$E\{x\} = \frac{wX-rB}{w+q}$$
$$Var\{x\} = \frac{f^2}{2(w+q)} \tag{15}$$

According to eq(15) the mean and variance can exhibit four patterns. The mean can change without affecting the variance through an inverse change in B. The variance can change independent of the mean by a proportional change in f. The mean and variance can move together by an inverse change in q or in an opposite manner with w, with an increase in w producing an increase in the mean and a decrease in the variance.

To demonstrate the application of the theory, the mean and variance of winter and summer nutrient observations from a marine environment are compared. The probability distributions of intertidal

concentrations of nitrate, phosphate and silicate collected from a site at Seahurst Beach on the main basin of Puget Sound (47°28'N, 122°21.5'W) are illustrated as histograms in Figure 1. The samples were collected in 6-week periods about the summer and winter solstices in 1982. The samples were frozen in plastic bottles and analyzed with a Technicon Analyzer using the methods of Strickland and Parsons (1968).

Removing high and low observations associated with excessive land runoff the histograms have normal probability distributions as supported by a chi-square goodness of fit test at the $\alpha = 0.05$ level. For all nutrients the coefficients of variation are less than 0.5 and the mean values in the winter are larger than the summer values. For nitrate and phosphate the variance increases significantly in the summer but for silicate it decreases slightly (Table 1).

In terms of the model, the increase in winter nutrient levels is best attributed to a decrease in phytoplankton biomass B, which results in a decrease in nutrient uptake. An order of magnitude decrease in phytoplankton chlorophyll biomass from summer to winter was observed, with 4.9 mg chl/m^3 about the summer solstice and 0.4 mg chl/m^3 about the winter solstice.

The increase in the variance of phosphate and nitrate associated with the decrease in the mean values could be the result of an increase in the stochastic factor f, or a decrease in the mixing parameter w. In general, biological rates increase in the summer so because an increase in q would result in a decrease in the variance this factor is

probably not important. The ratio of summer to winter variances is different for each nutrient. These differences would not be expected from w since the mixing factor should be similar for the three nutrients. Thus the changes in variance are likely the result of changes in the stochastic factors f.

In general, the model suggests that seasonal changes in the mean values of the nutrients is a result of seasonal changes in phytoplankton biomass and nutrient uptake. The seasonal changes in variance are different for each nutrient which suggests that each nutrient's stochastic factor has a unique seasonal pattern that controls the variance. The final result of the model is that nutrient histograms should be sufficiently approximated by the normal probability distribution.

In contrast to nutrients, the rate of change of plankton is determined by first and higher order rate processes (Levins 1969; Costantino and Desharnais 1981; Dennis and Patil 1984; and Anderson in review). Where steady-state nutrient probability distributions are normally distributed with a variety of possible correlations between the mean and the variance, plankton probability distributions are often positively skewed and the variance increases with the mean (Barnes 1952; Cassie 1962; O'Connell 1971). Thus the statistical properties of nutrients are fundamentally different from those of plankton. Whereas plankton distributions require special statistical methods, nutrient distributions can be described with the simple arithmetic mean and variance.

ACKNOWLEDGMENTS

This work was supported under a contract from the Municipality of Metropolitan Seattle. The nutrient samples were graciously collected by students at the Occupational Skills Center, Highline Public Schools Marine Laboratory at Seahurst Park, under the direction of Mr. Lauren Rice.

REFERENCES

Anderson, J. J. Why log transforms of population data have normal frequency distributions. Submitted to J. Theor. Biol.

Barnes, H. J. 1952. The use of transformations in marine biological statistics. J. Cons. Explor. Mer. 18:61-71.

Cassie, R. M. 1962. Frequency distribution models in ecology of plankton and other organisms. J. Anim. Ecol. 31:65-91.

Costantino, R. F. and R. A. Desharnais. 1981. Gamma distributions of adult numbers for Tribolium populations in regions of their steady states. J. Anim. Ecol. 50:667-681.

Dennis, B. and G. P. Patil. 1984. The gamma distribution and weighted multimodal gamma distributions as models of population abundance. Math. Biosci. 68:187-212.

Goel, N. S. and N. Richtery-Dyn. 1974. Stochastic Models in Biology. Academic Press, New York. 269 pp.

Karlin, S. and H. M. Taylor. 1981. A Second Course in Stochastic Processes. Academic Press, New York. 542 pp.

Levins, R. 1969. The effects of random variations of different types on populations growth. Proc. Nat. Acad. Sci. U.S.A. 62:1061-1065.

Nisbet, R. M. and W. S. C. Gurney. 1982. Modelling Fluctuating Populations. John Wiley, Chichester. 379 pp.

O'Connell, C. P. 1971. Variability of near-surface zooplankton off southern California, as shown by towed-pump sampling. Fish. Bull. 69:681-697.

Stickland, J. D. H. and T. R. Parsons. 1968. A practical handbook of seawater analysis. Fish. Res. Board Can., Bull. 167. 311 pp.

Table 1. Statistical properties of Seahurst Beach intertidal nutrients collected about the summer and winter solstices in 1982. Concentrations are in mg-at/m^3. CV is coefficient of variation. Mean w/s and var w/s are the ratios of means and variances between summer and winter solstices.

	Phosphate		Nitrate		Silicate	
	Summer	Winter	Summer	Winter	Summer	Winter
Number of points	15	26	13	24	11	30
Mean	1.3	2.7	6.1	26.9	35.0	68.6
Variance	0.05	0.02	6.9	0.8	25.7	31.8
CV	0.17	0.05	0.43	0.03	0.14	0.08
Mean w/s	2.7		3.6		2.0	
Var w/s	0.4		0.1		1.2	
Chi-square	1.2	4.8	5.1	1.9	6.3	13.2
Chi-square ($\alpha = 0.05$)	9.5	7.8	7.8	11.1	12.6	16.9
Degrees of freedom	4	3	3	5	6	9

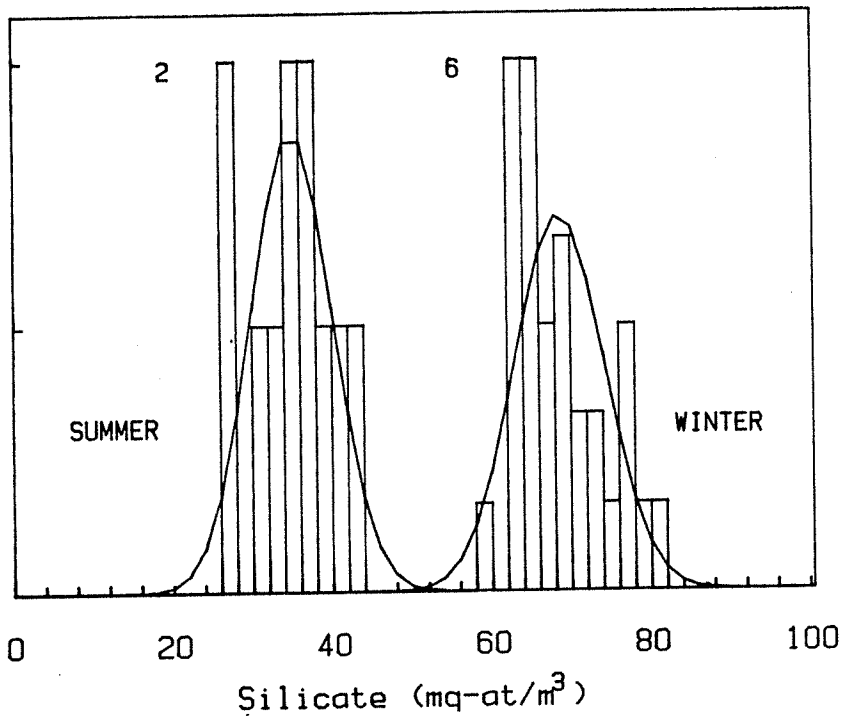

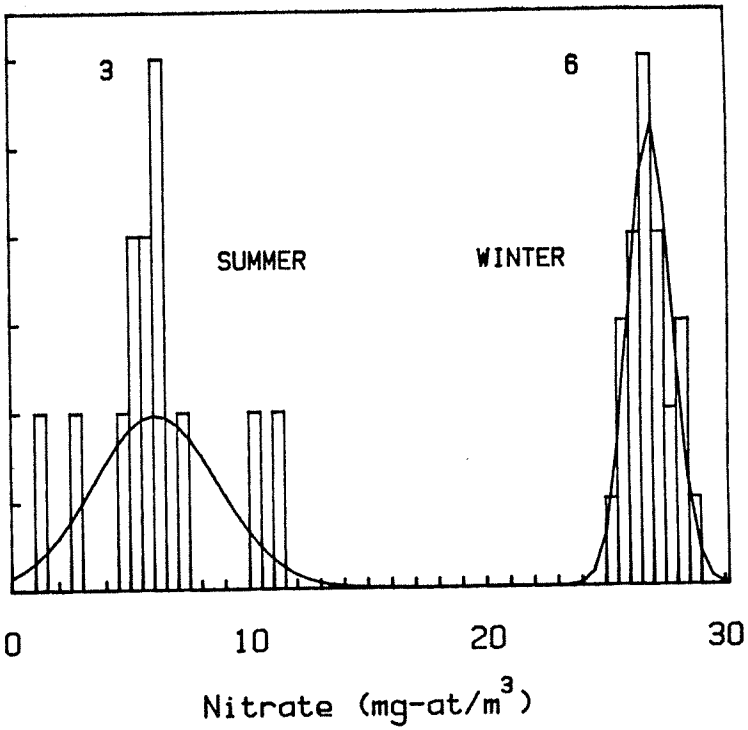

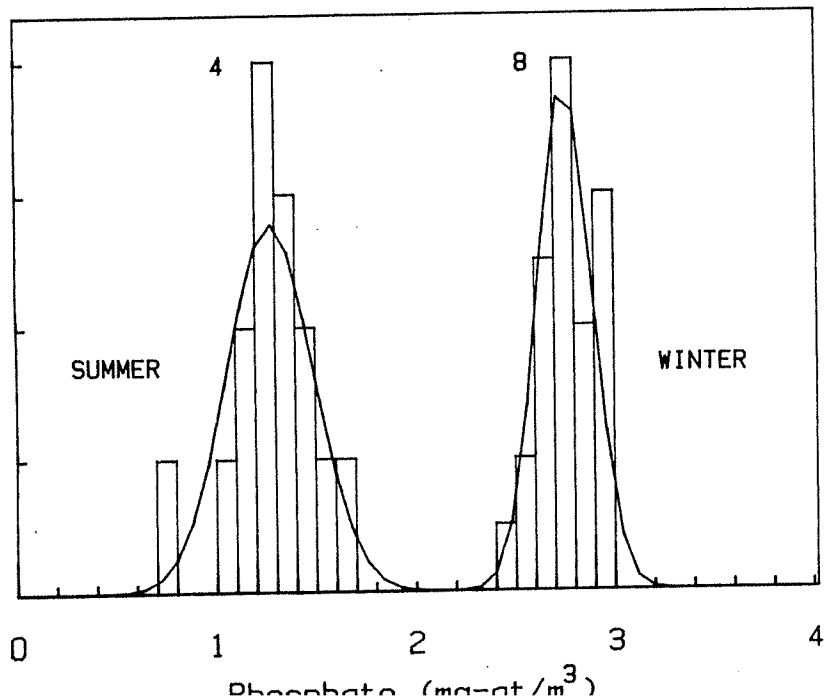

Fig. 1 Histograms of silicate, nitrate and phosphate collected about the summer and winter solstices in 1982 at the Seahurst Beach intertidal site. Numbers beside each mode designates the total number of observations in the mode. A normal probability distribution is fit through each group of observations.

Appendix 4.D

Appendix 4.D. Methods and data to calculate the probability of specified levels of plankton and nutrients in summer and winter seasons.

Seasonal probability distributions of plankton properties are defined according to eq(7) Section 4.3.4.2. The probability that x will fall between the range y0 and y1, where the gamma scale and shape parameters are b and c, is given by the algorithm below.

```
BASIC program to determine P(Y0 < X < Y1)
using the Gamma probability density function

10 DISP "INPUT b,c"
20 INPUT b,c
30 G1 = EXP(-c)*c^(c-.5)*SQR(2*PI)
40 G2 = 1+1/(12*c)+1/(288*c^2)
50 G3 = -139/(51840*c^3)-571/(2488320*c^4)
60 G = G1*(G2+G3+G4)
70 DISP "INPUT Y0,Y1"
80 INPUT Y0,Y1
90 I = (Y1-Y0)/200
100 P = 0
110 FOR X = Y0 TO Y1 STEP I
120 P = I*(X/b)^(c-1)*EXP(-X/b)/b/G + P
130 NEXT X
140 DISP P
150 GOTO 20
160 END
```

The scale and shape parameters for the probability distributions in figures 4.13, 4.16, 4.18, and 4.20 follow.

Seasonal probability distributions of nurtients near steady state conditions are defined by the normal pdf according to eq(13) Section 4.3.4.4. The probability that x will fall between the range y0 to y1 is given as a function of the mean M and variance V and can be computed with the algorithm below.

```
BASIC program to determine P(Y0 < x < Y1)
using the Normal probabiality density function

10 DISP "INPUT M,V"
20 INPUT M,V
30 DISP "INPUT Y0,Y1"
40 INPUT Y0,Y1
50 I = (Y1-Y0)/200
60 P = 0
70 A =1/SQR(V*2*PI)
80 B = 2*V
90 FOR X = Y0 TO Y1 STEP I
100 P = A*EXP(-(X-M)^2/B)*I + P
110 NEXT X
120 DISP P
130 GOTO 10
140 END
```

The mean and variance for the normal probability distributions in figures 4.44, and 4.45 follow. For Fig 4.45 the gamma shape and scale parameters are also given.

FOR DATA SET NEAR LITE Z INT CONC
X VARIABLE = PPmgm2
RANGE VARIABLE, LOWER VALUE, UPPER VALUE
JDAY 172 264

22 DATA POINTS SELECTED

Summer 82

STATISTICS
Mean = 1385.66770644
Std Dev = 706.40890392
Log Mean = 7.045972071
Log Std Dev = .4875964238
Exponent of Log Mean = 1148.22444919
Exponent of Log Std Dev = 1.62839753485
Geometric Mean = 1148.22444918

90 % confidence limits on gamma statistics

parameter	0.05 limit	best estimate	0.95 limit
Scale parameter b	319.427	513.634	903.344
Shape parameter c	4.098	2.619	1.569
Carrying capacity (gamma mean)			
mean = bc = K	1109.478	1345.428	1783.952
% error on K	17.537	0	32.593
Randomness coeff.			
R = 1/c	.243	.381	.637
% error on R	36.095	0	66.894

FOR DATA SET NEAR LITE Z INT CONC
X VARIABLE = PPmgm2
RANGE VARIABLE, LOWER VALUE, UPPER VALUE
JDAY 340 424

winter 83

6 DATA POINTS SELECTED

STATISTICS
Mean = 71.1
Std Dev = 33.2551343404
Log Mean = 4.13337636228
Log Std Dev = .3126280605
Exponent of Log Mean = 62.3882129362
Exponent of Log Std Dev = 1.36701299033
Geometric Mean = 62.388212937

90 % confidence limits on gamma statistics

parameter	0.05 limit	best estimate	0.95 limit
Scale parameter b	9.442	23.963	93.162
Shape parameter c	7.188	2.955	.966
Carrying capacity (gamma mean)			
mean = bc = K	54.937	70.818	98.282
% error on K	22.425	0	38.78
Randomness coeff.			
R = 1/c	.139	.338	1.035
% error on R	58.888	0	205.911

FOR DATA SET NEAR LITE Z INT CONC
X VARIABLE = PPmgm2
RANGE VARIABLE, LOWER VALUE, UPPER VALUE
JDAY 537 629

SUMMER 83

26 DATA POINTS SELECTED

STATISTICS
Mean = 1363.12905769
Std Dev = 760.712295071
Log Mean = 7.09108949235
Log Std Dev = .2404264077
Exponent of Log Mean = 1201.21580338
Exponent of Log Std Dev = 1.27179133634
Geometric Mean = 1201.21580337

90 % confidence limits on gamma statistics

parameter	0.05 limit	best estimate	0.95 limit
Scale parameter b	223.37	345.922	577.34
Shape parameter c	5.865	3.863	2.403
Carrying capacity (gamma mean)			
mean = bc = K	1151.526	1336.544	1641.454
% error on K	13.842	0	22.813
Randomness coeff.			
R = 1/c	.17	.258	.415
% error on R	34.125	0	60.728

FOR DATA SET NEAR LITE Z INT CONC
X VARIABLE = PPmgm2
RANGE VARIABLE, LOWER VALUE, UPPER VALUE
JDAY 720 800

winter 84

6 DATA POINTS SELECTED

STATISTICS
Mean = 109.446833333
Std Dev = 61.0583710582
Log Mean = 4.50530650627
Log Std Dev = .4689256033
Exponent of Log Mean = 90.4960774136
Exponent of Log Std Dev = 1.59827608786
Geometric Mean = 90.4960774141

90 % confidence limits on gamma statistics

parameter	0.05 limit	best estimate	0.95 limit
Scale parameter b	20.539	52.127	202.655
Shape parameter c	4.988	2.083	.711
Carrying capacity (gamma mean)			
mean = bc = K	81.012	108.621	162.398
% error on K	25.417	0	49.508
Randomness coeff.			
R = 1/c	.2	.479	1.406
% error on R	58.23	0	193.068

Data for Figure 4.13

FOR DATA SET NEAR LITE 2 INT CONC
X VARIABLE = CHLm2
RANGE VARIABLE, LOWER VALUE, UPPER VALUE
JDAY 172 264

Summer 82

44 DATA POINTS SELECTED

STATISTICS
Mean = 70.0984517318
Std Dev = 40.7775392975
Log Mean = 4.05144196905
Log Std Dev = .454831142
Exponent of Log Mean = 57.4802821033
Exponent of Log Std Dev = 1.57590725602
Geometric Mean = 57.4802821033

90 % confidence limits on gamma statistics

parameter	0.05 limit	best estimate	0.95 limit
Scale parameter b	18.706	26.227	38.386
Shape parameter c	3.516	2.582	1.844
Carrying capacity (gamma mean)			
mean = bc = K	60.098	67.741	82.958
% error on K	11.281	0	22.463
Randomness coeff.			
R = 1/c	.284	.387	.542
% error on R	26.539	0	39.998

FOR DATA SET NEAR LITE 2 INT CONC
X VARIABLE = CHLm2
RANGE VARIABLE, LOWER VALUE, UPPER VALUE
JDAY 340 424

Winter 83

19 DATA POINTS SELECTED

STATISTICS
Mean = 5.15847368421
Std Dev = 1.53242192545
Log Mean = 1.59896309763
Log Std Dev = .08443078613
Exponent of Log Mean = 4.94789927508
Exponent of Log Std Dev = 1.08809753018
Geometric Mean = 4.9478992751

90 % confidence limits on gamma statistics

parameter	0.05 limit	best estimate	0.95 limit
Scale parameter b	.276	.461	.854
Shape parameter c	18.381	11.114	6.157
Carrying capacity (gamma mean)			
mean = bc = K	4.57	5.128	5.871
% error on K	10.879	0	14.483
Randomness coeff.			
R = 1/c	.054	.089	.162
% error on R	39.535	0	80.502

FOR DATA SET NEAR LITE 2 INT CONC
X VARIABLE = CHLm2
RANGE VARIABLE, LOWER VALUE, UPPER VALUE
JDAY 537 629

Summer 83

59 DATA POINTS SELECTED

STATISTICS
Mean = 158.355668235
Std Dev = 80.4261716474
Log Mean = 4.90672771419
Log Std Dev = .3811594524
Exponent of Log Mean = 135.19628889
Exponent of Log Std Dev = 1.46398102209
Geometric Mean = 135.19628889

90 % confidence limits on gamma statistics

parameter	0.05 limit	best estimate	0.95 limit
Scale parameter b	35.564	47.663	65.934
Shape parameter c	4.105	3.231	2.54
Carrying capacity (gamma mean)			
mean = bc = K	140.678	154.042	179.776
% error on K	8.675	0	16.705
Randomness coeff.			
R = 1/c	.243	.309	.393
% error on R	21.278	0	27.218

FOR DATA SET NEAR LITE 2 INT CONC
X VARIABLE = CHLm2
RANGE VARIABLE, LOWER VALUE, UPPER VALUE
JDAY 720 800

Winter 84

15 DATA POINTS SELECTED

STATISTICS
Mean = 19.4167504345
Std Dev = 5.98970992995
Log Mean = 2.91709675551
Log Std Dev = .10400132079
Exponent of Log Mean = 18.4875356342
Exponent of Log Std Dev = 1.10960192047
Geometric Mean = 18.4875356343

90 % confidence limits on gamma statistics

parameter	0.05 limit	best estimate	0.95 limit
Scale parameter b	1.175	2.089	4.257
Shape parameter c	16.174	9.235	4.754
Carrying capacity (gamma mean)			
mean = bc = K	16.686	19.294	22.892
% error on K	13.514	0	18.645
Randomness coeff.			
R = 1/c	.061	.108	.21
% error on R	42.897	0	94.242

Data for Figure 4.16

FOR DATA SET NEAR LITE Z INT CONC
X VARIABLE = CHL
RANGE VARIABLE, LOWER VALUE, UPPER VALUE
JDAY 172 264
CHL 0 20

Summer 82

43 DATA POINTS SELECTED

STATISTICS
Mean = 3.77875758614
Std Dev = 4.05336125287
Log Mean = .873323874451
Log Std Dev = .898130289134
Exponent of Log Mean = 2.39485784561
Exponent of Log Std Dev = 2.45500866098
Geometric Mean = 2.39485784561

90 % confidence limits on gamma statistics

parameter	0.05 limit	best estimate	0.95 limit
Scale parameter b	2.045	2.879	4.234
Shape parameter c	1.614	1.195	.869
Carrying capacity (gamma mean)			
mean = bc = K	3.019	3.441	4.884
% error on K	12.277	0	41.91
Randomness coeff.			
R = 1/c	.619	.836	1.149
% error on R	25.947	0	37.433

FOR DATA SET NEAR LITE Z INT CONC
X VARIABLE = CHL
RANGE VARIABLE, LOWER VALUE, UPPER VALUE
JDAY 537 629
CHL 0 20

Summer 83

57 DATA POINTS SELECTED

OFF SET = 0 NUMBER OF CELLS = 20 CELL WIDTH = 1

STATISTICS
Mean = 6.27329679354
Std Dev = 3.90153495607
Log Mean = 1.61449873074
Log Std Dev = .50757959986
Exponent of Log Mean = 5.02536822939
Exponent of Log Std Dev = 1.66126539789
Geometric Mean = 5.02536822938

90 % confidence limits on gamma statistics

parameter	0.05 limit	best estimate	0.95 limit
Scale parameter b	1.908	2.57	3.578
Shape parameter c	2.987	2.343	1.833
Carrying capacity (gamma mean)			
mean = bc = K	5.449	6.024	7.309
% error on K	9.535	0	21.334
Randomness coeff.			
R = 1/c	.334	.426	.545
% error on R	21.575	0	27.828

FOR DATA SET NEAR LITE Z INT CONC
X VARIABLE = CHL
RANGE VARIABLE, LOWER VALUE, UPPER VALUE
JDAY 340 424

Winter 83

19 DATA POINTS SELECTED

STATISTICS
Mean = .225892967376
Std Dev = 5.31377299007E-2
Log Mean =-1.51483163338
Log Std Dev = .05680052313
Exponent of Log Mean = .219845196325
Exponent of Log Std Dev = 1.05844465411
Geometric Mean = .219845196325

90 % confidence limits on gamma statistics

parameter	0.05 limit	best estimate	0.95 limit
Scale parameter b	.007	.013	.024
Shape parameter c	28.148	16.98	9.374
Carrying capacity (gamma mean)			
mean = bc = K	.204	.225	.25
% error on K	9.035	0	11.387
Randomness coeff.			
R = 1/c	.035	.058	.106
% error on R	39.675	0	81.131

FOR DATA SET NEAR LITE Z INT CONC
X VARIABLE = CHL
RANGE VARIABLE, LOWER VALUE, UPPER VALUE
JDAY 720 800

Winter 84

15 DATA POINTS SELECTED

STATISTICS
Mean = .838616250027
Std Dev = .347162246291
Log Mean =-.273558584771
Log Std Dev = .216394225778
Exponent of Log Mean = .760667771503
Exponent of Log Std Dev = 1.24159175001
Geometric Mean = .760667771503

90 % confidence limits on gamma statistics

parameter	0.05 limit	best estimate	0.95 limit
Scale parameter b	.098	.175	.357
Shape parameter c	8.213	4.726	2.473
Carrying capacity (gamma mean)			
mean = bc = K	.68	.828	1.059
% error on K	17.805	0	27.968
Randomness coeff.			
R = 1/c	.121	.211	.404
% error on R	42.454	0	91.117

Data for Figure 4.18

X VARIABLE = PHAEO

RANGE VARIABLE,	LOWER VALUE,	UPPER VALUE
JDAY	172	264
PHAEO	0	2

Summer 82

39 DATA POINTS SELECTED

OFF SET = 0 NUMBER OF CELLS = 20 CELL WIDTH = .1

STATISTICS
Mean = .483378729228
Std Dev = .381501693363
Log Mean =-1.01275655398
Log Std Dev = .60549970065
Exponent of Log Mean = .363216372799
Exponent of Log Std Dev = 1.83216751548
Geometric Mean = .363216372798

90 % confidence limits on gamma statistics

parameter	0.05 limit	best estimate	0.95 limit
Scale parameter b	.175	.251	.377
Shape parameter c	2.548	1.824	1.258
Carrying capacity (gamma mean)			
mean = bc = K	.398	.458	.6
% error on K	13.039	0	31.104
Randomness coeff.			
R = 1/c	.392	.548	.794
% error on R	28.393	0	44.964

FOR DATA SET NEAR LITE Z INT CONC
X VARIABLE = PHAEO

RANGE VARIABLE,	LOWER VALUE,	UPPER VALUE
JDAY	340	424

Winter 83

19 DATA POINTS SELECTED

STATISTICS
Mean = .133421850534
Std Dev = 5.02534194729E-2
Log Mean =-2.06545490024
Log Std Dev = .09262174482
Exponent of Log Mean = .126760614017
Exponent of Log Std Dev = 1.09704669318
Geometric Mean = .126760614016

90 % confidence limits on gamma statistics

parameter	0.05 limit	best estimate	0.95 limit
Scale parameter b	.008	.014	.027
Shape parameter c	14.986	9.075	5.039
Carrying capacity (gamma mean)			
mean = bc = K	.116	.132	.154
% error on K	11.864	0	16.29
Randomness coeff.			
R = 1/c	.066	.11	.198
% error on R	39.444	0	80.096

FOR DATA SET NEAR LITE Z INT CONC
X VARIABLE = PHAEO

RANGE VARIABLE,	LOWER VALUE,	UPPER VALUE
JDAY	537	629

Summer 83

59 DATA POINTS SELECTED

STATISTICS
Mean = 1.12862630121
Std Dev = .978465466688
Log Mean =-.235189612893
Log Std Dev = .778141246653
Exponent of Log Mean = .790420961414
Exponent of Log Std Dev = 2.17742121274
Geometric Mean = .790420961413

90 % confidence limits on gamma statistics

parameter	0.05 limit	best estimate	0.95 limit
Scale parameter b	.519	.696	.962
Shape parameter c	1.898	1.508	1.203
Carrying capacity (gamma mean)			
mean = bc = K	.951	1.049	1.363
% error on K	9.367	0	29.83
Randomness coeff.			
R = 1/c	.526	.662	.83
% error on R	20.544	0	25.309

FOR DATA SET NEAR LITE Z INT CONC
X VARIABLE = PHAEO

RANGE VARIABLE,	LOWER VALUE,	UPPER VALUE
JDAY	720	800

Winter 84

15 DATA POINTS SELECTED

STATISTICS
Mean = .294035132309
Std Dev = .131889356353
Log Mean =-1.32853634824
Log Std Dev = .21993949566
Exponent of Log Mean = .264864647339
Exponent of Log Std Dev = 1.24600133982
Geometric Mean = .264864647339

90 % confidence limits on gamma statistics

parameter	0.05 limit	best estimate	0.95 limit
Scale parameter b	.036	.065	.133
Shape parameter c	7.679	4.423	2.319
Carrying capacity (gamma mean)			
mean = bc = K	.237	.29	.374
% error on K	18.265	0	29.173
Randomness coeff.			
R = 1/c	.13	.226	.431
% error on R	42.393	0	90.725

Data for Figure 4.20

```
FOR DATA SET    NEAR LITE Z INT CONC
X VARIABLE = NH3
RANGE VARIABLE,        LOWER VALUE,          UPPER VALUE
   JDAY                   172                   264
```

Summer 82

```
 76 DATA POINTS SELECTED

OFF SET = 0    NUMBER OF CELLS = 10    CELL WIDTH = .3

          STATISTICS
          Mean = .950139436905
          Std Dev = .627575900867
          Log Mean =-.343996138799
          Log Std Dev = .721457635073
          Exponent of Log Mean = .708931665372
          Exponent of Log Std Dev = 2.05743000813
          Geometric Mean = .708931665373

          Gamma Mean = .896406250444
          Gamma mode = .403187309067
          Gamma Scale Parameter b = .493218941377
          Gamma Shape Parameter c = 1.81746112171
```

```
FOR DATA SET    NEAR LITE Z INT CONC
X VARIABLE = NH3
RANGE VARIABLE,        LOWER VALUE,          UPPER VALUE
   JDAY                   355                   445
```

winter 83

```
 23 DATA POINTS SELECTED

          STATISTICS
          Mean = .297794639049
          Std Dev = .118592675966
          Log Mean =-1.28722338096
          Log Std Dev = .1555066576
          Exponent of Log Mean = .276036167286
          Exponent of Log Std Dev = 1.16824971378
          Geometric Mean = .276036167286

          Gamma Mean = .294475750396
          Gamma mode = .247573800716
          Gamma Scale Parameter b = 4.69019496799E-2
          Gamma Shape Parameter c = 6.27853964293
```

Data for Figure 4.45

```
FOR DATA SET    NEAR LITE Z INT CONC
X VARIABLE = NH3
RANGE VARIABLE,        LOWER VALUE,          UPPER VALUE
   JDAY                   537                   629
```

Summer 83

```
 57 DATA POINTS SELECTED

OFF SET = 0    NUMBER OF CELLS = 10    CELL WIDTH = .3

          STATISTICS
          Mean = .627146622137
          Std Dev = .442384604612
          Log Mean =-.708933158514
          Log Std Dev = .507387472389
          Exponent of Log Mean = .492168983769
          Exponent of Log Std Dev = 1.66094625383
          Geometric Mean = .49216898377

          Gamma Mean = .599335790317
          Gamma mode = .321262607723
          Gamma Scale Parameter b = .278073182594
          Gamma Shape Parameter c = 2.15531675772
```

```
FOR DATA SET    NEAR LITE Z INT CONC
X VARIABLE = NH3
RANGE VARIABLE,        LOWER VALUE,          UPPER VALUE
   JDAY                   720                   800
```

winter 84

```
 15 DATA POINTS SELECTED

OFF SET = 0    NUMBER OF CELLS = 10    CELL WIDTH = .1

          STATISTICS
          Mean = .110492035055
          Std Dev = 4.65961488453E-2
          Log Mean =-2.34907144955
          Log Std Dev = .41887037064
          Exponent of Log Mean = 9.54577584207E-2
          Exponent of Log Std Dev = 1.52024327385
          Geometric Mean = 9.54577584209E-2

          Gamma Mean = .108327007463
          Gamma mode = 7.45265688459E-2
          Gamma Scale Parameter b = 3.38004386173E-2
          Gamma Shape Parameter c = 3.20489945973
```

Summer 1982

```
FOR DATA SET   NEAR LITE Z INT CONC
X VARIABLE = NO3
RANGE VARIABLE,      LOWER VALUE,          UPPER VALUE
   JDAY                153                   158

 6 DATA POINTS SELECTED

OFF SET = 0   NUMBER OF CELLS = 10   CELL WIDTH = 1

        STATISTICS
        Mean = 4.55389915763
        Std Dev = 2.2445438832
        Log Mean = 1.30878061278
        Log Std Dev = .61691225996
        Exponent of Log Mean = 3.7016572056
        Exponent of Log Std Dev = 1.85319700783
        Geometric Mean = 3.70165720559

        Gamma Mean = 4.51211322641
        Gamma mode = 2.16785026953
        Gamma Scale Parameter b = 2.34426295688
        Gamma Shape Parameter c = 1.92474705671
```

Summer 1983

```
FOR DATA SET   NEAR LITE Z INT CONC
X VARIABLE = NO3
RANGE VARIABLE,      LOWER VALUE,          UPPER VALUE
   JDAY                518                   536

 16 DATA POINTS SELECTED

OFF SET = 0   NUMBER OF CELLS = 10   CELL WIDTH = 1

        STATISTICS
        Mean = 3.87365293455
        Std Dev = 1.72153255591
        Log Mean = 1.25603668509
        Log Std Dev = .20347112217
        Exponent of Log Mean = 3.5114767837
        Exponent of Log Std Dev = 1.22564976302
        Geometric Mean = 3.51147678369

        Gamma Mean = 3.82413377491
        Gamma mode = 3.01610849069
        Gamma Scale Parameter b = .808025284222
        Gamma Shape Parameter c = 4.7326907333
```

Winter 1983

```
FOR DATA SET   NEAR LITE Z INT CONC
X VARIABLE = NO3
RANGE VARIABLE,      LOWER VALUE,          UPPER VALUE
   JDAY                382                   424

 11 DATA POINTS SELECTED

OFF SET = 0   NUMBER OF CELLS = 1   CELL WIDTH = 1
OFF SET = 25   NUMBER OF CELLS = 10   CELL WIDTH = .5

        STATISTICS
        Mean = 27.495271133
        Std Dev = .46582491668
        Log Mean = 3.31388266008
        Log Std Dev = .0002636517
        Exponent of Log Mean = 27.4916592888
        Exponent of Log Std Dev = 1.00026368646
        Geometric Mean = 27.4916592889

        Gamma Mean = 27.4712955373
        Gamma mode = 27.4627952975
        Gamma Scale Parameter b = 8.50023984556E-3
        Gamma Shape Parameter c = 3231.8259292
```

Winter 1984

```
FOR DATA SET   NEAR LITE Z INT CONC
X VARIABLE = NO3
RANGE VARIABLE,      LOWER VALUE,          UPPER VALUE
   JDAY                733                   775

 10 DATA POINTS SELECTED

        STATISTICS
        Mean = 25.6011465223
        Std Dev = .398720595572
        Log Mean = 3.24252857712
        Log Std Dev = .0002165328
        Exponent of Log Mean = 25.5983674283
        Exponent of Log Std Dev = 1.00021655624
        Geometric Mean = 25.5983674283

        Gamma Mean = 25.5713084784
        Gamma mode = 25.5646516939
        Gamma Scale Parameter b = 6.65678444581E-3
        Gamma Shape Parameter c = 3841.39049214
```

Data for Figure 4.44

Appendix 4.E

Appendix 4.E. List of zooplankton taxa encountered in this study, classified to the smallest taxonomic level identified.

Phylum Arthropoda
  Subphylum Crustacea
    Class Maxillopoda
      Subclass Copepoda
        Order Calanoida
          Calanus pacificus
          Calanus marshallae
          Microcalanus sp.
          Paracalanus sp.
          Pseudocalanus spp.
          Aetidius divergens
          Metridia lucens
          Centropages abdominalis
          Tortanus discaudatus
          Acartia clausii
          Acartia longiremus
          Epilabidocera longipedata
        Order Cyclopoida
          Corycaeus anglicus
          Oithona similis
          Oithona spinirostris
          Cyclopoina sp.
        Order Harpacticoida
      Subclass Cirripedia
          Larvae (nauplii and cyprid stages)
    Class Branchiopoda
      Subclass Diplostraca
        Order Cladocera
          Evadne nordmanni
          Podon leuckarti
    Class Malacostraca
      Subclass Eumalacostraca
        Order Mysidacea
        Order Amphipoda
          Calliopius laeviusculus
          Cyphocaris challengeri
          Parathemisto pacifica
        Order Euphausiacea
          Larvae (eggs, nauplii, calyptopis, furcilia, juveniles)
          Adults
        Order Decapoda
          Pasiphaea pacifica
          Crab larvae (zoeae, megalops)
          Shrimp larvae
Phylum Mollusca
    Class Gastropoda
          Larvae
    Class Bivalvia
          Larvae
Phylum Annelida
    Class Polychaeta
          Tomopteris sp.
          Larvae

Phylum Ctenophora
Pleurobrachia pileus
Phylum Cnidaria
Class Hydrozoa
Order Siphonophora
Chelophyes appendiculata
Phylum Chordata
Class Larvacea
Oikopleura dioica
Oikopleura labradorensis
Fritillaria borealis
Phylum Chaetognatha
Sagitta elegans
Phylum Bryozoa
Cyphonautes larvae
Phylum Echinodermata
Larvae